Technical Report Documentation Page

1. Report No. FHWA/TX-12/0-6374-2	2. Government Accession No.	3. Recipient's Catalog No.
4. Title and Subtitle Effect of New Prestress Loss Estimates on Pretensioned Concrete Bridge Girder Design		5. Report Date October 2012, Rev. June 2013, Published August 2013
		6. Performing Organization Code
7. Author(s) David Garber, José Gallardo, Dean Deschenes, David Dunkman, and Oguzhan Bayrak		8. Performing Organization Report No. 0-6374-2
9. Performing Organization Name and Address Center for Transportation Research The University of Texas at Austin 1616 Guadalupe Street, Suite 4.202 Austin, TX 78701		10. Work Unit No. (TRAIS)
		11. Contract or Grant No. 0-6374
12. Sponsoring Agency Name and Address Texas Department of Transportation Research and Technology Implementation Office P.O. Box 5080 Austin, TX 78763-5080		13. Type of Report and Period Covered Technical Report 09/01/08-08/31/12
		14. Sponsoring Agency Code

16. Abstract

In 2008, TxDOT initiated Project 0-6374 to investigate prestress losses in pretensioned concrete girders. The prestress loss estimates in the AASHTO LRFD Bridge Design Specifications had been recalibrated in 2005 to be more accurate for "high-strength [conventional] concrete." Greater accuracy implies less conservatism, the result of which may be flexural cracking of beams under service loads. Project 0-6374 was therefore funded to provide an experimental evaluation and an engineering recommendation of whether implementation of the new prestress loss estimates (currently outlined in AASHTO LRFD 2012) is appropriate for TxDOT. The primary objectives of TxDOT Project 0-6374 were: (1) to *assess the conservatism and accuracy* of the current prestress loss provisions, (2) to *identify the benefits and weaknesses* of using the AASHTO LRFD 2004 and 2012 prestress loss provisions, and (3) to *make recommendations to simplify* the prestress loss provisions of AASHTO LRFD 2012. These objectives were accomplished through (1) the fabrication, conditioning, and testing of 30 field-representative girders, (2) the assembly and analysis of a prestress loss database, (3) a parametric study of the design implications of the various prestress loss provisions. The database evaluation, coupled with the experimental results, revealed that use of the AASHTO LRFD 2012 prestress loss provisions resulted in underestimation of the prestress loss in nearly half of all cases. With this in mind, new prestress loss provisions were developed through simplification and recalibration of the method outlined in AASHTO LRFD 2012. The TxDOT Project 0-6374 prestress loss provisions were found to be simpler, more conservative, and more precise than the current methods outlined within the AASHTO LRFD Bridge Design Specifications.

17. Key Words Prestress Losses, Prestressed, Pretensioned, Concrete, Girder, Design, Full-Scale, Experimental, Parametric	18. Distribution Statement No restrictions. This document is available to the public through the National Technical Information Service, Springfield, Virginia 22161; www.ntis.gov.		
19. Security Classif. (of report) Unclassified	20. Security Classif. (of this page) Unclassified	21. No. of pages 300	22. Price

Form DOT F 1700.7 (8-72) Reproduction of completed page authorized

This page is intentionally left blank

EFFECT OF NEW PRESTRESS LOSS ESTIMATES ON PRETENSIONED CONCRETE BRIDGE GIRDER DESIGN

David Garber
José Gallardo
Dean Deschenes
David Dunkman
Oguzhan Bayrak

Disclaimers

Author's Disclaimer: The contents of this report reflect the views of the authors, who are responsible for the facts and the accuracy of the data presented herein. The contents do not necessarily reflect the official view or policies of the Federal Highway Administration or the Texas Department of Transportation (TxDOT). This report does not constitute a standard, specification, or regulation.

Patent Disclaimer: There was no invention or discovery conceived or first actually reduced to practice in the course of or under this contract, including any art, method, process, machine manufacture, design or composition of matter, or any new useful improvement thereof, or any variety of plant, which is or may be patentable under the patent laws of the United States of America or any foreign country.

Engineering Disclaimer

NOT INTENDED FOR CONSTRUCTION, BIDDING, OR PERMIT PURPOSES.

Project Engineer: Oguzhan Bayrak
Professional Engineer License State and Number: Texas No. 106598
P. E. Designation: Research Supervisor

Acknowledgments

TABLE OF CONTENTS

LIST OF FIGURES

This page is intentionally left blank

LIST OF TABLES

This page is intentionally left blank

CHAPTER 1
Introduction

1.1 INTRODUCTION

A study of the prestress losses in pretensioned concrete beams conducted under Project 0-6374 is presented in this report; this project was initiated by the Texas Department of Transportation (TxDOT). The research was undertaken by The University of Texas at Austin (UT) at the Ferguson Structural Engineering Laboratory (FSEL). The main objectives of the project were: (1) verify the performance of the current AASHTO LRFD Bridge Design Specifications (AASHTO LRFD 2012) loss estimation procedures, and (2) recommend a simplified and conservative procedure to estimate final prestress losses. These objectives were accomplished through: assembly of an extensive prestress loss database, experimental assessment of 30 full-scale field-representative girders, and a comprehensive parametric study. It was concluded that the AASHTO LRFD 2012 procedures can result in underestimation of the prestress losses and result in an insufficient amount of prestress. As a major outcome of this project, a simple, conservative and precise procedure for estimation of final prestress losses is introduced.

1.2 PRESTRESS LOSSES

Prestressing is used in reinforced concrete beams to reduce the potential for cracking by pre-compressing the concrete, thereby reducing or even eliminating the tensile stresses imposed by both superimposed dead loads and live loads. Prestressed concrete beams are broadly used for their superior serviceability and low maintenance requirements. The effectiveness of the applied prestress declines over time due to various phenomena; this process is referred to as prestress loss and is the central point of this study. Prestress loss depends on a number of parameters, including material properties, prestress level, girder dimensions, environmental conditions, and loading.

The magnitude of the prestress loss needs to be estimated during the design process to verify that the girder stresses will not exceed the concrete tensile stress limits under service loads. An unconservative estimate of the prestress loss may lead to an insufficient amount of prestressing steel, higher concrete tensile stresses and premature service load cracking. On the other hand, large overestimations of prestress loss result in over-designed sections and increased costs. Methods for the estimation of prestress loss should therefore strike a balance between conservatism and accuracy.

1.3 PROJECT MOTIVATION

In the 1990s, the use of high-performance concrete became widespread among state Departments of Transportation (DOTs). Among some individuals, concern arose that while the equations developed in the 1970s had been proven effective for estimating prestress losses in bridge girders fabricated with normal-strength concrete, they might do so too conservatively for girders of higher strength concrete. As a result, National Cooperative Highway Research Program (NCHRP) Project 18-07 was funded in 2000, and the University of Nebraska – Lincoln (UNL) was tasked to "provide reliable estimates for high-strength concrete bridge girders". The

end product of this research project was NCHRP Report 496 (2003), which provided new approximate and refined methods to estimate prestress losses. The NCHRP 496 methods were then incorporated into the 2005 Interim Revisions of the AASHTO LRFD Bridge Design Specifications with minimal modification. The methods have persisted within the Section 5.9.5 of the Specifications, "Loss of Prestress", and will be referenced in this report via the most current edition (i.e. prestress loss provisions of AASHTO LRFD 2012).

The AASHTO LRFD 2012 prestress loss provisions account for a large number of factors that are thought to influence prestress losses, with the objective of achieving accurate estimations. The resulting complexity of the method far exceeds that of the preceding provisions of the 2004 AASHTO LRFD Bridge Design Specifications. Many have commented that the current method is difficult to implement because it requires the calculation and interpretation of a large number of variables and equations. Moreover, the relevance of some of the input parameters can be questioned when considering that their effect is far surpassed by the large variability of other, more relevant parameters.

Most importantly, introduction of the new provisions created a substantial amount of curiosity and concern within the bridge design community. The prestress loss estimates of AASHTO LRFD 2012 are considerably less than those of AASHTO LRFD 2004 in some cases; prompting TxDOT and others to question the conservatism of the method. Prior to implementation of the AASHTO LRFD 2012 prestress loss provisions in routine design, TxDOT Bridge Division sought additional experimental/analytical verification through Project 0-6374.

1.4 PROJECT OBJECTIVES

The primary objectives of TxDOT Project 0-6374 were:

1. To *assess the conservatism and accuracy* of the current prestress loss provisions, introduced in the 2005 Interim Revision of the AASHTO LRFD Bridge Design Specifications, and still included in the 2012 Edition of the Specifications.

2. To *identify the benefits and weaknesses* of using the prestress loss provisions contained within the 2004 and 2012 Editions of the AASHTO LRFD Bridge Design Specifications.

3. To *make recommendations to simplify* the prestress loss provisions of the 2012 AASHTO LRFD Bridge Design Specifications such that the final prestress loss can easily be estimated without the consideration of time.

1.5 PROJECT TASKS

The project objectives were accomplished through a combination of experimental and analytical efforts. The conservatism and accuracy of the AASHTO LRFD Bridge Design Specifications were evaluated through the use of a prestress loss database that included 30 field-representative girders - fabricated and tested within the context of the current study. Implementation and implications of the current prestress loss provisions were examined within an extensive literature review and parametric study. Synthesis of the experimental and analytical results supported the development of reasonably conservative, precise prestress loss provisions. Work completed during each of the major project tasks is outlined below:

1. *Literature Review*: The origin of the prestress loss expressions was investigated in order to understand the logic and reasoning behind each expression. Recent efforts examining the performance of the new loss procedure and recommending simplifications to the procedure were also studied.

2. *Database Assembly*: A comprehensive database of available experimental investigations pertaining to prestress loss was compiled as part of the project. This database contains information on 237 specimens, including 140 specimens for which prestress loss was reported or enough accurate information was provided to calculate prestress loss that occurred at the time of testing. Compared with previously assembled databases, the database assembled in this project is unmatched in size and diversity. The use of this database was invaluable in evaluation of the current prestress loss provisions and the project recommendations.

3. *Fabrication, Conditioning and Experimental Evaluation of Pretensioned Girders*: A total of 30 full-scale prestressed concrete beams were fabricated to provide a relevant experimental basis for assessment of the existing prestress loss provision (and for the development of new provisions). These specimens were representative of a broad range of the most influential factors that may affect prestress losses in structures fabricated within the State of Texas including:

   - type of concrete (CC and SCC),

   - coarse aggregate (Limestone and River Gravel),

   - sectional geometry (Type C and Tx46), and

   - climate (humidity from 51% to 63%).

   Prestress loss monitoring was conducted on 18 of the specimens through the use of internal instrumentation. As part of the experimental program, tests for compression, tension and modulus of elasticity were conducted on a large number of cylinders at multiple concrete ages. These concrete properties were used to assess the effect of the different concrete mixes. Flexural testing was conducted at the end of the conditioning period, and the load at the time of first cracking (together with measured concrete tensile strength) was used to back-calculate the total prestress loss. Results from the flexural testing were compared with results from the internal instrumentation and included in the database for evaluation.

4. *Parametric Study of Design Implications*: In order to assess the impact of the new prestress loss provisions of the 2012 AASHTO LRFD Bridge Design Specifications, a comprehensive parametric study was completed. Over 1800 different bridge designs were completed to account for all of the influential design parameters, including:

   - cross-section type,

   - girder spacing,

   - bridge span length, and

   - concrete release strength.

Through completion and comparison of the 2004 and 2012 AASHTO LRFD bridge designs, it was possible to identify the impact of the new loss provisions on the design of standard TxDOT bridges, summarized in terms of:

- flexural reinforcement,

- flexural capacity,

- shear capacity, and

- camber.

5. *Development of Design Recommendations*: New prestress loss provisions were developed through simplification of the method outlined in AASHTO LRFD 2012. The simplification process included consideration of the results obtained from experimental and analytical efforts outlined above. The primary objectives of the simplification were:

- To exclude prestress loss components with a minor contribution and/or limited relevance to the final prestress loss estimate.

- To account for typical materials and construction practices in calculation of the prestress loss components for simple span, pretensioned girders.

- To eliminate time-dependency of the provisions and limit estimation of the prestress loss to that corresponding to the full service life of a girder.

- To introduce additional conservatism where warranted by comparison of measured and estimated prestress losses.

It should be noted that this study was limited to pretensioned members used for the construction of simple span bridges. Post-tensioned, multi-stage construction was not examined within the context of this study.

1.6 ORGANIZATION

The remainder of this report is divided into six chapters. Essential background on prestress loss in pretensioned concrete is provided in Chapter 2, including a presentation of the current estimation methods as well as an introduction to the TxDOT Project 0-6374 prestress loss database. The fabrication, conditioning and testing of 30 full-scale pretensioned girders is then discussed within Chapter 3 - it covers all essential aspects of the experimental program. Results of the experimental program are examined in Chapter 4. Variation of the prestress losses with respect to the experimental parameters is covered therein. The implications of the current prestress loss provisions (AASHTO LRFD 2004 and 2012) on the design and construction of standard TxDOT bridges are evaluated in Chapter 5. New prestress loss provisions – developed through synthesis of the experimental and analytical results – are presented and evaluated in Chapter 6. The full scope of the study and the resulting conclusions are summarized in Chapter 7.

CHAPTER 2
Background on Prestress Loss in Pretensioned Concrete

2.1 OVERVIEW

Over the years, many procedures have been developed to estimate the prestress losses that occur immediately after release and over the life of a pretensioned concrete bridge girder. Historically, procedures for estimating prestress loss have been simple and conservative. With the implementation of a new loss procedure in the 2005 AASHTO LRFD Bridge Design Specification Interim Revisions, there was a profound shift in philosophy from conservatism to accuracy. When a loss is estimated unconservatively, the resulting design may have an insufficient amount of prestressing. Undesirable service load cracking can occur in these under-designed beams. It was found, using the Evaluation Database assembled for this project, that the measured losses for 30 of the 140 specimens are unconservatively estimated by as much as 41 percent using the AASHTO LRFD 2005 procedure. In addition to unconservative estimates, the "interpretation and use of [AASHTO LRFD 2005] provisions is difficult, and the existing commentary offers little clarification" (Roller 2011).

A detailed review of the two most recent approaches to prestress loss estimation is preceded by a review of the fundamental mechanisms of prestress loss. This review will highlight the influential variables to be considered in estimation of prestress loss. Due to the limitations of the scope of this report, only the procedures for calculating prestress loss contained in the 2004 and 2012 AASHTO LRFD Bridge Design Specifications will be discussed. The origin and implementation of the expressions found in both procedures will be explored in order to begin to show where simplifications can and should be made. The reader will benefit from detailed derivations of each specification's approach. These discussions will also support future simplifications of the code made in Chapter 6.

The performance of both code approaches will be evaluated against a database of field- and laboratory-measured prestress losses. Collection, analysis and filtering of Texas Department of Transportation (TxDOT) Project 0-6374 prestress loss database will be briefly discussed in advance of the code evaluations. The conservatism, accuracy and precision of the prestress loss estimates provided by each code approach will be summarized with respect to the full database of measurements. On the basis of the results from this investigation, an additional level of conservatism should be added to the estimate procedure through the simplification of expressions and recalibration of factors.

This study was limited to pretensioned members used for the construction of simple span bridges with panelized, cast-in-place decks. Post-tensioned, multi-stage construction was not examined within the context of this study. Throughout this chapter and the remainder of this report, prestress loss is positive and any stress gain is negative. This sign convention is consistent with that found in the specifications.

2.2 MECHANISMS OF PRESTRESS LOSS

During the life of a prestress beam, the stress in the prestressing strand will decrease due to both events occurring outside the beam and internal behavior of concrete; this change in

prestress is called prestress loss. This section will outline the influential factors and mechanisms that cause changes in the prestress.

The time-dependent variation of tensile stress within the prestressing strands of a pretensioned girder is illustrated in Figure 2.1. The instantaneous and gradual losses of stress from the time of prestress transfer (Point C in Figure 2.1) to the end of the girder's serviceable life (Point K) are collectively referred to as the "total prestress loss." A corresponding illustration of the compressive stress within the bottommost concrete fiber of the same pretensioned girder is provided in Figure 2.2. Resistance of the pretensioned girder to service load cracking is directly dependent on the magnitude of the stress in the prestressing strands; highlighting the need for proper estimation of the total prestress loss.
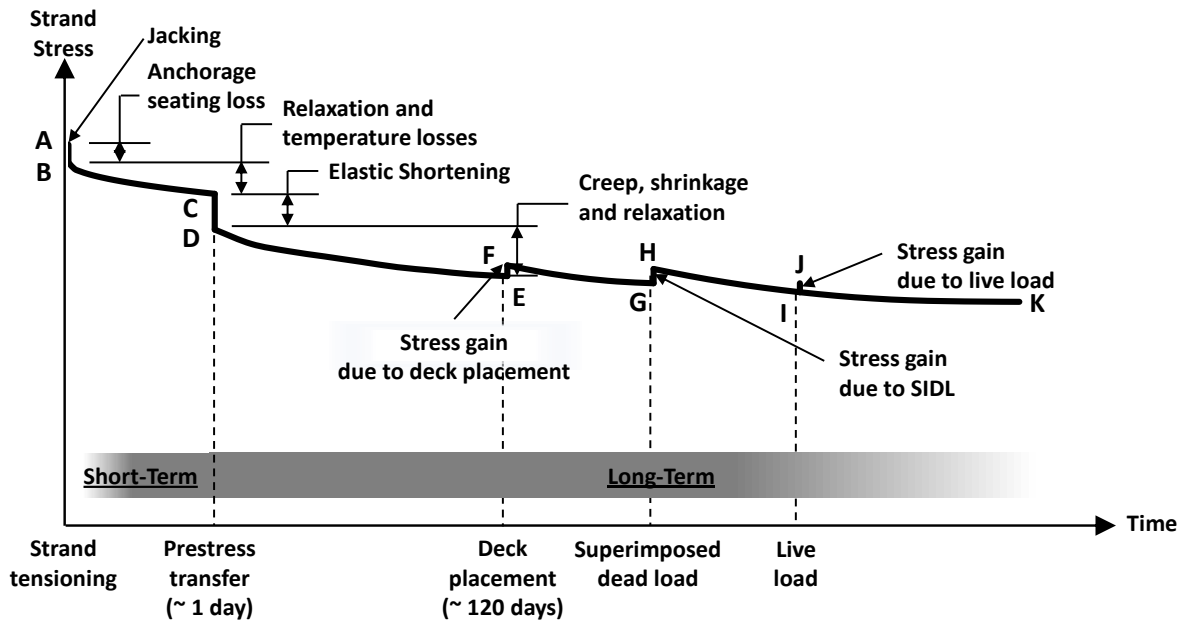
Figure 2.1 - Effective prestress (adapted from Tadros et al., 2003)
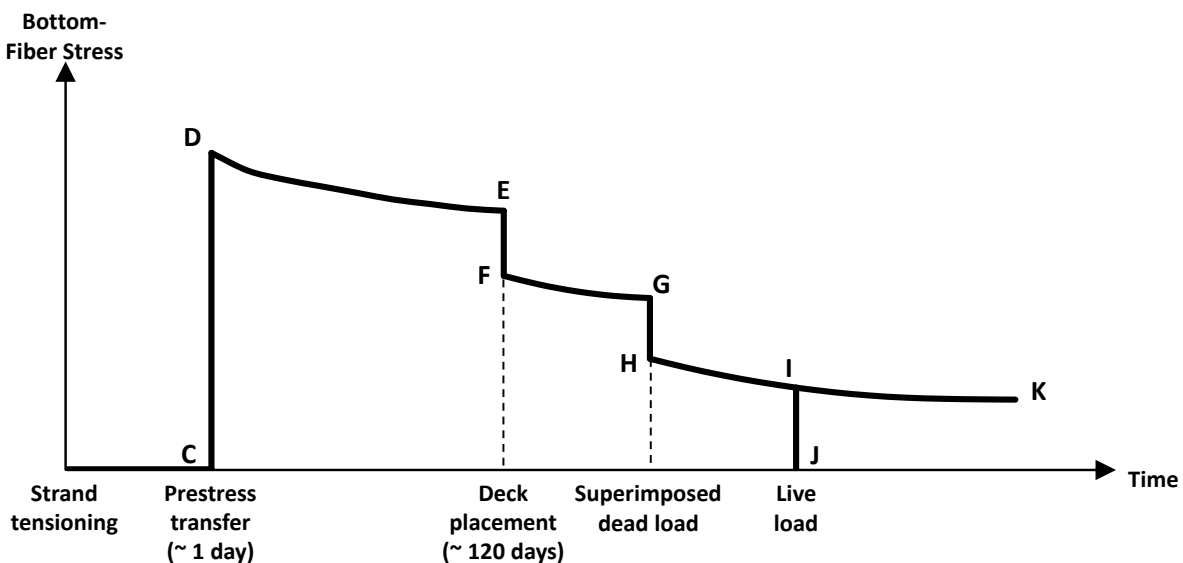
Figure 2.2 – Bottom-fiber compressive stress over the life of a pretensioned girder

6

The major events that typically occur during the life of the girder are shown on the horizontal axis of Figure 2.1 and Figure 2.2: strand tensioning, prestress transfer, deck placement, and addition of any other superimposed dead load and live load.

After all of the strands are pulled the full length of the prestressing bed, the strands are stressed to approximately 75 percent of their ultimate strength; corresponding to point A in Figure 2.1. Strand tensioning can either be done individually, strand by strand, or collectively through the use of a gang-stressing apparatus. Strands were tensioned individually for all of the beams fabricated during this project.

After the initial tensioning (or jacking), the first prestress loss observed is anchorage seating loss. Anchorage seating loss (A-B) occurs when the strands are initially stressed and seated before casting. Precast fabricators will typically overstress the strands so that after seating loss the strand stress is the desired initial prestressing force. The next observed losses are relaxation and temperature losses (B-C). Temperature-related losses are small, temporary losses caused by a change in ambient temperature and are not accounted for in most design procedures. Strand relaxation is the phenomenon in which the stress in a strand will decrease over time if held at a constant strain.

After the strands are tensioned, the cage is built around the strands, the concrete is cast and the beam is cured. When the desired initial concrete strength (f'_{ci}) is reached, the formwork is stripped and the stress in the prestressing strands is transferred from the jacking equipment to the beam; this is generally called transfer or release. Release is typically done in two stages: first a portion of the stress is released from all of the strands using the jacking apparatus and then the remainder of the stress is released by torch cutting the strands individually. The compressive stresses imposed at transfer cause the beam to elastically shorten (C-D) and compatibility between the beam and prestressing strands thereby results in the loss of pre-strain and prestress within the strands. After transfer, the beam is taken off of the line and stored at the precast plant until the bridge is erected. It is at this point immediately following transfer that the long-term losses (D-K) begin to occur. Long-term loss is primarily a result of creep and shrinkage of the girder concrete and the relaxation of the prestressing strands, which will be discussed in more detail in the following sections. Because of these long-term losses, the compressive stress in the bottom-most fiber of the beam will also decrease, as seen in Figure 2.2 D-E.

The beams are next erected at the bridge site and the deck is placed. Typically, the deck consists of a cast-in-place deck placed on 4-inch-thick precast, pretensioned deck panels, resulting in an 8-inch-thick deck slab. Deck placement will cause an increase in the tensile stresses in the bottom portion of the beam, both in the prestressing strands and the concrete. This increase in tensile stress can be seen by the stress gain in Figure 2.1 E-F and the decrease in the compressive stress in the bottom-most concrete fiber in Figure 2.2 E-F. Any additional superimposed dead loads or live loads will have a similar effect on the system as deck placement, with the exception that superimposed loads will be resisted by the composite cross-section.

The long-term prestress losses will continue to occur throughout the remainder of the life of the bridge. The majority of the long-term loss occurs early in the life of the bridge, with typically over 70 percent of creep and shrinkage loss occurring before deck placement and over 90 percent within the first year (as indicated by TxDOT Project 0-6374 measurements).

Among the prestress losses illustrated in Figure 2.1, the most significant contributions to the total prestress loss are elastic shortening, shrinkage and creep of the girder concrete and relaxation of the prestressing strands. The relative contribution of each component to the total

prestress loss calculated for a typical pretensioned girder is shown in Figure 2.3. Minor contributions to the total prestress loss (i.e. seating loss) are typically accounted for during the manufacturing process.
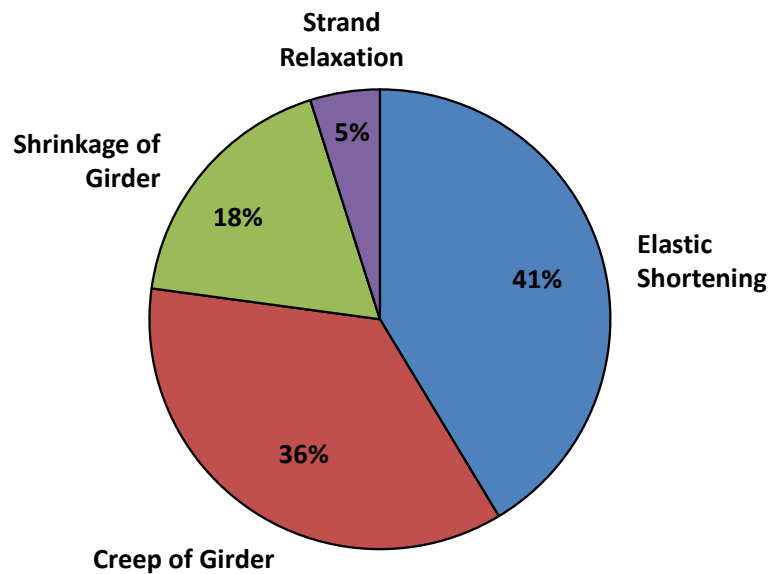
Figure 2.3 – Typical breakdown of total prestress loss (from parametric study of Chapter 5)

Prestressing strands are most commonly stressed to seventy-five percent of their specified tensile strength before transfer (i.e. $f_{pbt} = 0.75f_{pu} = 0.75 \cdot 270$ ksi = 202.5 ksi). To provide perspective, the total prestress losses estimated by AASHTO LRFD 2004 range between 25 and 105 ksi (or 12 and 52 percent of f_{pbt}) for typical pretensioned girders utilized by the TxDOT. The actual loss of prestress in the field will be influenced by the girder design, fabrication sequence, material properties, and environmental conditions. As noted by Tadros et al. (2003):

Accurate prediction of prestress losses requires accurate prediction of long-term properties of concrete and prestressing strands, which is a very complex process because of the uncontrollable variables involved. The material properties that vary with time and affect prestress losses are compressive strength, modulus of elasticity, shrinkage (stress independent), and creep (stress dependent) of concrete and relaxation of strands... The rate at which concrete properties change with time depends on a number of factors, including type and strength of cement, type, quality, and stiffness (i.e. modulus of elasticity) of aggregates, and quantity of coarse aggregates; type and amount of admixtures; water/cement ratio; size and shape of the girder; stress level; and environmental conditions (humidity and temperature).

The underlying mechanisms of the most significant prestress loss components (elastic shortening, shrinkage, creep and relaxation) are discussed in the next three sections. The discussions will collectively highlight the most influential factors to be considered during code-based estimation of prestress loss.

2.2.1 Prestress Loss Due to Elastic Shortening

A concrete member subjected to an external force will shorten instantaneously. The amount of shortening will depend on the magnitude of the applied force and the stiffness of the concrete. When the prestress force is transferred from the stressing blocks to the concrete beams, the stress in the strands is transferred to the surrounding (hardened) concrete via bond stresses. Relative shortening of the girder at the level of prestressing (ε_c) may be calculated on the basis of the imposed compressive stresses (f_{cgp}) and the concrete modulus of elasticity (E_{ci}); refer to Equation (2.1). The concrete compressive stress at the level of the prestressing (f_{cgp}) may be determined through sectional equilibrium of the strand stresses, concrete stresses, dead and superimposed loads. Assuming perfect bond between the prestressing strands and surrounding concrete, compatibility would require the concrete strain due to elastic shortening to be equivalent to the strain change in the prestressing strands (ε_p). The loss of prestress due to elastic shortening may then be calculated on the basis of the strand modulus of elasticity (E_p); refer to Equation (2.2).

$$\varepsilon_c = \frac{f_{cgp}}{E_{ci}} = \varepsilon_p \tag{2.1}$$

$$\Delta f_{pES} = E_p \varepsilon_p = \frac{E_p}{E_{ci}} f_{cgp} \tag{2.2}$$

2.2.2 Prestress Loss Due to Creep and Shrinkage

Prestress loss due to creep is primarily dependent on the stiffness of the concrete, which varies with concrete strength and aggregate type, and on the magnitude of the stress sustained on the concrete. Prestress loss due to shrinkage is heavily dependent on the material properties of the concrete (i.e. concrete stiffness, concrete strength, aggregate type and quantity, paste content, etc.). A brief discussion of the mechanisms that cause both creep and shrinkage is provided in this section. The mechanisms are introduced to provide the reader with a general understanding of both creep and shrinkage as they are two of the most influential and least agreed upon components of prestress loss.

Concrete creep may be more accurately identified as basic creep and drying creep. Basic creep is the long-term shortening of the concrete member under the effect of external stresses imposed on the girder at constant moisture content with no moisture migration to the environment. Drying creep is the shortening that occurs in a specimen exposed to the environment and allowed to dry. The total creep that a specimen undergoes is primarily a combination of basic and drying creep. The various creep theories are debated because the mechanism of creep is not as well understood as that of shrinkage. The factors effecting creep behavior are summarized in Table 2.1. Similar to elastic shortening and shrinkage, creep is largely dependent on the modulus of elasticity of the concrete. This dependency on modulus means that creep is largely influenced by the aggregate quantity and stiffness. The magnitude of the load placed on the concrete is also important; the larger the magnitude of load placed on the concrete, the larger the creep.

Conventionally, concrete shrinkage is classified according to the conditions under which it is observed. This classification usually includes four types of shrinkage: thermal, autogenous, drying, and carbonation shrinkage:

- *Thermal shrinkage* is generated by the cooling of concrete mainly during the first hours after set.
- *Autogenous shrinkage* is defined as the (non-thermal) shortening, primarily caused by water loss, observed in concrete under no transfer of moisture from or to the environment.
- *Drying shrinkage* is due to migration of water from the concrete to the environment.
- *Carbonation shrinkage* is initiated by chemical changes that take place when carbon dioxide reacts with the calcium in the cement paste.

Drying and the autogenous shrinkage make up the largest fraction of total shrinkage. Drying shrinkage is especially relevant in concretes with high permeability, high water-to-cement ratios and exposed to low relative humidity environments. In the opposite case, autogenous shrinkage makes up the largest fraction of total shrinkage. In short, the loss of water from the concrete system (into the atmosphere or through further cement hydration) is the main cause of concrete shrinkage.

Shrinkage is mainly affected by the paste content of the concrete; higher paste content will result in higher shrinkage. Because the paste content is the most influential factor, anything that decreases paste content (e.g. greater quantity of aggregate, larger maximum aggregate size, less water, etc.) while other parameters are kept constant will result in lower shrinkage. An aggregate with a high modulus of elasticity will also result in less shrinkage, as the aggregate stiffness will resist shrinkage-induced stresses.

Table 2.1 – Main factors influencing shrinkage and creep behavior (Italics emphasizes importance)

	Drying Shrinkage	**Creep**
Mixture Effects	- Size/grading of aggregate - *Water-to-cement ratio* - *Aggregate properties* - Cement characteristics - Admixtures	- *Quantity of aggregate* - Size/grading of aggregate - *Water-to-cement ratio* - *Aggregate properties* - Admixtures
Environment Effects	- Relative humidity - Temperature	- Relative humidity - Temperature
Design and Construction Effects	- Period of curing - Type of curing - Specimen size and shape	- *Load magnitude and duration* - Period of curing - Type of curing - Specimen size and shape

2.2.3 Prestress Loss Due to Relaxation

Intrinsic strand relaxation is the phenomenon in which the stress in a strand will decrease over time if the strand is held at a constant strain. In general, relaxation loss will be larger with a larger initial stress and at higher temperatures. Although high temperatures (above 130°F) will greatly increase the relaxation loss for a strand under a small initial stress, there will be no temperature effect when a large stress is applied (Magura 1964). The other influential variable in relaxation magnitude is the type of prestressing tendon. Low-relaxation prestressing strands undergo considerably less relaxation than stress-relieved strands, and are almost exclusively used today.

The generally accepted, empirically derived expression used for strand relaxation of a prestressing strand being held at a constant strain, presented in Equation (2.3), was first developed by Magura et al. in 1964. Similar expressions have been used to model relaxation where strains remain near constant (i.e. prior to transfer). After transfer occurs, the strand strain will change due to the other types of prestress loss. Various modifications to this expression have been proposed to account for the strain change in the strands.

$$\Delta f_{pR} = \frac{f_{pi}}{45}\left(\frac{f_{pi}}{f_{py}} - 0.55\right)\log\left(\frac{24t_2 + 1}{24t_1 + 1}\right) \qquad (2.3)$$

Where:

f_{pi} = initial prestress stress, typically 75% of ultimate strength (ksi)
f_{py} = yield stress of strand, typically 90% of ultimate strength (ksi)
t_1 = age of concrete at the beginning of the period (days)
t_2 = age of concrete at the end of the period (days)

2.3 ESTIMATION OF PRESTRESS LOSS

The estimation of prestress loss generally depends on the magnitude of concrete stresses and strains at the level of the prestressing. This magnitude of concrete stress and strain, estimated at the centroid of the prestressing steel, changes due to elastic shortening, creep, and shrinkage. When estimating these stresses, material properties and modular ratios are required and are influential. In addition to the loss caused by stress changes in the concrete, an expression is also used to estimate the prestress loss due to strand relaxation. The losses that occur instantaneously (e.g. elastic shortening) are generally calculated separately from those that occur over time (e.g. creep, shrinkage and strand relaxation).

The prestress loss provisions of the 2004 and 2012 AASHTO LRFD Bridge Design Specifications are presented and briefly discussed in the following sections. The provision of AASHTO LRFD 2004 is the current standard for prestress loss estimation at TxDOT. There have been relatively few issues with girders in the field designed using this specification. The procedure found in AASHTO LRFD 2012 is being investigated to assess its merit as the new standard. There are currently a small number of field implementations of AASHTO LRFD 2012 in Texas.

There are several differences between the two procedures that will be first introduced. The expressions presented in the AASHTO LRFD 2004 specification are simple, empirically derived expressions that are based on normal strength concrete (f'$_{ci}$ less than 6 ksi). In AASHTO

LRFD 2005, a more theoretically based procedure was introduced that greatly increased the complexity of the expressions. In addition to the improved theoretical accuracy of the procedure, the materials expressions were calibrated for specimens with high strength concrete (f'$_{ci}$ greater than 6 ksi).

The provisions are presented as they are found in the specification; specifically, the calculations are divided into the estimation of short-term (elastic shortening) and long-term loss components. All expressions taken from the specification body and commentary are accompanied by their corresponding equation number and/or the relevant section heading. The performance of the Specifications will not be analyzed here; a comparison of the two approaches within the context of an experimental database is provided in Section 2.4.

2.3.1 AASHTO LRFD 2004

The prestress loss provisions found in the 2004 AASHTO LRFD Bridge Design Specification were introduced in the 1977 standards and have remained virtually unchanged (Tadros 2003). The total loss expression is separated into the short- and long-term components previously discussed, shown in Equation (2.4). The prestress loss consists of elastic shortening loss (Δf_{pES}), shrinkage loss (Δf_{pSR}), creep loss (Δf_{pCR}), and steel relaxation loss (Δf_{pR2}). The prestress losses estimated using this procedure are full-term, design-life losses; there is no time dependency.

(2.4)
$$\Delta f_{pT} = \Delta f_{pES} + \Delta f_{pSR} + \Delta f_{pCR} + \Delta f_{pR2}$$

AASHTO 04 (5.9.5.1-1)

Where:

Δf_{pES} = sum of all losses or gains due to elastic shortening or extension at the time of application (ksi)

Δf_{pCR} = prestress loss due to creep (ksi)

Δf_{pSR} = prestress loss due to shrinkage (ksi)

Δf_{pR2} = prestress loss due to relaxation of steel after transfer (ksi)

2.3.1.1 Elastic Shortening

The elastic shortening expression in AASHTO LRFD 2004 is here replicated as Equation (2.5); this expression is equivalent to Equation (2.2). The concrete stress at the centroid of the prestressing strands (f_{cgp}) may be directly calculated by assuming that the stress in the prestressing strands immediately after transfer will be $0.7 f_{pu}$, as shown in Equation (2.7).

$$\Delta f_{pES} = \frac{E_p}{E_{ci}} f_{cgp} \qquad (2.5)$$

Where:

E_p = modulus of prestressing tendons (ksi)
E_{ci} = modulus of concrete at time of release (ksi)

$$E_{ci} = 33,000w_c{}^{1.5}\sqrt{f'_{ci}} \qquad (2.6)$$

w_c = unit weight of the concrete (kcf)
f'_{ci} = compressive strength at release (ksi)
f_{cgp} = concrete stress at center of gravity of prestressing steel at transfer (ksi)

$$f_{cgp} = 0.7 f_{pu} A_{ps} \left(\frac{1}{A_g} + \frac{e_p{}^2}{I_g} \right) - \frac{M_g e_p}{I_g} \qquad (2.7)$$

f_{pu} = ultimate strength of p/s strand (ksi)
A_{ps} = total p/s strand area (in.^{2})
A_g = area of gross section (in.^{2})
I_g = moment of inertia of gross section (in.^{4})
e_p = eccentricity of prestressing tendons (in)
M_g = dead load moment (in-kips)

Alternatively, the prestress loss due to elastic shortening may be calculated directly using Equation (2.8). This approximate expression, taken from the code commentary (AASHTO LRFD 2004 §C5.9.5.2.3a), was derived using transformed section properties and a few minor approximations.

$$\Delta f_{pES} = \frac{A_{ps} f_{pbt} \left(I_g + e_m{}^2 A_g \right) - e_m M_g A_g}{A_{ps} \left(I_g + e_m{}^2 A_g \right) + \dfrac{A_g I_g E_{ci}}{E_p}} \qquad (2.8)$$

Where:

f_{pbt} = stress in prestressing steel immediately prior to transfer (ksi)
       = *0.75f_{pu}* (for low-relaxation strands)
e_m = average prestressing steel eccentricity at midspan (in)

2.3.1.2 Creep and Shrinkage

The expression used to estimate the prestress loss due to creep is presented in Equation (2.9). The calculated creep loss is dependent on the stress at the center of gravity of the prestressing strands due to prestressing force and self-weight (f_{cgp}), presented in Equation (2.7), and due to deck placement and superimposed dead load (Δf_{cdp}), presented in Equation (2.10).

The constants in front of each of these terms in Equation (2.9) are empirically derived and related to the modular ratio and creep coefficients. Evaluation of the AASHTO LRFD 2004 creep expression through the use of the TxDOT Project 0-6374 prestress loss database revealed that the constants were calibrated for conservatism. Details of the evaluation can be found in Appendix C.

$$\Delta f_{pCR} = 12.0 f_{cgp} - 7.0 \Delta f_{cdp} \geq 0$$

<div align="right">(2.9)</div>

<div align="right">*AASHTO 04 (5.9.5.4.3-1)*</div>

Where:

f_{cgp} = concrete stress at center of gravity of prestressing steel at transfer (ksi), same as used in Elastic Shortening

Δf_{cdp} = change in concrete stress at center of gravity of prestressing steel due to permanent loads, with the exception of the load acting at the time the prestressing force is applied. Values of Δf_{cdp} should be calculated at the same section or at sections for which f_{cgp} is calculated (ksi)

$$\Delta f_{cdp} = \frac{M_{sd} e_p}{I_g}$$

<div align="right">(2.10)</div>

M_{sd} = superimposed dead load moment (in-kips)

The expression used to calculate prestress loss due to shrinkage of the girder concrete through the entire life of the girder is presented in Equation (2.11). Shrinkage loss, which is a product of shrinkage strain and the modular ratio, was simplified empirically to the following expression, which only varies with the average relative humidity of the location where the girder will be placed.

$$\Delta f_{pSR} = (17.0 - 0.150H)$$

<div align="right">(2.11)</div>

<div align="right">*AASHTO 04 (5.9.5.4.2-1)*</div>

Where:

H = average relative humidity (%)

2.3.1.3 Strand Relaxation

The estimation of prestress losses due to strand relaxation is separated into two time periods within AASHTO LRFD 2004: (1) prior to prestress transfer and (2) after prestress transfer.

Prior to prestress transfer, the strain in the prestressing strands remains nearly constant and the expression developed by Magura et al. (1964) may be applied as presented in Equation (2.12). It is stated in the code that this loss is generally accounted for by the fabricator. This allows the fabricator to overstress the strands to compensate for the relaxation losses occurring between strand stressing and prestress transfer. The relaxation loss invoked by Equation (2.4)

and presented in Equation (2.13), occurs after transfer. Given the varying state of strain (generally declining) within the prestressing strand, relaxation must be accounted for through an empirically derived expression that accounts for the effects of elastic shortening and ongoing shrinkage and creep. The expression, as shown in Equation (2.13), is calibrated for stress-relieved strands; for low relaxation strands, the relaxation loss can be taken as 30% of the loss calculated from the shown expression, using the variable K.

$$\Delta f_{pR1} = \frac{\log(24.0t)}{10.0}\left[\frac{f_{pbt}}{f_{py}} - 0.55\right] f_{pj}$$

<div align="right">(2.12)

AASHTO 04 (5.9.5.4.4b-2)</div>

Where:

t = time estimated in days from stressing to transfer (days)
f_{py} = specified yield strength of prestressing steel (ksi)

$$\Delta f_{pR2} = K\left[20.0 - 0.3\Delta f_{pES} - 0.2\left(\Delta f_{pSR} + \Delta f_{pCR}\right)\right]$$

<div align="right">(2.13)

AASHTO 04 (5.9.5.4.4c-1)
(Modified)</div>

Where:

K = 1 for stress-relieved strands and 0.3 for low-relaxation strands

2.3.2 AASHTO LRFD 2012

Research completed during the course of NCHRP Project D18-07 was summarized by Tadros et al. within NCHRP Report 496, "Prestress Losses in Pretensioned High-Strength Concrete Bridge Girders." The purpose of the research was to improve the accuracy of the prestress loss estimations provided by the AASHTO LRFD Bridge Design Specifications. Tadros et al. intended to improve accuracy by combining a theoretical understanding of the girder behavior with empirically accurate expressions for the material properties. Previously available expressions for prestress loss were calibrated using data from tests with concrete compressive strengths less than 6 ksi. In order to observe the effect of high strength concrete, creep, shrinkage, strength and modulus of elasticity tests on 16 different high strength concrete mix design from four different states were completed by Tadros et al. New material property expressions were derived on the basis of the new test results.

Along with the material testing, seven girders placed in bridges in four states were instrumented with vibrating wire gages to measure prestress losses. Expressions for prestress loss were theoretically derived and compared with the measured prestress losses from this research project as well as results from 31 previously reported experiments.

The material property expressions and prestress loss procedure proposed in NCHRP 496 were adopted into the 2005 AASHTO LRFD Bridge Design Specifications. A few minor modifications and simplifications were made to the expressions and procedure prior to implementation in the bridge specification.

The total prestress loss estimated in AASHTO LRFD 2012 is separated into short- and long-term components, shown in Equation (2.14).

$$\Delta f_{pT} = \Delta f_{pES} + \Delta f_{pLT}$$

(2.14)

AASHTO (5.9.5.1-1)

The long-term prestress loss expression provided in AASHTO LRFD 2012 is presented in Equation (2.15). Four different behaviors (girder creep, girder shrinkage, strand relaxation and deck shrinkage) are accounted for over two separate time spans (transfer to deck placement and deck placement to final time). This separation was made in order to account for the effects of composite action after deck placement. The time span separation is also the main complication in the AASHTO LRFD 2012 procedure versus that found in AASHTO LRFD 2004.

$$\Delta f_{pLT} = \left(\Delta f_{pSR} + \Delta f_{pCR} + \Delta f_{pR1}\right)_{id} + \left(\Delta f_{pSD} + \Delta f_{pCD} + \Delta f_{pR2} - \Delta f_{pSS}\right)_{df}$$

(2.15)

AASHTO 12 (5.9.5.4.1-1)

Where:

$\left(\Delta f_{pSR} + \Delta f_{pCR} + \Delta f_{pR1}\right)_{id}$
   = sum of time-dependent prestress losses between transfer and deck placement (ksi)

$\left(\Delta f_{pSD} + \Delta f_{pCD} + \Delta f_{pR2} - \Delta f_{pSS}\right)_{df}$
   = sum of time-dependent prestress losses after deck placement (ksi)

Δf_{pSR} = prestress loss due to shrinkage of girder concrete between transfer and deck placement (ksi)

Δf_{pCR} = prestress loss due to creep of girder concrete between transfer and deck placement (ksi)

Δf_{pR1} = prestress loss due to relaxation of prestressing strands between time of transfer and deck placement (ksi)

Δf_{pR2} = prestress loss due to relaxation of prestressing strands between deck placement and final time (ksi)

Δf_{pSD} = prestress loss due to shrinkage of girder concrete between time of deck placement and final time (ksi)

Δf_{pCD} = prestress loss due to creep of girder concrete between time of deck placement and final time (ksi)

Δf_{pSS} = prestress gain due to shrinkage of deck in composite section (ksi)

Some derivations and graphical representations of the expressions are provided in this section for the benefit of the reader.

2.3.2.1 Elastic Shortening

The elastic shortening loss expression presented in the body of AASHTO LRFD 2012 is shown in Equation (2.16). Rather than utilizing an approximation of the stress present immediately after transfer, the expression and accompanying commentary requires that the stress be solved for exactly. The procedure to calculate the prestress force after release is summarized in the specification in §C5.9.5.2.3 as follows:

> *For the combined effects of initial prestress and member weight, an initial estimate of prestress after transfer is used. The prestress may be assumed to be 90 percent of the initial prestress before transfer and* **the analysis iterated until acceptable accuracy is achieved**.

The iterative process is outlined in Figure 2.4. The beam is placed under an initial, assumed, prestress force and the stress in the concrete at the centroid of the prestressing strands due to this prestress force and member self-weight are calculated ($f_{cgp,1}$). The stress that is lost in the strands is subtracted out of the assumed initial prestress force, giving $f_{p,1}$. This stress is then applied onto the section and the stresses in the concrete at the centroid of the prestressing strands is recalculated ($f_{cgp,2}$). This procedure is repeated until $f_{cgp,n}$ converges, which is accomplished, to a satisfactory degree, after three or four iterations. The convergence of the stress shows the system in equilibrium prior to any long-term prestress losses or additional external loads.

There is a paragraph included within §C5.9.5.2.3a allowing for elastic shortening loss to be "implicitly accounted for" when transformed section properties are used to calculate concrete stresses (f_{cgp}). This concrete stress can then be used to calculate the creep loss and relaxation loss. The inconvenience with this approach is the strand area is required for calculation of the transformed section properties, meaning that each time loss is calculated transformed section properties need to be recalculated.

$$\Delta f_{pES} = \frac{E_p}{E_{ci}} f_{cgp}$$

(2.16)

AASHTO 12 (5.9.5.2.3a-1)

Where:
E_p = modulus of prestressing tendons (ksi)
E_{ci} = modulus of concrete at time of release (ksi)

(2.17)

$$E_{ci} = 33{,}000 K_1 w_c^{1.5} \sqrt{f'_{ci}}$$

AASHTO 12 (5.4.2.4-1)

w_c = unit weight of the concrete (kcf)
f'_{ci} = compressive strength at release (ksi)
f_{cgp} = the concrete stress at center of gravity of prestressing tendons due to the prestressing force **immediately after transfer** and the self-weight of the member at the section of maximum moment (ksi)

K_1 = correction factor for source of aggregate, to be taken as 1.0 unless determined by physical test and properly approved

Iteration 1

$$f_{cgp,1} = f_{pi}A_{ps}\left(\frac{1}{A_g}+\frac{e_p^2}{I_g}\right) - \frac{M_{SW}e_p}{I_g}$$

$$f_{p,1} = f_{pi} - f_{cgp,1}\frac{E_p}{E_{ci}}$$

(arrow →) ... *(arrow ←)* f_{pi}

Iteration 2

$$f_{cgp,2} = f_{p,1}A_{ps}\left(\frac{1}{A_g}+\frac{e_p^2}{I_g}\right) - \frac{M_{SW}e_p}{I_g}$$

$$f_{p,2} = f_{pi} - f_{cgp,2}\frac{E_p}{E_{ci}}$$

(arrow ←) $f_{p,1}$

Iteration n

$$f_{cgp,n} = f_{p,n-1}A_{ps}\left(\frac{1}{A_g}+\frac{e_p^2}{I_g}\right) - \frac{M_{SW}e_p}{I_g}$$

$$f_{p,n} = f_{pi} - f_{cgp,n}\frac{E_p}{E_{ci}}$$

(arrow ←) $f_{p,n-1}$
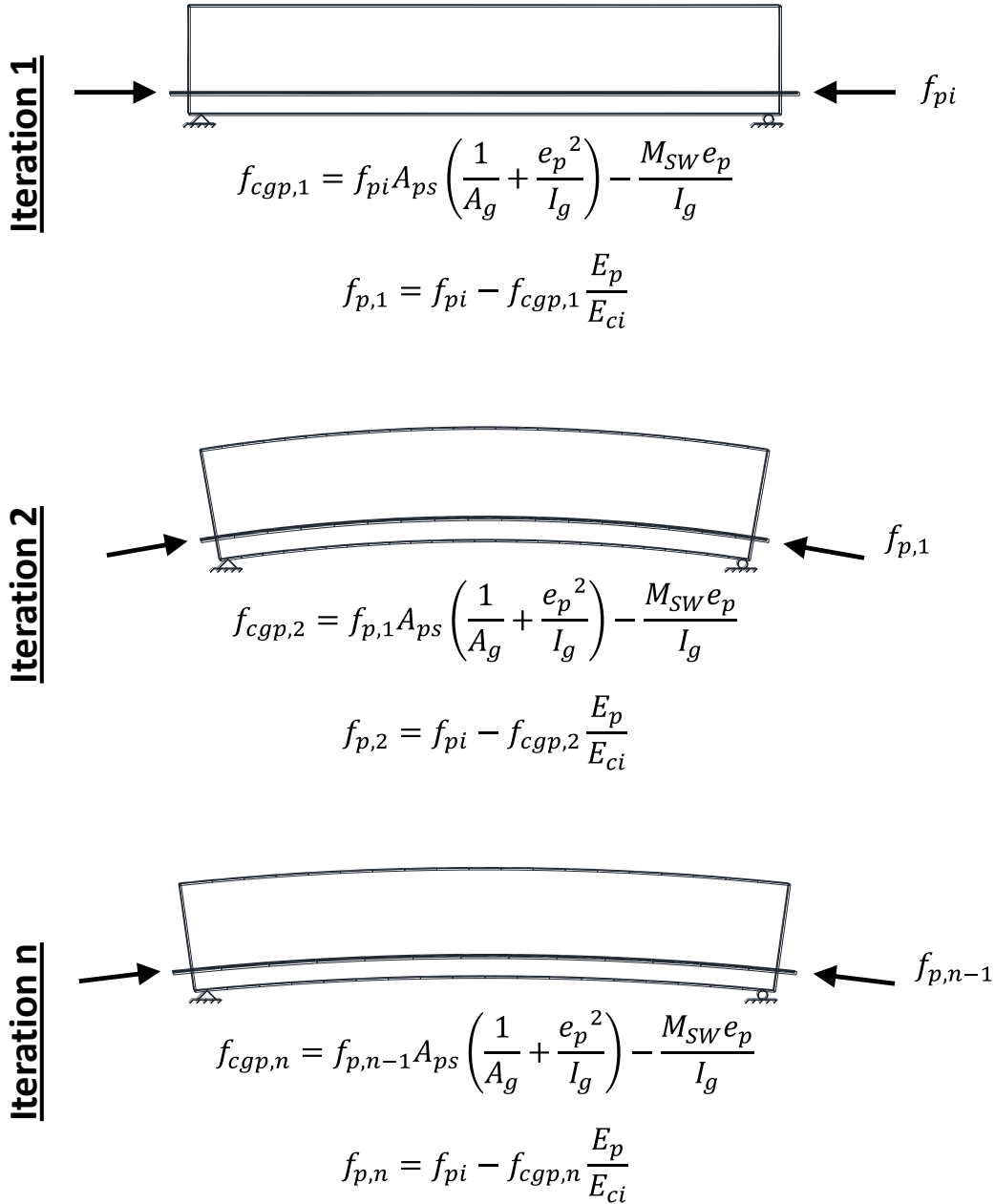
Figure 2.4 – AASHTO LRFD 2012 Bridge Specification Elastic Shortening Iterative Procedure

The influence of source aggregate stiffness and quantity on the elastic shortening (and long-term losses) may be accounted for through the use of the modulus of elasticity, presented in Equation (2.18). The only difference in this expression versus the modulus used in previous specifications is the introduction of the correction factor (K_1). The correction factor, presented in Equation (2.19), allows a designer to use a measured modulus of elasticity rather than the

calculated modulus. It allows designers to adjust the elastic modulus for aggregates of different stiffness and other material factors. The correction factor is to be taken as 1.0 unless it is determined otherwise by physical testing.

$$E_c = 33,000K_1 w_c{}^{1.5}\sqrt{f'_c}$$

(2.18)

AASHTO 12 (5.4.2.4-1)

Where:

K_1 = correction factor for source aggregate, to be taken as 1.0 unless determined by physical test and properly approved

$$K_1 = \frac{E_{c,measured}}{E_c}$$

(2.19)

w_c = unit weight of concrete, not more than 0.155 kcf
f'_c = strength of concrete at time in question (ksi)

AASHTO LRFD 2012 commentary allows for an alternate elastic shortening equation to be used to avoid iteration altogether. The alternate equation is presented in Equation (2.8) above and is taken from AASHTO LRFD 2004.

2.3.2.2 Creep and Shrinkage

Compared to the expressions for creep and shrinkage prestress loss found in AASHTO LRFD 2004, the expressions found in the AASHTO LRFD 2012 procedure are much more complicated. When the prestress loss procedure found in AASHTO LRFD 2012 was implemented, a new set of expressions to model the material properties and behavior were also introduced. Both the update to the material properties section and the prestress loss section were the result of research conducted by Tadros et al. (2003).

The general approach to account for creep and shrinkage includes (1) calculation of the material dependent coefficients, (2) use of these material coefficients in the calculation of the creep and shrinkage strain, and (3) converting these girder strains to prestress loss through the use of the modular ratio. Tadros et al. also accounted for the time-dependent interaction of the concrete and steel through the use of transformed section coefficients (K_{id} before deck placement and K_{df} after deck placement).

2.3.2.2.1 Material Properties Expressions

The shrinkage and creep expressions presented in the AASHTO LRFD 2012 materials properties section (Article 5.4) were developed specifically for use with the prestress loss procedure. These equations are not "expected to yield results with errors less than ±50 percent" without the physical testing or prior experience with the material (AASHTO LRFD 2012 §C5.4.2.3.1). The rationale for implemented such a complex procedure in the context of such high variability will be scrutinized in Chapter 6. The expression that accounts for the shrinkage strain (ε_{sh}) is presented in Equation (2.20). All of the material factors used in the shrinkage strain

expression are found in Table 2.2. From the discussion in Section 2.2.2, it can be seen that these expressions account for three of the major variables that are traditionally assumed to affect drying shrinkage (concrete strength, relative humidity and specimen size and shape). If the equations are calibrated properly, they should provide greater sensitivity than the expression provided in AASHTO LRFD 2004, which only accounts for changes in relative humidity.

Table 2.2 – Material factors found in AASHTO LRFD 2012 §5.4.2.3

Influential Factor	Shrinkage Expression	Creep Expression
Humidity (**H**)	$k_{hs} = 2.0 - 0.014H$ *AASHTO 12 (5.4.2.3.3-2)*	$k_{hc} = 1.56 - 0.008H$ *AASHTO 12 (5.4.2.3.2-3)*
Volume-to-surface ratio (**V/S**)	$k_s = 1.45 - 0.13(V/S)$ *AASHTO 12 (5.4.2.3.2-2)*	
Concrete Release Strength (**f'**_{ci})	$k_f = \dfrac{5}{1 + f'_{ci}}$ *AASHTO 12 (5.4.2.3.2-4)*	
Time (**t**)	$k_{td} = \dfrac{t}{61 - 4f'_{ci} + t}$ *AASHTO 12 (5.4.2.3.2-5)*	

$$\varepsilon_{sh} = k_s k_{hs} k_f k_{td} 0.48 * 10^{-3}$$

(2.20)

AASHTO 12 (5.4.2.3.3-1)

Where:

k_{hs} = humidity factor for shrinkage
k_s = factor for the effect of the volume-to-surface ratio of the component
k_f = factor for the effect of concrete strength
k_{td} = time development factor
t = age of concrete after loading (days)
H = average relative humidity (%)
V/S = volume to surface ratio (in)

The expression used to calculate the creep coefficient (ψ) in AASHTO LRFD 2012 is presented in Equation (2.21). This expression is affected by the same factors as shrinkage but is also dependent on the age of the concrete when the load is applied. When the factors included in the expression are compared with those listed within Table 2.1, it can be seen that the aggregate information is the only important factor not taken into account. As with shrinkage strain, this would suggest the creep coefficient expression should yield a more sensitive prestress loss estimate.

$$\psi(t, t_i) = 1.9 k_{vs} k_{hc} k_f k_{td} t_i^{-0.118}$$

(2.21)

AASHTO 12 (5.4.2.3.2-1)

Where:

k_{hc} = humidity factor for creep
t_i = age of concrete when load is applied (days)

2.3.2.2.2 Concrete and Steel Interaction

The time-dependent strains are applied at the centroid of the pretensioned girder, as shown for shrinkage in Figure 2.5. If the girder was a non-prestressed, reinforced concrete beam, it would undergo the shrinkage strain shown in Figure 2.5 (b). In a beam where prestressing is present, it is assumed that the strands restrain the shrinkage of the concrete, shown in Figure 2.5 (c).
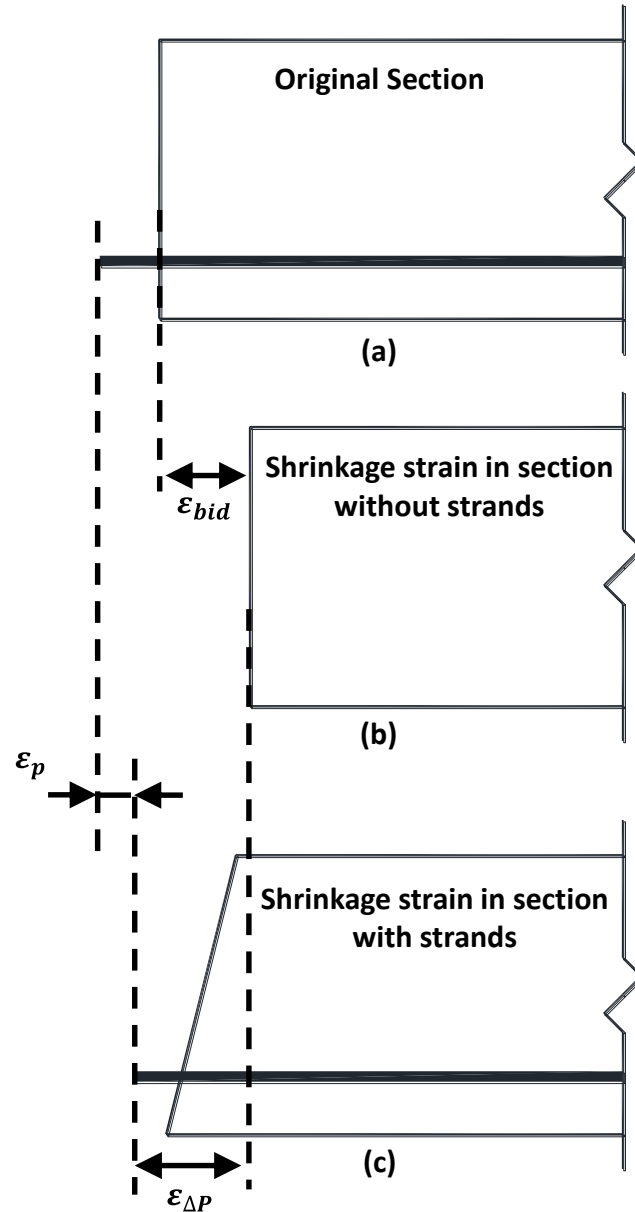
Figure 2.5 – Assumed effect of shrinkage strain on concrete girder for K_{id} derivation; (a) original section, (b) shrinkage strain in section without strands, and (c) shrinkage strain restrained by prestressing strands

This behavior is accounted for in AASHTO LRFD 2012 using transformed section coefficients (K_{id} and K_{df}), which account for the time-dependent interaction between the concrete and bonded steel in the section being considered. There is one coefficient for the time period between transfer and deck placement (K_{id}) and one for the time period between deck placement and final time (K_{df}). These coefficients are derived from enforcement of compatibility between the prestressing tendons and the surrounding concrete. The derivation of the expression for the prestress loss due to girder shrinkage is shown in Table 2.3.

Table 2.3 – Derivation of AASHTO LRFD 2012 shrinkage loss expression

Enforce Compatibility	$\Delta\varepsilon_p = \Delta\varepsilon_c$
- Strains from Figure 2.5	$\varepsilon_p = \varepsilon_{bid} - \varepsilon_{\Delta P}$
- Substitute in strain values	$\dfrac{\Delta P_p}{A_{ps}E_p} = \varepsilon_{bid} - \left(\dfrac{\Delta P_p}{E''_{ci}A_g} + \dfrac{\Delta P_p}{E''_{ci}}\dfrac{e_{pg}{}^2}{I_g}\right)$
- Simplify	$\dfrac{\Delta P_p}{A_{ps}}\left[1 + \dfrac{E_p}{E''_{ci}}\dfrac{A_{ps}}{A_g}\left(1 + \dfrac{A_g e_{pg}{}^2}{I_g}\right)\right] = \varepsilon_{bid}E_p$
- Define E''_{ci}	$E''_{ci} = \dfrac{E_{ci}}{\left(1 + \chi\psi_b(t_f, t_i)\right)}$
- Define K_{id}	$K_{id} = \dfrac{1}{\left[1 + \dfrac{E_p}{E_{ci}}\dfrac{A_{ps}}{A_g}\left(1 + \dfrac{A_g e_{pg}{}^2}{I_g}\right)\left(1 + \chi\psi_b(t_f, t_i)\right)\right]}$
- Substitute K_{id} into expression	$\Delta f_{pSR} = \dfrac{\Delta P_p}{A_{ps}} = \varepsilon_{bid}K_{id}E_p$

Where:

ε_p = strain in prestressing strand caused by concrete shrinkage

$\varepsilon_{\Delta P}$ = strain in concrete due to the resistance provided by the prestressing strands

E''_{ci} = age-adjusted effective modulus of elasticity of concrete (ksi)

χ = aging coefficient that accounts for concrete stress variability with time and may be considered constant for all concrete members at age 1 to 3 days = 0.7

ΔP_p = change in force in the prestressing strands due to concrete shrinkage (kips)

ε_{bid} = concrete shrinkage strain of girder between the time of transfer and deck placement per Eq. 5.4.2.3.3-1 (Equation (2.20))

The prestressing steel is assumed to also provide some restraint against the creep of the concrete. The derivation of the creep expression including the transformed section coefficient is shown in Table 2.4; this derivation is similar to that for shrinkage loss.

Table 2.4 – Derivation of AASHTO LRFD 2012 girder creep loss expression

Enforce Compatibility	$\Delta\varepsilon_p = \Delta\varepsilon_c$
- Strains similar to those from Figure 2.5	$\varepsilon_p = \varepsilon_{cr} - \varepsilon_{\Delta P}$
- Substitute in strain values	$\dfrac{\Delta P_p}{A_{ps}E_p} = \dfrac{f_{cgp}}{E'_{ci}} - \left(\dfrac{\Delta P_p}{E''_{ci}A_g} + \dfrac{\Delta P_p}{E''_{ci}}\dfrac{e_{pg}^2}{I_g}\right)$
- Simplify	$\dfrac{\Delta P_p}{A_{ps}}\left[1 + \dfrac{E_p}{E''_{ci}}\dfrac{A_{ps}}{A_g}\left(1 + \dfrac{A_g e_{pg}^2}{I_g}\right)\right] = \left(\dfrac{f_{cgp}}{E'_{ci}}\right)E_p$
- Define E'_{ci}	$E'_{ci} = \dfrac{E_{ci}}{\psi_b(t_d, t_i)}$
- Definition of E''_{ci} from shrinkage derivation	$E''_{ci} = \dfrac{E_{ci}}{\left(1 + \chi\psi_b(t_f, t_i)\right)}$
- Definition of K$_{id}$ from shrinkage derivation	$K_{id} = \dfrac{1}{\left[1 + \dfrac{E_p}{E_{ci}}\dfrac{A_{ps}}{A_g}\left(1 + \dfrac{A_g e_{pg}^2}{I_g}\right)\left(1 + \chi\psi_b(t_f, t_i)\right)\right]}$
- Substitute K$_{id}$ and E'_{ci} into expression	$\Delta f_{pCR} = \dfrac{\Delta P_p}{A_{ps}} = \dfrac{E_p}{E_{ci}}f_{cgp}K_{id}\psi_b(t_d, t_i)$

The age-adjusted effective modulus of elasticity (E''_{ci}) is used in the derivation of the transformed section coefficients. Because concrete ages and gains strength over time, the modulus would need to be calculated in small time intervals in order for the effective modulus to be calculated in a theoretically exact manner. The aging coefficient (χ) was introduced by Bažant (1972) in order to allow for the effective modulus to be calculated in one step. Tadros (2003) assumes the aging coefficient to be 0.7. While this is a reasonable assumption for concrete loaded at an early age (1 to 3 days), concrete loaded at a later age has an aging coefficient closer

to 0.9. This does not theoretically affect the before deck placement losses, but does raise a question regarding the appropriateness of the after deck placement coefficient (K_{df}).

2.3.2.2.3 Long-Term Losses: From Release to Deck Placement

Now that the interactions between the steel and the concrete, and the age-adjusted effective modulus have been discussed, the estimation of the prestress loss due to shrinkage and creep of the girder concrete will be outlined. The creep and shrinkage loss are divided into before and after deck placement losses; the former being introduced here.

The prestress loss caused by the shrinkage of the girder concrete (Δf_{pSR}) is presented in Equation (2.22). Within this expression are the concrete shrinkage strain (ε_{bid}) and the transformed section coefficient (K_{id}), both discussed above and shown in Equations (2.20) and (2.23), respectively.

$$\Delta f_{pSR} = \varepsilon_{bid} K_{id} E_p$$

<div align="right">

(2.22)

AASHTO 12 (5.9.5.4.2a-1)
</div>

Where:

ε_{bid} = concrete shrinkage strain of girder between the time of transfer and deck placement

K_{id} = transformed section coefficient that accounts for time-dependent interaction between concrete and bonded steel in the section being considered for time period between transfer and deck placement

$$K_{id} = \frac{1}{1 + \dfrac{E_p}{E_{ci}} \dfrac{A_{ps}}{A_g} \left(1 + \dfrac{A_g e_{pg}^2}{I_g}\right) \left(1 + 0.7\psi_b(t_f, t_i)\right)}$$

<div align="right">

(2.23)

AASHTO 12 (5.9.5.4.2a-2)
</div>

e_{pg} = eccentricity of prestressing force with respect to centroid of girder (in.); positive in common construction where it is below girder centroid

$\psi_b(t_f, t_i)$ = girder creep coefficient at final time due to loading introduced at transfer

t_f = final age (days)

t_i = age at transfer (days)

A_{ps} = area of prestressing steel (in.^{2})

A_g = gross area of section (in.^{2})

E_{ci} = modulus of elasticity of concrete at transfer (ksi)

E_p = modulus of elasticity of prestressing tendons (ksi)

I_g = moment of inertia of the gross concrete section (in.^{4})

The expression used to account for the prestress loss due to the long-term shortening of the girder caused by the prestressing force, or girder creep loss, is presented in Equation (2.24). The creep loss expression is dependent on the concrete stress at the center of gravity of the prestressing tendons (f_{cgp}). This stress is the same as that calculated for elastic shortening via the

iterative procedure of Section 2.3.2.1. The creep coefficient is taken from time of transfer until deck placement.

$$\Delta f_{pCR} = \frac{E_p}{E_{ci}} f_{cgp} K_{id} \psi_b(t_d, t_i) \qquad \textbf{(2.24)}$$

AASHTO 12 (5.9.5.4.2b-1)

Where:

f_{cgp} = the concrete stress at center of gravity of prestressing tendons due to the prestressing force immediately after transfer and the self-weight of the member at the section of maximum moment (ksi); same as calculated for Elastic Shortening

$\psi_b(t_d,t_i)$= girder creep coefficient at time of deck placement due to loading introduced at transfer

t_d = age of concrete at time of deck placement (days)

2.3.2.2.4 Long-Term Losses: From Deck Placement to Final Time

Within the AASHTO LRFD 2012 prestress loss procedure, prestress loss due to the shrinkage of girder concrete, creep of concrete, and shrinkage of deck concrete after deck placement are accounted for separately from prestress loss occurring prior to deck placement. In theory, this separation should result in a more accurate behavioral model of the system than accounting for the loss all in one step. In reality, due to the variation associated with the design and fabrication of the deck as well as difficulty in accurately modeling the actual behavior of the system, this separation results in a more complicated procedure with lower conservatism and increased variability.

Within the AASHTO LRFD 2012 prestress loss procedure, the prestress loss due to the shrinkage of the girder concrete from the time of deck placement to final time is presented in Equation (2.25). This expression is the continuation of the before deck placement shrinkage loss expression (2.22) and has the same derivation, shown in Table 2.3.

Within this shrinkage loss expression there is the transformed section coefficient (K_{df}), presented in Equation (2.26). The only difference between the transformed section coefficient from before deck placement (K_{id}) and after deck placement (K_{df}) is the use of composite sections when calculating the after deck placement coefficient. The use of composite sections yields an after deck placement coefficient slightly higher than the before deck placement coefficient.

$$\textbf{(2.25)}$$
$$\Delta f_{pSD} = \varepsilon_{bdf} K_{df} E_p$$

AASHTO 12 (5.9.5.4.3a-1)

Where:

ε_{bdf} = shrinkage strain of girder between time of deck placement and final time

K_{df} = transformed section coefficient that accounts for time-dependent interaction between concrete and bonded steel in the section being considered for time period between deck placement and final time

$$K_{df} = \cfrac{1}{1 + \cfrac{E_p}{E_{ci}}\cfrac{A_{ps}}{A_c}\left(1 + \cfrac{A_c e_{pc}{}^2}{I_c}\right)\left(1 + 0.7\psi_b(t_f, t_i)\right)} \qquad \text{(2.26)}$$

AASHTO 12 (5.9.5.4.3a-2)

e_{pc} = eccentricity of prestressing force with respect to centroid of composite section (in.); positive in common construction where it is below centroid of section

$\psi_b(t_f, t_i)$ = girder creep coefficient at final time due to loading introduced at transfer

t_f = final age (days)

t_i = age at transfer (days)

A_c = area of section calculated using the gross composite concrete section properties of the girder and the deck and the deck-to-girder modular ratio (in.^{2})

I_c = moment of inertia of section calculated using the gross composite concrete section properties of the girder and the deck and the deck-to-girder modular ratio at service loading (in.^{4})

The prestress loss due to the creep of the girder concrete from the time of deck placement to final time (Δf_{pCD}) is presented in Equation (2.27). This creep loss is composed of two separate components. The prestress loss caused by the continued creep of the concrete due to the initial prestressing force and self-weight is accounted for in the first component (Δf_{pCD1}), presented in Equation (2.28). The prestress loss caused by the stress change in the concrete at the strand centroid due to prestress loss prior to deck placement and any superimposed dead loads is accounted for by the second component (Δf_{pCD2}), shown in Equation (2.29). The expression used to calculate the change in concrete stress at the strand centroid (Δf_{cd}) is presented in Equation (2.30) and the prestress loss force (P_Δ) in Equation (2.31). It should be noted that prestress loss calculated from this second component is always negative, implying an increase in strand stress. This increase in strand stress is termed a "gain" in AASHTO LRFD 2012.

$$\Delta f_{pCD} = \frac{E_p}{E_{ci}} f_{cgp} K_{df}\left[\psi_b(t_f, t_i) - \psi_b(t_d, t_i)\right] \ldots \qquad \text{(2.27)}$$

$$+ \frac{E_p}{E_{ci}} \Delta f_{cd}\psi_b(t_f, t_d) K_{df} \qquad \textit{AASHTO 12 (5.9.5.4.3b-1)}$$

$$\Delta f_{pCD1} = \frac{E_p}{E_{ci}} f_{cgp} K_{df}\left[\psi_b(t_f, t_i) - \psi_b(t_d, t_i)\right] \qquad \text{(2.28)}$$

$$\Delta f_{pCD2} = \frac{E_p}{E_{ci}} \Delta f_{cd}\psi_b(t_f, t_d) K_{df} \qquad \text{(2.29)}$$

Where:

f_{cgp} = the concrete stress at center of gravity of prestressing tendons due to the prestressing force immediately after transfer and the self-weight of the member at the section of maximum moment (ksi); same as calculated for Elastic Shortening

Δf_{cd} = change in concrete stress at centroid of prestressing strands due to long-term losses between transfer and deck placement, combined with deck weight and superimposed loads (ksi)

$$\Delta f_{cd} = \frac{P_\Delta}{A_g} + \frac{P_\Delta e_{pg}^{\ 2}}{I_g} - \frac{M_{sd}e_{pc}}{I_c} \tag{2.30}$$

$\psi_b(t_f,t_d)$= girder creep coefficient at final time due to loading introduced at deck placement

M_{sd} = moments due to deck weight and other superimposed dead loads (in-kips)

P_Δ = total long-term prestress losses prior to deck placement (kips)

$$P_\Delta = -\left(\Delta f_{pSR} + \Delta f_{pCR} + \Delta f_{pR1}\right)A_{ps} \tag{2.31}$$

Δf_{pSR} = shrinkage losses prior to deck placement (ksi)

Δf_{pCR} = creep losses prior to deck placement (ksi)

Δf_{pR1} = relaxation losses prior to deck placement (ksi)

At the time of deck placement, the majority of the shrinkage of the girder concrete will have already occurred. In AASHTO LRFD 2012, it is assumed that when the deck concrete undergoes shrinkage, the girder will resist the stress caused by the deck shrinkage, shown in Figure 2.6. This behavior is based on the assumption that the entire slab is cast-in-place, shown in Figure 2.6 (a), and may not accurately model the behavior of precast slab solutions.

The expression presented in AASHTO LRFD 2012 for the prestress gain due to the shrinkage of the deck concrete is presented in Equation (2.32). The derivation of this equation is similar to the derivation for shrinkage, presented in Table 2.3. The change in concrete stress at the centroid of the prestressing strands due to the shrinkage of the deck concrete is presented in Equation (2.33). This equation is a mechanics-based expression that assumes the shrinkage of the deck concrete imposes a notional force (P_{sd}), shown in Equation (2.34), at an eccentricity of e_d on the system.

$$\Delta f_{pSS} = \frac{E_p}{E_{ci}} \Delta f_{cdf} K_{df} \left[1 + \psi_b\left(t_f, t_d\right)\right] \tag{2.32}$$

AASHTO 12 (5.9.5.4.3d-1)

Where:

Δf_{cd} = change in concrete stress at centroid of prestressing strands due to shrinkage of deck concrete (ksi)

$$\Delta f_{cdf} = \frac{\varepsilon_{ddf} A_d E_{cd}}{\left[1 + 0.7\psi_d\left(t_f, t_d\right)\right]} \left(\frac{1}{A_c} - \frac{e_{pc}e_d}{I_c}\right) \tag{2.33}$$

AASHTO 12 (5.9.5.4.3d-2)

ε_{ddf} = shrinkage strain of deck concrete between placement and final time

A_d = area of deck concrete (in.^{2})

E_{cd} = modulus of elasticity of deck concrete (ksi)

e_d = eccentricity of deck with respect to the gross composite section, positive in typical construction where deck is above girder (in.)

$\psi_b(t_f,t_d)$ = creep coefficient of deck concrete at final time due to loading introduced shortly after deck placement (i.e. overlays, barriers, etc.)

$$P_{sd} = \frac{\varepsilon_{ddf} A_d E_{cd}}{[1 + 0.7\psi_d(t_f, t_d)]} \tag{2.34}$$

It should be noted that there is likely a misprint or mislabel present in Article 5.9.5.4.3d of AASHTO LRFD 2012. The creep coefficient of the deck concrete should be labeled $\psi_d(t_f, t_d)$ rather than $\psi_b(t_f, t_d)$ in the variable definitions. The creep coefficients appear to be subscripted properly in the equations. The timing that should be implemented for calculation of deck creep coefficient could benefit from further clarification.

(a)

(b)

(c)
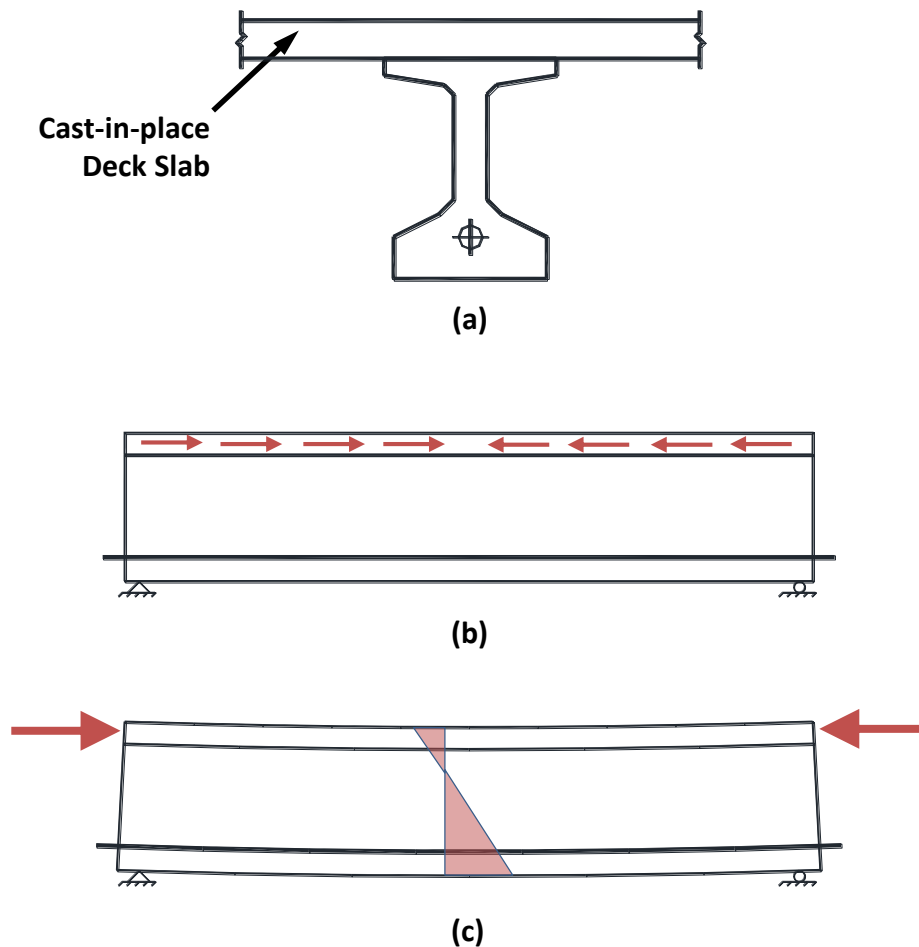
Figure 2.6 – For shrinkage of deck concrete the cast-in-place slab in the (a) assumed section causes (b) a differential shrinkage force that is (c) resisted by the beam

2.3.2.3 Strand Relaxation

The expressions for the prestress loss due to strand relaxation in the AASHTO LRFD 2012 procedure are presented in Equation (2.35), for before deck placement, and Equation (2.36), for after deck placement. The expressions are equal because it is assumed that there is an equal amount of relaxation loss before and after deck placement. These expressions are simplifications of Equation (2.37), which is found in the specification commentary.

$$\Delta f_{pR1} = \frac{f_{pt}}{K_L}\left(\frac{f_{pt}}{f_{py}} - 0.55\right)$$

(2.35)

AASHTO 12 (5.9.5.4.2c-1)

Where:
f_{pt} = stress in prestressing strands immediately after transfer, taken not less than 0.55f'$_c$ (ksi)
K_L = 30 for low relaxation strands and 7 for other prestressing steel, unless more accurate manufacturer's data are available
f_{py} = yield stress of prestressing strands (ksi)

$$\Delta f_{pR2} = \Delta f_{pR1}$$

(2.36)

AASHTO 12 (5.9.5.4.3c-1)

The expression found in the commentary, Equation (2.37), is taken directly from recommendations made by Tadros et al. (2003). Equation (2.3) from Magura et al. (1964) was refined to include a transformed section coefficient (K_{id}) and the reduction factor (ϕ_i) presented in Equation (2.38), which reflects the steady decrease in strand prestressing due to the creep and shrinkage of the concrete. The expressions found in the body of the specification are derived by inserting the assumed values of Table 2.5 into Equation (2.37).

$$\Delta f_{pR1} = \left[\frac{f_{pt}}{K'_L}\frac{\log(24t)}{\log(24t_i)}\left(\frac{f_{pt}}{f_{py}} - 0.55\right)\right]\left[1 - \frac{3\left(\Delta f_{pSR} + \Delta f_{pCR}\right)}{f_{pt}}\right]K_{id}$$

(2.37)

AASHTO 12 (C5.9.5.4.2c-1)

$$\phi_i = 1 - \frac{3\left(\Delta f_{pSR} + \Delta f_{pCR}\right)}{f_{pt}}$$

(2.38)

Where:
K'_L = 45 for low relaxation strands and 10 for other prestressing steel, unless more accurate manufacturer's data are available
t_i = time estimated in days from stressing to transfer (days)
t = time estimated from transfer to deck placement (days)

K_{id} = transformed section coefficient that accounts for time-dependent interaction between concrete and bonded steel in the section being considered for time period between transfer and deck placement

Δf_{pCR} = prestress loss due to girder creep prior to deck placement (ksi)

Δf_{pSR} = prestress loss due to girder shrinkage prior to deck placement (ksi)

Table 2.5 – Assumed variables in Equation (2.36) to derive Equation (2.35)

$$t_i = 0.75 \text{ days}$$

$$t = 120 \text{ days}$$

$$\left[1 - \frac{3\left(\Delta f_{pSR} + \Delta f_{pCR}\right)}{f_{pt}}\right] = 0.67$$

$$K_{id} = 0.8$$

2.3.3 Summary

The prestress loss procedure presented in AASHTO LRFD 2012 was implemented with the intention of making the procedure theoretically correct and more accurate. The resulting AASHTO LRFD 2012 procedure for calculating prestress loss is significantly more complicated than the procedure of AASHTO LRFD 2004. The accuracy and conservatism of the new procedure will be discussed in Section 2.6 after the database is introduced.

2.4 RECENT RESEARCH ON PRESTRESS LOSS IN PRETENSIONED CONCRETE

Engineers recognized that the prestress loss procedure introduced in 2005 AASHTO LRFD Bridge Design Specifications (and included in AASHTO LRFD 2012) would result in notably different designs than those produced by legacy methods for high strength concrete specimens. This realization led to a number of research studies aimed at verifying the provisions prior to full-scale implementation. The publications that provided key insights and guidance during the course of TxDOT Project 0-6374 are summarized here.

Following a brief overview of limited scope implementation studies, more extensive investigations of the AASHTO LRFD 2005 prestress loss provisions will be reviewed. Roller et al. (2011) instrumented a bridge in Louisiana and made several recommendations for improvement of the provisions on the basis of their results. Swartz et al. (2010) conducted an analytical study to investigate simplification of the otherwise complex method.

2.4.1 Implementation Studies

Several states (Virginia, Missouri, and Utah) funded research to investigate the conservatism of the new loss provisions. The research was generally conducted on a small scale, limited scope basis and will be reviewed here.

In Virginia, three different prestressed reinforced concrete bridges were instrumented with vibrating wire gages to measure the prestress loss occurring over the life of the girders (Cousins 2005). The results from these three bridges were combined with a database containing 24 other specimens. These results were compared to predictions calculated using multiple different prestress loss procedures: AASHTO Standard 1996, AASHTO LRFD 1998 (similar to 2004), PCI-1975, PCI-BDM and the procedure proposed by Tadros (NCHRP 496). From the database evaluation of the different procedures, Cousins et al. recommended the use of NCHRP 496 Refined and Approximate methods for estimating prestress losses and noted that the continued use of the method in AASHTO LRFD 2004 was "overly conservative but acceptable" until the NCHRP 496 methods could be adopted by AASHTO.

In Missouri, the prestress losses within one bridge were monitored for two years through the use of vibrating wire gages installed by the University of Missouri (Yang 2006). Monitoring results from the bridge led the researchers to recommend the use of NCHRP 496 methods for routine design work at the Missouri Department of Transportation (MoDOT).

In Utah, the behavior of six, high performance, self-consolidating concrete, prestressed bridge girders was measured using embedded vibrating wire gages (Barr 2009). The data from these girders was compared with prestress loss estimations from both the 2004 and 2005 AASHTO LRFD Bridge Design Specifications. The researchers concluded that "design practices are improving, and that prestress losses for high strength self-consolidating concrete can be predicted with them."

2.4.2 Rigolets Pass Bridge - Roller et al. (2011)

The Louisiana Department of Transportation and Development (LADOTD) has introduced the use of high-strength concrete bridge construction in recent years. Two spans of a 62-span bridge were constructed with high strength concrete in 2006. Roller et al. installed vibrating wire gages within four girders of one of the high strength concrete spans. These gages were used to observe the structural behavior of the high strength concrete girders.

The measured prestress losses (elastic shortening loss, long-term loss and total loss) were compared with the values estimated by AASHTO LRFD 2005 on the basis of both design and actual material properties. The researchers commented that "interpretation and use of [the AASHTO LRFD 2005] provisions is difficult, and the existing commentary offers little clarification." The researchers continued to comment about difficulties related to proper sign convention and poorly defined terms. They also commented that the provisions for estimating prestress loss should be simplified and clarified so that users will not have to look to other sources for interpretation.

The recommendations made by Roller et al. are summarized and examined below. The following discussion includes interpretations made by the TxDOT Project 0-6374 researchers.

- *Eliminate Iterative Calculation of Δf_{pES}*: Commentary Equation (C5.9.5.2.3a-1) should be used rather than Equation (5.9.5.2.3a-1).

$$\Delta f_{pES} \text{ Iterative} \longrightarrow \Delta f_{pES} = \frac{A_{ps} f_{pbt}(I_g + e_m{}^2 A_g) - e_m M_g A_g}{A_{ps}(I_g + e_m{}^2 A_g) + \frac{A_g I_g E_{ci}}{E_p}}$$

- *Refine the Commentary for Δf_{pES}*: Commentary discussion in Article 5.9.5.2.3 should be reworded and should only include explanation applicable to the section. This commentary is lengthy, confusing and should be reworded. It also includes some discussion on time-dependent losses that would serve better in later sections.

- *Expand the Applicability of Creep and Shrinkage Expressions*: Further refinements should be made to the creep and shrinkage expressions to account for a wider range of concrete mixture proportions (specifically type and quantity of cement replacement materials, initial curing conditions, initial concrete stress level, and aggregate properties) and bridge design conditions. These expressions should be expanded to account for both high and low strength concretes, conventional and self-consolidating concrete mixes, and different aggregate stiffness.

- *Clarify Prestress Loss Sign Conventions*: Clarification of sign convention should be made in several expressions (Δf_{ss} and Δf_{cd}). It needs to be clarified in the specification whether these components add or subtract from the total prestress loss. From the definitions of these variables, it can be deduced what sign should be applied, but the signs should be explicitly stated.

- *Clarify the Calculation of After Deck Concrete Stresses*: Further guidance should be provided for the determination of the change in concrete stress at the centroid of prestressing strands due to long-term losses and deck placement (Δf_{cd}). It is unclear what section properties should be used for which load application and what loads should be applied. The language would suggest that a load placed at the centroid of the prestressing strands representing the prestress loss between transfer and deck placement should be included, but this should be more directly stated.

- *Eliminate the Calculation of Prestress Gains*: Prestress gains due to shrinkage of deck concrete (Δf_{pSS}) should be eliminated. This procedure is complicated for the small amount of gain estimated. The process also likely does not represent the actual behavior of the system.

2.4.3 The Direct Method - Swartz et al. (2010)

Swartz et al. (2010) noticed that many "practitioners have expressed concerns about the complex nature of the equations and the seemingly less conservative results when compared with other prestress loss estimating methods." In order to address these concerns, the researchers recommended several simplifications and clarifications to the prestress loss procedure in AASHTO LRFD 2005. Through these simplifications, the differentiation between before and after deck placement was eliminated. The researchers called the resulting procedure the "Direct Method." The Direct Method was verified with results from a Monte Carlo simulation. The goal of this simulation was to ensure that the mean results from the Direct Method compared well with results from AASHTO LRFD 2005.

The material coefficient and timing recommendations are summarized in Table 2.6. The recommended values for the shape factor (k_s) were determined from common volume-to-surface area ratios for typical bridge girders. The time development factor (k_{td}) was determined from examination of the entire bridge life in one step. The assumption for the release strength of the concrete (f'_{ci}) was based on recommendations of Tadros et al. (2003). The transformed section coefficients for both shrinkage and creep (K_{id-SH} and K_{id-CR}, respectively) reflect typical numerical results from the analytical study. The recommended timing for release and deck placement (t_i and t_d, respectively) reflect conservative estimates for typical fabrication practices.

Table 2.6 – Recommendations by Swartz et al. (2010)

$$k_s = 1.0$$

$$k_{td} = 1.0$$

$$f'_{ci} = 0.8f'_c$$

$$K_{id-SH} = 0.9$$

$$K_{id-CR} = 0.85$$

$$t_i = 1.0 \text{ day}$$

$$t_d = 120 \text{ days}$$

Equations (2.39) and (2.40) resulted from substitution of the recommended coefficients into the AASHTO LRFD 2005 expressions for shrinkage and creep. The following expressions were modified to keep a consistent sign convention through this report, considering compression (or decrease in the tension) as positive.

$$\Delta f_{pSH} = E_p \left(\frac{140 - H}{1.3 + f'_c} \right) (3.8 \ x \ 10^{-5}) \quad\quad\quad \textbf{(2.39)}$$

$$\Delta f_{pCR} = 0.04 \left(\frac{E_p}{E_c}\right) \left(\frac{195 - H}{1.3 + f'_c}\right) \left(2 f_{cgp} + \Delta f_{cdp} + \Delta f_{cps}\right) \tag{2.40}$$

Where:

f_{cgp} = the concrete stress at center of gravity of prestressing tendons due to the prestressing force immediately after transfer and the self-weight of the member at the section of maximum moment (ksi)

Δf_{cdp} = change in concrete stress at centroid of prestressing strands due to the application of deck load and superimposed dead loads (ksi)

$$\Delta f_{cdp} = -\frac{M_{sd} e_{pc}}{I_c} \tag{2.41}$$

Δf_{cds} = change in concrete stress at centroid of prestressing strands due to shrinkage and relaxation losses, and differential shrinkage between the deck and girder

$$\Delta f_{cds} = P_\Delta \left(\frac{1}{A_g} + \frac{e_p{}^2}{I_g}\right) + P_{deck} \left(\frac{1}{A_c} - \frac{e_d e_{pc}}{I_c}\right) \tag{2.42}$$

A_g = area of gross section (in.^{2})
I_g = moment of inertia of gross section (in.^{4})
e_p = eccentricity of prestressing tendons in gross section (in)
M_{sd} = moments due to deck weight and other superimposed dead loads (in-kips)
I_c = moment of inertia of composite section (in.^{4})
e_{pc} = eccentricity of prestressing tendons in composite section (in)
e_d = eccentricity of deck with respect to the gross composite section, positive in typical construction where deck is above girder (in.)
P_Δ = total long-term prestress losses, other than creep loss (kips)

$$P_\Delta = -\left(\Delta f_{pSH} + \Delta f_{pR}\right) A_{ps} \tag{2.43}$$

Δf_{pSH} = total shrinkage loss (ksi)
Δf_{pR} = total relaxation loss (ksi)
A_{ps} = total p/s strand area (in.^{2})

Swartz et al. also attempted to clarify the effect of differential shrinkage of the deck concrete on prestress loss. As previously mentioned, the current bridge specification refers to the stress gain due to the differential shrinkage of the deck concrete a "prestress gain." The researchers suggested that the language was misleading, since the bottom concrete fiber also experiences an increase in stress. An effective force accounting for the differential shrinkage of the deck (P_{deck}), shown in Equation (2.44), was derived in order to clarify the way that this component should be properly accounted for without error. This force is to be applied to the

system at the centroid of the deck to calculate the change in concrete stress at the centroid of the prestressing strands.

$$P_{deck} = 1.2 \ x \ 10^{-4} \left[\frac{(140 - H) \left[\frac{5}{1 + f'_{cd}} - \frac{1}{f'_c} \right]}{17 + \frac{195 - H}{1.3 + f'_{cd}}} \right] A_d E_{cd} \qquad \textbf{(2.44)}$$

These recommendations and those made by Roller et al. were taken into consideration during the development of the recommendations provided in Chapter 6 of this report.

2.5 TXDOT PROJECT 0-6374 PRESTRESS LOSS DATABASE

A thorough literature review was conducted during the length of the research project. All relevant and potentially relevant research conducted on pretensioned girders was collected and assembled into a database. The database was assembled in order to enable evaluation of the past and present prestress loss provisions of the AASHTO LRFD Bridge Design Specification as well as the recommendations outlined in Chapter 6 of this report. The specimens and the corresponding prestress losses contained in the database represent a broad range of materials (including high strength concrete) and girder geometries. The specimens contained in this database are pretensioned girders only.

2.5.1 Data Collection and Filtering

The TxDOT Project 0-6374 research team identified a total of 29 prestress loss studies in literature published between 1970 and present. Prestress loss data for 237 specimens were extracted from the collection of studies.

Prestress loss was determined either by internal strain measurement or by back-calculating strand stress from service load testing results. Some of the studies explicitly reported the prestress losses that occurred within their specimens. These results were verified, if possible, through the use of other data reported within the study. If verification was not possible, the reported loss was given an accuracy rating. If the prestress loss was not explicitly reported, the loss was calculated using either service load testing results or reported internal strain measurements. When a loss was reported and could be determined from both internal strain measurements and cracking load test results, only the loss from the most accurate measurement method (internal strain measurement) was used in database analysis.

Once the results were fully vetted, a two-stage filtering process, shown in Table 2.7, was conducted to ensure that code performance would only be evaluated on the basis of relevant data. The filtering process provided assurance that: (1) the prestress loss measured in each specimen was an accurate representation behavior encountered in the field, and (2) the specimens were of representative scale and detailing.

The first filtering process was performed on the database to eliminate specimens for which critical details could not be ascertained; information deemed critical is shown in Table 2.7 and discussed here. The concrete tensile strength, compressive release strength, and prestressing strand area were essential to assessment of the load test results and estimation of the prestress

loses. A failure to report measurements (as opposed to design values) of these properties resulted in dismissal of the specimen from the database. Moreover, if the prestress loss was not reported and ancillary data could not be used to back-calculate the prestress loss, the specimen was similarly dismissed from the database.

Table 2.7 – Filtering of the prestress loss database

Collection Database			237 tests
Stage 1 Filtering	Critical information not reported - Concrete tensile strength - Concrete release strength - Prestress loss - Total prestressing area		- 57 tests
	Inaccurate prestress loss estimate		- 3 tests
Filtered Database			177 tests
Stage 2 Filtering	Height: $h > 20\ inches$		- 36 tests
	Concrete stress at release: $f_{c,bottom}/f_{ci} < 0.7$		- 1 tests
Evaluation Database			140 tests

The accuracy of the prestress loss calculated from or reported within the data of the studies was further evaluated. Assumption or calculation of key properties for a given specimen was deemed to be inferior to the measurement of those key properties. Each property was given an importance factor for the purposes of quantifying the accuracy of the resulting prestress loss estimate (Table 2.8). If assumptions and calculations within the study resulted in an inaccuracy ranking above a set threshold, the study was not included in the Evaluation Database.

Table 2.8 – Properties investigated to determine accuracy of prestress loss estimate reported by each study

	Property	Factor
w_c	Unit weight of concrete assumed	1
f_{pu}	Ultimate strength of strand assumed	1
E_p	Strand modulus assumed to be 28,500-ksi	1
f'_{cd}	Compressive strength of deck concrete assumed to be 4-ksi	2
t_i	Time of release assumed to be 0.75-days	1
t_d	Time of deck placement assumed to be 120-days	1
E_{ci}	Concrete modulus at release calculated using measured or specified f'$_c$	3
f'_c	Specified concrete strength used rather than measured	3
E_c	Concrete modulus calculated using measured or specified f'$_c$	1
f_{pi}	Strand stress prior to transfer assumed to be 202.5-ksi	1

The purpose of the first filtering process was to eliminate specimens with inaccurate or incomplete reported prestress losses. Each of the specimens in the Filtered Database is accompanied by sufficient detail to accurately estimate the prestress loss and compare it to a reported/calculated value. The second stage of the filtering process was conducted to ensure that the specimens within the Evaluation Database possessed field-representative scale and detailing. Two parameters (refer to Table 2.7) were examined to make this determination:

- *Specimen Height (h)*: The smallest section used by TxDOT is limited to a height of 20 inches. Moreover, a cursory database analysis revealed that the flexural cracking resistance of smaller specimens was generally exaggerated in relation to reported concrete tensile strength; resulting in lower than realistic prestress loss assessments. All specimens under 20 inches in depth were therefore eliminated from Evaluation Database.

- *Initial Bottom Fiber Stress ($f_{c,bottom}$)*: In the current bridge specification the limit for the maximum compressive stress at prestress transfer is $0.6 f_{ci}$. Research has been conducted to investigate the potential of increasing this limit, which would allow for longer span lengths, a reduction in harped or debonded strands, and a faster turnaround time for beams in prestressing beds. An upper limit of 0.65f$_{ci}$, recommended by TxDOT Project 0-5197, has been widely adopted by fabricators as well as TxDOT Bridge Designers. To be inclusive of slightly overstressed specimens, an upper limit of $0.7 f_{ci}$ was adopted for inclusion within the Evaluation Database.

The final Evaluation Database contains the specimens from the Filtered Database that met the height and initial stress qualifications outlined above. The origin of the reference, geometry of the specimens, concrete materials used, and amount of prestressing in the specimens included in the Evaluation Database will be briefly discussed in the following sections.

2.5.2 Evaluation Database Characteristics

The TxDOT Project 0-6374 prestress loss database was used heavily in evaluation of the past, present and future prestress loss provisions reviewed and proposed in this report. Due to the central role played by the database, it is important to demonstrate that the database provides a comprehensive representation of pretensioned girder design and fabrication in the State of Texas.

The methods used to measure the prestress loss in the specimens contained in the Evaluation Database are shown in Figure 2.7. The two primary methods of assessing prestress loss (vibrating wire gages and flexural cracking tests) make up the majority of the Evaluation Database. Vibrating wire gages, used in about half of the specimens, were found to be the most consistent means of prestress loss assessment; with flexural cracking being the second-most utilized, and consistent, means of assessment.
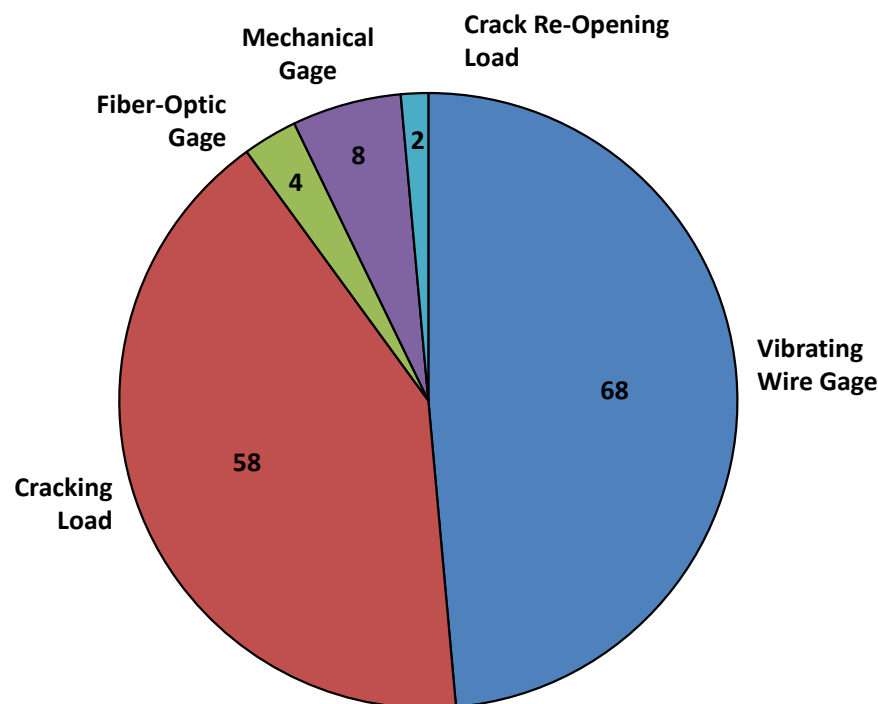
Figure 2.7 – Method used for measuring loss

The fabrication and conditioning locations of the specimens are presented in Figure 2.8. Although the majority of the specimens are from Texas, many other states are also represented, ensuring that various climates are captured by the database. The average relative humidity reported for the conditioning location is shown in Figure 2.9. It should be noted that the majority of Texas, and the entire country for that matter, has an average ambient relative humidity between 60 and 75 percent (Figure 5.4.2.3.3-1 - AASHTO 2012). The climatic exposure of a majority of the specimens within the Evaluation Database is consistent with that generalization.

No. of Specimens in Each State
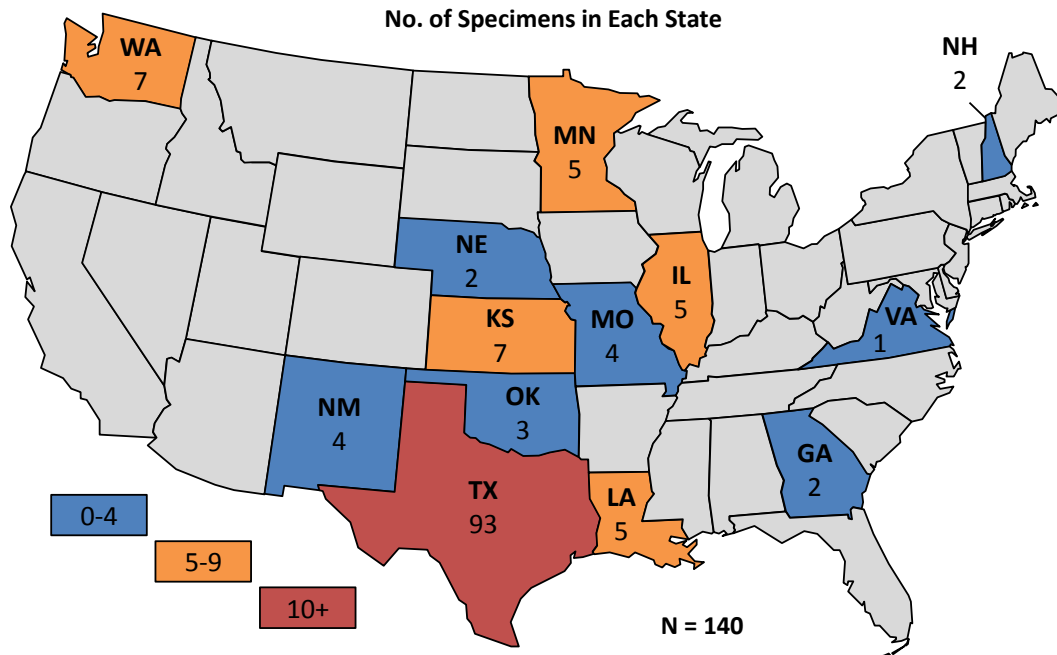
Figure 2.8 – Location where specimens were fabricated/conditioned
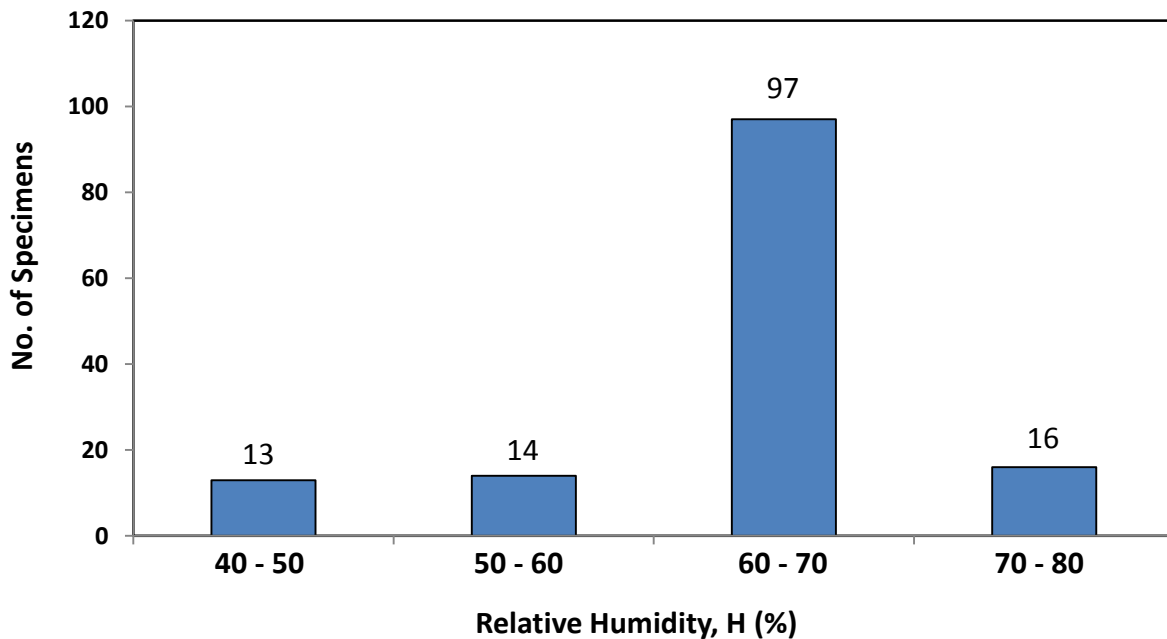
Figure 2.9 – Average reported relative humidity for location where specimens were conditioned

A variety of different specimen geometries are captured by the specimens included in the Evaluation Database. Variation of the specimen length and height are presented in Figure 2.10. The majority of the specimens are 25 to 75 feet in length and 20 to 60 inches in height, although longer spans and deeper cross-sections are also present.

The gross cross-sectional area and the volume-to-surface area ratio of the specimens are presented in Figure 2.11. It should be noted that the majority of the specimens have a volume-to-surface area ratio of between three and four; nearly all typical cross-sections have a volume-to-surface ratio within this range.
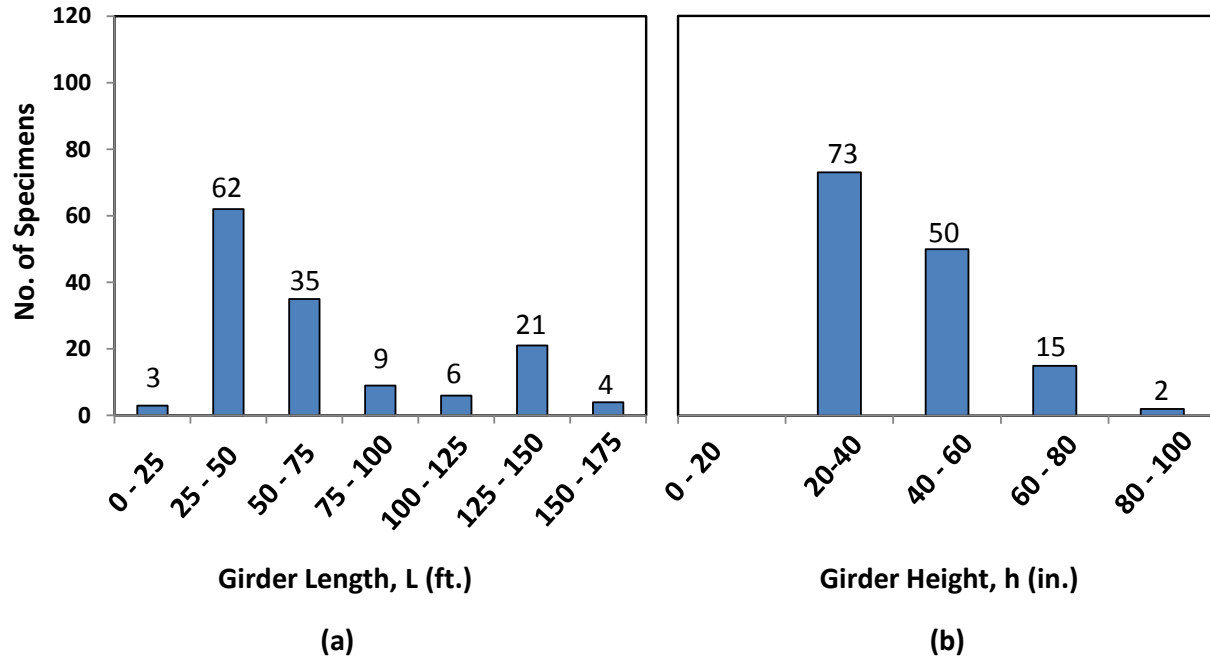
Figure 2.10 – (a) Girder length and (b) girder height of specimens
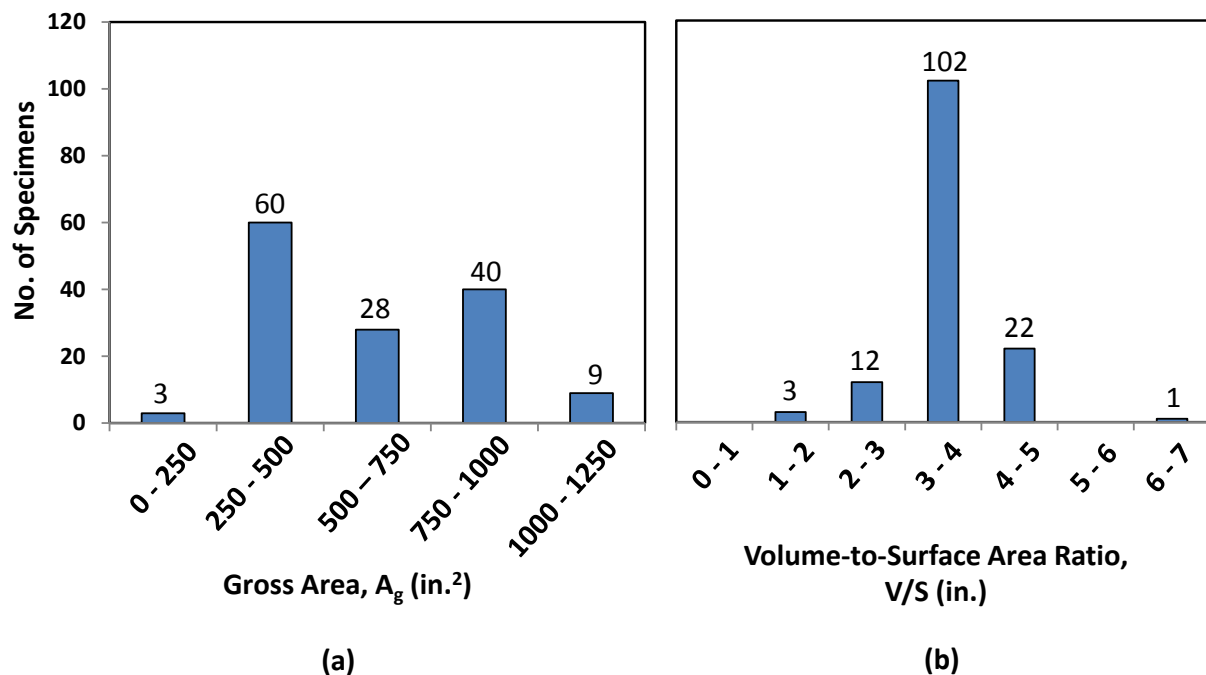
Figure 2.11 – (a) Gross area and (b) volume-to-surface area ratio of specimens

A variety of concrete mixtures with different types of aggregates are captured within the Evaluation Database, as shown in Figure 2.12. The majority of the specimens were fabricated using conventional concrete, although some specimens were fabricated using self-consolidating concrete. The two main types of course aggregate used in common practice, river gravel and limestone; make up the majority of the specimens in the database.

While previous material property and prestress loss equations were developed and verified using either only normal strength concrete (< 6 ksi) or only high strength concrete (> 6 ksi), the Evaluation Database contains a wide variety of concrete strengths, as shown in Figure 2.13. This wide variety for both release and 28-day compressive strengths helps to ensure that the loss equations are properly calibrated for all commonly used concrete strengths.

It should also be noted that 89 out of the 140 specimens included in the Evaluation Database attained a 28-day compressive strength of over 10 ksi. This number far exceeds the 38 high strength concrete specimens collected by Tadros et al. (2003) in support of the NCHRP 496 provisions.
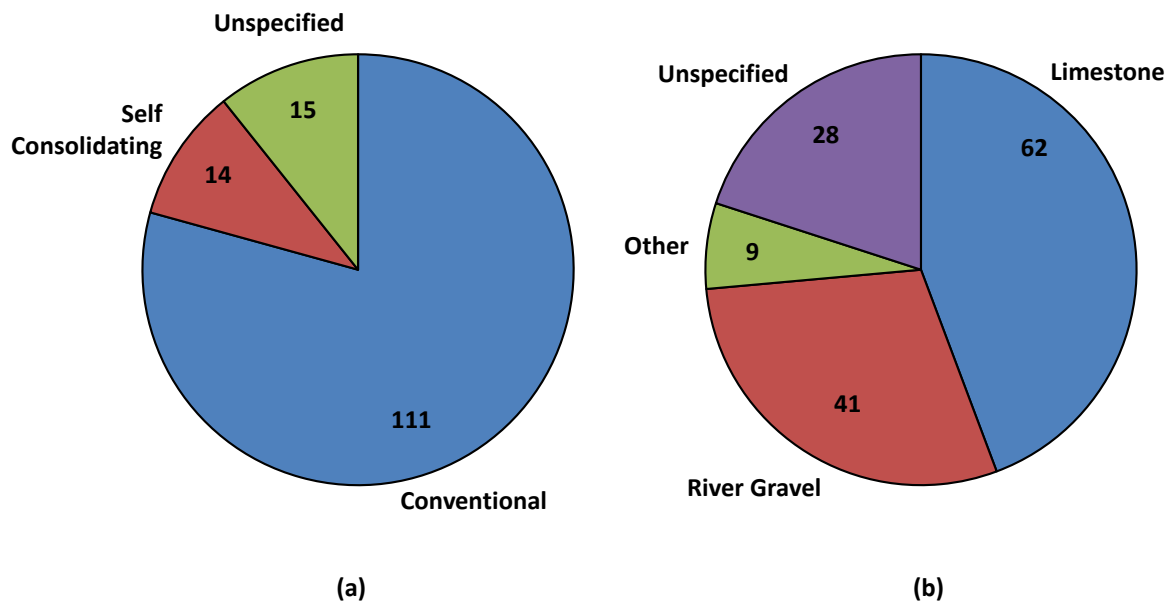
Figure 2.12 – (a) Type of concrete mixture and (b) type of aggregate used to construct specimens
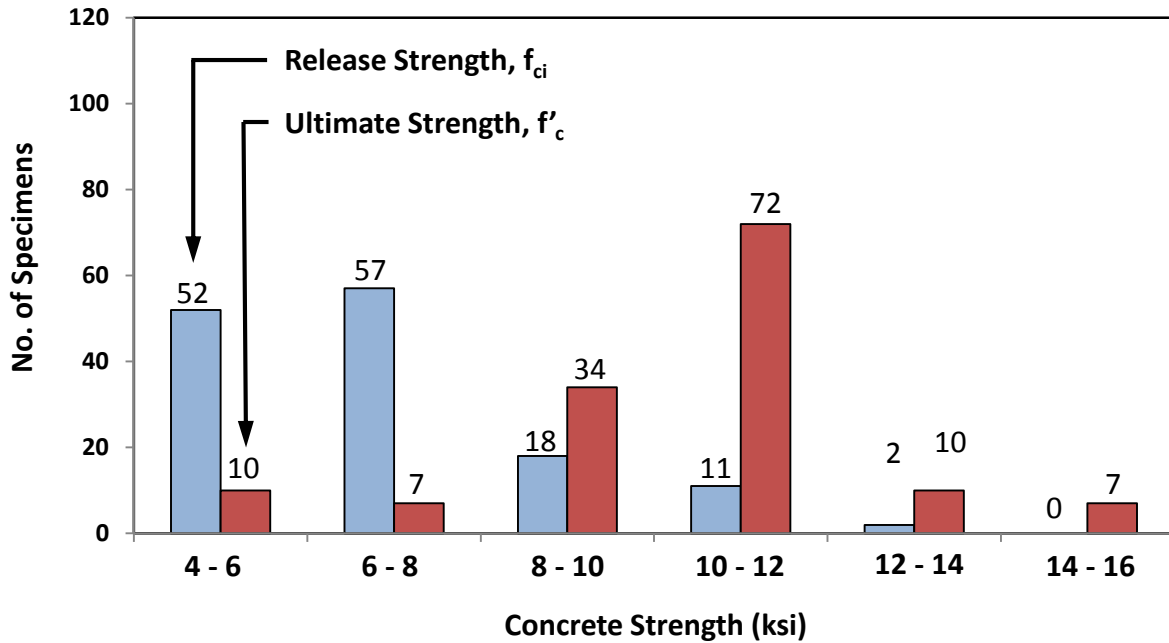
Figure 2.13 – Release strength and ultimate strength of concrete used to construct specimens

The prestressed reinforcement ratios for the specimens contained in the Evaluation Database are shown in Figure 2.14. In practice, it is not practical to have a prestress ratio higher than 1.5 percent, as these higher ratios lead to compressive stress concerns. This practical limit is reflected in the specimens contained in the Evaluation Database.
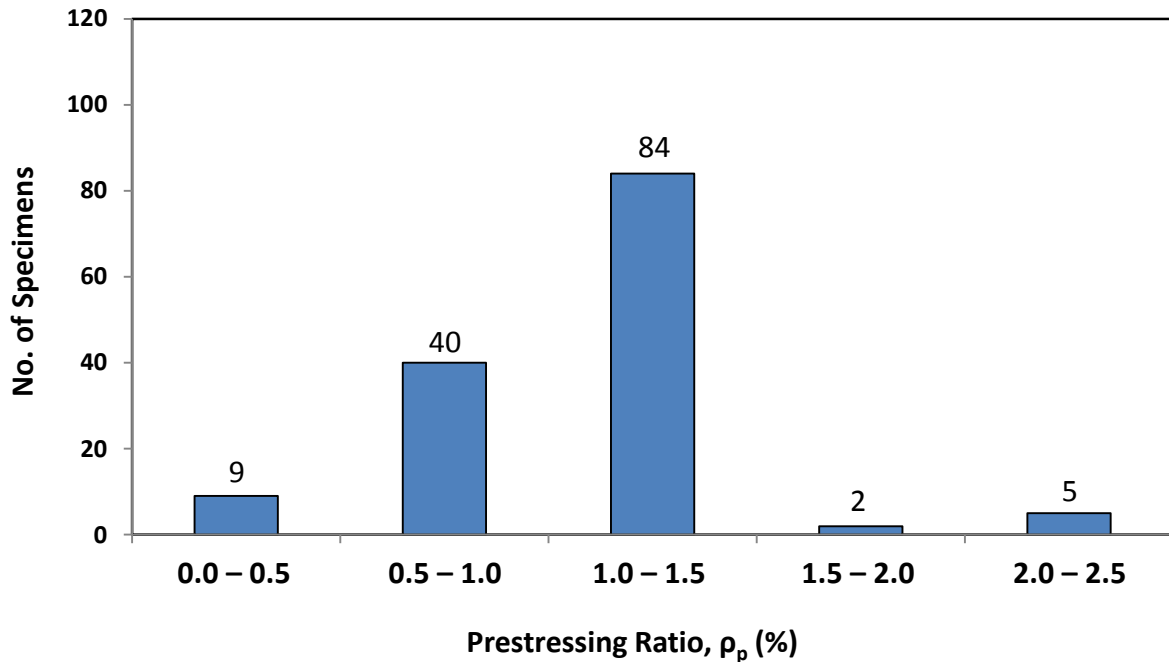
Figure 2.14 – Prestressing ratio of specimens

2.6 DATABASE EVALUATION OF CURRENT PRESTRESS LOSS PROVISIONS

The performance of the 2004 and 2012 (introduced in 2005) AASHTO LRFD Bridge Design Specifications will now be presented and discussed. The performance of each procedure is evaluated by comparing the estimated prestress loss to the measured prestress loss of each Evaluation Database specimen; calculation of the ratio of the estimated-to-measured prestress losses (*E/M*) is helpful in that regard. Key statistics from the *E/M* ratios calculated for the prestress loss expressions in AASHTO LRFD 2004 and 2012 are presented in Table 2.9. Please note that an accurate means of prestress loss estimation will be characterized by an average *E/M* ratio close to 1.00 (i.e. estimated and measured prestress losses are equal). More conservative means of prestress loss estimation will be characterized by an *E/M* ratio greater than 1.00 (i.e. estimated prestress losses exceed the measured prestress losses). Prestress loss estimates provided by AASHTO LRFD 2004 are clearly more conservative than those provided by AASHTO LRFD 2012.

Table 2.9 – Comparison of AASHTO LRFD 2004 and 2012 performance using estimated-to-actual ratio (*E/M*) from the Evaluation Database

	AASHTO 2004	AASHTO 2012
Minimum	0.86	0.59
Average	1.74	1.25
Maximum	3.69	2.20
Co. of Variation	0.26	0.24
St. Deviation	0.45	0.30

The relationship between the estimated prestress losses and the measured prestress losses is further examined in Figure 2.15 (AASHTO LRFD 2004) and Figure 2.16 (AASHTO LRFD 2012). All results contained within the Evaluation Database are plotted against the prestress loss estimate on the vertical axis and the measured prestress loss on the horizontal axis. If a procedure exhibits perfect precision, all of the specimens will fall on a straight line that originates from the origin. A procedure with no excess conservatism and perfect precision will place all of the specimens on the line of equality, which is the solid black line extending from the origin in Figure 2.15. It should also be noted that all of the specimens that fall below the line of equality are estimated unconservatively by the particular prestress loss provisions.
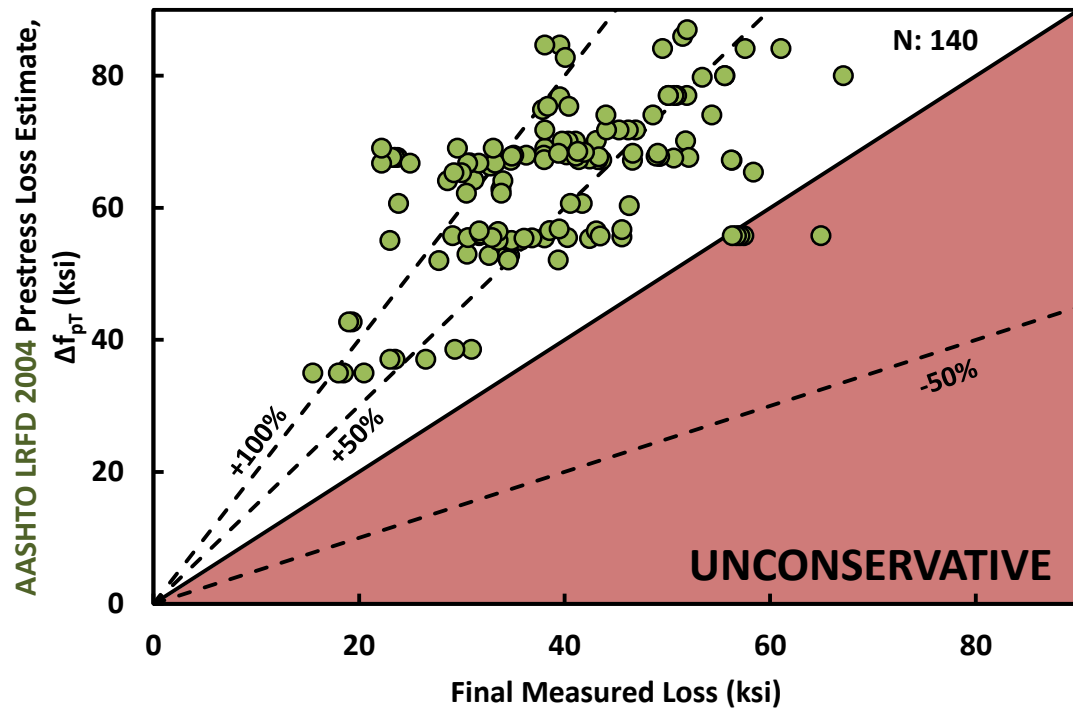
Figure 2.15 – AASHTO LRFD 2004 prestressed loss estimate vs. final measured loss
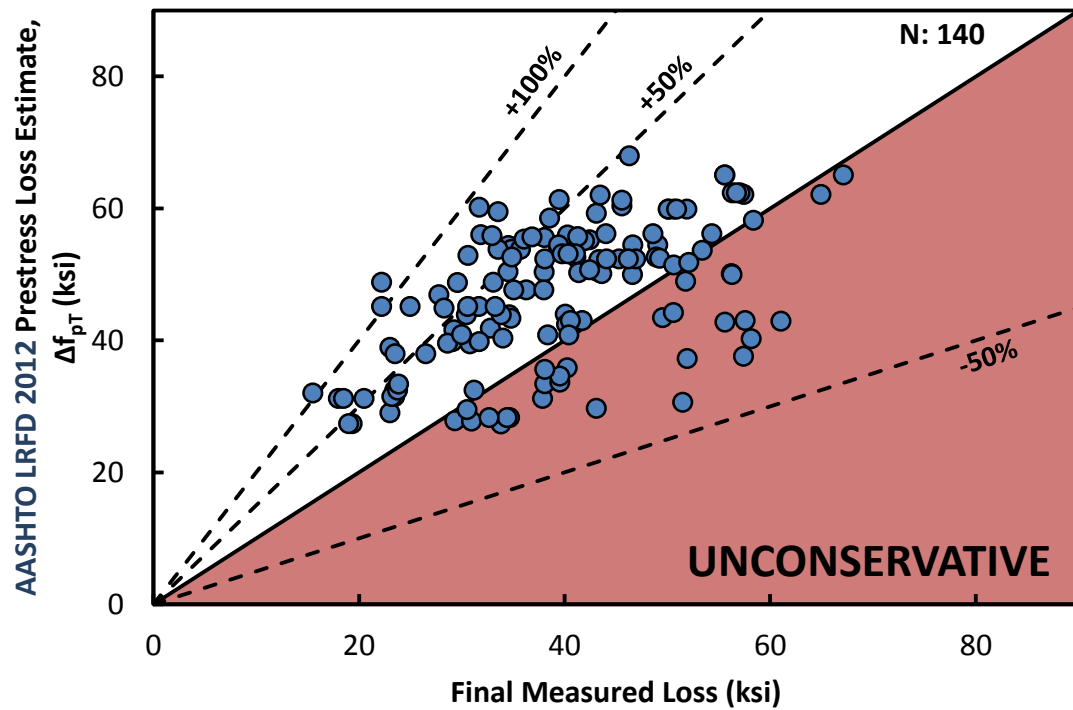
Figure 2.16 – AASHTO LRFD 2012 prestressed loss estimate vs. final measured loss

The AASHTO LRFD 2012 prestress loss provisions have clearly been calibrated to yield accurate estimates; the average E/M ratio is significantly less than the previous provisions. Moreover, the decreased level of conservatism is achieved through a substantial increase in complexity and virtually no improvement in the precision of the estimates (refer to the coefficient of variation in Table 2.9). The performance of both of these loss procedures will be further investigated in Chapter 6.

2.7 SUMMARY

The total prestress loss is a combination of short-term losses (elastic shortening) and long-term losses (creep, shrinkage and relaxation losses). Elastic shortening of a concrete girder is a well-understood phenomenon that may be accounted for via theoretically based analyses. Prestress loss due to creep is primarily dependent on the stiffness of the concrete, which varies with concrete strength and aggregate type, and on the magnitude of the stress sustained on the concrete. Prestress loss due to shrinkage is heavily dependent on the material properties of the concrete (i.e. concrete stiffness, concrete strength, aggregate type and quantity, paste content, etc.).

The total loss can be and has been estimated with varying degrees of complexity. In AASHTO LRFD 2004 an empirically derived procedure was provided that was simple, but perhaps overly conservative. The procedure contained in AASHTO LRFD 2012 was introduced to attempt to improve the theoretical accuracy and account for more of the contributing factors. In their efforts to include more contributing variables, the procedure was made to be much more complex and much less conservative.

Since the adoption of the new loss procedure into AASHTO LRFD in 2005, many studies have been conducted to look at the accuracy and application of the procedure. There have been questions raised as to whether the complexity is warranted and whether the loss in conservatism is acceptable. Some studies supported the implementation of the new loss procedure into their respective state's design practices based on a small sample of bridge instrumentations. Other studies saw the excessive complexity of the loss expressions and made recommendations to simplify and clarify the procedure. The "Direct Method" suggested by Swartz et al. (2010) successfully simplified the procedure, but did not change the level of conservatism.

The remainder of this report will investigate the results of this study. The experimental portion will first be discussed and is followed by an overview of the parametric study. Results from both the experimental work and the parametric study contributed to the development of the design recommendations made in Chapter 6.

CHAPTER 3
Experimental Program
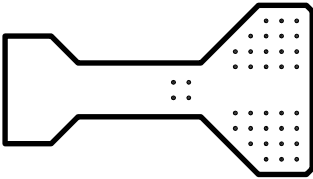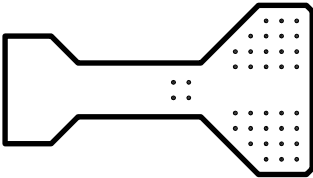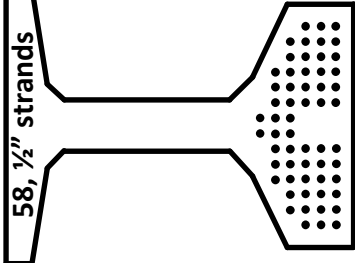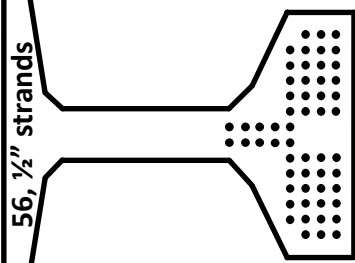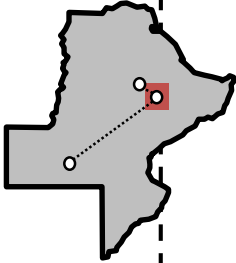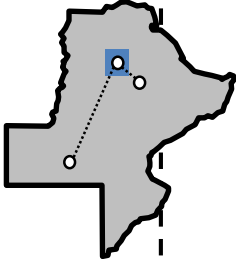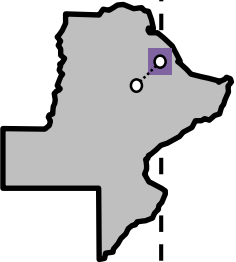
3.1 OVERVIEW

An extensive experimental program was conducted to provide an experimental basis for the assessment of existing prestress loss provisions (and the development of new provisions). Thirty full-scale prestressed concrete beams were fabricated and conditioned to enable comprehensive assessment of short- and long-term prestress losses. The specimens were representative of a fairly broad range of the most influential factors that may affect prestress losses in structures fabricated within the State of Texas, including type of concrete, prestress level, specimen geometry, fabrication techniques, and climate.

The scope of the experimental program is summarized in Table 3.1. About half of the specimens were Type C beams, while the other half were Tx46 beams. The concrete and coarse aggregate types were intentionally varied from series to series to investigate their effects on prestress loss: Series I and III were fabricated in San Antonio with conventional concrete and limestone coarse aggregate; Series II in Elm Mott using conventional concrete and river gravel coarse aggregate; Series IV near Victoria using conventional and self-consolidating concrete with river gravel coarse aggregate. The specimens were conditioned for periods ranging from 93 to 980 days (an average of 700 days) at a total of five storage locations in Texas: San Antonio, Austin, Lubbock, Elm Mott, and Victoria. The long-term loss of prestress within each specimen was assessed through the use of: (1) internal strain monitoring and (2) flexural testing.

The results of this experimental program are presented in Chapter 4. The results, in combination with information compiled in the database (Chapter 2), are used in Chapter 6 to assess the performance of prestress loss provisions: (1) outlined in the AASHTO LRFD Bridge Design Specifications and (2) proposed within Chapter 6 of this report.

Table 3.1 – Summary of main properties of the specimens

	Series I	Series II	Series III	Series IV
Cross-Section Type	38, ½" strands Type C	38, ½" strands Type C	58, ½" strands Tx46	56, ½" strands Tx46
Coarse Aggregate	Limestone	River Gravel	Limestone	River Gravel
Location (# of specimens) — Fabrication	San Antonio (8)	Elm Mott (8)	San Antonio (8)	Eagle Lake (6)
Location (# of specimens) — Storage	San Antonio (2) Austin (3) Lubbock (3)	Elm Mott (2) Austin (3) Lubbock (3)	San Antonio (2) Austin (3) Lubbock (3)	Austin (6) (3: SCC + 3: CC)

3.2 DEVELOPMENT OF FIELD-REPRESENTATIVE BEAM SPECIMENS

The specimens were designed, fabricated and conditioned to be representative of typical construction practices and field conditions in Texas. The cross-section types selected were Type C and Tx46. The amount of prestressing steel in each specimen varied from about 1.13 percent to 1.17 percent of the gross cross-sectional area. This large amount of prestressing steel, for this short of a span, was used in order to generate high initial compressive stresses, on the order of $0.65f'_{ci,design}$, to maximize the potential for prestress losses.

Specimens were fabricated at multiple precast plants to assess the influence of plant-specific materials and techniques on the development of prestress loss. The plants chosen were located in San Antonio, Elm Mott, and Eagle Lake. Overall, the main differences in the concrete mix between plants were the coarse aggregate type (river gravel versus limestone) and the type of concrete mix (conventional versus self-consolidating).

The conditioning of the specimens was conducted in four storage locations in order to observe the effect of different climate conditions. The specimens were conditioned in San Antonio, Elm Mott, Austin and Lubbock; this gave a range of relative humidity from 50 to 64 percent.

3.2.1 Design

Type C and Tx46 cross-sections were selected for the experimental program. Type C sections were selected by decision of the Texas Department of Transportation (TxDOT) Project Monitoring Committee (PMC) because they have been heavily used in the past. The Tx46 sections were selected because they were one of the most readily available TX girder sections at the time of this study. Both cross-sections can be referred to as mid-size when considering other TxDOT sections, as shown in Figure 3.1.

The prestressed reinforcement for specimens within Series I through IV was proportioned and configured to obtain a uniform stress of approximately $0.65f'_{ci,design}$ along the bottom flange. An approximately uniform stress condition was maintained along the length of each specimen through the use of harping, as shown in Figure 3.2 and Figure 3.3. A minor amount of mild reinforcement was placed within the top flange to control cracking due to unanticipated tensile stress demands.
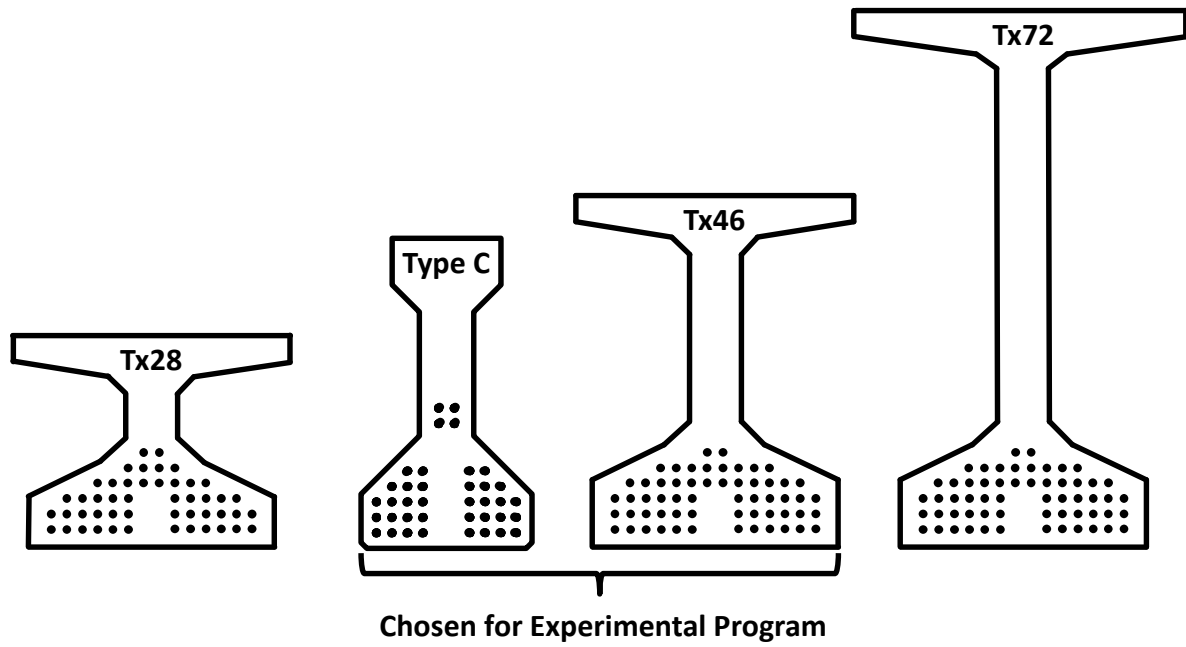
Figure 3.1 – Comparison of specimens and scale of Tx girders
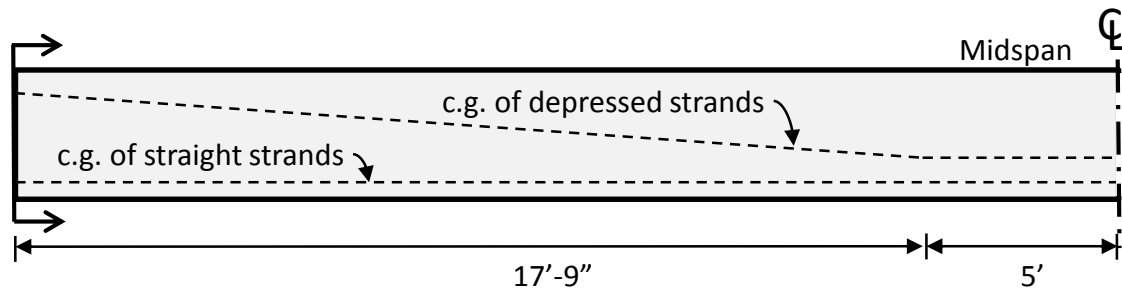
Figure 3.2 – Longitudinal elevation of specimens
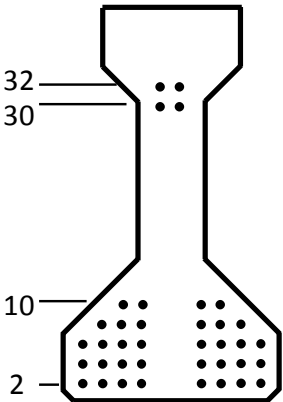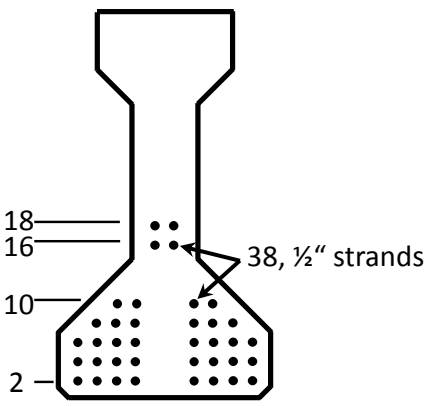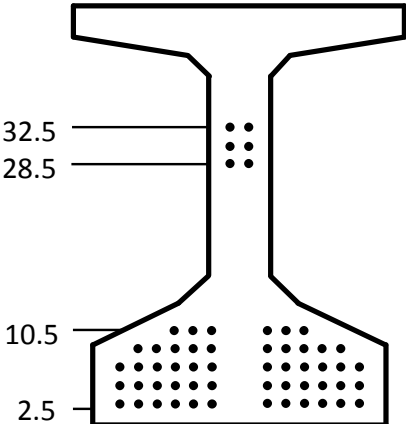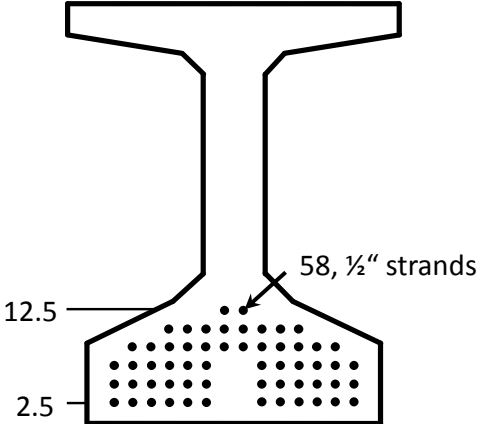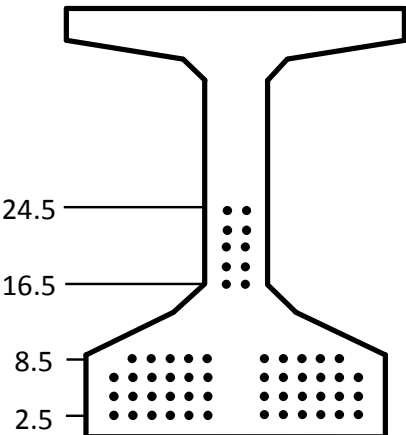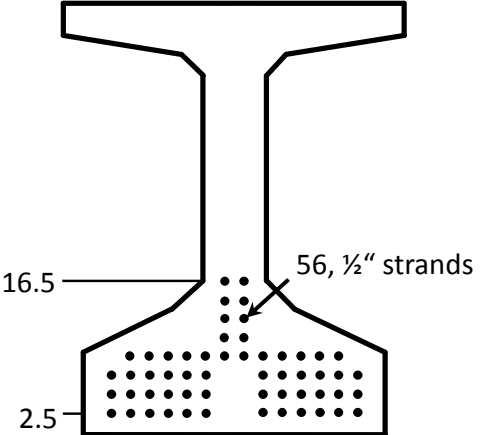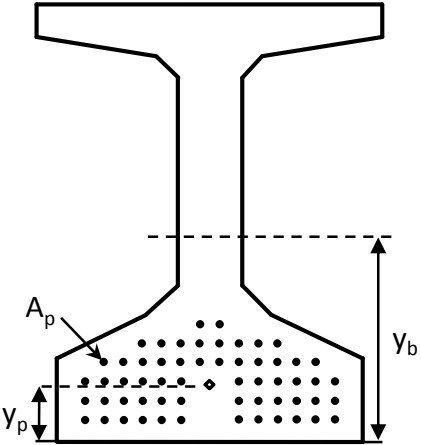
Figure 3.3 – Prestressing strand layout for all series (all dimensions are offsets from bottom of girder assuming a 2-inch grid)

The specimen length was selected through balanced consideration of the test objectives and the practicalities of girder transportation and handling. Due to space and overhead crane limitations, a beam equal to or less than fifty feet in length represented the most practical solution. The specimens were therefore kept as short as possible, while also ensuring that flexural cracking could be observed without significant risk of premature shear failure. In most cases, the standard shear reinforcement specified by TxDOT was sufficient for the anticipated demands.

Variations of the design parameters in each of the series of specimens are summarized in Table 3.2. The Tx46 section is slightly larger than the Type C section, as indicated by the larger gross cross-sectional area (A_g) and moment of inertia (I_g). A larger amount of prestressing steel was required in the Tx46 specimens to maintain a consistent bottom-fiber compressive stress across all series.

Table 3.2 – Design of Series I through Series IV specimens

Series (# of Specimens)	f'$_{ci\text{-}design}$	Strand diameter (in.)	A_p (in^2)	y_p (in)	Beam Type	y_b (in.)	A_g (in^2)	I_g (in^4)	V/S (in.)
I (8)	6.30 ksi	0.5	5.81	6.63	C	17.1	495	82600	3.96
II (8)	6.30 ksi	0.5	5.81	6.63					
III (8)	6.30 ksi	0.5	8.87	6.43	Tx46	20.1	761	198100	3.86
IV-SCC (3)	6.05 ksi	0.5	8.57	6.64					
IV-CC (3)	6.05 ksi	0.5	8.57	6.64					

A_p: Total area of strands

y_p: Centroid of strands

y_b: Height of the centroid

A_g: Total area

I_g: Moment of inertia

V/S: Ratio of volume to surface

SCC: Self-Consolidating Concrete

CC: Conventional Concrete

3.2.2 Fabrication

Specimens were obtained from multiple fabrication plants to assess the influence of plant-specific materials and techniques on the development of prestress loss. In the first few months of the project, concrete mixtures and fabrication techniques employed by various precast concrete plants throughout Texas were studied. The study was conducted on materials data

collected during the course of TxDOT Project 0-5197. The goal of this study was to identify a "most critical" combination of materials and fabrication techniques in regards to the loss of prestress. During the course of the study, the PMC and FSEL researchers ultimately agreed that such a determination was impractical given the project timeline. Final selection of the fabrication plants from a jointly-determined list was left to the discretion of Ferguson Structural Engineering Laboratory (FSEL). Selection of the fabricator for each series of specimens is described below.

- *Fabrication plant for Series I and II*: Plant A, in San Antonio, was noted for particularly low concrete stiffness at release and high long-term cambers, and was chosen to examine the effect of low concrete stiffness on prestress loss. Plant B, in Waco, was perceived to have moderate strength gain, and low long-term cambers. While some fabrication differences were noted between the two plants, the cause for variation between beams produced in the different plants seemed to be tied to the coarse aggregate supply. The siliceous river gravel used by Plant B is much harder than the crushed limestone used by Plant A; leading to a large disparity in elastic modulus between concretes used at the two plants (approximately 40% higher at Plant B). The decision was made to cast the first two series of research specimens at Plants A and B.

- *Fabrication plant for Series III*: Preliminary data from the internal instrumentation indicated that the initial prestress losses were much higher for the Series I beams fabricated at Plant A and the use of crushed limestone aggregate, as opposed to river gravel, was judged to be significant in terms of this disparity. It was therefore determined that the concrete mixture for Series III should contain crushed limestone coarse aggregate. Fabricator selection was further limited by a TxDOT PMC-directive to examine prestress loss development within a TX girder cross-section. The new standards for TX Girders were released immediately in advance of TxDOT Project 0-6374 and fabrication of TX girders was extremely limited at the time of the Series III letting process. Plant A was ultimately selected for Series III beams because it was the only fabricator that offered TX girders (Tx46) made with the required aggregate (limestone).

- *Fabrication plant for Series IV*: The specimens of Series IV were fabricated as part of a PCI-funded fellowship awarded to Dunkman and Bayrak in 2010. The primary objective of the fellowship work was to evaluate the impact of self-consolidating concrete (SCC) on the end region cracking in pretensioned girders; prestress losses were assessed in a secondary effort. A fabricator in Eagle Lake (Plant C) was selected on the basis of its experience with SCC (as approved by TxDOT) and its willingness to donate the specimens. Three of the six specimens within Series IV were fabricated with SCC, while the remaining specimens were fabricated with conventional concrete (CC). The influence of the concrete type on the long-term prestress losses is examined later in this report.

The most relevant details of each fabricator, including coarse aggregate type and average local humidity, are presented in Table 3.3. The geographic location of each fabricator is shown in Figure 3.8. Following the selection of each fabricator, specimen design documents were

submitted for review and a standard mixture was identified on the basis of the release strength requirements. The concrete mixtures utilized by each fabricator are presented in Table 3.4.

Table 3.3 – Fabricator information

Fabricator	Series	Location	Coarse Aggregate	Concrete Type	Average Humidity at Plant Location*
A	I and III	San Antonio	Limestone	Conventional	65%
B	II	Elm Mott	River Rock	Conventional	65%
C	IV	Eagle Lake	River Rock	Conventional and SCC	75%

*Based on Humidity map in AASHTO 2010

Table 3.4 – Typical concrete mixture proportions

Material	Units	Quantity				
		Series I	Series II	Series III	Series IV	
					SCC	CC
Type III Portland Cement	lb/cy	540	530	660	700	600
Fly Ash	lb/cy	170	170	220	230	200
CA	lb/cy	1850 (¾" Crushed Limestone)	1970 (¾" River Gravel)	1850 (¾" Crushed Limestone)	1540 (½" Natural Gravel)	1780 (½" Natural Gravel)
FA: Sand	lb/cy	1220	1310	1030	1240	1220
Water	lb/cy	180	115	180	270	220
HRWR Admixture	oz/cy	33	50	18	37	36
Set Retardant Admixture	oz/cy	31	14	44	9	12
Water/Cement Ratio		0.34	0.22	0.27	0.39	0.37
CNI Admixture	oz/cy	-	-	-	115	144
Viscosity-Modifying Admixture	oz/cy	-	-	-	15	-

The fabrication of each specimen was consistent with the practices used on a routine basis at local precast plants. The researchers of TxDOT Project 0-6374 did not intervene during, or impose special requirements on, the fabrication process to ensure that the prestress loss assessments would be representative of typical girders. Relevant aspects of the fabrication process are summarized in Figure 3.4.
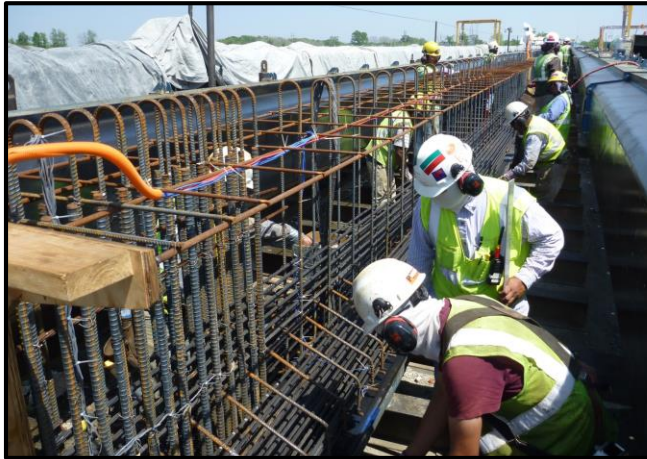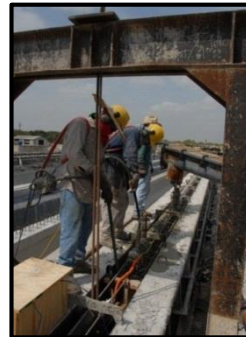
Figure 3.4 – Fabrication of a typical specimen: (a) harping of strands, (b) tensioning of strands, (c) placement of mild reinforcement, (d) installation of side forms, (e) concrete placement, (f) internal vibration, (g) external vibration

After the prestressing strands were loosely run the length of the pretensioning bed, the hardware required to achieve the harped strand profile was installed. Fabricator A utilized assemblies of coil rods, rollers and support structures to fully stress the prestressing strands in the final harped position (as shown in Figure 3.5). The rollers were used to guide the strands and limit the development of friction at the hold-down and hold/pull-up points. In contrast,

Fabricators B and C partially stressed the strands in a straight configuration and then utilized long-stroke hydraulic cylinders to push the strands down into the final harped position (as shown in Figure 3.6). The use of rollers by Fabricators B and C was limited to the support structures at the beam ends; the interface between the strands and each push-down assembly was fixed.

(a)   (b)
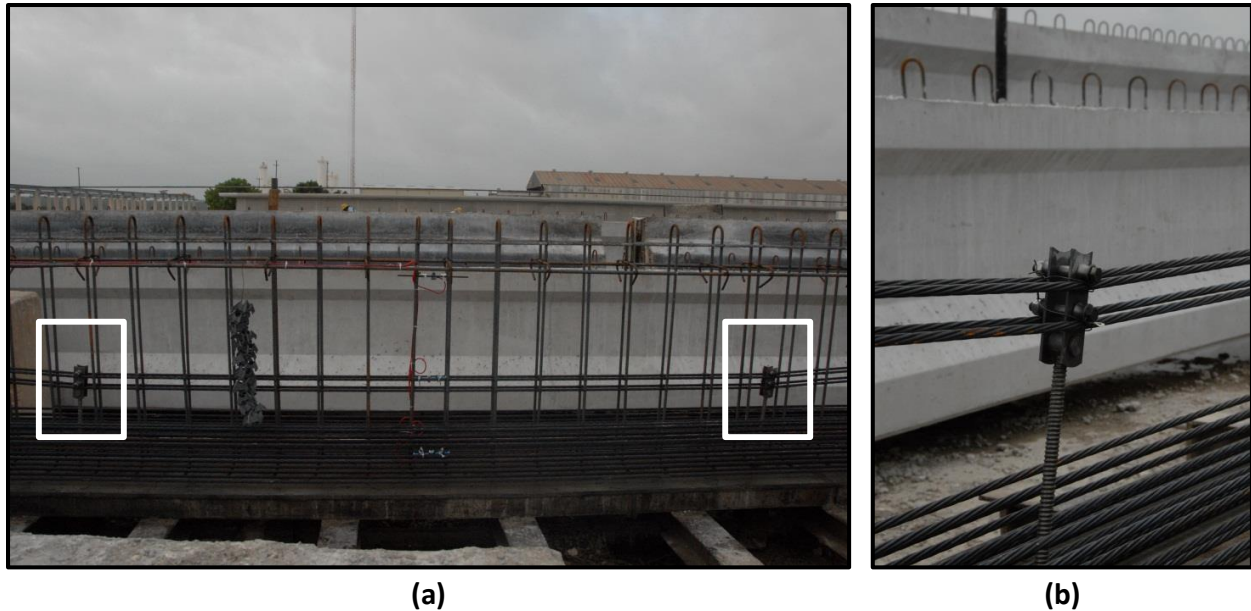
Figure 3.5 – Strand harping method at Fabricator A

(a)   (b)
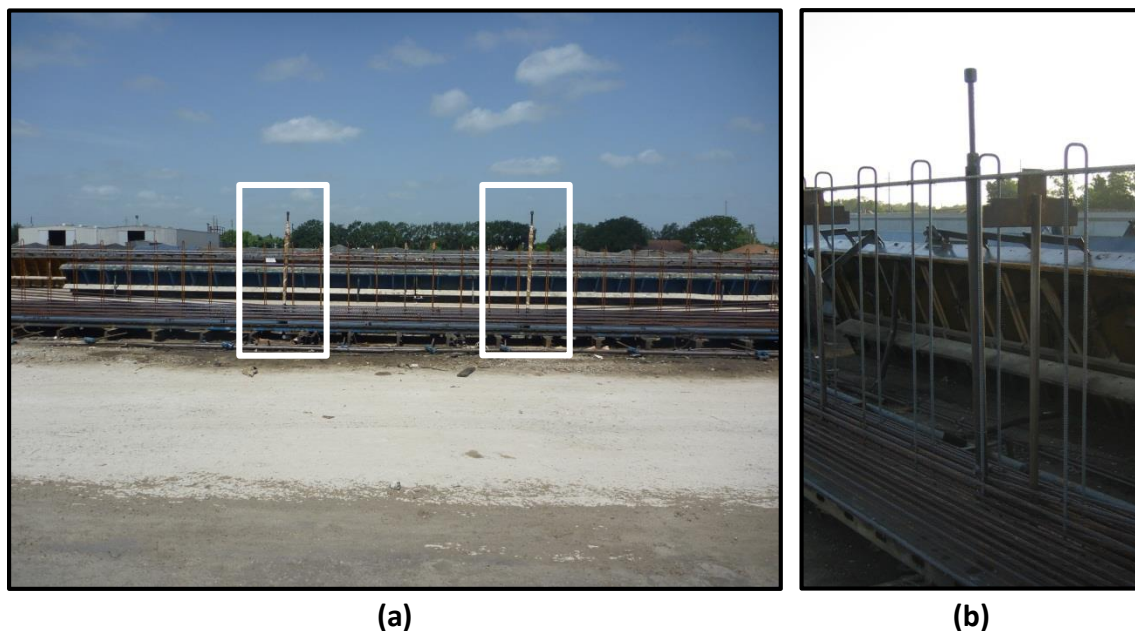
Figure 3.6 – Strand Harping Method at Fabricator B and C

Each fabricator tensioned the prestressing strands on an individual basis as shown in Figure 3.4 (b). All of the precast plants possessed the equipment necessary for group tensioning

of the strands, but individual strand tensioning allowed for more accurate control of the pretensioning operations. The reinforcement cages for each specimen were assembled around the fully stressed strands and the internal vibrating wire gages (refer to Section 3.3 for more detail) were installed thereafter. All of the concrete was batched at the precast plant; mix proportions can be found in Table 3.4. Both external and internal vibrators were used during placement of the conventional concrete mixtures to ensure proper consolidation.

The beams were moist cured until the specified release strength (f'_{ci}) was attained. At that time, the formwork was removed and the prestressing force was transferred from the pretensioning bed to the specimens. Torch-cutting of the strands at the beam ends and release of the hold-down devices completed transfer of the prestressing force. A counterweight, shown in Figure 3.7 (b), was utilized as necessary to minimize the potential for cracking during prestress transfer. The beams were placed in the precast storage yard until a shipment could be arranged.

(a)

(b)

(c)

(d)
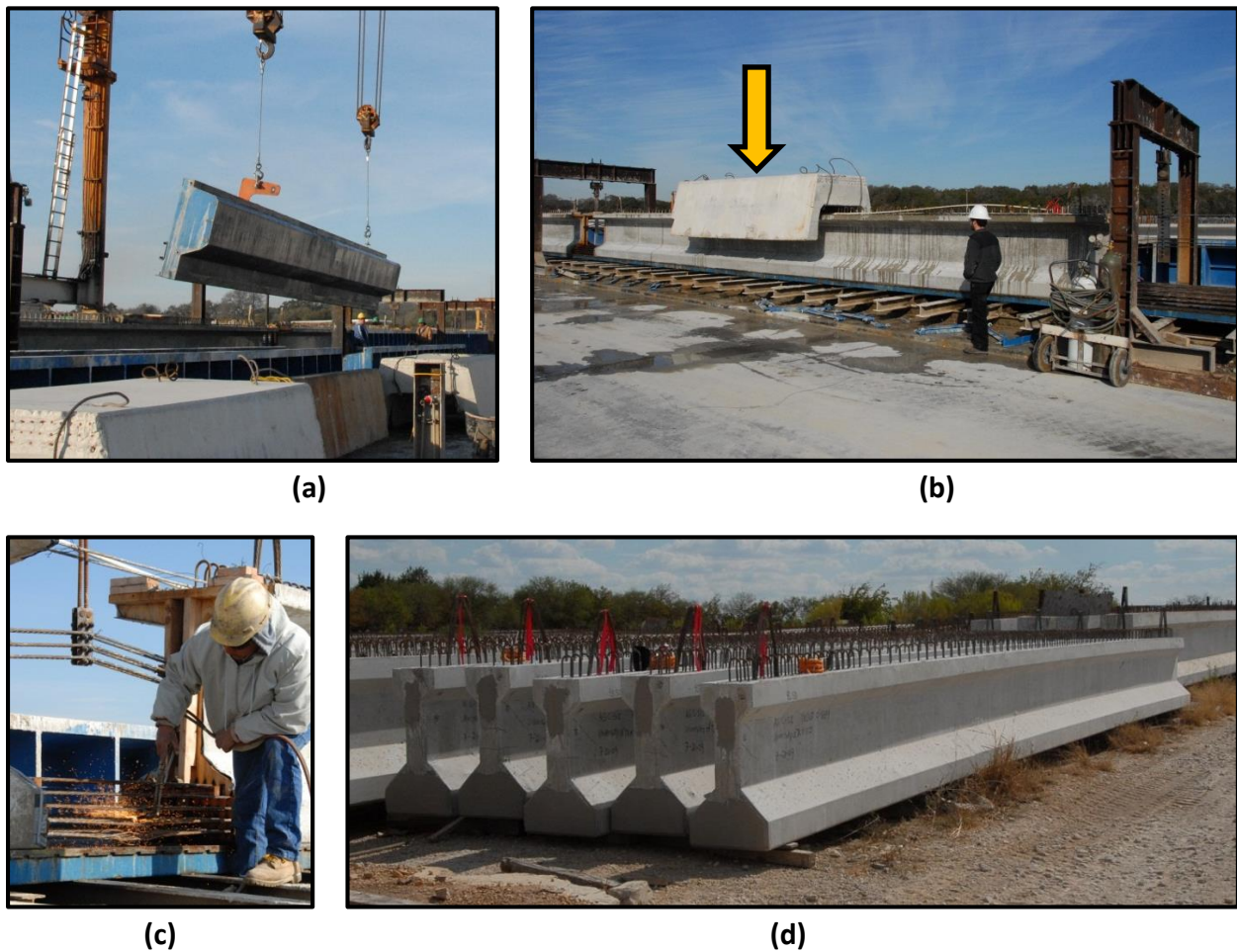
Figure 3.7 – Fabrication of a typical specimen: (a) form removal, (b) counterweight location, (c) torch-cutting of strands, (d) temporary storage in precast yard

3.2.3 Conditioning

Previous research (ACI 209R 2008) has indicated that climatic conditions (i.e. humidity and temperature) have a notable effect on the shrinkage and creep of concrete. The study of long-term prestress loss (as driven by creep and shrinkage) in different climatic conditions was therefore an essential consideration for the current effort.

The fabrication of each series was generally completed in less than three days and the specimens were shipped to their conditioning locations within two to three weeks of initial prestress transfer. The specimens remained in their respective conditioning locations until the time of flexural testing at FSEL. The five conditioning locations are characterized below. Meteorological data was obtained from the National Climatic Data Center (NOAA 2012).

- *Lubbock:* The climate of Lubbock is classified as mild, semiarid. The annual average relative humidity is 71 percent in the morning and 53 percent in the afternoon. Approximately 19 inches of precipitation falls each year, including 10 inches of sleet and snow. Lubbock experiences approximately 160 clear days and 102 partly cloudy days each year under an average wind speed of 12 miles per hour. In comparison to the Central Texas cities outlined below, the semiarid, windy climate of Lubbock was expected to have the greatest influence on development of the prestress losses.

- *Austin:* The climate of Austin is classified as humid subtropical. The annual average relative humidity is 81 percent in the morning and 64 percent in the afternoon. Approximately 34 inches of precipitation falls each year over approximately 136 cloudy days and 114 partly cloudy days. The average annual wind speed in Austin is 8 miles per hour. The climate of Austin is similar to that of other large cities along the I-35 corridor of Texas (e.g. Dallas, Fort Worth, Waco and San Antonio) and it therefore provided a convenient means for representative conditioning of the specimens.

- *San Antonio and Elm Mott:* The climatic conditions in San Antonio (Fabricator A) and Elm Mott (Fabricator B) are very similar to that found in Austin. Nevertheless, storage of a subset of specimens in these locations offered an opportunity to account for the climatic variation along the I-35 corridor.

Six of the eight specimens within Series I through III were evenly split between the two primary storage locations of Austin and Lubbock. The remaining two of eight specimens within each Series I through III were placed into storage by the fabricator (four specimens in San Antonio and two specimens in Elm Mott). All of the Series IV beams were transported to and stored in Austin. The fabricator locations and conditioning sites are shown in Figure 3.8. The timeline of the fabrication-conditioning-testing process for each series is detailed in Table 3.5.
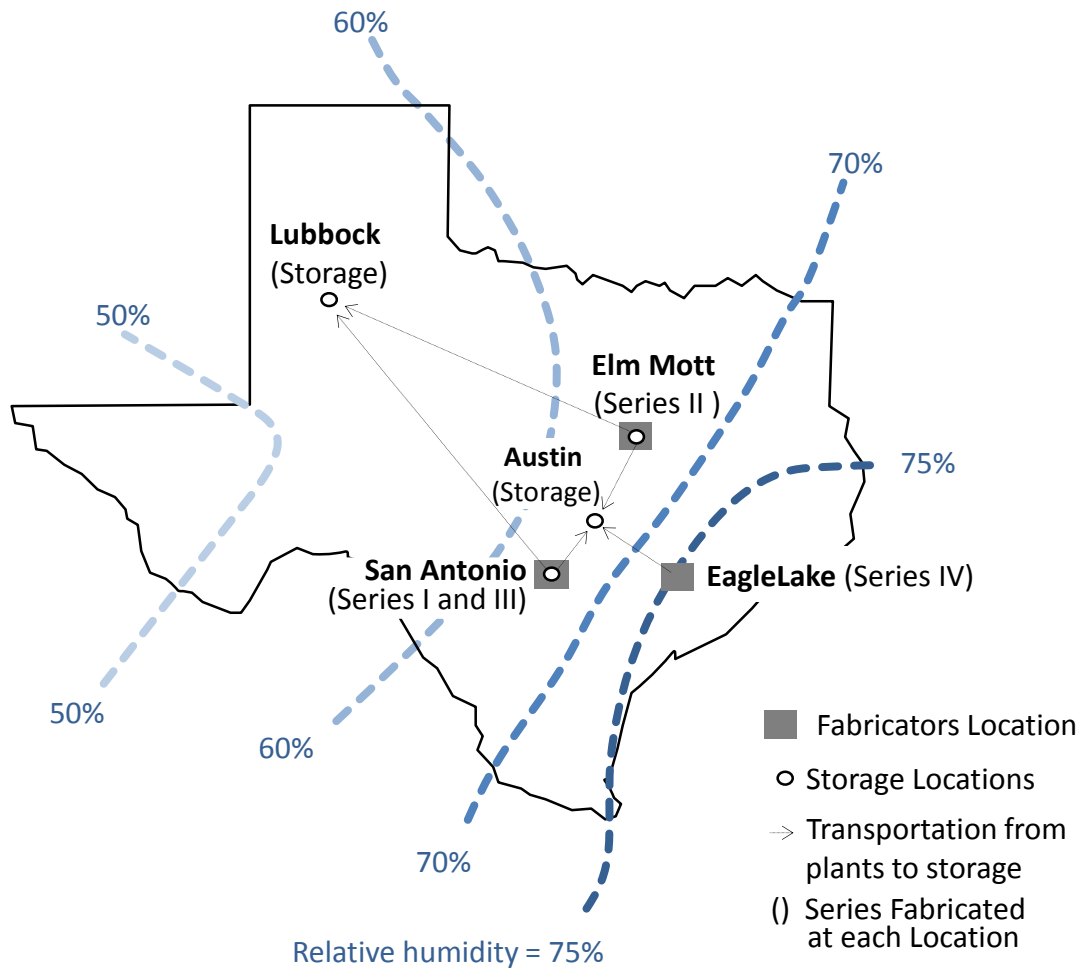
Figure 3.8 – Fabrication and storage locations

Table 3.5 – Timeline of beam conditioning

Series	'08	2009	2010	2011	2012
I	Fabrication →				
II					
III					
IV				← Testing	

Storage of the specimens in Austin and Lubbock is shown in Figure 3.9 and Figure 3.10, respectively. During storage, each of the specimens was supported on both ends, creating a span length of approximately 44 feet (similar to the flexural testing span). The specimens remained uncovered (fully exposed to the site climate) during the conditioning time and were periodically monitored for changes in strain (as indicative of prestress losses) and camber.

Figure 3.9 – Austin storage site (Series I, II, III and IV)

Figure 3.10 – Lubbock conditioning site (Series I, II and III)

The variation of relative humidity and temperature at each of the storage locations is summarized in Figure 3.11. Despite significant variation of the climatic conditions during the course of TxDOT Project 0-6374 (i.e. Central Texas drought), the average temperature and humidity at each of the conditioning sites was relatively consistent with the historical data referenced above. Specimens stored in Lubbock were exposed to an average relative humidity of approximately 50 percent, while those stored in Austin were exposed to an average relative humidity of approximately 60 percent. The data reported here was taken from the nearest weather stations as reported by the National Climate Data Center.
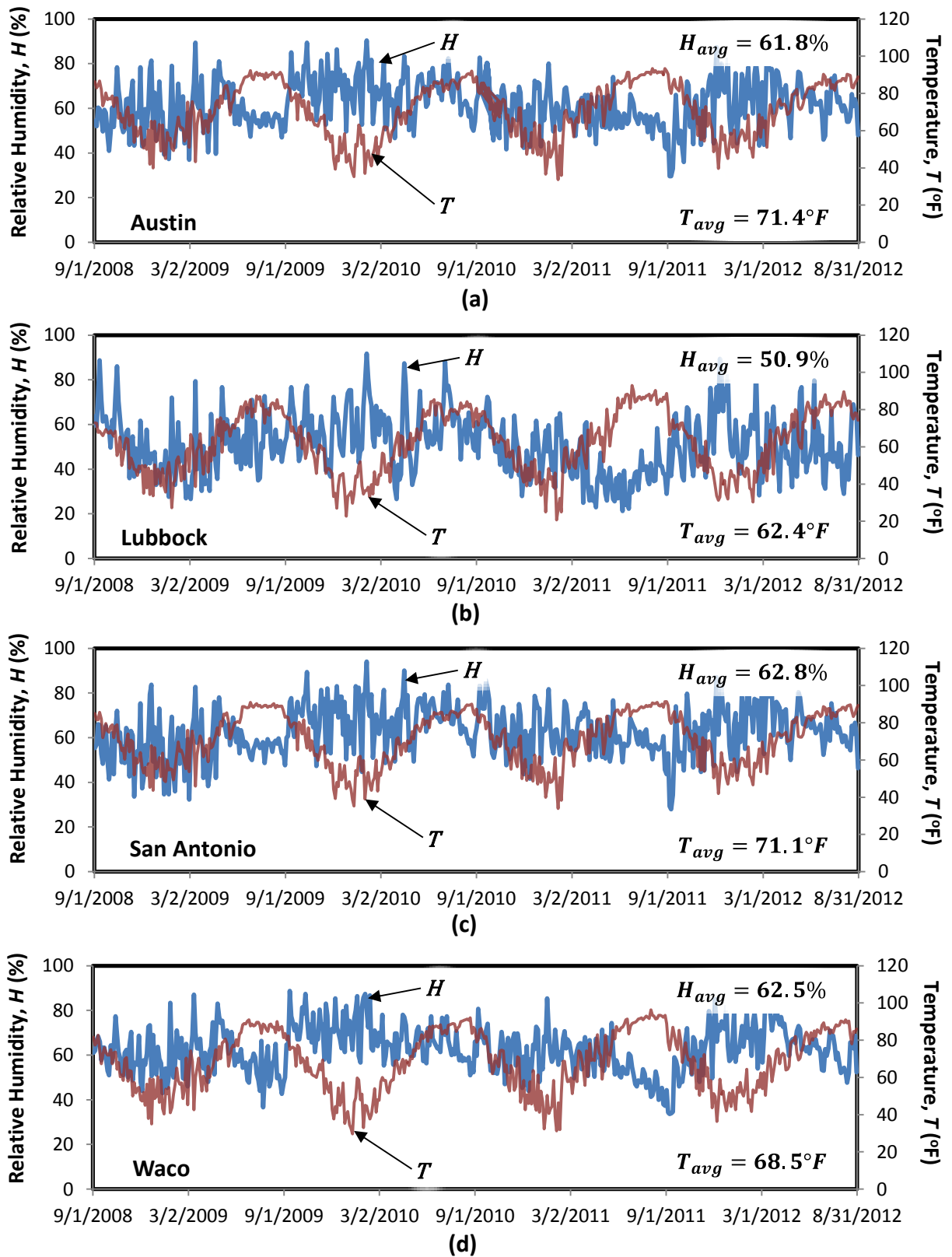
Figure 3.11 – Record of relative humidity and temperature at each conditioning site (NOAA 2012)

3.3 ASSESSMENT OF PRESTRESS LOSS VIA INTERNAL STRAIN MONITORING

The development of prestress loss within 18 of the 30 specimens was monitored through the use of internal strain instrumentation. Concrete strains and temperatures were measured at several points through the depth of each instrumented cross-section and used to calculate the change of strain at the centroid of the prestressing strands. Due to compatibility between the prestressing strands and the surrounding concrete, it was possible to further calculate the loss in prestressing force on the basis of the prestressing strand modulus and area.

The concrete strain and temperature were measured periodically throughout the conditioning of each specimen. Internal concrete strains were capture through the use of vibrating wire gages (VWGs) that were well suited to the long-term measurements completed during the course of TxDOT Project 0-6374. Gage installation, periodic monitoring techniques and formal assessment of the prestress losses are examined within the following sections.

3.3.1 Vibrating Wire Gage Installation

A vibrating wire gage consists of a length of steel wire stretched between two end blocks; the wire is enclosed and free to deform with the movement of the end blocks. When embedded in concrete, the vibrating wire gage can be used to measure concrete strain: the wire in the gage is plucked electromagnetically and the change in the resonant frequency of its response indicates the change in strain of the wire, which is the same as that of the surrounding concrete.

Vibrating wire gages (as opposed to foil strain gages) were chosen because of the long-term stability of their readings and their durability in the highly alkaline environment of hardened concrete. Confidence in the latter of these benefits was provided by a past TxDOT project (Gross and Burns, 2000) involving the measurement of prestress losses; the attrition of vibrating wire gage functionality over the course of a five year period was much less than that of foil strain gages.

Typical installation of the vibrating wire gages within the TxDOT Project 0-6374 specimens is illustrated in Figure 3.12. Installation of the vibrating wire gages was completed immediately after the mild reinforcement was fully tied, with little interruption to the typical fabrication process. Three to four gages were installed at three distinct heights within the midspan cross-section and oriented to measure strains along the longitudinal axis of the specimen. Spacers were used to install each of the vibrating wire gages a sufficient distance from the surrounding reinforcement to ensure the free movement necessary for accurate measurements. To protect the lead wires from damage during concrete placement, they were routed under the prestressing strands to a location where all of the leads exited the beam.
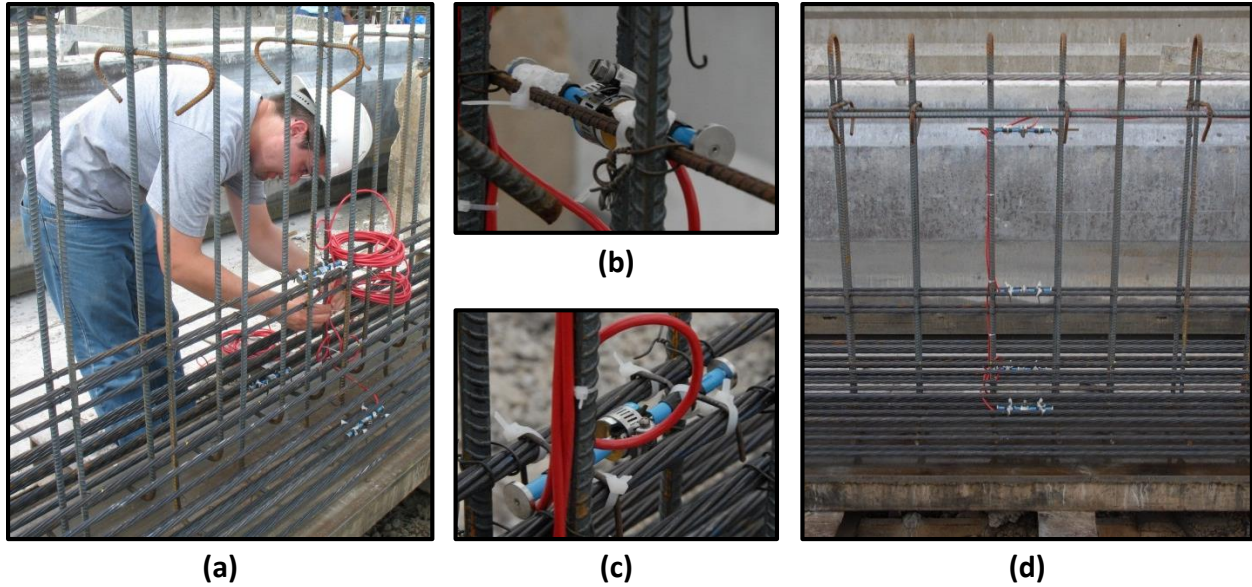
Figure 3.12 – Vibrating wire gage installation: (a) cable routing, (b) gage supported by auxiliary reinforcement, (c) gage supported by a strand, (d) midspan distribution of gages

The VWG embedment locations for each series of specimens are illustrated in Figure 3.13. All of the gages in each specimen were installed at the midspan cross-section. Placement of the gages at this location ensured that prestress losses assessed via the two methods (internal strain monitoring and flexural testing) would correspond to the same region of the beam. Moreover, the middle portion of the beam was subject to the greatest pre-compression (no harping) and potential for prestress loss.
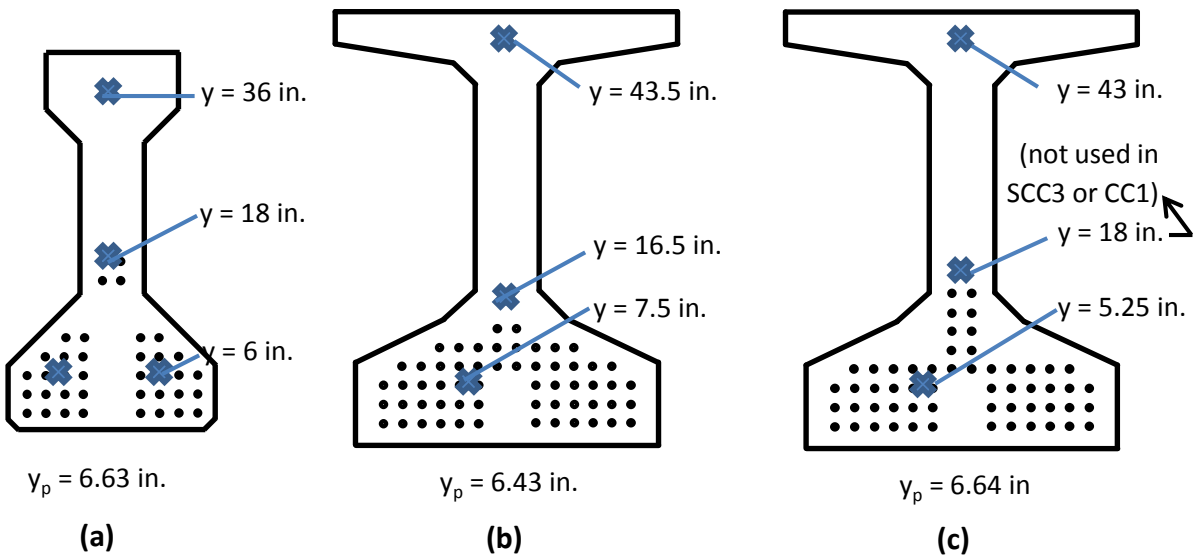
Figure 3.13 – VWG embedment locations

3.3.2 Periodic Monitoring Efforts

The concrete strains were measured before and after prestress transfer - to assess the prestress loss due to elastic shortening - and periodically throughout the conditioning process – to assess long-term prestress losses due to creep and shrinkage. It should be noted that by monitoring the beams in this manner, the total long-term prestress losses, not the individual components or creep and shrinkage, were measured.

The vibrating wire gage measurements were taken through the use of a handheld reader and/or a remote Data Acquisition System (DAQ). The remote DAQ, fabricated at FSEL, and deployed in Lubbock is shown in Figure 3.14. It consisted of a datalogger, cellular modem and solar power supply. The DAQ was programmed to periodically interrogate the VWGs (approximately once per hour) and store the concrete strains in memory. All of the data recorded by the DAQ was accessible from FSEL via cellular modem.

(a)   **(b)**
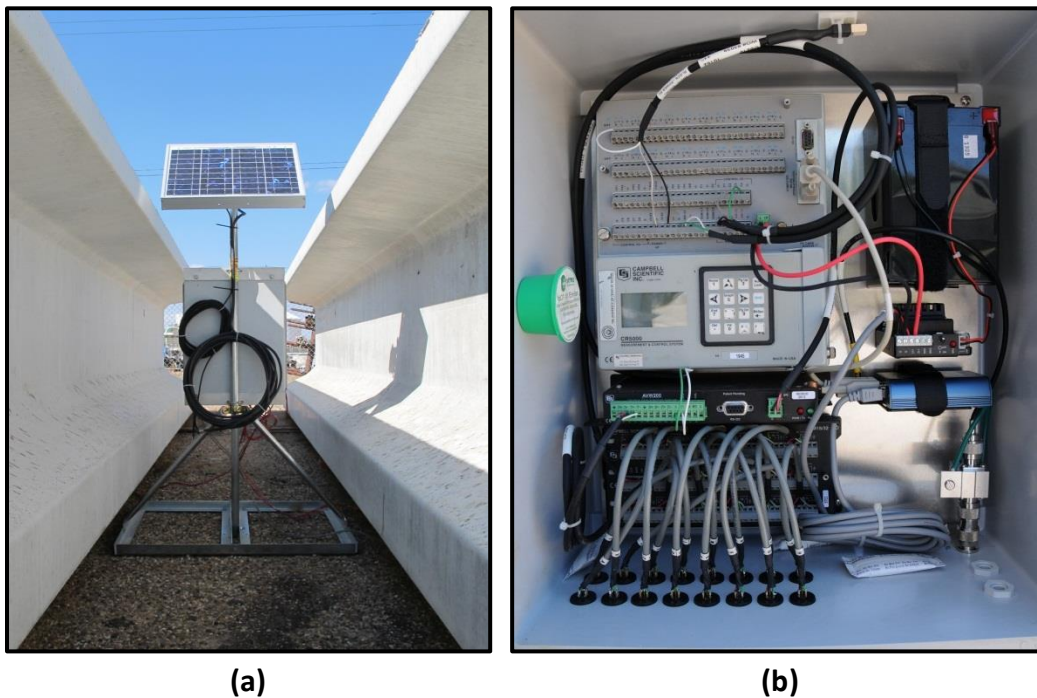
Figure 3.14 – Remote DAQ system: (a) General view and (b) electronic components

3.3.3 Prestress Loss Calculation / Analysis

Measurement of the change in concrete strain from the time of prestress transfer to the time of interest provided a means of assessing the total prestress loss in each specimen. The relationship between prestress loss, strand and concrete strains is summarized in Equation (3.1). Determination of the strain in the prestressing strands is illustrated in Figure 3.15.

$$\Delta f_p = \Delta \varepsilon_p \cdot E_p + \Delta f_{pRE} = \Delta \varepsilon_c \cdot E_p + \Delta f_{pRE} \qquad \textbf{(3.1)}$$

where:

Δf_p = Prestress losses (ksi)

$\Delta \varepsilon_p$ = Strain change in the strand

$\Delta \varepsilon_c$ = Strain change in the concrete
E_p = Modulus of elasticity of the strand (ksi)
Δf_{pRE} = Relaxation of the strand (ksi)

With the VWGs distributed through the depth of the midspan cross-section, a linear strain profile could be developed and the longitudinal strain at a location of interest (the centroid of the prestressing force or the bottom fiber of concrete, for example) could be determined by linear interpolation or extrapolation. Using linear methods to find the strain at the locations of interest was appropriate as plane sections remained plane within the specimens; a tenet of beam theory that was verified by the VWG readings. For a given point in time, the effective prestress loss could therefore be calculated by taking the change in concrete strain at the centroid of the prestressing strand, compared to the measurements taken just before prestress transfer, and multiplying it by the modulus of elasticity of the prestressing strand; as done in Equation (3.1).
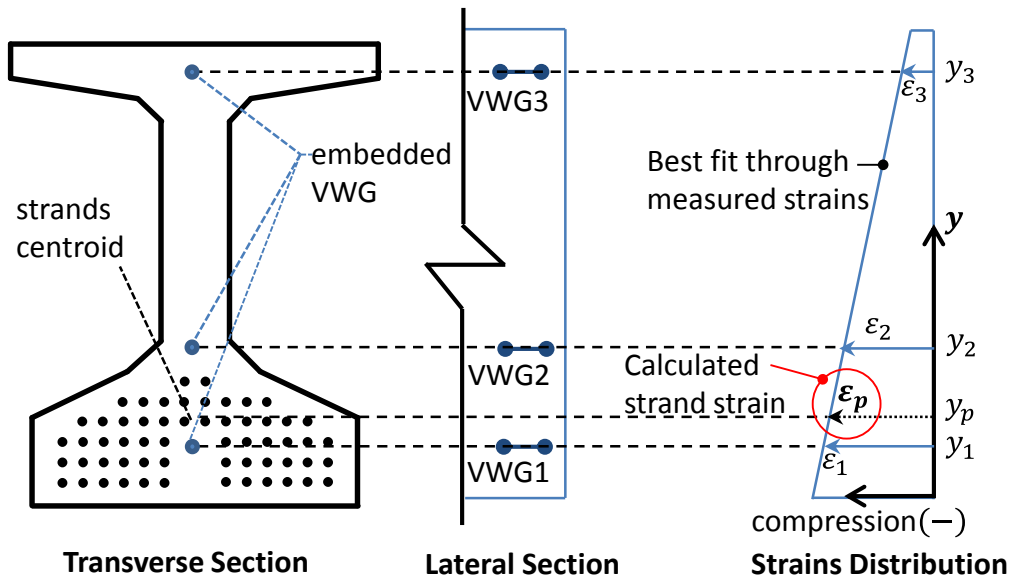
Figure 3.15 – Determination of strain in prestressing strands

It is important to note that the strain monitoring technique is incapable of capturing the prestress losses due to strand relaxation as the phenomenon leads to a loss of stress without a corresponding change in strain. Resolution of the discrepancy, among others, through processing and analysis of the data is outlined here.

- *Accounting for Relaxation*: It should be noted that this monitoring method is limited to strain-related stress changes, so relaxation of the strands is not directly captured. This limitation was overcome by using existing equations that estimate the well-known phenomenon which accounted for less than 5 percent of total final losses in most of the cases.

- *Need for Uniform Stress Conditions*: It is important to avoid regions with disturbed stress fields (e.g. within the strand transfer length) to ensure that plane sections will remain plane and that the concrete and strand strains will indeed be compatible. The

specimen length (45.5 ft.) was at least an order of magnitude longer than the strand transfer length in this study, ensuring that the gages were not placed in a region with a disturbed stress field.

- *Consideration of Temperature Effects*: There was a dependence observed between temperature and the losses assessed using the strain monitoring approach. These fluctuations reflect a real change in stress that occurs in the strands. When the temperature drops, the concrete and the strands would shorten individually according to their coefficients of thermal expansion. As these two materials are bonded the concrete restricts the strand from shortening and a stress in the strand develops; this stress is proportional to the difference in coefficients of thermal expansion of the steel as compared to that for the concrete. The change in stress is temporary and for ages at which the losses are in general stable, the losses appear to be reduced during some months and increased during others. A correction to eliminate this fluctuation (outlined below) was conducted as it was beneficial to assess the losses that permanently affected the stress in the strands.

Correction for the temperature effects consisted of subtracting the thermally induced stress from the calculated stress, as shown in Equation (3.2) using a datum temperature of 95°F. Coefficients of thermal expansion based on measurements conducted on Series I through III were used for this correction.

$$\Delta f_{p\_corrected} = \Delta \varepsilon_p \cdot E_p - (\alpha_{steel} - \alpha_{concrete})(-\Delta T) \cdot E_p \qquad \textbf{(3.2)}$$

where:

$\Delta f_{p\_corrected}$ = Temperature corrected prestress losses (ksi)
$\Delta \varepsilon_p$ = Strain change measured by VWG
E_p = Modulus of elasticity of the strand (ksi)
ΔT = Temperature change respective to datum temperature (°C)
α_{steel} = Coefficient of thermal expansion of steel (12 με/°C)
$\alpha_{concrete}$ = Coefficient of thermal expansion of concrete (με/°C) (see Section 4.2.1)

3.4 ASSESSMENT OF PRESTRESS LOSS VIA FLEXURAL CRACKING

The flexural demands (e.g. moment due to load) under which a pretensioned girder will crack is uniquely dependent on the beam geometry, concrete tensile strength, and effective prestressing force. Measurement of the cracking moment and concrete tensile strength and knowledge of the beam geometry should therefore enable back-calculation of the effective prestressing force, and by association, the prestress losses.

The long-term prestress loss within all 30 specimens was assessed via flexural cracking. Four-point loading of the specimens created a constant moment region in which flexural cracking could be positively identified and correlated to the flexural demands. Visual inspection and load-deflection analysis techniques were used to identify the flexural cracking load. The test setup and testing protocol are described in Sections 3.4.1 and 3.4.2, respectively.

3.4.1 Test Setup

The flexural demand necessary to crack the specimens was applied through a four-point loading scheme. Each of the specimens were centered underneath a four-column test frame capable of resisting 800 kips of force, as illustrated in Figure 3.16 and photographed in Figure 3.18. A hydraulic ram, attached to the test frame, pushed down on the specimens through an assembly consisting of a spherical head, load cell, and transfer beam. The loading assembly was carefully centered on the specimen to minimize the potential for eccentric loading and premature flexural cracking. The transfer beam reacted against the specimen through small neoprene bearing pads placed 33½ inches from midspan, thereby creating a constant moment region of suitable length for the identification of first flexural cracking.
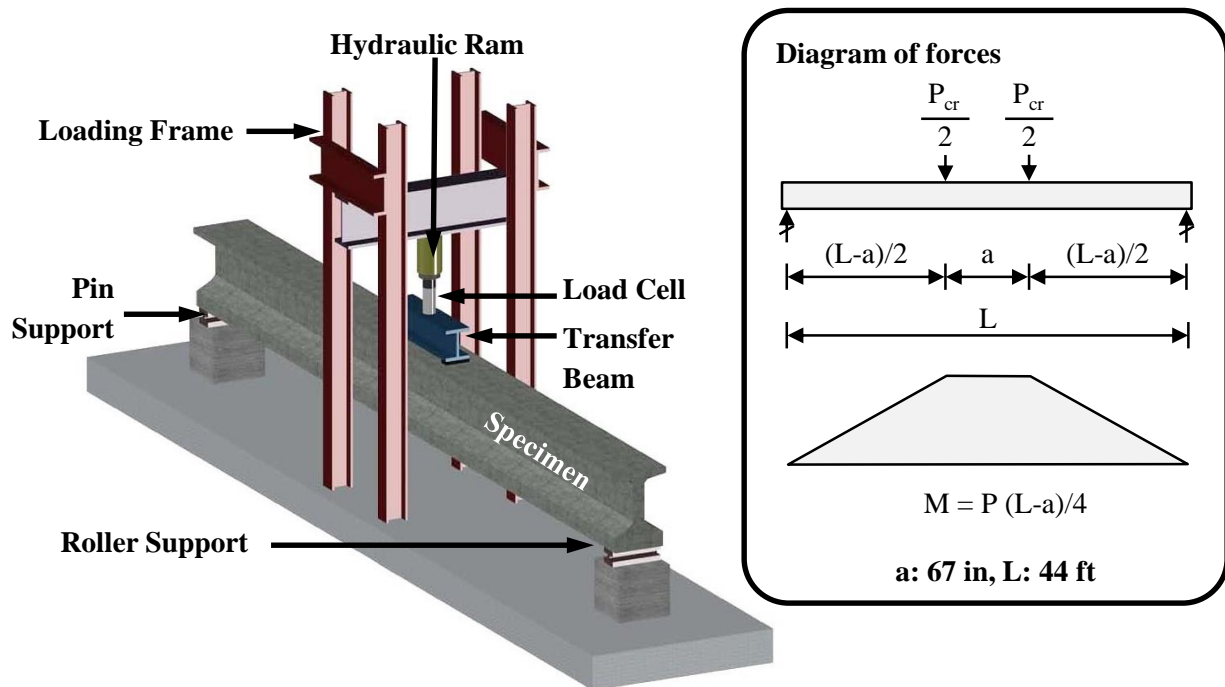
Figure 3.16 – Schematic of flexural test setup

Each of the specimens was simply supported, with a pin or a roller (i.e. free to translate along the longitudinal axis of the beam) at opposite supports, as exemplified in Figure 3.17. The center-to-center distance of the pin and roller supports was 44 feet, leaving 9 inches of specimen overhang at either support. The pin and roller assemblies were mounted on concrete blocks to provide necessary access to the bottom of each specimen for crack inspection purposes.

Figure 3.17 – Typical support assembly

Linear potentiometers were placed at the midspan and supports of each specimen as shown in Figure 3.18 and Figure 3.19. The linear potentiometer at each support was used to measure support settlement (if any) during the course of each flexural test. The linear potentiometers placed on either side of the beam at midspan allowed for: (1) measurement of the midspan deflection (taken as the average output of the two potentiometers) and (2) identification and resolution of eccentric loading (as indicated by specimen twist and uneven side-to-side deflection). The full flexural response of each specimen was characterized by the load and deformation measurements obtained from the load cell and linear potentiometers, respectively.

Linear
Potentiometers
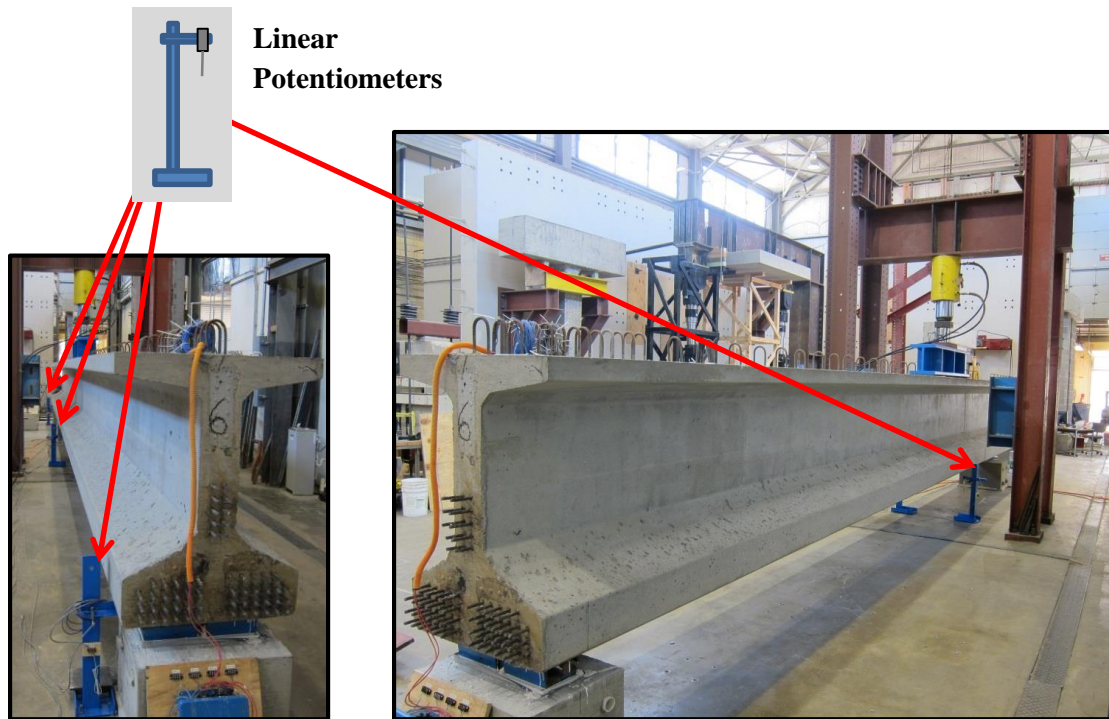
Figure 3.18 – Typical location of linear potentiometers

(a)

(b)
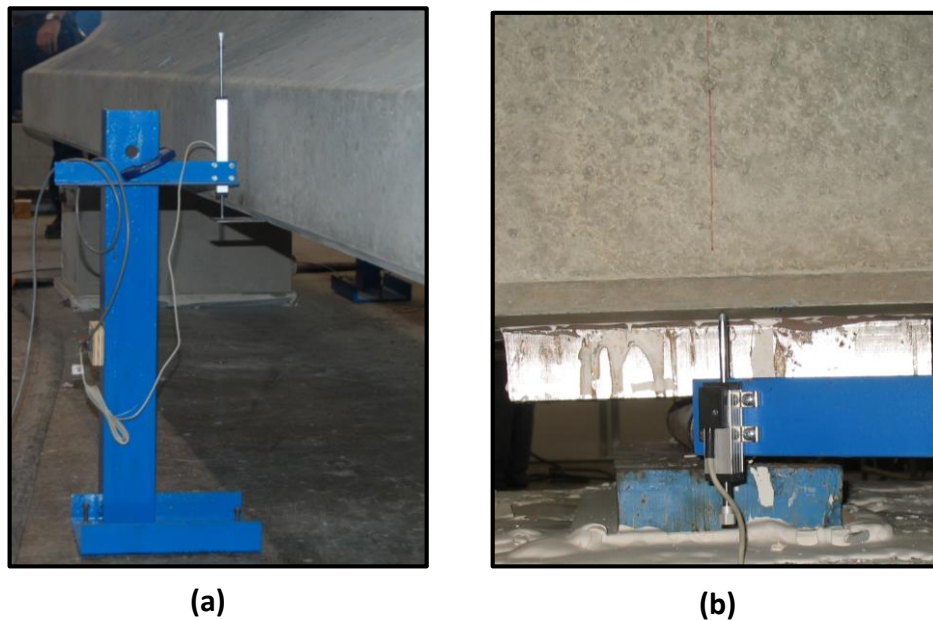
Figure 3.19 – Linear potentiometers installed at (a) midspan and (b) support

3.4.2 Flexural Testing Protocol

Prior to testing, the concrete tensile strength was measured via split cylinder tests. After the tensile strength was determined, the beams were loaded at a rate of approximately ½-kip per second up to 75 percent of the estimated cracking load. At this point, additional load was applied in 10-kip increments (less than 6 percent of the measured cracking loads on average) until the

first crack was visually detected. After cracking, the loading was continued in increments of 20 to 50 kips until extensive cracking was observed. The load and deflection, obtained from the external instrumentation, was continuously recorded during the test. Between each load step: (1) the specimen was visually inspected for crack initiation and growth, (2) new cracks were marked on the specimen surface and (3) the test region was photographed to record the crack progression.

The testing procedure is illustrated in Figure 3.20. Crack growth and widening were observed using a microscope on various beams. In general, the crack width was in the range of 1×10^{-3} in. when detected by visual inspection, and larger than 3×10^{-3} in. when extensive cracking was observed (see Figure 3.21).
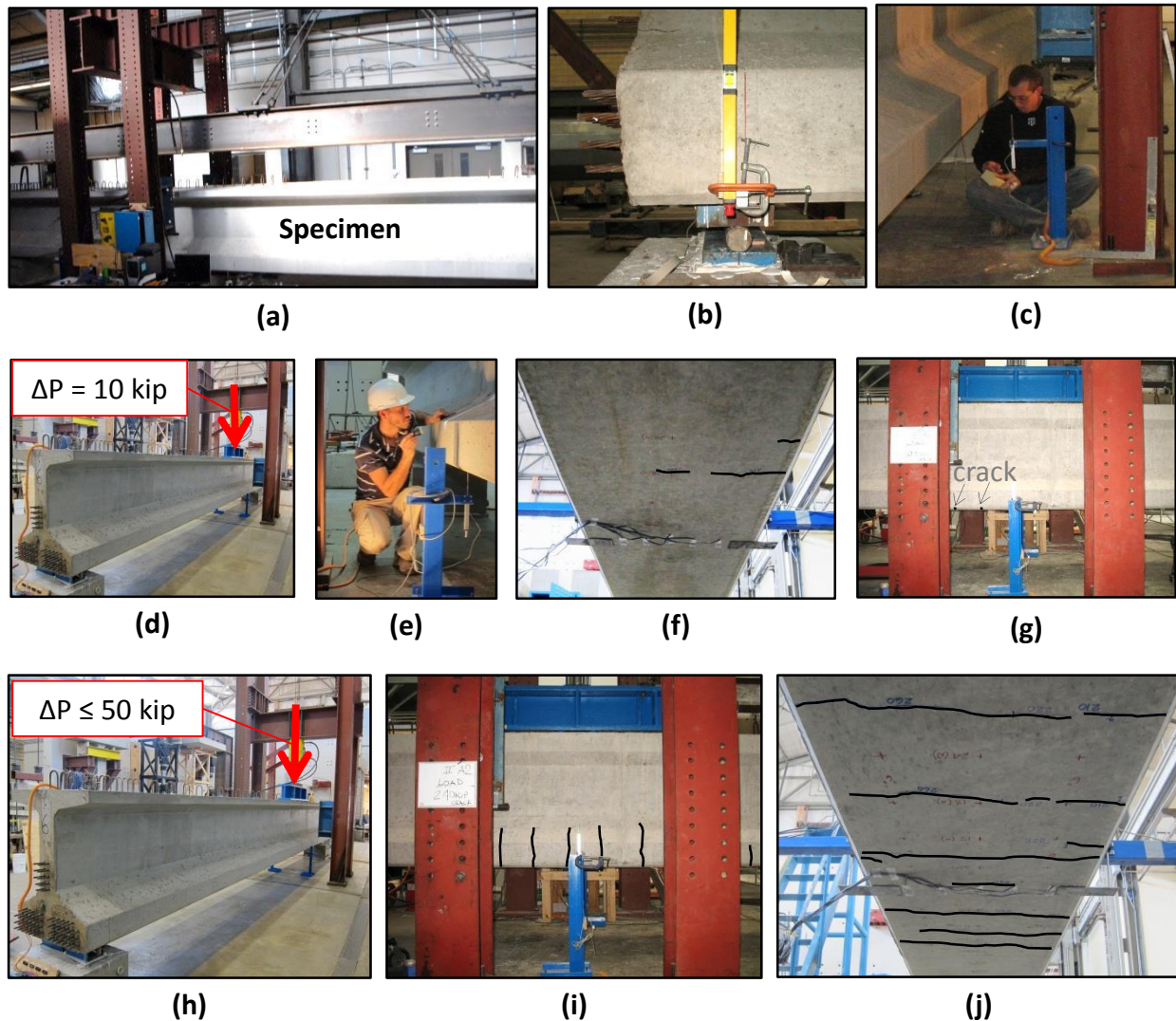
Figure 3.20 – Testing procedure: (a) installation of beam, (b) preparation of roller support, (c) installation of external instrumentation, (d) load step prior to cracking, (e) visual detection of cracking, (f) bottom of beam at first cracking, (g) side of beam at first cracking, (h) load step after cracking, (i) side of beam (extensive cracking), (j) bottom of beam at end of test

(a)   **(b)**

Figure 3.21 – Crack width: (a) at first cracking (width ≈ 1x10^{-3} in.), (b) at extensive cracking (width ≥ 3x10^{-3} in.)

3.4.3 Cracking Load Identification

The first flexural cracking was identified by: (1) visual inspection and (2) load-deflection analysis. Of the two methods, visual detection of first flexural cracking resulted in prestress loss assessments of more significant variability. The increased variability is attributed to a number of factors.

- *Premature cracking*: Small cracks may appear in localized areas of the beam fascia that are subject to higher stresses and/or lower concrete tensile strengths. These cracks may not be representative of the average response of the specimen, but are still subject to identification via visual inspection.

- *Human error*: Detection of the first crack relied on the ability of the researchers to perceive the crack, which is highly dependent on the individual and circumstances under which the visual inspections were conducted. Examination of the full surface of the bottom flange with a microscope was not practical, though it may have led to more repeatable identification of first flexural cracking.

- *Surface condition*: Detection of the earliest flexural cracks was also influenced by the condition of the concrete (shrinkage cracks, concrete surface roughness, color uniformity, etc.). In some cases the beams had rough surfaces and were significantly rust stained from conditioning; this made visual crack detection much more difficult.

A consistent method for identification of first flexural cracking was therefore developed on the basis of the measured load-deflection response. Assessments made on the basis of the load-deflection measurements were indicative of the global response of the specimen and were not influenced by the variation of the specimen condition, material properties or researcher capabilities. The procedure for determining the first cracking load on the basis of the load-deflection response is illustrated in Figure 3.22. This procedure includes:

- *Discretization of response*: The data from the load-deflection response was discretized into displacement steps of 0.02 inches. This discretization allowed for the stiffness of the response to be consistently calculated between each step and from specimen to specimen.

71

- *Calculation of stiffness*: The stiffness was calculated as $\Delta_{force}/\Delta_{displacement}$ for each displacement step. During the inspection stages (on which the loading was suspended) creep of the specimen resulted in the loss of load at a constant displacement. These drops were not related to crack occurrence and the stiffness was not calculated for the steps that coincided with inspection stages.

- *Calculation of moving average*: The moving average of the stiffness was calculated and plotted. These represented the average behavior of the beam from the beginning of the test to the beginning of each of the loading steps.

- *Identification of stiffness drop*: At the beginning of each test, the flexural stiffness varied within a well-defined band centered about the moving average; behavior that was indicative of an uncracked flexural response. Cracking was therefore noted to occur when the flexural stiffness consistently fell below the moving average; cracks reduced the effective area (and consequently the inertia) of the concrete that resists the flexural demands. This point marked the end of the linear behavior and was identified as first flexural cracking.

- *Determination of first cracking load*: The deflection corresponding to first flexural cracking was utilized within the context of the load-deflection response to obtain the flexural cracking load.
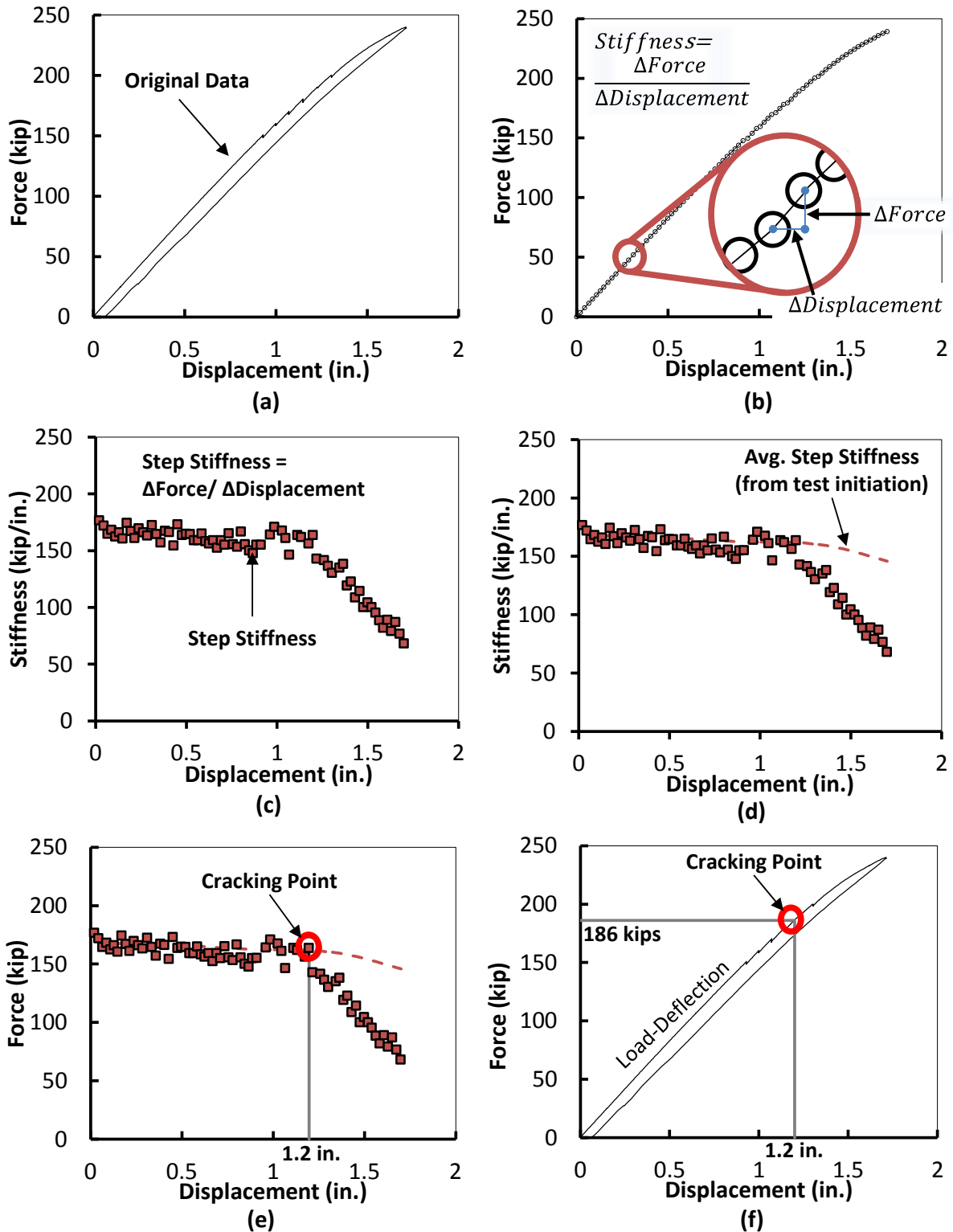
Figure 3.22 – Load-deflection analysis: (a) load-deflection response, (b) discretization of response, (c) calculation of stiffness, (d) calculation of moving average, (e) identification of stiffness drop, (f) determination of first cracking load

3.4.4 Prestress Loss Calculation / Analysis

The final prestress loss within each specimen was calculated on the basis of the flexural testing results. Specifically, the flexural cracking load - as identified by means of the load-deflection analysis and confirmed by visual crack identification - was used to back-calculate the effective prestressing and corresponding prestress losses. It is important to note that the prestress losses assessed in this manner included all potential components, including those due to elastic shortening, creep, shrinkage and relaxation.

A derivation of the expressions used to back-calculate the prestress losses is provided in Equations (3.3) through (3.6). These expressions illustrate the dependence of the prestress loss assessments on the measured tensile strength of concrete (f_{ct}) and first cracking moment of the specimen (M_{cr}). The expressions were obtained by imposing sectional equilibrium to calculate the stress at the bottom fiber of the cross-section, shown in Equation (3.3). At the point of cracking the beam experiences the effect of various loads: self-weight (M_g), strand force ($f_{pe}A_{ps}$), and externally applied moment (M_{cr}). The state of stress that these loads place on the beam is shown in Figure 3.23 and all effects were taken into account during the final analyses.
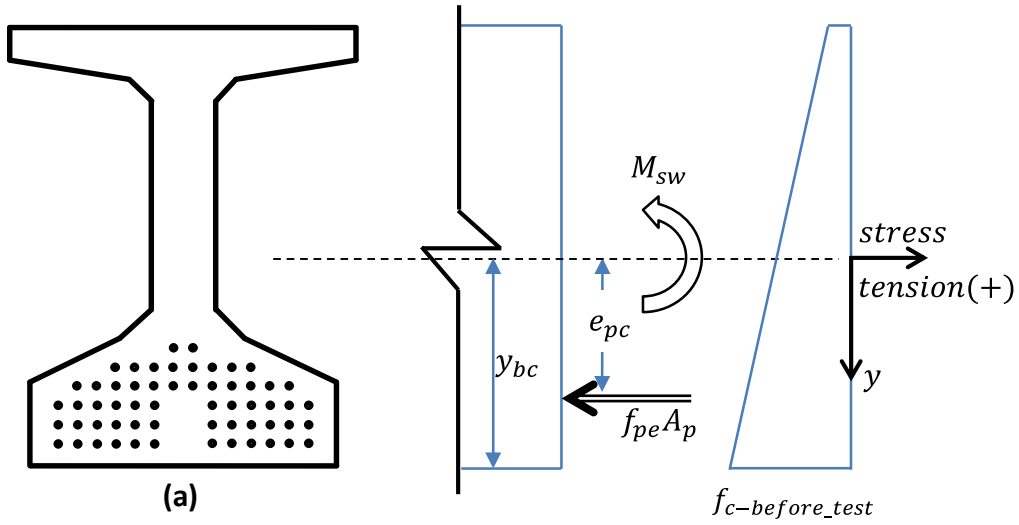
$$f_{c-before\_test} = M_{sw}\frac{y_{bc}}{I_c} - f_{pe}A_p\left(\frac{1}{A_c} + \frac{e_{pc}y_{bc}}{I_c}\right)$$
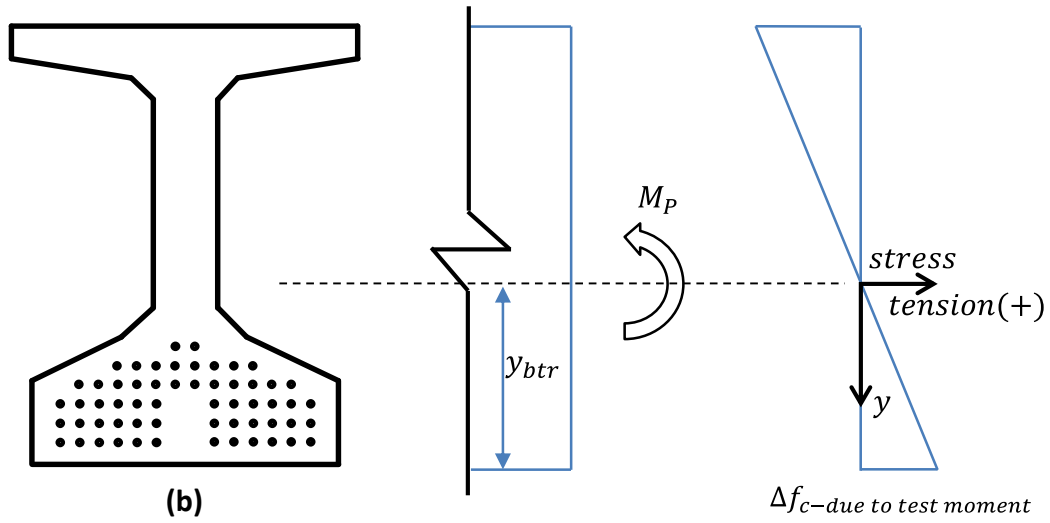
$$\Delta f_{c-due\ to\ test\ moment} = M_P\frac{y_{btr}}{I_{tr}}$$

Figure 3.23 – Determination of concrete stress (a) due to prestress and self-weight acting on concrete section (b) due to flexural test demands acting on transformed section

$$f_{c-crack} = M_{sw}\frac{y_{t\_c}}{I_c} - f_{pe}A_{ps}\left(\frac{1}{A_c} + \frac{e_{pc}y_{t\_c}}{I_c}\right) + M_{P-crack}\frac{y_{t\_tr}}{I_{tr}} \qquad \textbf{(3.3)}$$

$$f_{c-crack} \approx f_{ct} \tag{3.4}$$

$$f_{pe} = \frac{M_g \dfrac{y_{t\_c}}{I_c} - f_{ct} + M_{P-crack} \dfrac{y_{t\_tr}}{I_{tr}}}{A_{ps}\left(\dfrac{1}{A_c} + \dfrac{e_{pc} y_{t\_c}}{I_c}\right)} \tag{3.5}$$

$$\Delta f_p = f_{pj} - f_{pe} \tag{3.6}$$

where:

M_g = moment due to self-weight at studied section (midspan) (kip-in.)

$M_{P-crack}$ = moment due to cracking load at studied section (midspan) (kip-in.)

y_{t_c} = distance from extreme tension fiber to centroid of concrete section (in.)

y_{t_tr} = distance from extreme tension fiber to centroid of transformed section (in.)

I_c, I_{tr} = moment of inertia of concrete section and transformed section, respectively (in.[4])

f_{pj}, f_{pe} = average stress in the strands at jacking and at final age (before testing), respectively (ksi)

A_{ps}, A_c = total sectional area of strands and area of concrete section, respectively (in.[2])

e_{pc} = distance from centroid of concrete section to centroid of prestress strands (in.)

$f_{c-crack}$ = stress in the bottom of the beam at cracking load (ksi)

f_{ct} = tensile strength of concrete determined from split cylinder test (ksi).

Results of the flexural tests are summarized in Chapter 4. Due to a number of factors explained therein, the prestress loss assessments provided by the internal instrumentation (where available) are utilized as the final assessment of the prestress losses within the TxDOT Project 0-6374 specimens.

3.5 SUMMARY

The experimental program included the assessment of prestress losses in 30 full-size standard bridge girders. The specimens were designed, fabricated and conditioned considering influential variables that may affect prestress losses in structures fabricated within the State of Texas, including type of concrete, prestress level, specimen geometry, fabrication techniques, and climate. The cross-section types selected were Type C and Tx46. The amount of prestressing steel in each specimen varied from about 1.13 percent to 1.37 percent of the gross cross-sectional area.

Specimens were fabricated at multiple precast plants to assess the influence of plant-specific materials and techniques on the development of prestress loss. Overall, the main differences in the concrete mix between plants were the coarse aggregate type (river gravel versus limestone) and the type of concrete mix (conventional versus self-consolidating). The conditioning of the specimens was conducted in four storage locations (San Antonio, Elm Mott,

Austin and Lubbock) in order to observe the effect of different climate conditions (relative humidity ranging from 50 to 64 percent). The final variation of the parameters within the experimental program is summarized in Table 3.6.

Table 3.6 – Variation of specimen characteristics with respect to influential parameters

	Influential Parameter	Specimen Characteristics	
		As Designed	**As Built***
Conditioning	Final Age of Beam	--	230-980 days
	Storage Humidity	55% - 65%	49% - 65%
Concrete	Concrete type	Conventional and SCC	
	Coarse aggregate type	River Rock and Limestone	
	Release Strength (f'$_{ci}$)	6 – 6.5 ksi	5.8 – 7 ksi
	Standard Strength (f'$_c$)	8.5 – 12 ksi	9.6 – 12 ksi
	Max. stress/strength at midspan	0.65	0.57 – 0.62
Beam Geometry and Reinforcement	Length	45.5 ft	
	Sectional Area	495-761 in^2	
	V/S	3.86 – 3.96 in.	
	Prestress Reinforcement	1.13%-1.37%	

*As built properties are presented only when these deviate from design values

The development of prestress loss within 18 of the 30 specimens was monitored through the use of internal strain instrumentation; vibrating wire gages (VWG) were used for this effort. Concrete strains and temperatures were measured at several points through the depth of each cross-section and used to calculate the change of strain at the centroid of the prestressing strands. Due to compatibility between the prestressing strands and the surrounding concrete, it was possible to further calculate the loss in prestressing force on the basis of the prestressing strand modulus and area.

In addition to the monitoring of loss through the use of VWGs, final loss was assessed via flexural cracking within all 30 specimens. The flexural demands (e.g. moment due to load) under which a pretensioned girder will crack is uniquely dependent on the beam geometry, concrete tensile strength, and effective prestressing force. Measurement of the cracking moment and concrete tensile strength and knowledge of the beam geometry should therefore enable back-calculation of the effective prestressing force, and by association, the prestress losses. Visual inspection and load-deflection analysis techniques were used to identify the flexural cracking load of specimens subjected to four point loading tests.

The results obtained from the internal strain monitoring and flexural cracking tests, in combination with information compiled in the database (Chapter 2), are used in Chapter 6 to assess the performance of prestress loss provisions: (1) outlined in the AASHTO LRFD Bridge Design Specifications and (2) proposed within Chapter 6 of this report.

This page is intentionally left blank

CHAPTER 4
Experimental Results and Analysis

4.1 OVERVIEW

A total of 30 specimens were fabricated, conditioned and tested during the course of the experimental program. At the time of final prestress loss assessment, the four series (6 to 8 specimens each) were representative of a fairly broad range of concrete materials, precast fabrication processes, and climatic conditions encountered in the State of Texas. Limestone or river gravel was utilized as coarse aggregate in conventional and self-consolidating concrete mixtures. Type C and Tx46 girder cross-sections were fabricated at three different precast plants and transported to arid (Lubbock) and humid (Austin) locations for the long-term development of prestress losses. Further details of the experimental program are provided in Chapter 3.

Assessment of the specimens through long-term monitoring and structural testing methods provided the data necessary to assess the impact of time, concrete properties, climate conditions and cross-sectional geometry on the development of prestress losses in the State of Texas. A general summary of the experimental results is provided below to support detailed examination of the program variables; the summary includes a review of the concrete material properties measured for each series of beams.

A summary of the material test results and measured losses from the experimental program are presented and briefly discussed in this chapter. The results are organized to aid in the investigation of the effect of (1) modulus of elasticity, (2) relative humidity, and (3) cross-sectional geometry on prestress losses. The measured loss results are then compared with the loss estimations of AASHTO LRFD 2012. The experimental database was expanded with the addition of data collected during the experimental program. This data and associated insights will enable definitive assessment of the code provisions, and further provide insights that will guide simplifications of the AASHTO LRFD 2012 procedure in Chapter 6.

4.2 SUMMARY OF EXPERIMENTAL RESULTS

The experimental results will be summarized in this section. A review of the concrete material properties is necessary to later appreciate their influence on the measured prestress losses. Results of both loss assessment methods (i.e. internal strain monitoring and flexural testing) will be reviewed independently, but only one will be used for the purpose of final result reporting.

4.2.1 Concrete Properties

The mechanical properties of the concrete mixtures used for each series were determined through extensive testing of companion 4-inch by 8-inch cylinders. Compressive strength, tensile strength (splitting tension) and modulus of elasticity tests were completed by researchers at Ferguson Structural Engineering Laboratory (FSEL). Testing was conducted as necessary to facilitate assessment of the prestress losses. The compressive strength (f'_{ci}) and modulus of elasticity (E_{ci}) of each mixture were determined approximately one hour after release ("At Release" in Table 4.1), as these concrete properties are influential in the estimation and real magnitude of prestress loss. The compressive (f'_c) and tensile strength (f_{sp}) were also measured at

the time of flexural testing; these properties are needed for back-calculation of the prestress loss on the basis of the flexural cracking load.

The relevant concrete materials properties measured at release, 28 days, and time of testing are shown in Table 4.1. In addition to the materials tests conducted at FSEL, the coefficients of thermal expansion were also measured by a subcontractor. The coefficients of thermal expansion were found to be 6 x10^{-6}/°C for the limestone concretes (Series I and III) and 10 x10^{-6}/°C for river gravel concrete (Series II).

Table 4.1 – Summary of concrete properties

Series	At Release					28 days		At Test	
	Age (days)	$f'_{ci,design}$ *(ksi)*	$f'_{ci,measured}$ *(ksi)*	$E_{ci,design}$ *(ksi)*	$E_{ci,measured}$ *(ksi)*	$f'_{c,design}$ *(ksi)*	$f'_{c,measured}$ *(ksi)*	$f'_{c,measured}$ *(ksi)*	$f_{sp,test}$ *(ksi)*
I	1.08	6.2	7.0	4800	4490	8.5	10.7	10.6	0.83
II	0.98	6.2	6.6	4800	6140	8.5	11.6	12.7	1.00
III	1.77	6.5	6.6	4900	3990	8.5	9.6	11.8	0.91
IV-SCC	0.74	6.05	6.3	4716	4810	12	11.5	15.0	1.06
IV-CC			6.9		5440		12.0	14.1	1.06
SCC = self-consolidating concrete; CC = conventional concrete									

The stiffness of the concrete at time of release (E_{ci}) strongly influences the estimation of prestress losses. For design purposes, this stiffness is calculated on the basis of the prescribed strength of the concrete at time of release (f'_{ci}) and may be estimated using Equation (4.1). If the concrete unit weight is 0.145 kips per cubic foot then Equation (4.2) is equivalent. These estimations can be adjusted using the K_1 parameter, which depends primarily on the coarse aggregate used.

In order to evaluate the AASHTO LRFD 2012 expression for estimation of the concrete modulus, the actual concrete stiffness was measured at time of release and time of testing; results are plotted in Figure 4.1. The AASHTO LRFD 2012 expression for the concrete modulus of elasticity - as adjusted by K_1 values of 0.9, 1.0 and 1.2 - is also plotted in Figure 4.1. It should be noted that the extreme K_1 values respectively correspond to overestimation of the concrete stiffness by 10 percent and underestimation by 20 percent. There is generally good agreement between measured and estimated modulus of elasticity through the use of $K_1 = 1.2$ for conventional concrete made using river gravel coarse aggregate and $K_1 = 0.9$ for conventional concrete made using limestone coarse aggregate. For self-consolidating concrete (SCC), the measured modulus of elasticity fell both above and below the estimated modulus using $K_1 = 1$.

As will be shown when investigating the prestress losses, the concrete stiffness significantly impacts the total loss. Beams made with stiffer concrete, as was seen in the concrete with river gravel aggregate, will experience smaller prestress loss than beams made with softer concrete, as seen with limestone aggregate.

(4.1)

$$E_c = 33,000K_1 w_c^{1.5}\sqrt{f'_c}$$

AASHTO 12 (5.4.2.4-1)

$$E_c = 1820K_1\sqrt{f_c'}$$

(derived for 0.145 kcf)

where:

E_c	= modulus of elasticity of concrete (ksi)
K_1	= correction factor for source of aggregate
w_c	= unit weight of concrete (kcf)
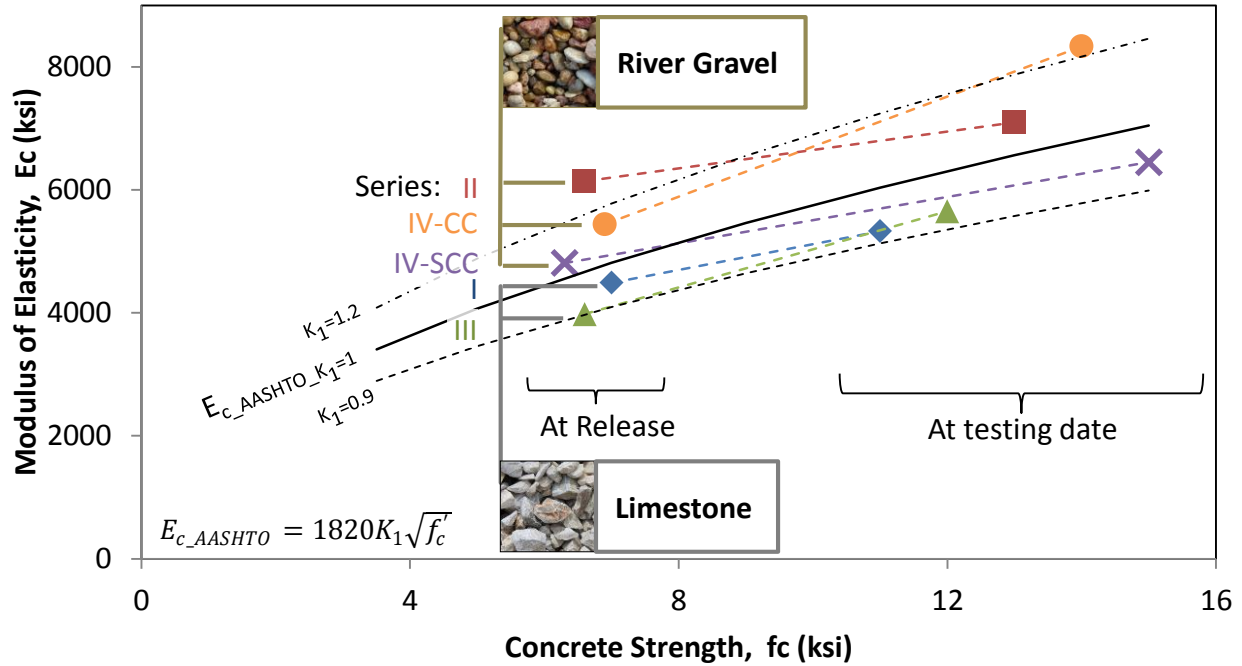
Figure 4.1 – Concrete modulus of elasticity

Split cylinder tests were conducted to measure the tensile strength of the concrete. This test method measures the global tensile capacity of the concrete, as microcracking is observed prior to the failure load being reached. The split cylinder test results were used to back-calculate the prestress loss from service load cracking, suggesting that a global method of crack detection would be most appropriate.

The results from the split cylinder tests are shown for all series in Figure 4.2, where measured concrete compressive strength (f'_c) versus tensile strength (f_{sp}) is shown. The modulus of rupture, specified as $0.24\sqrt{f'_c}$ in Article 5.4.2.6 of AASHTO LRFD 2012, is shown with the measured results. The measured concrete tensile strength, as indicated by split cylinder tests, consistently exceeded the AASHTO LRFD 2012 estimate the modulus of rupture.
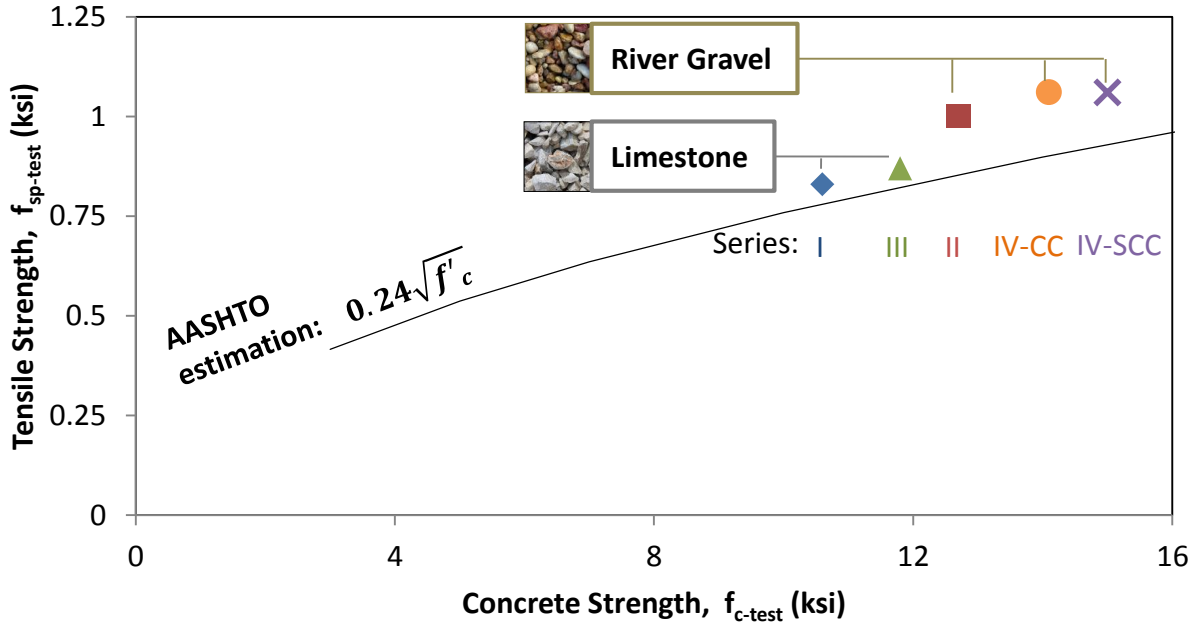
Figure 4.2 – Concrete tensile strength

4.2.2 Prestress Losses from Internal Strain Measurement

Vibrating wire gages (VWGs) were installed in 18 of the 30 specimens of the experimental program to allow for the development of prestress loss to be monitored over time. As mentioned in Chapter 3, the method could not directly capture the prestress losses due to strand relaxation, which occurs without a corresponding change in the concrete strain. This limitation was overcome by using the Equation (4.3) to estimate this well-known phenomenon that accounted for around 5 percent of total final losses in most of the cases. The calculated relaxation loss was added to the strain-related losses to estimate the total losses. Final prestress losses obtained from internal strain measurement are reported in Table 4.3.

(4.3)

$$\Delta f_{p\_Relaxation} = 2 \cdot \frac{f_{pt}}{30}\left(\frac{f_{pt}}{243\ ksi} - 0.55\right)$$

Modified from AASHTO 12 (5.9.5.4.2c-1)

where:

f_{pt} = stress in the strands after transfer (ksi)

82

4.2.3 Prestress Losses from Flexural Cracking

All 30 of the specimens were subjected to flexural demands to assess the prestress losses on the basis of first flexural cracking. The load-deflection data was analyzed, as discussed in Section 3.4.3, to detect the displacement, load and corresponding moment at first flexural cracking. The cracking moment was then used to back-calculate the prestress loss at the time of testing. There were two main purposes for the flexural testing program: (1) to verify the prestress losses assessed by internal strain monitoring and (2) to provide an independent means of assessment of the final prestress losses.

Many of the reported prestress losses included in the Evaluation Database (Chapter 2) were obtained through the use of either internal instrumentation or flexural testing. In the context of TxDOT Project 0-6374, the prestress losses back-calculated from flexural test results were comparable with, yet less consistent than, those obtained through internal strain monitoring. Moreover, the final observations and conclusions did not change during examination of one dataset or the other. Results of the flexural testing effort are presented in Table 4.2.

Table 4.2 – Cracking Loads and Back-Calculated Prestress Losses

A_p (in²)	f_{ct} (ksi)	S_c (in³)	S_{transf} (in³)	A_c (in²)	e_c (in)	M_d (kip-in)	f_{pi} (ksi)	Beam ID	P_{test} (kip)	$M_{cr,test}$ (kip-in)	f_{pe} (ksi)	Loss (ksi)
5.81	0.83	4760	5130	489	10.6	1500	203	I-1	184	21 200	146	57
								I-2	193	22 200	154	49
								I-3	193	22 200	154	49
								I-4	201	23 200	162	41
								I-5	191	22 000	152	51
								I-6	186	21 400	147	56
								I-7	192	22 100	153	50
								I-8	192	22 100	153	50
5.81	1.00	4760	5040	489	10.6	1500	203	II-1	217	25 000	172	31
								II-2	208	24 000	164	39
								II-3	219	25 200	174	29
								II-4	216	24 900	172	32
								II-5	225	25 900	179	24
								II-6	204	23 500	160	43
								II-7	224	25 800	179	24
								II-8	204	23 500	160	43
8.87	0.91	9690	10500	752	13.8	2300	209	III-1	404	46 600	154	55
								III-2	407	46 900	155	54
								III-3	405	46 700	154	55
								III-4	406	46 800	155	54
								III-5	402	46 300	153	56
								III-6	402	46 300	153	56
								III-7	405	46 700	154	55
								III-8	407	46 900	155	54
8.57	1.06	9700	10360	752	13.6	2300	203	IV-SCC1	400	46 100	155	48
								IV-SCC2	386	44 500	148	54
								IV-SCC3*	--	--	--	--
8.57	1.06	9700	10230	752	13.6	2300	203	IV-CC1	407	46 900	161	42
								IV-CC2	409	47 100	162	41
								IV-CC3	399	46 000	157	46

*Data from flexural test for beam IV-SCC3 is unreliable.

4.2.4 Final Prestress Losses

A summary of the properties and results is presented for all the specimens in Table 4.3. This table contains the material properties for each series, relevant information for each specimen, elastic shortening losses, and the final prestress loss as assessed via flexural testing (P-Δ) and internal strain monitoring (VWGs).

Table 4.3 – Summary of prestress loss assessments

Series Properties			Storage Location (RH)	Beam ID	Shortening (ksi)		Final Age (days)	Final Loss (ksi)			
								P-Δ	VWG	Reported	
Section:	Type-C	*SERIES I*	Lubbock (52%)	I-1	26		980	57	46	46	Avg.
Coarse Ag.:	Limestone			I-5	27		975	51	51	51	49
L:	45.5 ft			I-6	n/a		973	56	n/a	56	
A_p:	5.81 in^2		Austin (63%)	I-2	n/a	Avg. 27	939	49	n/a	49	Avg.
f_{pi}:	203 ksi			I-3	26		948	49	46	46	47
f_{ci}:	7.0 ksi			I-7	27		946	50	49	49	
E_{ci}:	4490 ksi		San Antonio (64%)	I-4	n/a		962	41	n/a	41	Avg.
				I-8	n/a		966	50	n/a	50	46
Section:	Type-C	*SERIES II*	Lubbock (51%)	II-1	16		955	31	32	32	Avg.
Coarse Ag.:	River Gravel			II-5	n/a		952	24	n/a	24	29
L:	45.5 ft			II-6	17		949	43	36	36	
A_p:	5.81 in^2		Austin (63%)	II-2	n/a	Avg. 17	922	39	n/a	39	Avg.
f_{pi}:	203 ksi			II-3	17		932	42	34	34	34
f_{ci}:	6.6 ksi			II-8	16		923	43	33	33	
E_{ci}:	6140 ksi		Elm Mott (63%)	II-4	n/a		936	32	n/a	32	Avg.
				II-7	n/a		937	24	n/a	24	28
Section:	TX-46	*SERIES III*	Lubbock (49%)	III-1	29		695	55	58	58	Avg.
Coarse Ag.:	River Gravel			III-5	29		703	56	58	58	55
L:	45.5 ft			III-8	n/a		700	54	n/a	54	
A_p:	8.87 in^2		Austin (61%)	III-3	29	Avg. 29	677	55	54	54	Avg.
f_{pi}:	209 ksi			III-4	n/a		675	54	n/a	54	52
f_{ci}:	6.6 ksi			III-7	29		681	55	53	53	
E_{ci}:	3990 ksi		San Antonio (63%)	III-2	n/a		689	54	n/a	54	Avg.
				III-6	n/a		687	56	n/a	56	55
Section:	TX-46	*SERIES IV*	Austin (57%)	IV-SCC1	22	Avg. 22	249	48	43	43	Avg.
Coarse Ag.:	River Gravel			IV-SCC2	22		259	54	42	42	40
L:	45.5 ft			IV-SCC3	22		230	n/a	43	43	
A_p:	8.57 in^2			IV-CC1	21	Avg. 21	237	42	39	39	Avg.
f_{pi}:	202 ksi			IV-CC2	20		257	41	38	38	36
f_{ci}:	SCC: 6.3 ksi CC: 6.9 ksi			IV-CC3	22		251	46	40	40	
E_{ci}:	SCC: 4810 ksi CC: 5440 ksi										

Official reporting of the final prestress loss measured within each specimen (designated "Reported" in Table 4.3) was completed on the basis of the VWG results when available; the flexural test results were used otherwise. This approach was selected given: (1) the consistent nature of the VWG-based assessments within virtually identical specimens, and (2) the many sources of variability related to the flexural testing method (refer to Chapter 3 for greater detail).

4.3   ANALYSIS OF EXPERIMENTAL RESULTS

The influence of several parameters on the development and final magnitude of the measured prestress losses is examined in this section. The time dependency of prestress loss is investigated through review of the internal strain monitoring results. The effects of the concrete properties, climate conditions, and cross-sectional geometries included in the experimental program are also identified. This is accomplished through analysis of the final prestress losses reported in Table 4.3. This effort, in combination with the parametric study of Chapter 5, enabled identification of the key parameters for prestress loss estimation and form the basis of the recommendations made in Chapter 6.

4.3.1   Time Dependency of Losses

The time-dependent development of the prestress losses was examined to assess the value of accounting for construction activities within the context of the prestress loss estimates. Please recall that the prestress loss provisions within the 2012 AASHTO LRFD Bridge Design Specifications are currently divided as "before deck" and "after deck" losses. The value of such an approach should be established through balanced consideration of: (1) the potential serviceability/strength implications and (2) the complexity introduced by the associated concepts and calculations. The complexity of the prestress loss provisions within AASHTO LRFD 2012 was one of the primary motivations for the creation of TxDOT Project 0-6374.

The time-dependent development of the strain related prestress losses within all of the specimens that were conditioned for one year or longer is plotted in Figure 4.3. The prestress loss in a given specimen at a given point in time is normalized by the prestress loss measured at one year. The prestress loss measured at one year was selected as it is a fair representation of the full-term losses measured during the course of TxDOT Project 0-6374; prestress losses increased by less than 10 percent after the first year. The most notable aspect of Figure 4.3 is that more than 90 percent of the prestress losses generally occurred within the first four months (or 120 days) of transfer of the prestressing force. It is important to note that commentary associated with the AASHTO LRFD 2012 prestress loss provisions cites a typical deck placement time of 120 days.

Given a sufficiently conservative set of prestress loss provisions, it would not be imprudent – and would indeed be more conservative - to utilize the final estimate of losses to conduct serviceability stress checks at the time of deck placement. Calculation of the prestress losses at the time of deck placement would be superfluous.
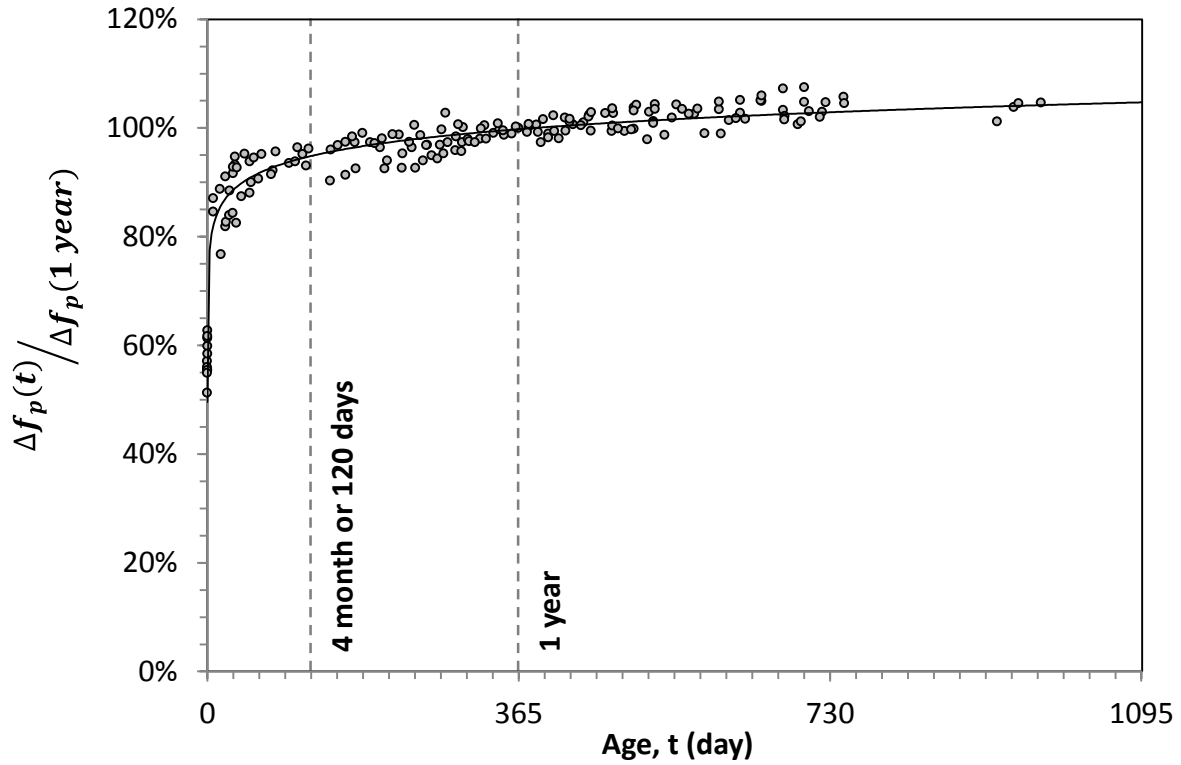
Figure 4.3 – Prestress loss ($\Delta f_p(t)$) normalized by loss occurring by one year after placement ($\Delta f_p(1\ year)$)

Prior to examining the next parameter, one additional aspect of the time-dependent loss measurements should be noted. The vibrating wire gages, installed in 18 of the 30 specimens, enabled independent assessment of the prestress losses resulting from elastic shortening and long-term creep/shrinkage; flexural testing only resulted in assessment of the combined effects of the short- and long-term prestress loss components. The instantaneous and long-term development of prestress loss within the Series III specimens stored in Austin is depicted in Figure 4.4.
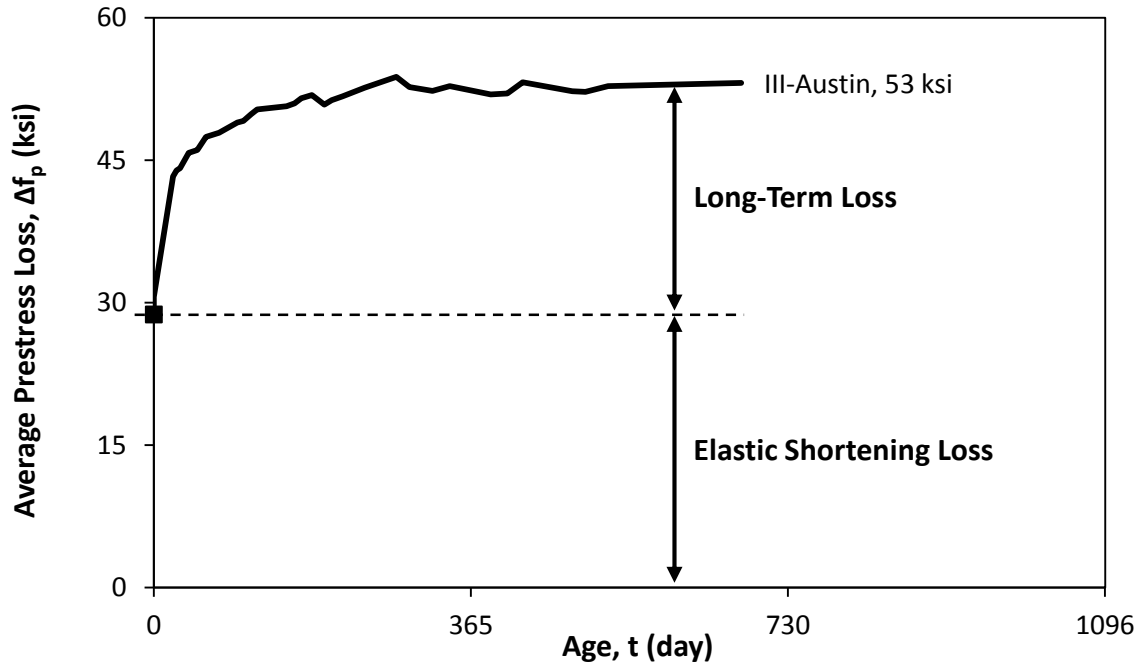
Figure 4.4 – Short- and long-term prestress losses in Series III specimens

Independent measurement of the short-term and long-term loss components permitted comparison of the real prestress loss due to elastic shortening and the corresponding estimate outlined in AASHTO LRFD 2012 (as done in Section 4.4).

4.3.2 Influence of Concrete Properties

The concrete modulus of elasticity associated with each series of specimens was strongly influenced by the type, quality and quantity of the coarse aggregate. The specimens of Series I and III were constructed using concrete containing crushed limestone coarse aggregate; those in Series II and IV were constructed with river gravel coarse aggregate. The effect of the different coarse aggregate type can be seen in Figure 4.5, where the average modulus of elasticity is shown for each series. The concrete with the river gravel coarse aggregate was significantly stiffer than the concrete with crushed limestone; by as much as 50 percent.
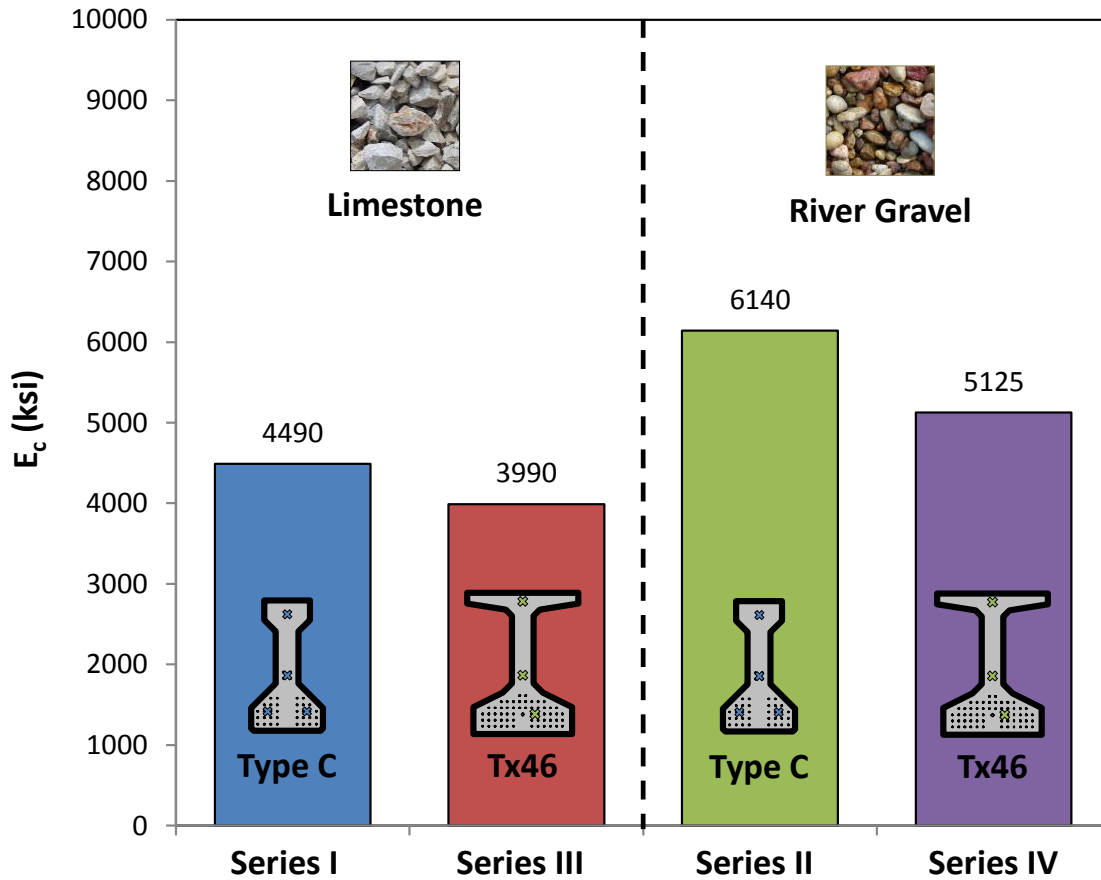
Figure 4.5 –Average measured modulus of elasticity (E_c) for each series

The total prestress losses were in turn greatly influenced by the stiffness of the concrete. The average final prestress loss for all the series is shown in Figure 4.6. The total loss is broken into elastic shortening (Δf_{pES}) and long-term (Δf_{pLT}) loss components to help illustrate the effect of the stiffness on each. The series of specimens constructed with stiffer, river gravel concrete experienced significantly smaller total prestress loss: Series I and III experienced total losses of 47 ksi and 54 ksi, respectively, while Series II and IV only experienced total losses of 31 ksi and 39 ksi, respectively.

The concrete stiffness also influenced the long-term losses greater than the elastic shortening. This can be seen through comparison of the loss components of Series I and III as well as comparison of Series II and IV. The elastic shortening loss decreased from 27 ksi (Series I) to 19 ksi (Series III) when a stiffer concrete was used, a decrease of 30 percent; the long-term loss decreased from 20 ksi to 12 ksi (40 percent) in the same specimens. The same trend was observed when comparing the specimens in Series II with the specimens in Series IV: elastic shortening loss decreased from 29 ksi to 23 ksi (20 percent) and the long-term loss from 25 ksi to 16 ksi (36 percent). These observations are consistent with common assertions that creep and shrinkage are heavily influenced by the coarse aggregate properties (ACI 209R, 2008).
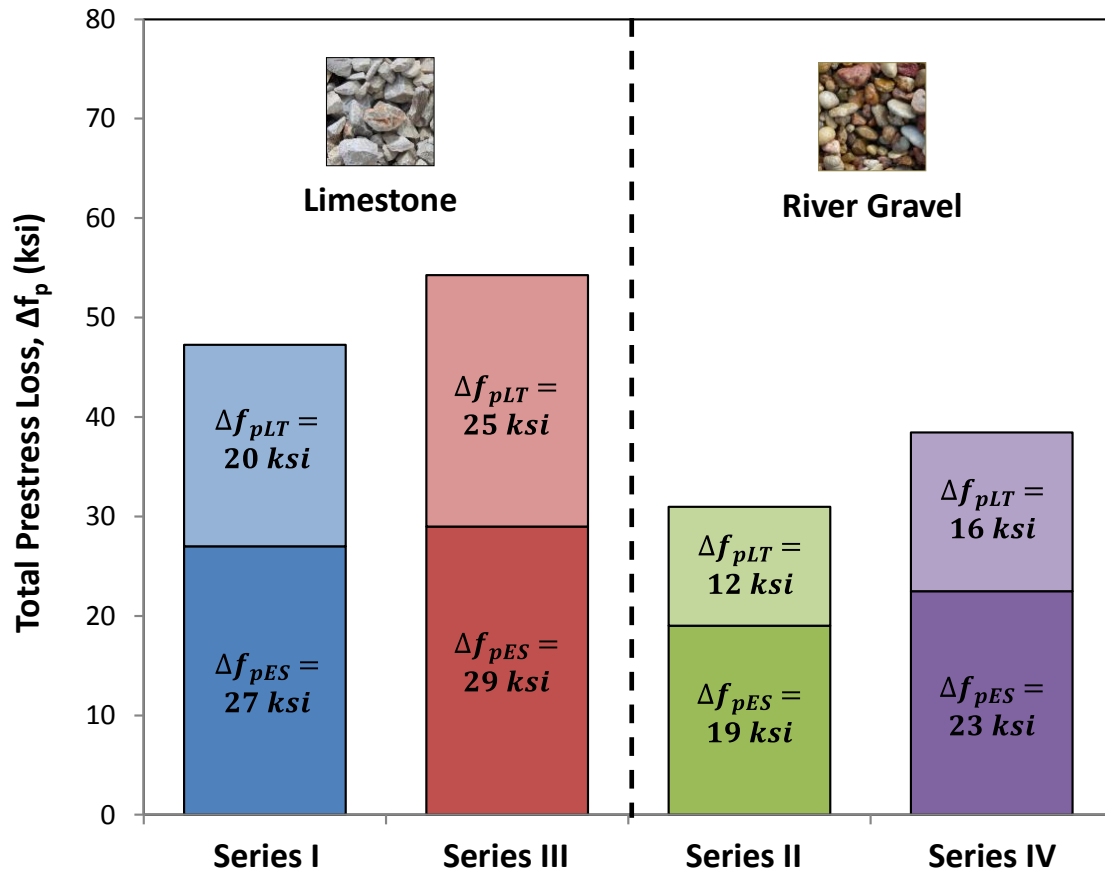
Figure 4.6 – Total prestress loss for each series divided into elastic shortening (Δf_{pES}) and long-term loss components (Δf_{pLT})

The time-dependent variation of prestress losses for all internally instrumented specimens is shown in Figure 4.7. As noted above, the specimens comprised of river gravel coarse aggregate (Series II and IV) consistently exhibited lower prestress losses than those comprised of limestone coarse aggregate (Series I and III).
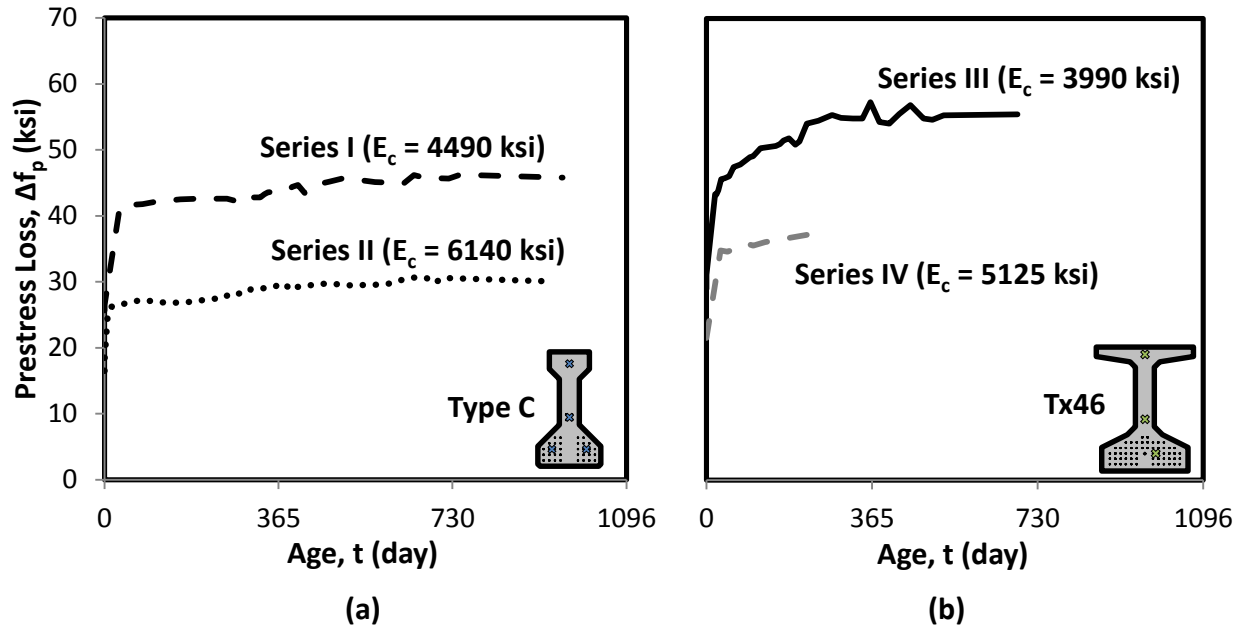
Figure 4.7 – Average losses vs. time for (a) Series I and II and (b) Series III and IV

The effect of the proportion of coarse aggregate in the concrete mixture was also investigated. In Series IV, three of the six beams were fabricated using self-consolidating concrete (SCC), which typically has a lower concentration of coarse aggregate than conventional concrete (CC) mixes; the other three beams were fabricated with conventional concrete. It was found that the conventional concrete was slightly stiffer than the self-consolidating concrete, with stiffness of 5,540 and 4,810 ksi respectively. The stiffer concrete translated to slightly smaller loss in the CC specimens versus the SCC specimens, 38.0 and 41.1 ksi respectively. This shows that the concentration of coarse aggregate may affect the concrete stiffness and total prestress loss, but not as significantly as the coarse aggregate properties.

During implementation of the AASHTO LRFD 2012 prestress loss provisions, the variation of concrete stiffness (as a result of constituent properties and/or mixture proportions) may be accounted for through use of the K_1 factor, as introduced in Section 4.2.1, Equation (4.1) above. Given measurements of the concrete modulus and compressive strength, K_1 may be calculated as the ratio of the measured concrete modulus and the concrete modulus estimated on the basis of the measured compressive strength; as done in Table 4.4. The K_1 factor for each of the concrete mixtures used in the current project varied between 1.15 and 1.20 for conventional mixtures with river gravel coarse aggregate and between 0.87 and 0.91 for mixtures with limestone coarse aggregate.

Table 4.4 – Average K₁ correction factor for each series

Series	Aggregate Type	$E_{ci,estimated}$ (ksi)	$E_{ci,measured}$ (ksi)	Average K_1 (at release)
I	Limestone	4934	4490	0.91
II	River Gravel	5117	6140	1.20
III	Limestone	3897	3390	0.87
IV-SCC	River Gravel	4810	4810	1.00
IV-CC	River Gravel	4730	5440	1.15

The current language in AASHTO LRFD 2012 allows for K_1 to be taken as 1.0 if material testing is not conducted. A bridge designer generally does not know which fabricator or what aggregates will be used for a given structure until the design is complete and the bridge has been let for construction. They will likely default to use of the default K_1 value of 1.0. Moreover, it is likely - given the Chapter 2 assessments of AASHTO LRFD 2012 and the results discussed above – that such an approach will result in unconservative estimates of prestress loss, especially for pretensioned girders fabricated with limestone coarse aggregate. It is therefore recommended for the State of Texas that a K_1 of 0.85 be used when calculating material properties for AASHTO LRFD 2012 estimation of prestress loss unless either (1) material testing is conducted or (2) there is accepted knowledge that the aggregate type produces concrete with adequate stiffness.

4.3.3 Influence of Climate Conditions

Within each series, a portion of the specimens were conditioned in Lubbock, with an average annual ambient relative humidity of around 50 percent, and a portion in Austin, with a relative humidity of around 60 percent. This was done in order to investigate the influence of various climate conditions on the development of prestress losses.

The time dependent variation of prestress loss in Series III specimens conditioned in Lubbock and Austin are shown in Figure 4.8. It can be seen that the elastic shortening loss in both sets of specimens is identical, as was expected. The long-term loss was slightly larger in the specimens conditioned in Lubbock versus those conditioned in Austin, 58 and 53 ksi respectively. The prestress loss increase attained through conditioning in a lower humidity environment is consistent with the concrete creep and shrinkage models presented in ACI 209R and included in Article 5.4.2.3 of AASHTO LRFD 2012. It should be noted that comparison of the identical specimens within Series I and II did not reveal any significant effect of the conditioning environment.

The fact that the climate conditions had a noticeable effect in Series III, while not noticed in Series I and II, is related to the permeability and age of the concrete at the time of shipping to the conditioning sites. The largest fraction of the losses occurs in the first few weeks after casting. For this reason, the storage conditions during this period have a larger effect on prestress losses than the storage conditions at later ages. Series I and II were stored at the fabricator for longer times (51 and 22 days respectively) than Series III (18 days), contributing to specimens in Series III being more sensitive to climate differences between Austin and Lubbock.
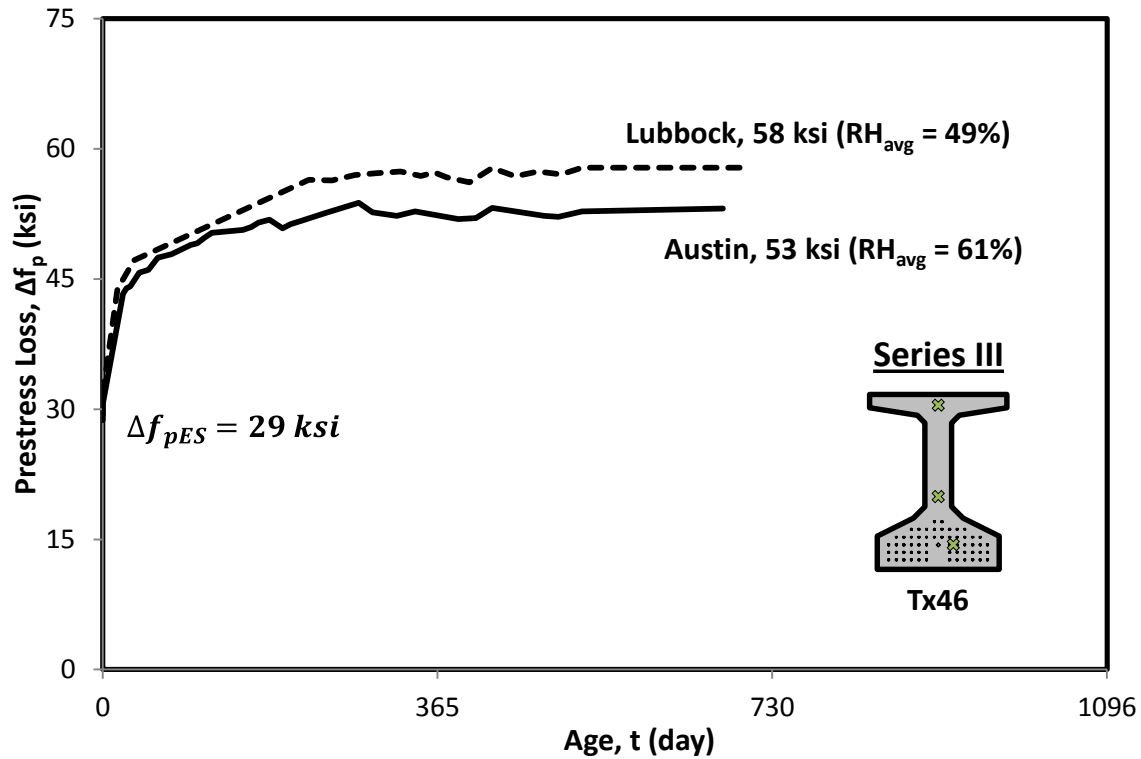
Figure 4.8 – Average prestress loss vs. time for Series III specimens

The ambient relative humidity is considered in the estimation of prestress loss in both AASHTO LRFD 2004 and 2012. In both specifications, the estimation of prestress loss due to shrinkage considers relative humidity, while in AASHTO LRFD 2012 relative humidity is also a factor in the creep loss expression. These expressions can be found in Chapter 2. Due to the observations made here, ambient relative humidity is retained as an influential parameter during simplification of the AASHTO LRFD 2012 prestress loss expressions in Chapter 6.

4.3.4 Influence of Cross-Sectional Geometry

Historically, the cross-sectional geometry has been thought to affect the creep and shrinkage of the concrete. A larger volume-to-surface area ratio (*V/S*) is thought to allow greater water transfer from the concrete to the atmosphere. Volume-to-surface area does not typically play a significant role in prestress concrete girder design, as most of the commonly used cross-section types have volume-to-surface area ratios of around 4.0 inches.

Through the course of the experimental research, two different cross-section types (Type C and Tx46) were investigated. The relevant cross-sectional geometric properties are shown in Table 4.5. It can be seen that both of the sections have similar volume-to-surface area and prestress ratios (ρ_p). The two sections do, however, have different bottom flange volume-to-surface ratios, which is the ratio considering the bottom flange separate from the rest of the section.

Table 4.5 – Summary of relevant cross-sectional geometry properties

Series	Section Type	$E_{ci,measured}$ (ksi)	Prestress Ratio (ρ_p)	Gross Area (in^2)	Volume-to-Surface Area Ratio (V/S) (in)	Bottom Flange V/S (in)
I	Type C	4490	0.012	494.9	4.0	4.1
II	Type C	6140	0.012	494.9	4.0	4.1
III	Tx46	3390	0.012	752.1	3.9	4.6
IV	Tx46	5125	0.012	752.1	3.9	4.6

The total final prestress loss for each series is shown in Figure 4.9 in order to show the effects of cross-section type on prestress loss. It can be seen that in both the specimens with limestone and river gravel coarse aggregate there was a slight increase in measured long-term losses when going from the Type C to Tx46 cross-section. This increase is likely due to the Tx46 specimens having less stiff concrete than the Type C girders. There is no definitive cross-sectional geometry effect between Type C and Tx46 cross-section types.
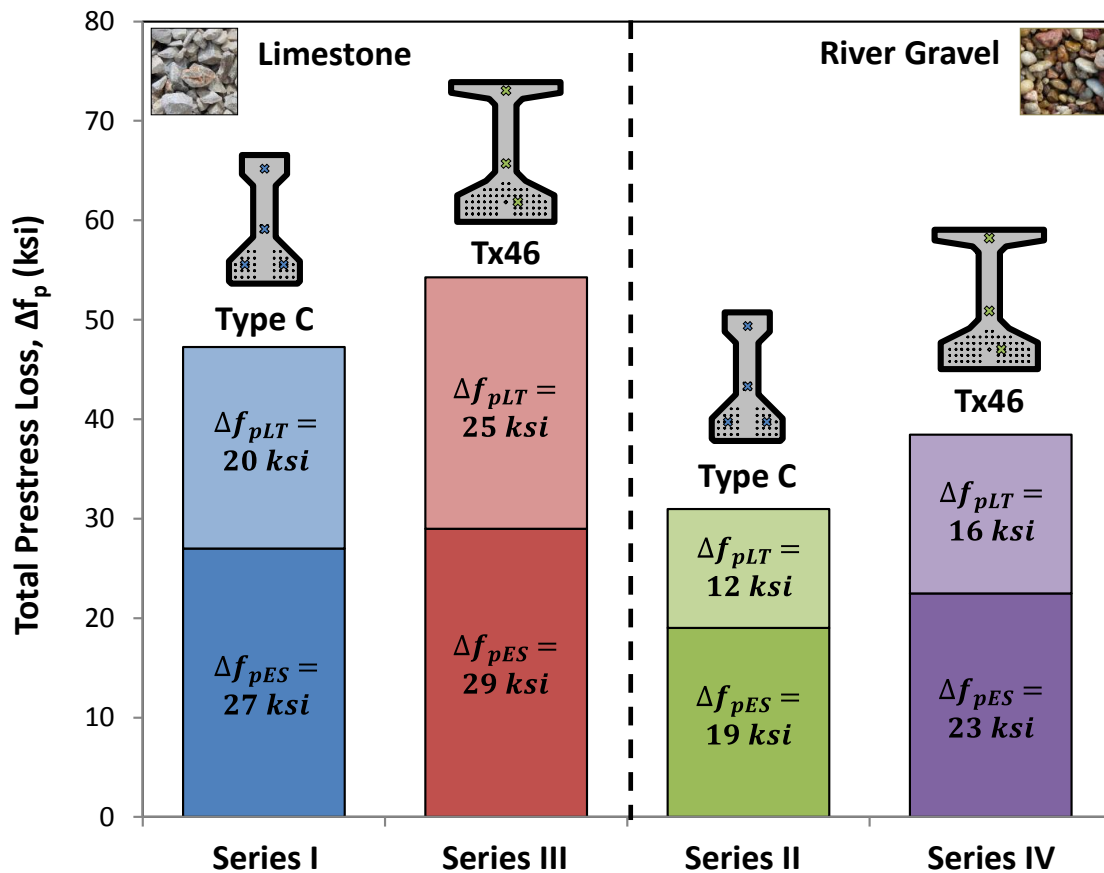
Figure 4.9 – Total prestress loss for each series divided into elastic shortening (Δf_{pES}) and long-term loss components (Δf_{pLT}), comparing geometry

4.4 EXPANDED EVALUATION OF CURRENT PRESTRESS LOSS PROVISIONS

A database evaluation of the prestress loss provisions in the 2012 AASHTO LRFD Bridge Design Specifications was presented in Chapter 2. In general, the provisions yielded unconservative estimates of the prestress loss for 30 of the 140 specimens. The average ratio of the estimated and measured prestress loss was 1.25 for the complete Evaluation Database.

The database evaluation of Chapter 2 is here extended to the results of the TxDOT Project 0-6374 experimental program. Evaluation of the short-term (elastic shortening) and long-term estimates (creep and shrinkage) provided by the current prestress loss provisions (AASHTO LRFD 2012) is depicted in Figure 4.10 and Figure 4.11, respectively. The prestress loss due to elastic shortening was only measured in the 18 specimens containing internal instrumentation and Figure 4.10 therefore contains 12 fewer data points than Figure 4.11. Similar evaluations of the prestress loss estimates provided by AASHTO LRFD 2004 are included in the Appendix C and in Chapters 2 and 6, for the specimens in the database.
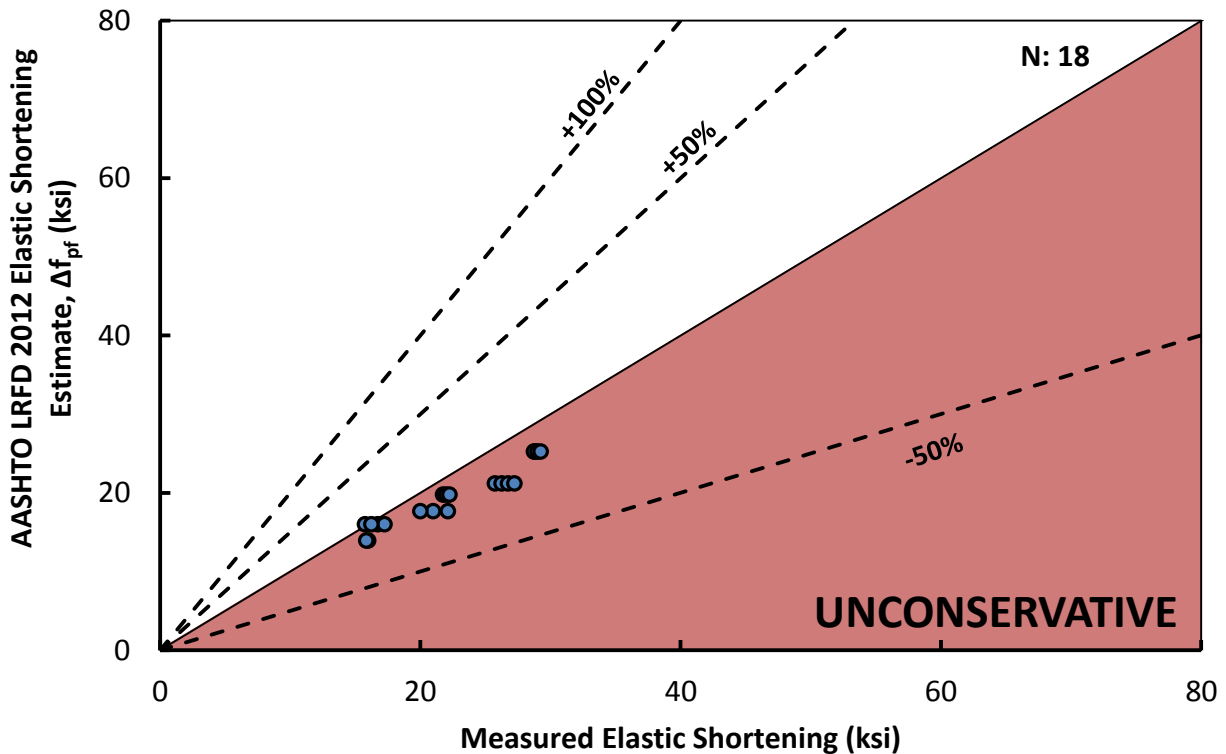
Figure 4.10 – AASHTO LRFD 2012 prestressed loss estimate vs. measured elastic shortening loss (VWG results)
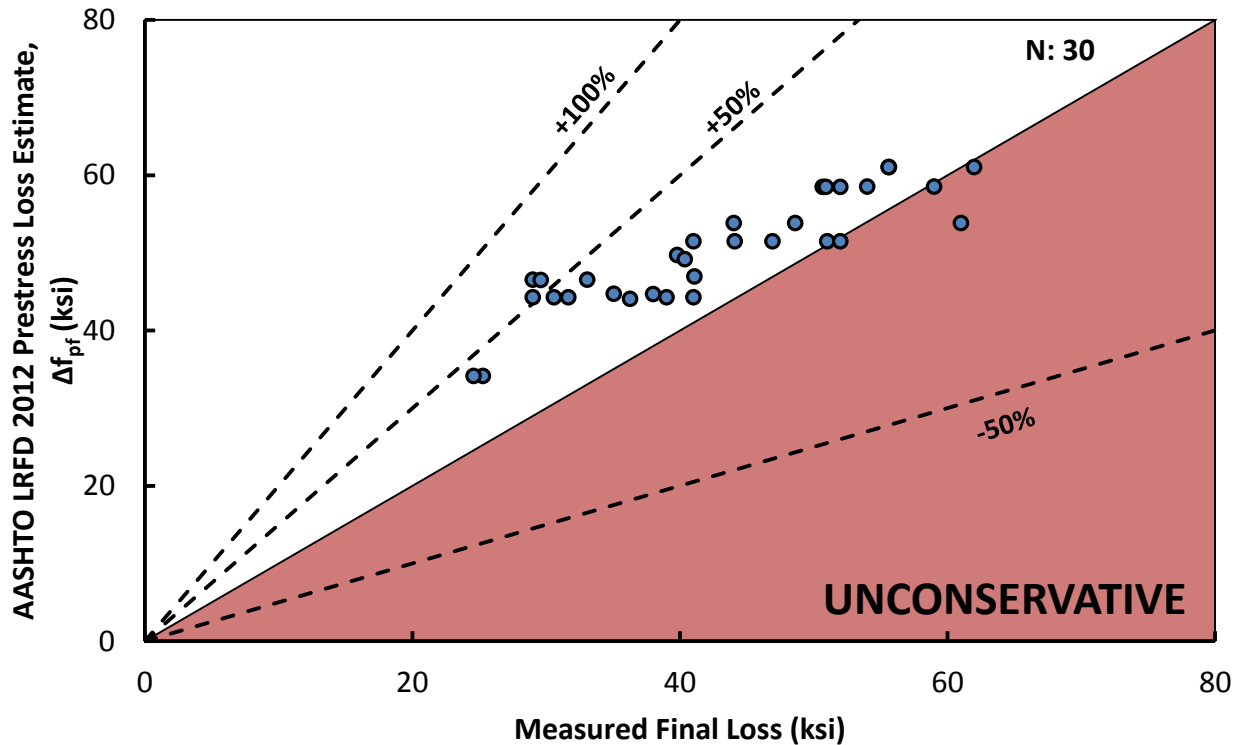
Figure 4.11 - AASHTO LRFD 2012 prestressed loss estimate vs. total measured loss

In both cases, a majority of the results lie close to the line of equality, though it does appear that the current provisions (AASHTO LRFD 2012) do result in consistent underestimation of the prestress loss due to elastic shortening.

Overall, the AASHTO LRFD 2012 prestress loss provisions provided fairly accurate estimation of the prestress losses measured during the experimental program. Given the somewhat negative (i.e. unconservative) characterization of AASHTO LRFD 2012 in Chapter 2, this outcome highlights the value of an extended database effort and evaluation. In spite of the experimental results, simplification of the AASHTO LRFD 2012 prestress loss provisions in Chapter 6 is completed with a desire to increase the conservatism of the estimates.

4.5 SUMMARY

Results of the experimental program were presented in this chapter. Because prestress loss is strongly dependent on the concrete material properties, both material properties and prestress losses were investigated.

Concrete strength fell between 5.8 to 7.0 ksi at release, and the elastic modulus fell between 4700 to 7200 ksi at the same age, both typical to what is found in the field. It was observed that the concrete made with river gravel concrete was stiffer than the concrete made with limestone. The measured tensile strengths at flexural testing were higher than $0.24\sqrt{f_c'}$, indicating that this estimation is conservative for all the specimens tested.

The final measured prestress losses ranged from 24 ksi to 61 ksi. A clear influence of the coarse aggregate type on the losses was observed. Concrete made from limestone coarse aggregate resulted in a lower modulus than concrete made with river gravel coarse aggregate. A

96

higher loss was observed in the specimens made with limestone aggregate concrete versus those with river gravel aggregate.

The losses measured in Series III beams stored in dryer conditions are larger than those stored in more humid environments (a 10 percent decrease in the relative humidity resulted in an increase of almost 9 percent in the long-term loss within otherwise identical specimens). Series I and II did not show considerable difference within beams stored at different humidity. The main factors leading to this difference in the effect of the relative humidity are related to the age and permeability of the concrete in the beams when first exposed to the storage conditions. The effect of different humidity was noticeable in the younger and most permeable beams (i.e. those from Series III). Also, there was no definitive cross-sectional geometric effect on prestress loss.

Both the measured elastic shortening losses and the final measured losses from the specimens in the experimental program were compared with losses estimated using AASHTO LRFD 2012. In both cases the results lie close to the equality line, though some cases of marginal underestimation were observed with respect to the prestress losses due to elastic shortening.

This page is intentionally left blank

CHAPTER 5
Parametric Study

5.1   OVERVIEW

In order to assess the impact of the new prestress loss provisions of the 2012 AASHTO LRFD Bridge Design Specifications, a comprehensive parametric study was completed. The current standard for the design of TxDOT bridges (2004 AASHTO LRFD Bridge Design Specifications) served as a basis for evaluation of the results, which focused on establishing the potential economic, strength and serviceability implications of the new provisions. The database evaluation completed in Chapter 2 provided preliminary insight into the implications: the accurate, less conservative approach assumed by AASHTO LRFD 2012 was expected to result in lower prestress loss estimates, and consequently, fewer prestressing strands.

The design implications of the new loss provisions were definitively quantified through the parametric study. Over 1800 different bridge designs were completed to account for all of the influential design parameters, whose variation was driven by a desire to account for the full spectrum of Texas materials and designs. The parameters varied during the course of the study included the girder cross-section type, girder spacing, bridge span length and concrete release strength. Through comparison of the 2004 and 2012 AASHTO LRFD bridge designs, it was possible to identify the impact of the new loss provisions on: (1) the flexural reinforcement, (2) the flexural capacity, (3) the shear capacity and (4) the camber of standard TxDOT bridges. All of the calculations and analyses were completed through the use of a parametric analysis tool, developed to provide capabilities otherwise unavailable within commercial design software.

Selection of the key parameters, development of the parametric analysis tool and review of a sample of results are discussed in this chapter. The parametric study also provided the opportunity to closely examine the variation of the input parameters for the prestress loss provisions of the 2012 AASHTO LRFD Bridge Design Specifications. While this secondary effort is not addressed within this chapter, the results were instrumental in simplification of the new loss provisions as discussed in Chapter 6.

5.2   DESIGN PARAMETERS

The main input parameters investigated during the study include girder type, girder spacing, span length, and concrete release strength. The variations of the parameters chosen for the parametric study are summarized in Table 5.1.

The variations were chosen to capture the entire range of typical Texas materials and design practices. The four main girder cross-section types used in TxDOT design are I-beams, box beams, bulb-T beams, and U-beams. The smallest and largest sections were chosen from each cross-section category, as well as the middle sized section for I-beams and bulb-T beams. The bridge configurations chosen (girder spacing and span length) represent the most commonly chosen configurations in actual bridges. The concrete release strength variations were chosen to represent up to the maximum release strength allowable by TxDOT. Within this section, the input parameters chosen and the reason behind the choice will be discussed.

Table 5.1 – Summary of parameter variation

Parameter:	*Section Type*	*Girder Spacing*	*Span Length*	*Release Strength*
Variations:	Type A Type C Type IV Type 4B20 Type 5B40 Tx28 Tx46 Tx70 Type U40 Type U54	6.67 ft. 8 ft. 8.7 ft.	$0.4L_{max}$ To L_{max} Varied by: $\sim 0.05L_{max}$	3.5 ksi To 6.5 ksi Varied by: 0.25 ksi

5.2.1 Girder Type

The cross-sections investigated in the parametric study are shown in Figure 5.1. Four different groups of cross-section types were investigated: I-beams, box beams, bulb-T beams, and U-beams, shown in Figure 5.1 (a) through (d) respectively. These four groups represent the majority of the girders fabricated in Texas. Within each group, a variety of different girder sizes were studied to ensure that the parametric study captured any size effects. The variety of cross-section types and sizes allows for the geometrically dependent variables in the design specifications to be properly investigated.
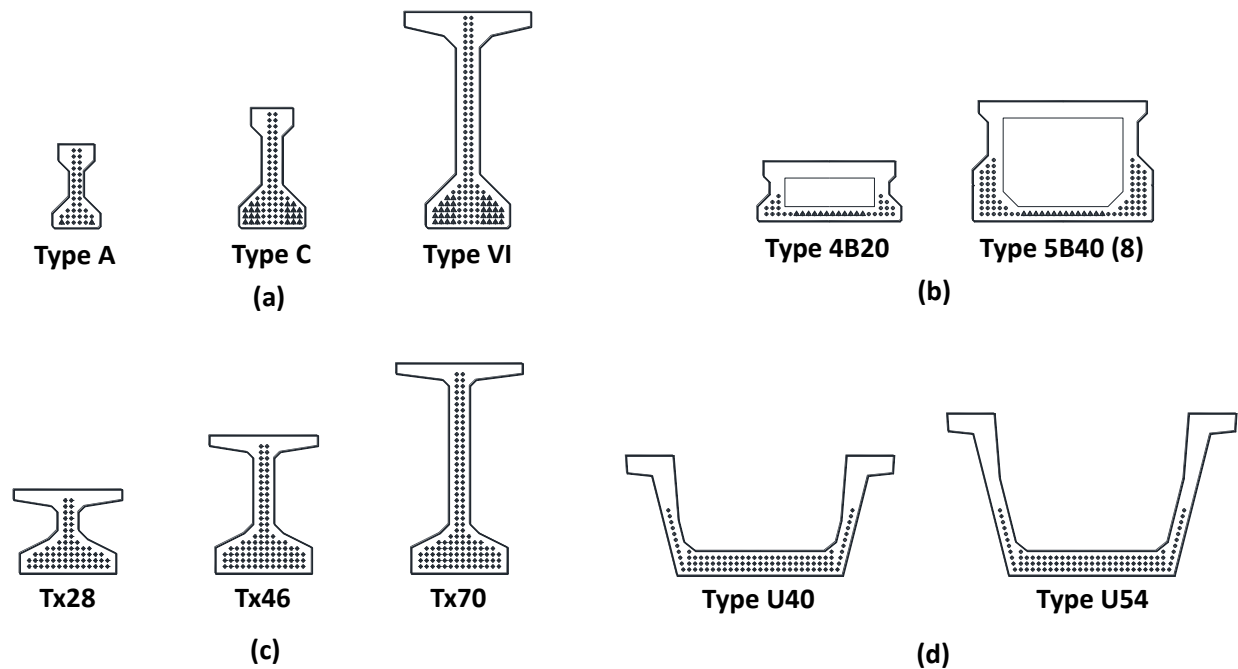
Figure 5.1 – Girder cross-sections investigated in parametric study; (a) I-beams, (b) box beams, (c) bulb-T, (d) U-beams

5.2.2 Girder Spacing and Span Length

For each girder cross-section type, three different girder spacing values were considered (6.7', 8' and 8.7'), as shown in Figure 5.2. The three girder spacing values encompass typical bridge configurations in Texas, which can be seen in the standard bridge widths presented in the TxDOT Bridge Design Manual (2011).

The TxDOT Bridge Design Manual presents a maximum allowable span length (L_{max}) for nearly all of their cross-section types, presented in Table 5.2. Multiple span lengths were considered for every combination of cross-section and girder spacing. The span lengths were determined on the basis of the maximum allowable span length, ranging from 40% of L_{max} to L_{max} and incremented by five to ten feet, as shown in Figure 5.3.

s = 6.7'

(a)

s = 8'

(b)

s = 8.7'

(c)
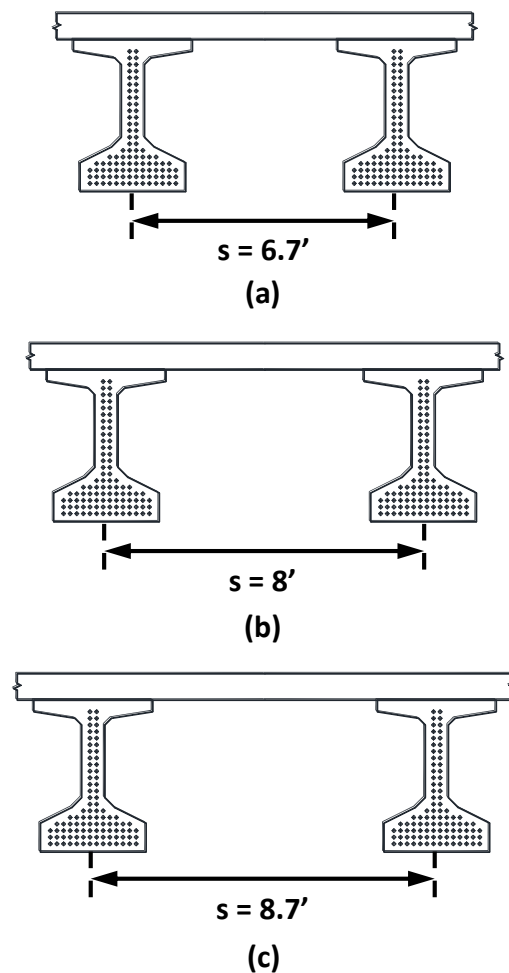
Figure 5.2 – Girder spacing values investigated: (a) 6.7', (b) 8', and (c) 8.7'
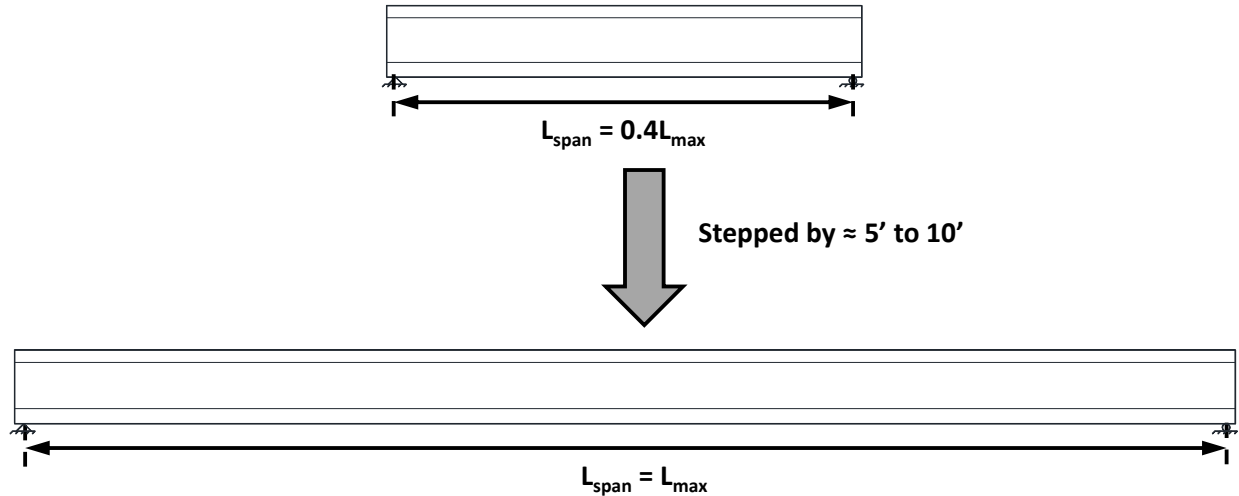
Figure 5.3 – Span lengths investigated

Table 5.2 – Maximum allowable span lengths (TxDOT 2011)

	Girder Type	L_{max} (ft)
I-Beam	Type A	55
	Type C	90
	Type VI	150
Bulb-T	Tx28	80
	Tx46	120
	Tx70	150
Box Beam	Type 4B20	65
	Type 5B40 (8)	120
U-Beam	Type U40	100
	Type U54	120

5.2.3   Concrete Release Strength (f'ci)

The effect of varying the release strength of the concrete was also investigated; varying the strength from 3-ksi to 6.5-ksi, stepped by 0.25-ksi. The concrete release strength has the largest direct impact on the release strength factor (k_f) in AASHTO LRFD 2012, shown in Figure 5.4. While the minimum allowable concrete release strength for design is 4-ksi, the minimum release strength chosen for this study was 3-ksi; this was chosen to investigate the effect of lower strength concrete. The high end of the range represents both the maximum allowable release strength allowed by TxDOT and the point where higher release strengths will not significantly change k_f.

102
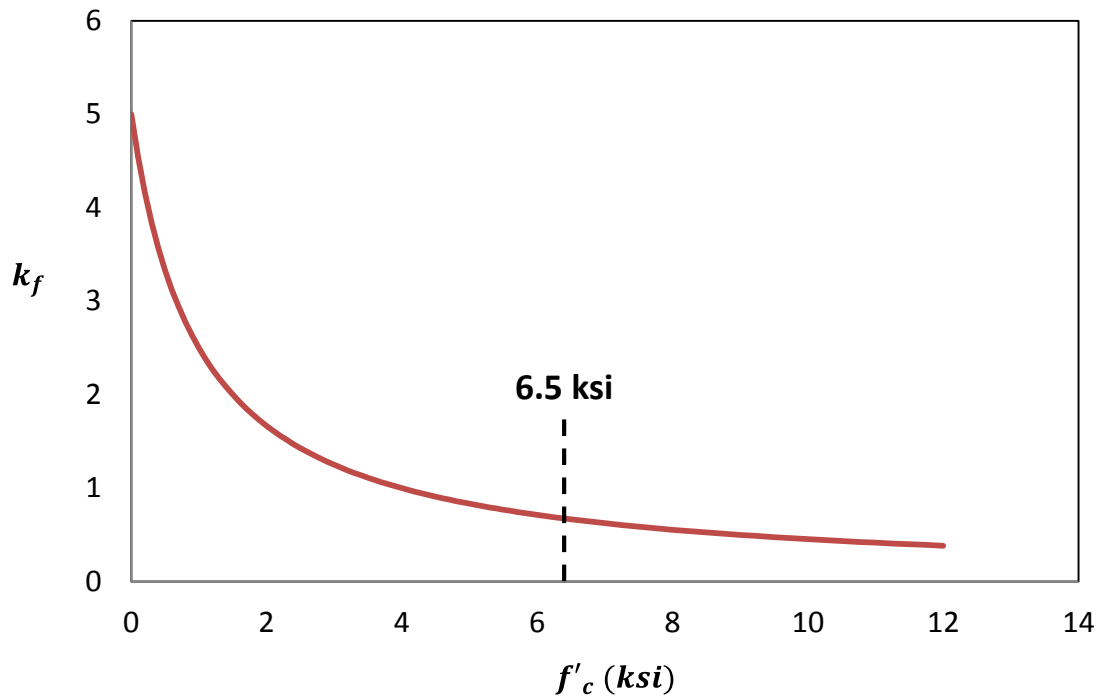
Figure 5.4 – Factor for effect of concrete release strength (k_f)

5.3 PARAMETRIC ANALYSIS TOOL

There are two different pieces of software used by Texas engineers to design prestressed concrete bridge girders, PSTRS14 and PGSuper. These pieces of software are valuable for the design and analysis of prestressed girders, but did not provide the flexibility, for both input and output variable, desired for the parametric study. This lack of flexibility led to the development of a spreadsheet-based analysis tool to facilitate completion of the parametric study and analysis of the results. In-house development of the analysis tool provided the opportunity to tailor the input and output data to the objectives of the parametric study.

The capabilities of commercially available software will first be reviewed to substantiate the need for the parametric analysis tool. Development of the tool will then be briefly discussed to show the scope and capability of the analysis tool. The output of the tool was verified through comparison with PGSuper results for a number of design scenarios; this comparison is provided after review of the development process.

5.3.1 Available Design Software

Two pieces of design software are primarily used by TxDOT to design prestressed concrete girders: PSTRS14 and PGSuper. PSTRS14 is a program developed and maintained in-house by TxDOT. PGSuper is an open-source Windows-based program developed and updated by BridgeSite, Inc. originally under supervision and direction from only the Washington State DOT (WSDOT). TxDOT, seeking forward looking prestress design software, contracted with BridgeSite, Inc. (April 2006) to enhance PGSuper per TxDOT's design policies, including the addition of the design algorithm from PSTRS14. While both programs now yield consistent pretensioned girder designs, TxDOT is encouraging bridge designers to transition to PGSuper.

5.3.1.1 *PSTRS14*

PSTRS14 was created to facilitate the design of I-beams, box beams, bulb-T beams, U-beams and non-standard beams per the requirements of the AASHTO Standard Specifications, AASHTO LRFD Bridge Design Specifications and AREMA Specifications. PSTRS14 design input and output variables are summarized in Table 5.3.

Table 5.3 – Input and output variable for PSTRS14, PGSuper and desired for the study

	PSTRS14	PGSuper	Desired
Input Variables	- Girder type - Girder spacing - Span length and skew - Distribution factors - Relative humidity - Slab thickness	- Girder type - Girder spacing - Number of girders - Span length and skew - Deck width - Slab thickness	- Girder type - Girder spacing - Number of girders - Span length and skew - Deck width - Slab thickness - ***Concrete properties (f'$_c$, f$_{ci}$, E$_c$, E$_{ci}$, K$_1$, etc.)*** - Fabrication timing - Relative humidity
Output Variables	- Number of strands required - Design load stresses - Req'd ultimate moment capacity - Moment capacity - Shear design - Camber and deflections - Concrete properties - Prestress loss information (components)	- Number of strands required - Design load stresses - Distribution factors - Req'd ultimate moment capacity - Moment capacity - Shear design - Camber and deflections - Concrete properties - Prestress loss information (components)	- Number of strands required - Design load stresses - Distribution factors - Req'd ultimate moment capacity - Moment capacity - Shear design - Camber and deflections - ***Prestress loss information (individual components and factors)***
Design Codes	- AASHTO LRFD 2004 - AASHTO LRFD 2012	- AASHTO LRFD 2004 - AASHTO LRFD 2012	- Any design specification

5.3.1.2 *PGSuper*

PGSuper was developed as a more user-friendly, Windows-based design software. PGSuper requires the cross-section of a new beam to be within the same family as an already defined section; this slightly restricts the freedom of cross-section selection for design and

analysis purposes. The software also has a preliminary design tool that will detail a girder (number of strands required, strength of concrete, shear reinforcement, etc.) based on the most basic input parameters (girder type, spacing, length, etc.). The input and output parameters of PGSuper are summarized in Table 5.3.

5.3.2 Motivation for Tool Development

There were three main motivations for development of the parametric analysis tool:

- *A need for greater control over the input and output parameters*: There was a desire to have better control of the design inputs, specifically the concrete material properties, and the design outputs, specifically prestress loss information, both highlighted in Table 5.3. Neither of the other programs allowed for the concrete strength (release or ultimate) to remain constant for the design. Having such capabilities was critical to independently studying the influence of each parameter.

- *Automated input to expedite analysis*: It was desired to have an input that would allow for multiple beams to be designed where the only variable changing between the designs would be girder type, span length, girder spacing, concrete release strength, or design specification. A simplified input would allow for a large time savings for the number of designs desired to be completed in the study.

- *Use of custom prestress loss procedure*: The two other programs only allowed for current or past loss procedures to be used for design. With one of the goals of the study to investigate the performance of the proposed loss procedure, the proposed loss procedure would need to be input and used in design.

Due to the complexities involved, adaption of PSTRS14 or PGSuper to the purposes of the current study was forgone in favor of a custom analysis tool. Both pieces of design software are well-suited for the purpose of routine girder design, but neither provides the flexibility required in this study.

5.3.3 Design Algorithm

The logic and design procedure implemented within the parametric analysis tool will be discussed briefly to establish the capabilities and use of the tool. The design procedure is outlined in Figure 5.5; relevant articles of the AASHTO LRFD Bridge Design Specifications are noted where appropriate.

The loading for the given bridge geometry was calculated first. Dead load was calculated based on member self-weight, deck weight, and other superimposed dead loads (such as barrier weight, additional overlay weight, etc.). Live loads were calculated using the appropriate combination of HL-93 design truck load and lane live load applied to the girder using live load distribution factors.

The initial total number of strands was determined through a flexural design using the above loads for the Strength I limit state. The number of strands was increased until the section had adequate flexural capacity. This number of strands was increased, if necessary, until all bottom fiber tensile checks were satisfied (at midspan and 40 percent of the girder length). It should be noted here that the estimated prestress loss will only have an effect on the bottom fiber tensile stress checks; the flexural capacity is calculated using the strand yield stress.

The strands were then harped as necessary to limit the tensile stresses at the transfer length. The adequacy of the concrete compressive strength was investigated by compression stress checks. If the concrete strength was found to be insufficient, a note was output to let the designer know the current design would fail.

Finally, the shear capacity of the section was determined. TxDOT currently specifies the transverse reinforcement spacing for each cross-section type within the design standards. The TxDOT-specified transverse reinforcement was used to calculate the shear capacity at the critical section.

1. Design input

2. Calculate Loads

3. Determine number of strands required

4. Determine number of strands to harp

5. Determine if f'$_{ci}$ and f'$_c$ are sufficient

6. Determine shear capacity based on TxDOT required shear reinforcement

Design Inputs

Calculate Loads
(3.6 and 4.6.2.2)

Strength Limit State
Flexural Capacity
(5.7.3.2)

Stress Limit State
Bottom-Fiber
(at 0.5L and 0.4L)
(5.9.4)

Top-Fiber
(at transfer length)
(5.9.4)

Top-Fiber
(at 0.5L and 0.4L)
(5.9.4)

Bottom-Fiber
(at transfer)
(5.9.4)

Shear Capacity
(5.8.3)

Figure 5.5 – Flow chart of the design process used in the analysis tool

5.3.4   Verification of Tool

Twelve design cases were completed through the use of both the parametric analysis tool and PGSuper to ensure that the tool would yield valid, consistent design results. Results from the verification runs are presented in Table 5.4. Designs were completed through the use of AASHTO LRFD 2004 and 2012, for two different girder types, various beam spacing values and two different beam lengths. Investigation of both short-spans (controlled by flexural capacity) and long-spans (controlled by stress checks) was completed to verify the accuracy of both the allowable stress and flexural capacity calculations.

Table 5.4 – Validation of Analysis Tool against PGSuper results

		1	2	3	4	5	6	7	8	9	10	11	12
Specification		AASHTO 2012				AASHTO 2004					AASHTO 2004		
Girder Type		Tx46				Tx46					Tx62		
Span Length, L_{span} (ft)		44	100	100	100	44	44	100	100	100	120	120	120
spacing, s (ft)		6.7	6.7	8	8.7	6.7	8	6.7	8	8.7	6.7	8	8.7
# required strands	Tool	12	46	52	54	12	14	46	52	56	56	60	64
	PG Super	12	46	52	54	12	14	46	52	56	56	60	64
M_n (k-ft)	Tool	2070	7110	7930	8220	2070	2350	7090	7910	8420	11400	12200	12900
	PG Super	2090	7030	7920	8230	2090	2440	7030	7910	8470	11300	12100	12900

A comparison of the results in Table 5.4 reveals that the parametric analysis tool and PGSuper required the same number of strands for all twelve design cases. The flexural capacities calculated using the tool are also similar to those calculated using PGSuper, generally within 1 percent of one another.

5.4 SAMPLE OF RESULTS

A sample of the final results from the parametric study is presented in this section. The effect of the design parameter variation (outlined in Section 5.2) on prestress loss, flexural reinforcement requirements, flexural strength, shear strength, camber and deflection was investigated through the completion of over 1800 design cases.

Results of the parametric study are typically presented as shown in Figure 5.6. The plots highlight the variation of the output parameter with increasing span length. The number of strands required for shorter design lengths is typically controlled by the flexural capacity, while longer spans are controlled by stress checks. The effect of the different loss estimation procedures on both designs controlled by flexural capacity and stress checks can be seen in these plots. The relevant bridge information (i.e. section type, maximum allowable span length, release and ultimate concrete strength) accompanies each of the plots.

Due to the large amount of data generated during the course of the parametric study, only a subset of the results is presented here and is sufficient to illustrate the common trends observed within the full dataset. The AASHTO LRFD 2012 loss procedure had the largest effect on the design of the Type C girders. For this reason, Type C girders were selected for demonstration of the common trends. Remaining results from the parametric study are presented in Appendix D.
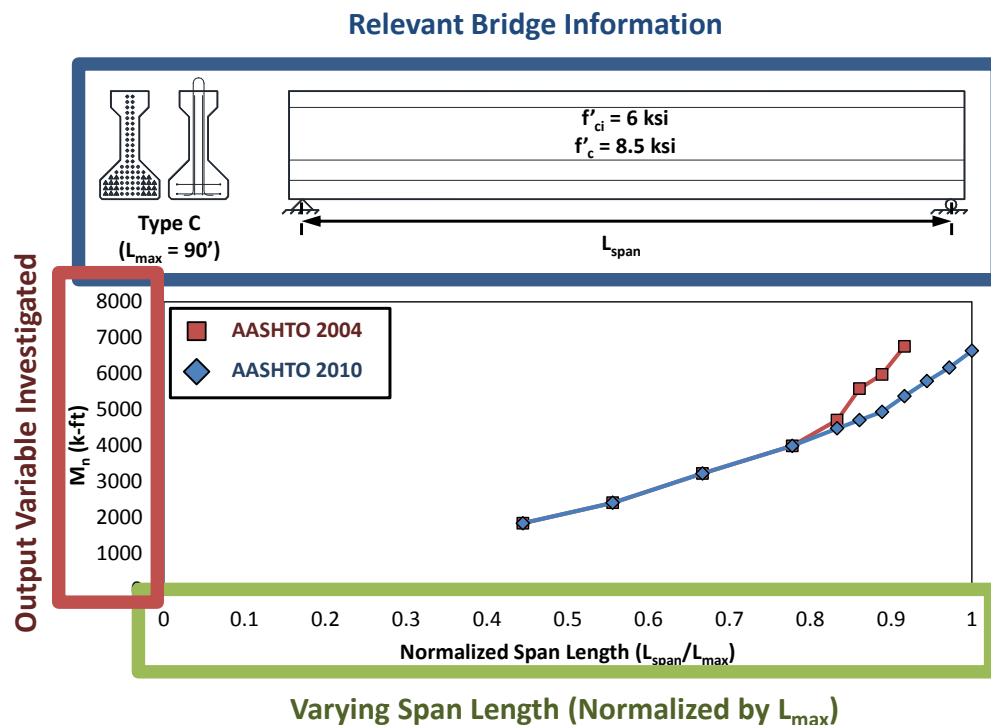
Figure 5.6 – Standard plot style from parametric study

109

5.4.1 Prestressing Strand

The total prestress loss, all of the individual loss components and all of the factors and coefficients influencing the loss components were investigated. Development of the design recommendations (as discussed in Chapter 6) was aided by study of the factors and coefficients (in terms of influence and variation) contributing to the calculation of the individual prestress loss components.

The prestress losses estimated per the recommendations of AASHTO LRFD 2004 and 2012 are shown in Figure 5.7. The short- and long-term losses are presented individually, in (a) and (b) respectively, and the total prestress loss is presented in Figure 5.7 (c).

In general, higher prestress losses mean that each strand is less effective; this will lead to more strands being required for the purpose of controlling stresses. Lower losses would imply the strands are more effective and less would be required to control stresses. Losses have no effect on the ultimate capacity of the strands and will not influence the flexural capacity of the girder for a given number of strands in a section.

A series of observations can and will be made. First, the short-term elastic shortening loss is very similar, if not identical, for shorter span lengths. In these shorter span designs, the designs are controlled by the flexural capacity and therefore the same numbers of strands are required for both specifications. Given a consistent number of strands, the only difference between the elastic shortening estimated using AASHTO LRFD 2004 and 2012 is the assumed strand stress. This would suggest that the approximation of 70% of the ultimate strand stress ($0.7f_{pu}$), which is used in AASHTO LRFD 2004, is a good approximation for the stress in the strands immediately after transfer, which is calculated using the iterative process discussed in Chapter 2 or using transformed section properties.
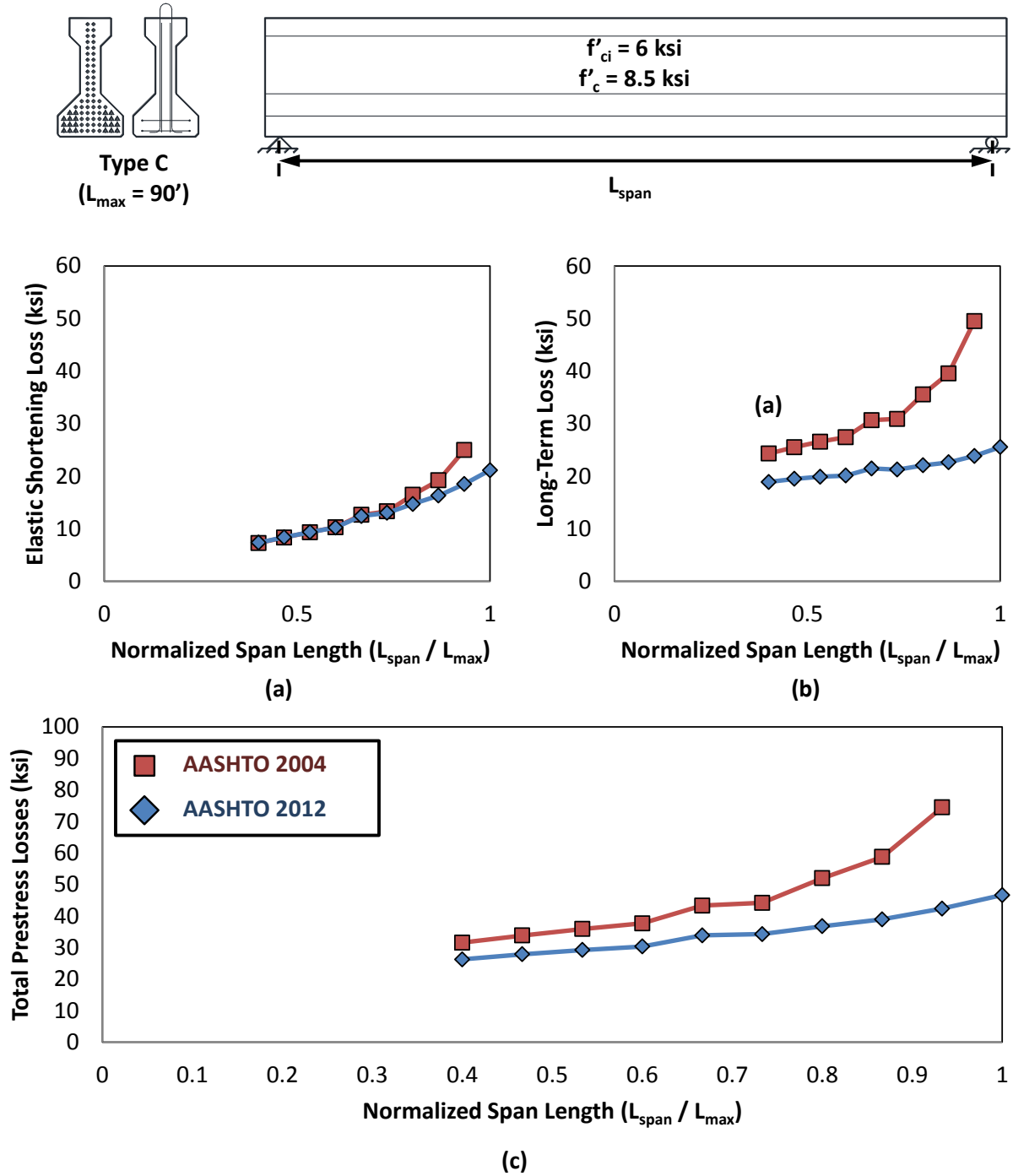
Figure 5.7 – (a) Elastic shortening loss, (b) Total long-term loss and (c) Total prestress loss for Type C girders of various lengths

The results from AASHTO LRFD 2004 and 2012 diverge at approximately 80 percent of the maximum normalized span length. The divergence is present for two interconnected reasons: (1) the designs for the longer spans are controlled by flexural stress, as opposed to flexural strength, requirements and (2) less strands were required by the AASHTO LRFD 2012

procedure. The number of strands required for both designs will be discussed in the following section.

The difference in the prestress loss estimated by AASHTO LRFD 2004 and 2012 is evident in the corresponding prestressing strand requirements. The lower prestress loss estimated by AASHTO LRFD 2012 resulted in fewer prestressing strands than those estimated by AASHTO LRFD 2004. This trend was observed for many different cross-section types, but is shown for the most extreme case in Figure 5.8.

The results from 16 individual Type C girder designs are plotted in Figure 5.8. The difference in the number of prestressing strands required by AASHTO LRFD 2004 and 2012 is shown for eight different span lengths. As noted previously, design of the shorter span lengths was controlled by flexural strength requirements, was unaffected prestress loss estimation method, and therefore resulted in identical prestressing strand requirements. Flexural capacity is dependent on the ultimate strength of the prestressing strands and independent of prestress loss. For the other cross-section types investigated, this transition point occurred between 75 and 85 percent of the maximum allowable span length.

The beginning of a difference between the strands required by the two specifications is an indicator that one, or both, of the designs are governed by stress limit checks. The controlling stress limit was typically the bottom fiber tension check at mid-span under service loads. Typically, the design for a span length immediately right of the transition point was governed by flexural capacity using AASHTO LRFD 2012 and governed by stress limit checks using AASHTO LRFD 2004. The larger strand differentiations occur when both designs are governed by stress limit checks.

The design with the largest strand differential is highlighted in Figure 5.8. The design of this Type C girder at a span length of around 90% of the maximum allowable span length using AASHTO LRFD 2012 will allow for 10 fewer strands than a design using AASHTO LRFD 2004; this is around a 25% reduction in the number of strands required.
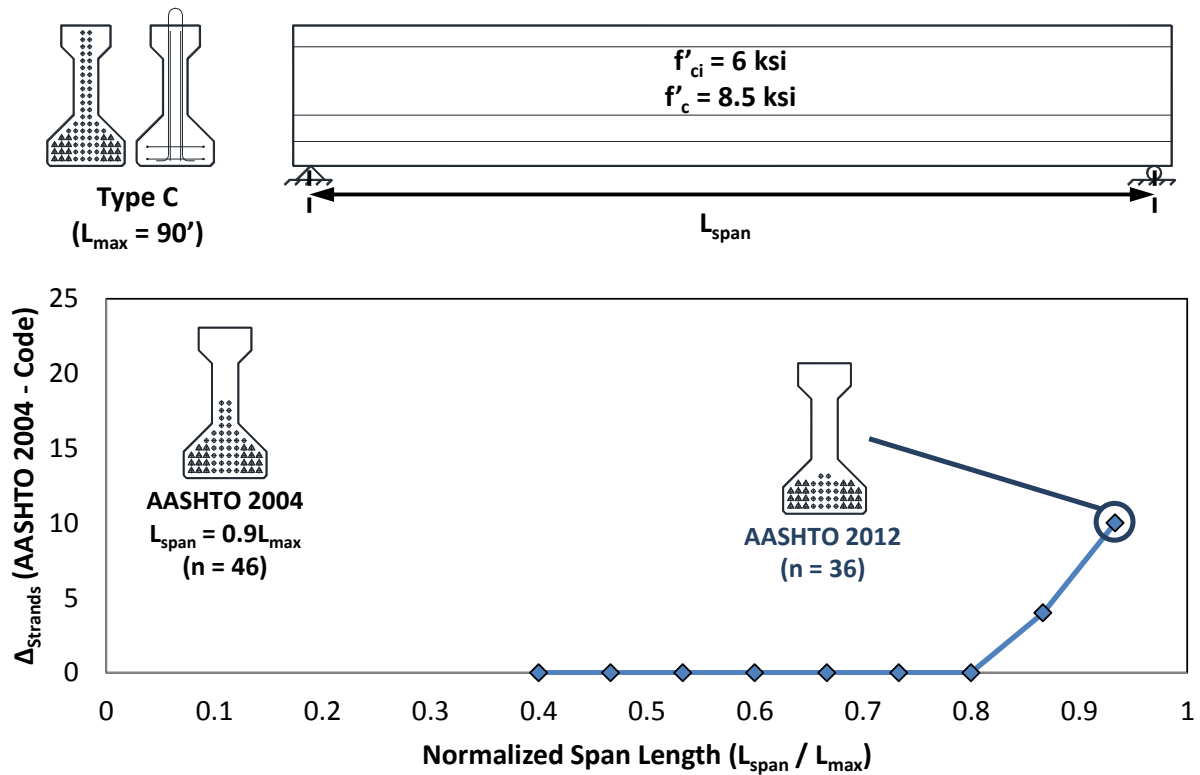
Figure 5.8 – Difference in total strands required by AASHTO LRFD 2004 vs. 2012

5.4.2 Flexural Strength

The flexural strength of a girder is primarily dependent on the number of prestressing strands provided in the design. The flexural capacities resulting from designs based upon the AASHTO LRFD 2004 and 2012 prestress loss estimates are shown in Figure 5.9. When the number of strands required by the two specifications was identical, there was no difference in calculated flexural capacity. The largest difference between the flexural capacities of the AASHTO LRFD 2004 and 2012 designs was around 25%, shown in Figure 5.9 at a span length of about 90% of the maximum design span. When a design required less strands, a lower flexural capacity was observed; the removal of about 25% of the strands resulted in around 25% decrease in flexural capacity.
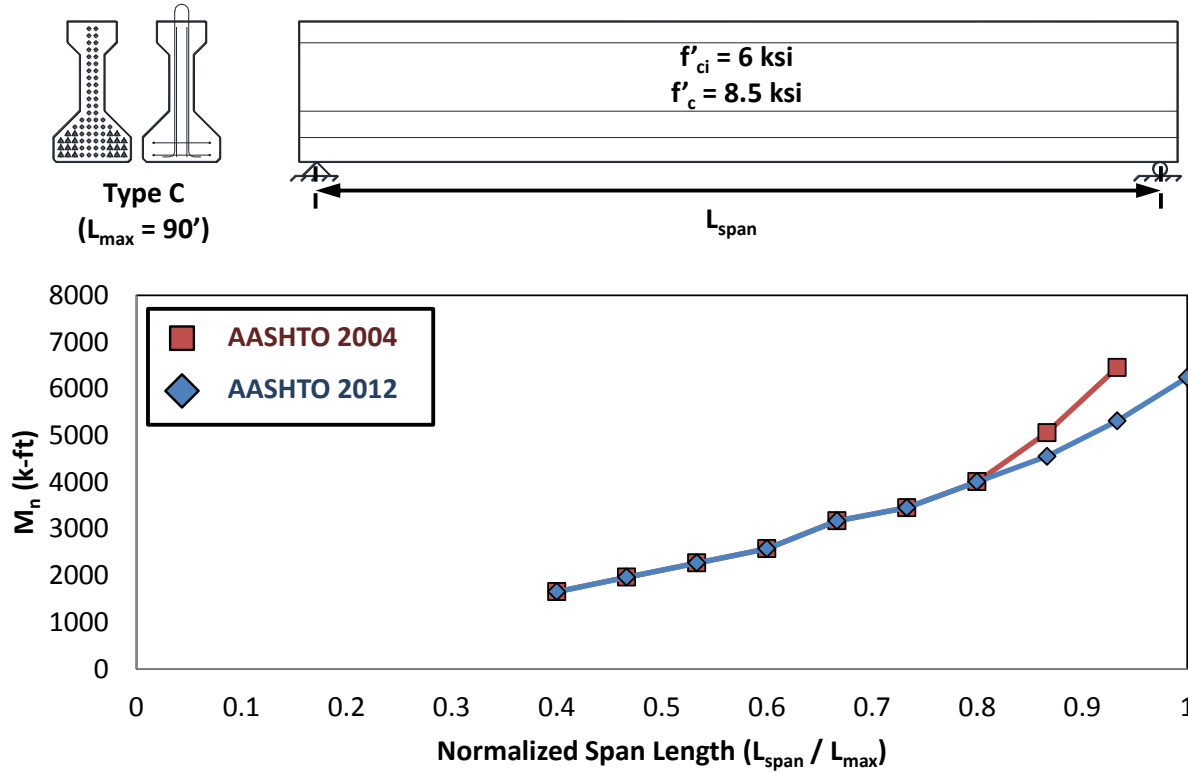
Figure 5.9 – Flexural capacity (M_n) calculated using AASHTO LRFD 2004 and 2012

5.4.3 Shear Capacity

The shear capacity at the critical section was calculated for all girders within the parametric study to investigate the effect of the different prestress loss procedures. The shear capacity was calculated using the modified compression field theory based approach presented in Article 5.8.3.4.2 of AASHTO LRFD 2012. The general procedure is presented below in Equations (5.1) through (5.6).

$$V_n = V_c + V_s + V_p$$

(5.1)

AASHTO 12 (5.8.3.3-1)

$$V_c = 0.0316\beta\sqrt{f'_c}b_v d_v$$

(5.2)

AASHTO 12 (5.8.3.3-3)

V_c determined by procedure provided in 5.8.3.4.2

114

$$V_s = \frac{A_v f_y d_v \cot \theta}{s}$$

(5.3)

AASHTO 12 (C5.8.3.3-1)

Where:

V_c = shear resistance provided by the tensile stresses in the concrete (kip)

V_s = shear resistance provided by transverse reinforcement (kip)

V_p = component in the direction of the applied shear of the effective prestressing force; positive if resisting the applied shear (kip)

b_v = effective web width taken as the minimum web width within the depth d_v as determined in Article 5.8.2.9 (in.)

d_v = effective shear depth as determined in Article 5.8.2.9 (in.)

s = spacing of transverse reinforcement measured in a direction parallel to the longitudinal reinforcement (in.)

β = factor indicating ability of diagonally cracked concrete to transmit tension and shear as specified in Article 5.8.3.4

$$\beta = \frac{4.8}{(1 + 750\varepsilon_s)}$$

(5.4)

AASHTO 12 (5.8.3.4.2-1)

θ = angle of inclination of diagonal compressive stresses as determined in Article 5.8.3.4 (degrees)

(5.5)

$$\theta = 29 + 3500\varepsilon_s$$

AASHTO 12 (5.8.3.4.2-3)

A_v = area of shear reinforcement within a distance s (in.^{2})

ε_s = net longitudinal tensile strain in the section at the centroid of the tension reinforcement

$$\varepsilon_s = \frac{\left(\frac{|M_u|}{d_v} + 0.5N_u + |V_u - V_p| - A_{ps}f_{po}\right)}{E_s A_s + E_p A_{ps}}$$

(5.6)

AASHTO 12 (5.8.3.4.2-4)

A_{ps} = area of prestressing steel on the flexural tension side of the member (in.^{2})

A_s = area of nonprestressed steel on the flexural tension side of the member at the section under consideration (in.^{2})

f_{po} = a parameter taken as modulus of elasticity of prestressing tendons multiplied by the locked-in difference in strain between the prestressing tendons and the surrounding concrete (ksi)

N_u = factored axial force, taken as positive if tensile and negative if compressive (kip)

$|M_u|$ = factored moment, not to be taken less than $|V_u - V_p|d_v$ (kip-in)

V_u = factored shear force (kip)

At this point in the design process, all the variables required in the above equations are known except for the spacing of the transverse reinforcement (*s*) and the area of shear reinforcement provided within this spacing (A_v). These two variables are prescribed for typical sections in the TxDOT Bridge Design Standard Drawings. The prescribed values were used in calculating the shear capacity, as shown in Equation (5.7).

$$V_n = 0.0316\beta\sqrt{f'_c}b_v d_v + \frac{(0.4\ in^2)f_y d_v \cot\theta}{(4\ in)} + V_p \qquad \textbf{(5.7)}$$

The shear capacity (V_n) for designs using both AASHTO LRFD 2004 and 2012 are presented in Figure 5.10. It can be seen that the design requiring more prestressing steel, from AASHTO LRFD 2004, will have a slightly smaller shear capacity. This is primarily due to the effective shear depth (d_v) decreasing when more prestressing strands are provided.
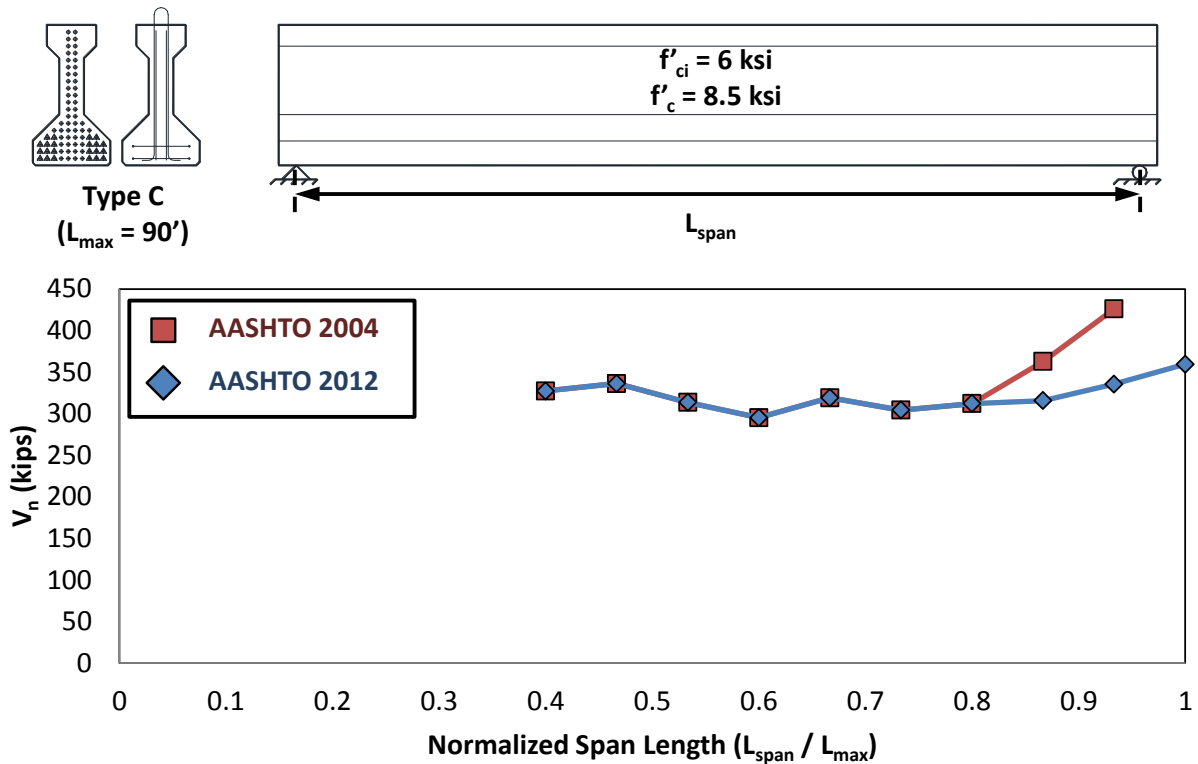
Figure 5.10 – Shear capacity (V_n) of beam using TxDOT recommended reinforcement calculated using AASHTO LRFD 2004 and 2012

5.4.4 Camber Prediction

The initial camber was investigated through use of the expression presented in Equation (5.8). A larger amount of (less effective) prestressing steel increases the force due to the prestressing after elastic shortening (P_i). This increased force will cause an increase in the calculated camber, which is represented as negative (upward) deflection by the expression. This behavior is shown in Figure 5.11, where camber calculated per AASHTO LRFD 2004 is larger at longer span lengths.

$$\Delta_i = \frac{-(2e_{cl} + e_e)P_i L_{span}^2}{24E_{ci}I_g} + \frac{5w_{sw}L_{span}^4}{384E_{ci}I_g} \tag{5.8}$$

Where:

e_{cl}	= eccentricity of prestressing tendons at mid-span (in.)
e_e	= eccentricity of prestressing tendons at end of girder (in.)
P_i	= force due to the prestressing tendons after elastic shortening (kip)
L_{span}	= design span length (in.)
E_{ci}	= modulus of concrete at time of release (ksi)
I_g	= moment of inertia of gross section (in.^{4})
w_{sw}	= girder self-weight (kip-in.)
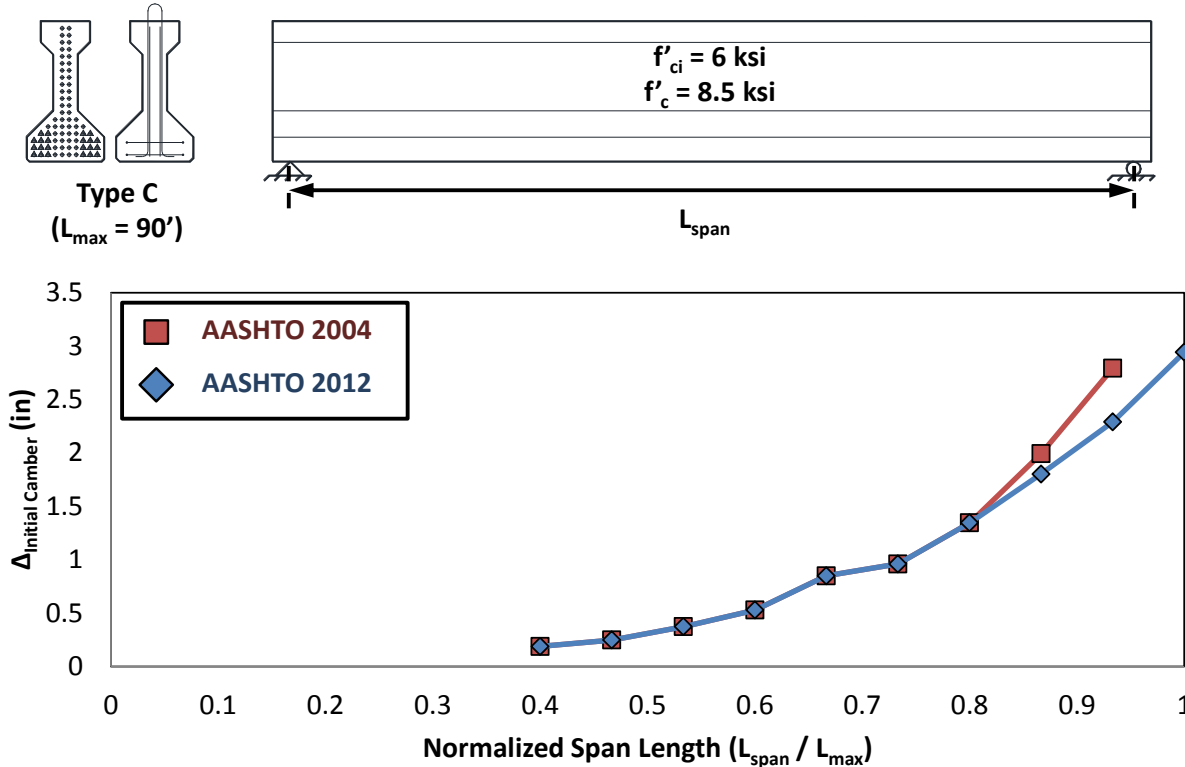
Figure 5.11 – Initial camber (Δ_i) calculated using AASHTO LRFD 2004 and 2012

5.5 SUMMARY

The parametric study was conducted with the intention of examining: (1) the design outcomes of both the AASHTO LRFD 2004 and AASHTO LRFD 2012 prestress loss estimation methods, and (2) the sensitivity of the different prestress loss components to the input variables of AASHTO LRFD 2012. A number of different influential design parameters were varied in order to properly account for the full spectrum of typical Texas materials and designs. These parameters included girder cross-section type, girder spacing, span length and concrete release strength. In order to investigate the effect of all the input variables on design and accomplish all the goals of the study, an analysis tool was developed and verified against current commercial design software.

Through the investigation of the results from the parametric study, summarized by the design of a series of Type C girders presented in this chapter, a few general trends were observed. Girders designed using AASHTO LRFD 2012 will have lower estimated total prestress loss than girders designed using AASHTO LRFD 2004. The lower estimated prestress loss leads to designs requiring less strands, leading to girders with lower flexural capacity, lower shear reinforcement requirements and smaller estimated camber. If the loss procedure in AASHTO LRFD 2012 does not accurately and conservatively estimate prestress loss, the girder designed will have questionable strength and serviceability performance.

The results obtained from the parametric study (fully disclosed in Appendix D) are used extensively in Chapter 6 to support extensive simplifications to the prestress loss provisions of the AASHTO LRFD Bridge Design Specifications.

CHAPTER 6
Recommendations for the Estimation of Prestress Loss

6.1 OVERVIEW

Design recommendations were developed on the basis of a thorough examination of the data gathered during the course of TxDOT Project 0-6374. The prestress loss provisions of the 2012 AASHTO LRFD Bridge Design Specifications were consistently found to be overly complicated and marginally unconservative during the course of the literature review, database analysis and parametric study. The development of new prestress loss provisions was therefore driven by two goals: (1) to reduce the unnecessary complexity of the AASHTO LRFD 2012 method and (2) to introduce additional conservatism through the use of lower bound constants and parameter expressions. The simplifications introduced during the process can be subdivided into three main categories: (i) dissociation of deck placement and long-term estimates, (ii) consideration of typical construction details, and (iii) reincorporation of select AASHTO LRFD 2004 recommendations. Each simplification is thoroughly examined and justified to ensure that the bases for the TxDOT Project 0-6374 prestress loss provisions are fully understood.

A final database evaluation of the TxDOT Project 0-6374 recommendations, presented at the end of this chapter, revealed that the simplification process resulted in a set of prestress loss provisions that was simpler, more conservative and more precise than the methods outlined in the 2004 and 2012 AASHTO LRFD Bridge Design Specifications.

6.2 BASIS FOR RECOMMENDATIONS

Development of design recommendations was accomplished through a synthesis of knowledge gathered during the course of the research project. The key findings (i.e. items for resolution) from each effort are outlined here.

- *Literature Review*: The loss estimation provisions found in AASHTO LRFD 2012 were found to be overly complicated through an investigation of the expressions. Since the procedure was introduced in 2005, a number of research studies have been conducted to make recommendations to simplify the procedure (Swartz 2010, Roller 2011, etc.). Many of these recommendations were taken into account during the development of the TxDOT Project 0-6374 prestress loss provisions.

- *Database Evaluation*: The most comprehensive prestress loss database ever assembled was used to evaluate the performance of the current prestress loss provisions. Despite detailed calibration of material expressions and consideration of transformed and composite properties, AASHTO LRFD 2012 does not offer any greater precision than AASHTO LRFD 2004. Although there was no greater precision, the conservatism of the code was lost with the introduction of the loss procedure in AASHTO LRFD 2005.

- *Experimental Study*: During the experimental study, the reliance of prestress losses on concrete properties, climate conditions, cross-section geometries and time were investigated. A strong correlation between the concrete properties (i.e. coarse

aggregate type and content) was observed, while the other factors had little effect on losses. These relationships were taken into account when developing the recommendations.

- *Parametric Study*: One of the goals of the parametric study was to investigate the design implications of the current loss procedures. It was found that drastic strand losses relative to AASHTO LRFD 2004 occurred with the use of AASHTO LRFD 2012; this may demonstrate a loss of conservatism. The other goal of the study was to inspect the variation of many parameters (considered by AASHTO LRFD 2012) within the bounds of typical design limitations. A lack of variation of some parameters was observed during the course of this study, further supporting the viewpoint that AASHTO LRFD 2012 is unnecessarily complex.

The design recommendations were developed on the basis of the findings noted above. The prestress loss provisions of AASHTO LRFD 2012 were used as a starting point and simplifications/adjustments were made when and where appropriate, as shown in Figure 6.1.

AASHTO LRFD 2012

1. **Dissociation of deck placement and long-term estimates (Section 6.3)** — $\Delta f_{ca,\Delta P}$ | $k_{td} = 1.0$ | Δf_{pSS}

2. **Consideration of typical construction details (Section 6.4)** — $K_{id} = 0.9$ | $k_s = 1.0$ | $t_i = 1.0$ day, $t_d = 120$ day

3. **Further Simplifications (Section 6.5)** — $k_f = \dfrac{7.2}{4.8 + f_{ci}}$ | Use $f_{pt} = 0.7 f_{pi}$ in Δf_{pES}, Δf_{pCR} and Δf_{pR}

Design Recommendations
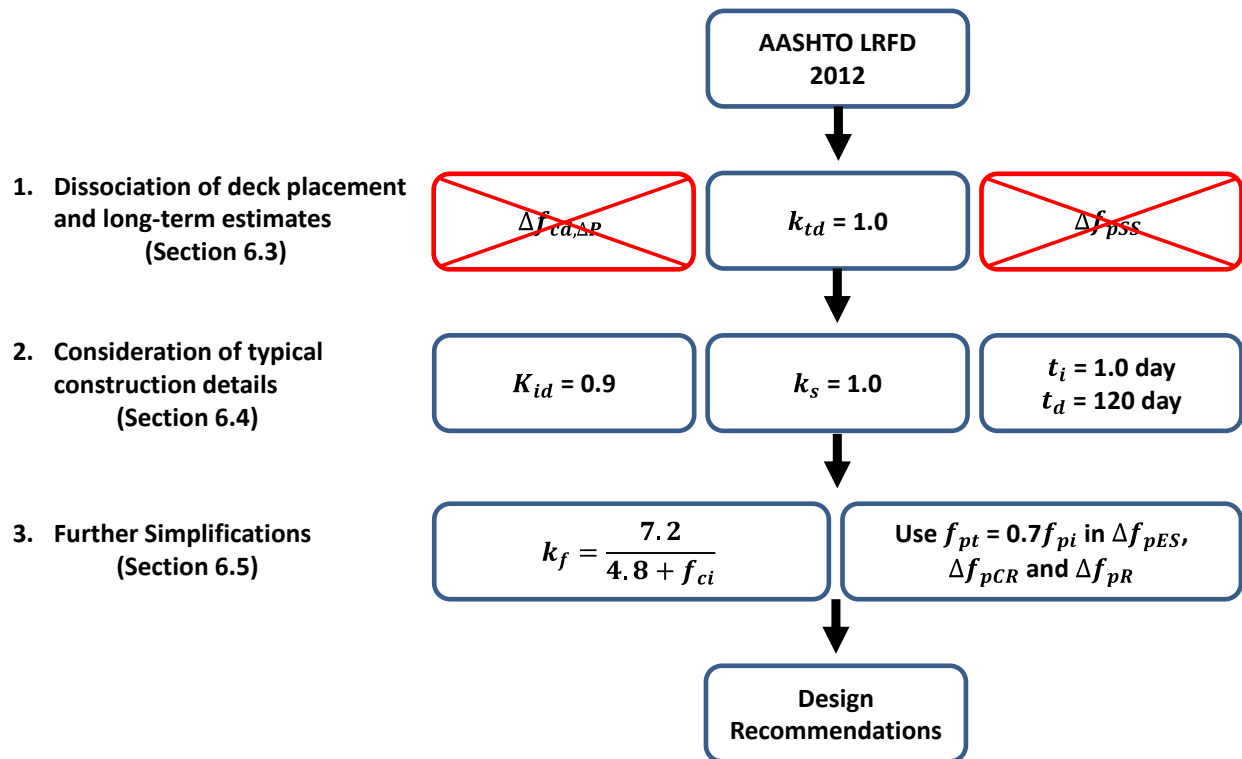
Figure 6.1 – Development of TxDOT Project 0-6374 Prestress Loss Provisions

6.3   DISSOCIATION OF DECK PLACEMENT AND LONG-TERM ESTIMATES

The prestress loss provisions of the 2012 AASHTO LRFD Bridge Design Specifications contain separate expressions for estimation of the long-term prestress losses occurring before and after deck placement. This approach was born out of a deficiency perceived by the NCHRP 496 researchers: "the current AASHTO-LRFD formulas do not consider the interaction between the precast pretensioned concrete girder and the precast or cast-in-place concrete deck" (Tadros et al.

2003). As noted above, this distinction adds unnecessary complexity to a method that is no more precise than its much simpler predecessor.

It is therefore recommended to eliminate the distinction between the long-term prestress losses occurring before and after deck placement. This may be accomplished, in large part, through simple combination of the before and after deck contributions of each long-term prestress loss mechanism: shrinkage, creep and relaxation. Minor components of the total prestress loss may also be neglected if the difficulty associated with its calculation outweighs the benefits to the estimation (in regards to precision and conservatism).

6.3.1 Girder Shrinkage

The AASHTO LRFD 2012 expression for the prestress loss due to girder shrinkage after deck placement (Δf_{pSD}) is presented in Equation (6.1). This component of the AASHTO LRFD 2012 loss estimate was previously introduced in Chapter 2; full definition of all parameters is provided therein. Dissociation of the shrinkage-related losses from the timing of deck placement will be accomplished by accounting for the after deck shrinkage within the before deck expression. While this approach will eliminate consideration of the composite section effects, it will do so with a minor loss of fidelity and a major gain in the simplicity of the calculations.

$$\Delta f_{pSD} = \varepsilon_{bdf} K_{df} E_p$$

(6.1)

AASHTO 12 (5.9.5.4.3a-1)

Where:

ε_{bdf} = shrinkage strain of girder between time of deck placement and final time

K_{df} = transformed section coefficient that accounts for time-dependent interaction between concrete and bonded steel in the section being considered for time period between deck placement and final time

$$K_{df} = \cfrac{1}{1 + \cfrac{E_p}{E_{ci}} \cfrac{A_{ps}}{A_c} \left(1 + \cfrac{A_c e_{pc}^2}{I_c}\right)\left(1 + 0.7\psi_b(t_f, t_i)\right)}$$

(6.2)

AASHTO 12 (5.9.5.4.3a-2)

The shrinkage occurring between the time of deck placement and fulfillment of the girder service life (ε_{bdf}) is defined as the difference between the full service life shrinkage (ε_{bif}) and the shrinkage occurring between the time of prestress transfer and deck placement (ε_{bid}). The estimated shrinkage of a girder over its full service life is presented in Equation (6.3). Within this expression are factors accounting for relative humidity (k_{hs}), volume-to-surface area ratio (k_s), and concrete strength (k_f). The only factor that is dependent on the timing of the deck placement is the time development factor (k_{td}).

$$\varepsilon_{bif} = -k_s k_{hs} k_f k_{td}(t_f, t_i)0.48 * 10^{-3}$$

(6.3)

AASHTO 12 (5.4.2.3.3-1)

$$\varepsilon_{bid} = -k_s k_{hs} k_f k_{td}(t_d, t_i)0.48 * 10^{-3}$$

(6.4)

AASHTO 12 (5.4.2.3.3-1)

$$\varepsilon_{bdf} = \varepsilon_{bif} - \varepsilon_{bid} \qquad \text{(6.5)}$$

Where:

    k_{td} = time development factor

$$k_{td} = \frac{t}{61 - 4f'_{ci} + t} \qquad \begin{array}{c}\text{(6.6)}\\ AASHTO\ 12\ (5.4.2.3.2\text{-}5)\end{array}$$

    t = age of concrete after loading (days)

The time development factor is a hyperbolic function that defines the progress of a long-term loss mechanism (0 to 100 percent) on the basis of the girder age. The time development factor approaches a value of one as a girder ages, where $k_{td} = 1.0$ corresponds to full development of the corresponding prestress loss (refer to Figure 6.2). In the context of the AASHTO LRFD 2012 shrinkage estimates, the timing of the deck placement simply defines the fractions of shrinkage occurring before and after deck placement. The timing of the deck placement does not affect the final magnitude of the shrinkage strains estimated by AASHTO LRFD 2012 (i.e. the sum of $k_{td}(t_d,t_i)$ and $k_{td}(t_f,t_d)$ equals 1.0).
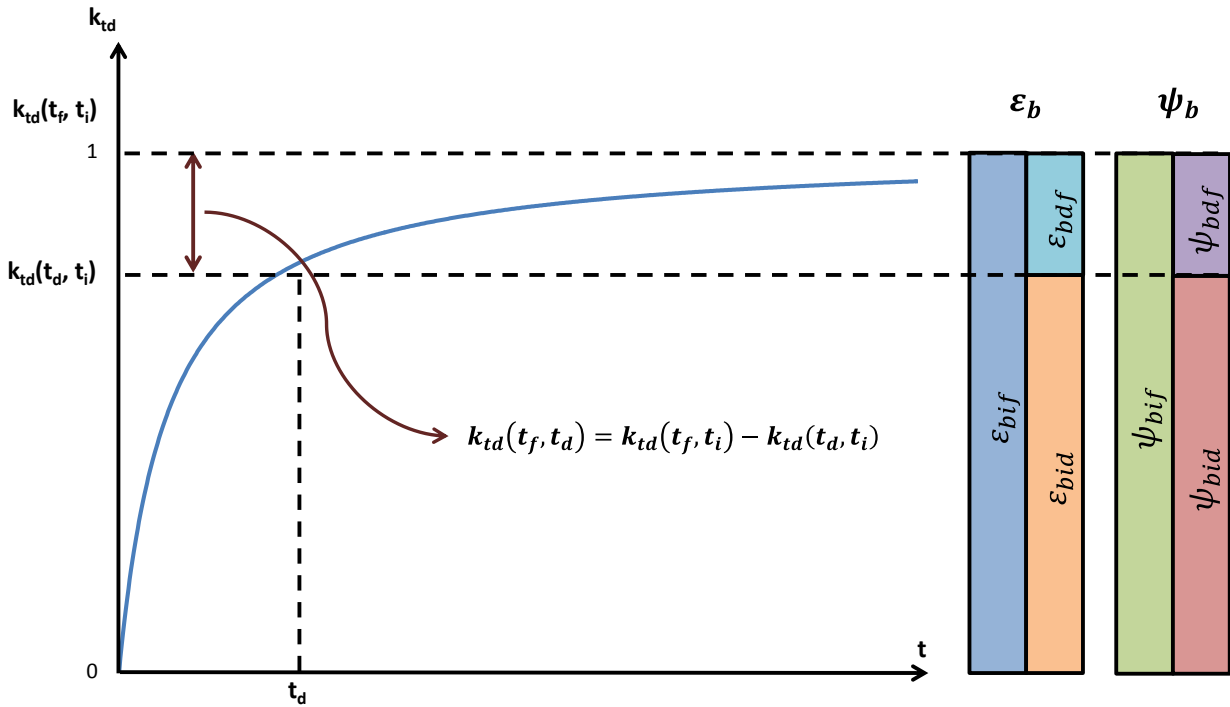
Figure 6.2 - k_{td} vs. time

The only potential refinement provided by the AASHTO LRFD 2012 approach is the ability to account for the effect of the composite section on the after deck development of the shrinkage strains and related prestress losses (through the use of the transformed section coefficient, K_{df}). For the sake of simplicity (and without a significant loss of precision), it is

therefore recommended that the prestress losses due to girder shrinkage be accounted for in one expression, where $k_{td} = 1.0$.

Time Development Factor
RECOMMENDATION: $\quad k_{td} = 1.0$

The impact of this recommendation on the AASHTO LRFD 2012 expression for the after deck prestress loss due to girder shrinkage is shown in Table 6.1. By setting $k_{td} = 1.0$, calculation of the after deck prestress loss due to girder shrinkage is eliminated. The service life prestress losses due to girder shrinkage are thereby accounted for within the AASHTO LRFD 2012 expression previously defined for shrinkage-related losses occurring before deck placement. Formal redefinition of the expression is completed later in this chapter.

Table 6.1 – Effect of $k_{td} = 1.0$ on shrinkage-related losses after deck placement

Equation (6.1)	$\Delta f_{pSD} = \varepsilon_{bdf} K_{df} E_p$
Recommendation	$k_{td} = 1$
Result	$\varepsilon_{bif} = \varepsilon_{bid}$ $\varepsilon_{bdf} = \varepsilon_{bif} - \varepsilon_{bid} = 0$ $\Delta f_{pSD} = 0$

The shrinkage-related prestress losses estimated for a series of girders are shown in Figure 6.3. The figure includes prestress loss estimates for various lengths of Tx46 girders of typical concrete release ($f_{ci} = 6$ ksi) and compressive strength ($f'_c = 8.5$ ksi). The prestress loss estimates correspond to one of the design series completed during the parametric study of Chapter 5.

The before and after deck contributions to the shrinkage-related prestress losses of AASHTO LRFD 2012 are shown in Figure 6.3 (a). A majority of the shrinkage-related prestress losses occur prior to deck placement (approximately 76 percent); a fact that further marginalizes the value of NCHRP-based corrections for the composite section. The total prestress losses due to girder shrinkage are shown in Figure 6.3 (b). The "AASHTO 2012" losses are the summation of the before and after deck contributions shown in Figure 6.3 (a). The "$k_{td} = 1.0$" losses result from implementation of the recommendations made above.

The resulting loss estimates are virtually the same. The most extreme difference is less than 2 percent and is attributable to manner in which the composite section effects are taken, or not taken (in the case of the combined estimate), into account. The transformed section

coefficient corresponding to before deck placement estimates (K_{id}) was calculated on the basis of the girder section properties, while the coefficient corresponding to after deck placement estimates (K_{df}) was calculated on the basis of composite (i.e. deck + girder) section properties. When the before and after deck placement loss contributions were combined, the transformed section coefficient was calculated on the basis of the girder properties alone and the effect of the deck was therefore neglected.
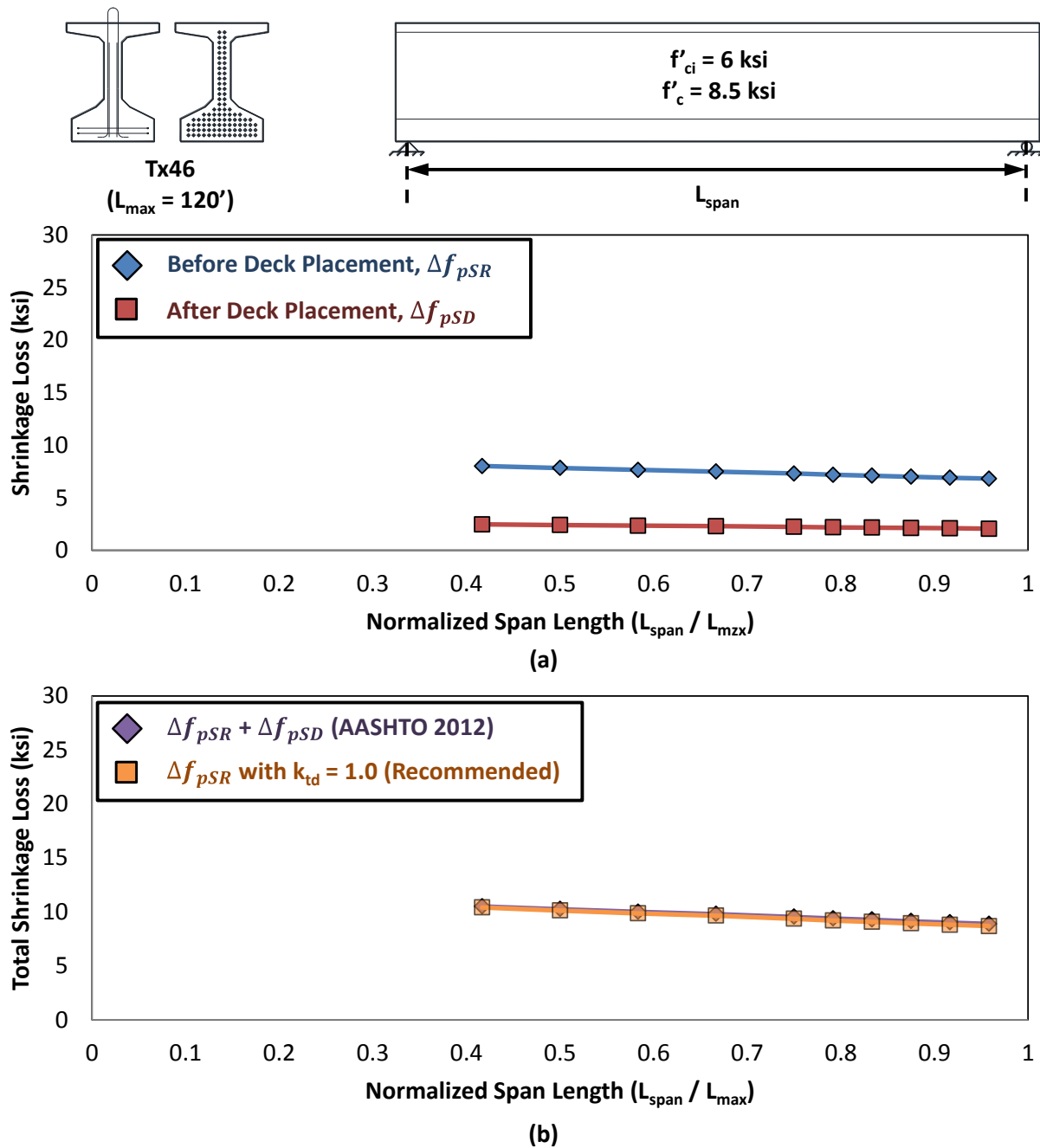
Figure 6.3 – Prestress loss due to shrinkage of the girder (a) broken into before and after deck contributions and (b) compared with $k_{td} = 1.0$

124

6.3.2 Girder Creep

The dissociation of creep-related prestress loss estimates and deck placement will be accomplished in a manner similar to that discussed for shrinkage: estimates for the prestress losses occurring after deck placement will be subsumed by the expression for creep-related prestress losses occurring before deck placement. Simplification of the creep expressions will require the elimination of time dependency (i.e. $k_{td} = 1.0$) and consideration of the deck placement effects on the section properties and long-term stresses.

The AASHTO LRFD 2012 expression for the prestress loss due to girder creep after deck placement (Δf_{pCD}) has been separated into two components, presented in Equations (6.7) and (6.8). The first component (Δf_{pCD1}) accounts for prestress loss due to creep of the girder concrete as resisted by the composite section and driven by the stresses imposed by the initial prestressing force and the self-weight of the girder. This component (Δf_{pCD1}) is a continuation of the creep occurring before deck placement and will be eliminated by setting $k_{td} = 1.0$. The second component (Δf_{pCD2}) accounts for the prestress loss due to the creep of girder concrete as resisted by the composite section and driven by changes in concrete stress (Δf_{cd}) occurring after the initial transfer of prestress. The after deck placement changes in concrete stress may be calculated through use of Equation (6.10). It should be noted that compression on the concrete is generally relieved by consideration of Δf_{cd}, resulting in creep recovery and a general reduction of the prestress loss estimate.

Analysis and simplification of the first creep component (Δf_{pCD1}) will be completed prior to consideration of the second creep component (Δf_{pCD2}). Recommendations made for the creep-related prestress loss estimates will result in full dissociation from timing of the deck placement.

$$\Delta f_{pCD1} = \frac{E_p}{E_{ci}} f_{cgp} K_{df} \left[\psi_b(t_f, t_i) - \psi_b(t_d, t_i) \right] \qquad \text{(6.7)}$$

$$\Delta f_{pCD2} = \frac{E_p}{E_{ci}} \Delta f_{cd} \psi_b(t_f, t_d) K_{df} \qquad \text{(6.8)}$$

$$\qquad \text{(6.9)}$$
$$\Delta f_{pCD} = \Delta f_{pCD1} + \Delta f_{pCD2}$$
AASHTO 12 (5.9.5.4.3b-1)

Where:

f_{cgp} = the concrete stress at center of gravity of prestressing tendons due to the prestressing force immediately after transfer and the self-weight of the member at the section of maximum moment (ksi); same as calculated for Elastic Shortening

K_{df} = transformed section coefficient that accounts for time-dependent interaction between concrete and bonded steel in the section being considered for time period between deck placement and final time

Δf_{cd} = change in concrete stress at centroid of prestressing strands due to long-term losses between transfer and deck placement, combined with deck weight and superimposed loads (ksi)

$$\Delta f_{cd} = \frac{P_\Delta}{A_g} + \frac{P_\Delta e_p{}^2}{I_g} - \frac{M_g e_{pc}}{I_c} \tag{6.10}$$

The creep-related prestress losses are calculated on the basis of the creep coefficient presented in Equation (6.11). Like the shrinkage strain, the only factor within the creep coefficient that is dependent on the timing of the deck placement is the time development factor (k_{td}). By setting $k_{td} = 1.0$, calculation of the after deck prestress loss due to girder creep under the initial concrete stresses (Δf_{pCD1}) may be eliminated as shown in Table 6.2.

$$\psi(t, t_i) = 1.9 k_{vs} k_{hc} k_f k_{td} t_i^{-0.118} \tag{6.11}$$

AASHTO 12 (5.4.2.3.2-1)

Table 6.2 - Effect of $k_{td} = 1.0$ on creep-related losses after deck placement

Equation (6.7)	$\Delta f_{pCD1} = \dfrac{E_p}{E_{ci}} f_{cgp} K_{df} \left[\psi_b(t_f, t_i) - \psi_b(t_d, t_i) \right]$
Recommendation	$k_{td} = 1$
Result	$\psi_b(t_f, t_i) = \psi_b(t_d, t_i)$ $\psi_b(t_f, t_i) - \psi_b(t_d, t_i) = 0$ $\Delta f_{pCD1} = 0$

AASHTO LRFD 2012 estimates of creep-related losses occurring before deck placement (Δf_{pCR}) and after deck placement (Δf_{pCD1}) are shown on an independent basis in Figure 6.4 (a) and as summed in Figure 6.4 (b). The creep-related prestress loss estimate, as dissociated from deck placement (i.e. $k_{td} = 1.0$), is also shown in Figure 6.4 (b). The observations and conclusions resulting from analysis of the plots are consistent with those made for shrinkage: (1) the after deck component of the creep-related loss is significantly less than the before deck component of the creep-related loss, (2) composite section effects on the prestress loss estimate should therefore be negligible, and (3) calculation of the creep-related losses on a full service life basis indeed results in minor differences that may be attributed to (justifiable) neglect of the composite section effects.
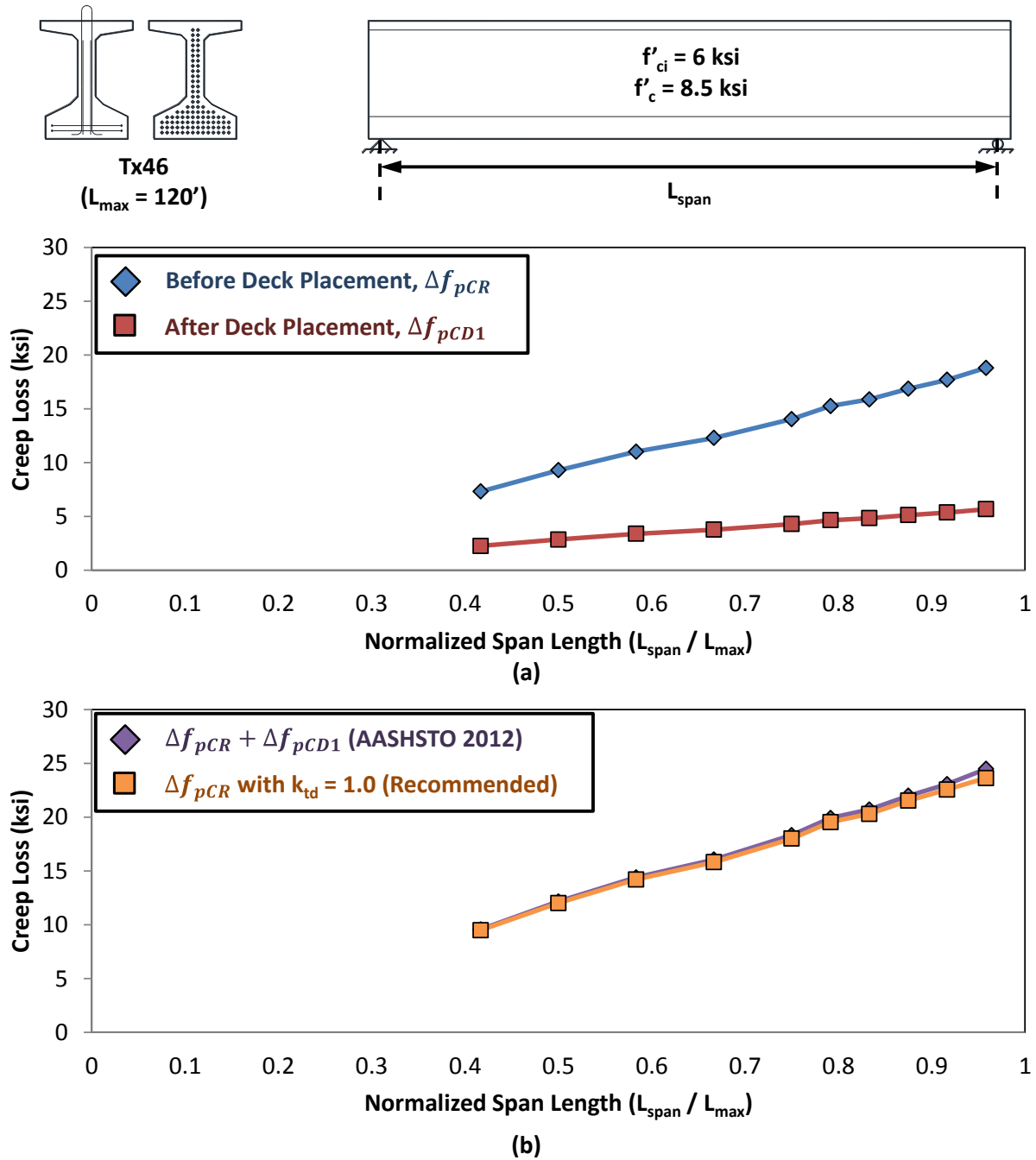
Figure 6.4 – Prestress loss due to creep of the girder (a) broken into before and after deck components and (b) compared with $k_{td} = 1.0$

The second component of the AASHTO LRFD 2012 creep expression (Δf_{pCD2}) accounts for changes in the concrete stress at the centroid of the prestressing strands. The change in the concrete stress is defined as Δf_{cd} and is inclusive of all internal and external effects occurring after initial prestress transfer, including: (1) long-term prestress losses, (2) deck weight and (3) superimposed dead loads. The change in concrete stress due to the long-term prestress losses

$(\Delta f_{cd,\Delta P})$ and dead load $(\Delta f_{cd,DL})$ is plotted for one of the parametric design series in Figure 6.5 (a).
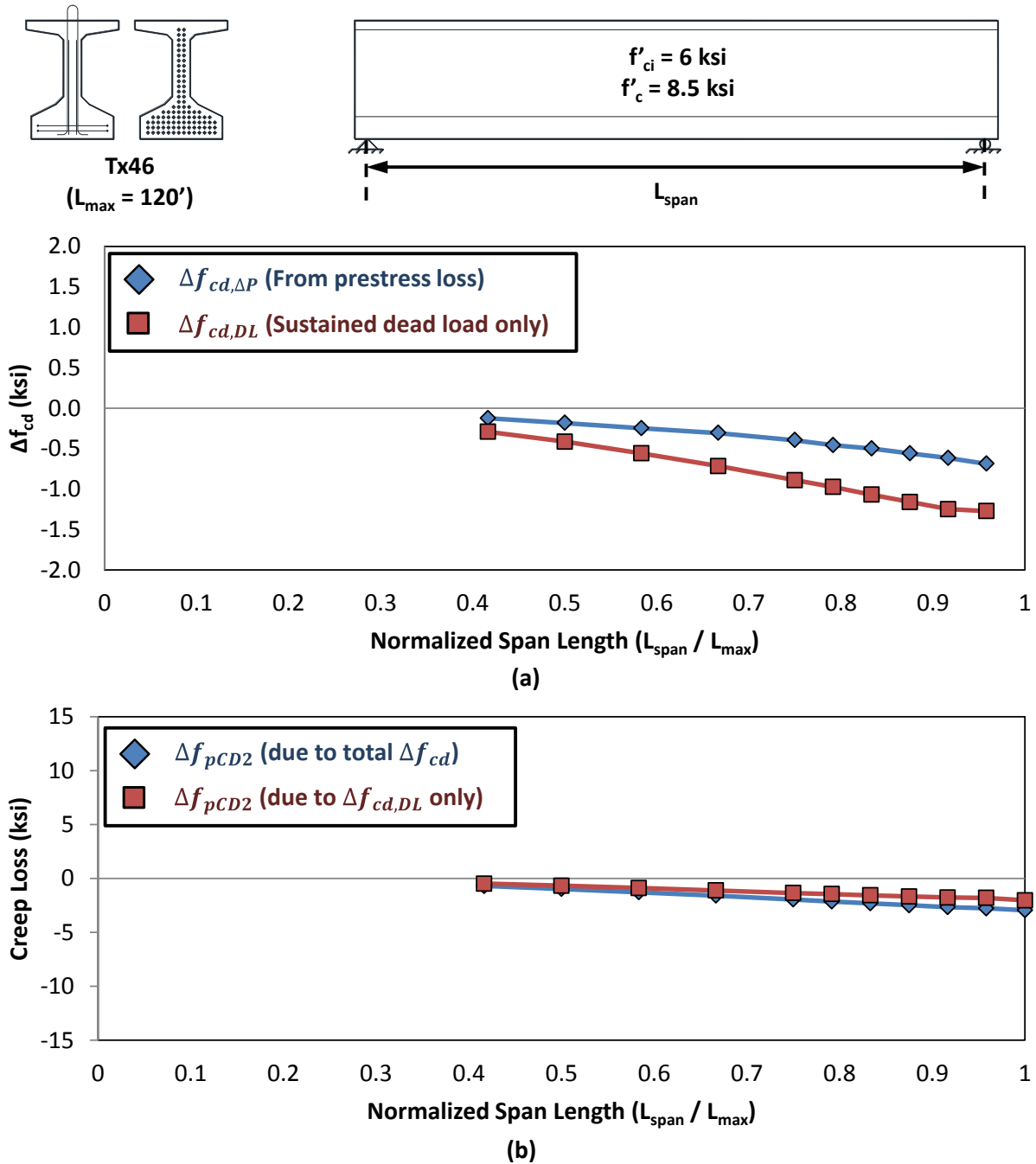
Figure 6.5 – (a) Change in concrete stress due to long-term prestress losses before deck placement $(\Delta f_{cd,\Delta P})$ and sustained dead load $(\Delta f_{cd,DL})$ and (b) Resulting creep loss due to total Δf_{cd} and $\Delta f_{cd,DL}$

As alluded to above, consideration of the long-term prestress losses and dead loads will generally reduce compression on, and creep of, the concrete; thereby resulting in lower service

life estimates of the prestress losses Figure 6.5 (b). While it would be conservative to neglect either or both of the concrete stress effects, consideration of the stress change resulting from the dead loads ($\Delta f_{cd,DL}$) may be accommodated with a minimal number of calculations and greater benefit than consideration of the stress change resulting from long-term prestress losses ($\Delta f_{cd,\Delta P}$). As shown in Figure 6.5 (a), the stress change caused by long-term prestress loss prior to deck placement ($\Delta f_{cd,\Delta P}$) is less than half of the stress change caused by the superimposed dead loads ($\Delta f_{cd,DL}$). It is therefore recommended that future prestress loss provisions neglect the effect of stress changes due to prestress losses occurring before deck placement.

<div style="border:1px solid">

After-Deck Creep Loss

RECOMMENDATION: Neglect $\Delta f_{cd,\Delta P}$

</div>

Estimates of the prestress losses resulting from after deck stress changes (Δf_{pCD2}) are plotted for one parametric design series in Figure 6.5 (b). The AASHTO LRFD 2012 estimates account for the effects of both $\Delta f_{cd,\Delta P}$ and $\Delta f_{cd,DL}$, while the recommended estimates only account for the effect of the superimposed dead load ($\Delta f_{cd,DL}$). In either case, calculation of the prestress loss estimate actually results in a "prestress gain" of less than 2.5 ksi; equivalent to about five percent of the total prestress loss encountered within a typical design scenario. Moreover, neglect of the loss-related stress change prior to deck placement ($\Delta f_{cd,\Delta P}$) will result in a discrepancy of less than 1 ksi in the most extreme circumstances.

6.3.3   Strand Relaxation

The AASHTO LRFD 2012 expressions for the prestress loss due to strand relaxation are outlined in Equations (6.12) and (6.13) for before and after deck placement, respectively. The strand relaxation occurring before deck placement is assumed to be equivalent to the strand relaxation occurring after deck placement.

$$\Delta f_{pR1} = \frac{f_{pt}}{K_L}\left(\frac{f_{pt}}{f_{py}} - 0.55\right)$$

(6.12)

AASHTO 12 (5.9.5.4.2c-1)

Where:

f_{pt} = stress in prestressing strands immediately after transfer, taken not less than $0.55f'_c$ (ksi)

K_L = 30 for low relaxation strands and 7 for other prestressing steel, unless more accurate manufacturer's data are available

$$\Delta f_{pR2} = \Delta f_{pR1}$$

(6.13)

AASHTO 12 (5.9.5.4.3c-1)

Dissociation of the relaxation-based prestress losses and the timing of deck placement may be accomplished by calculating the service life prestress loss (Δf_{pR}) as double the estimate provided in Equation (6.12).

Relaxation Loss	
RECOMMENDATION:	$\Delta f_{pR} = \dfrac{2 f_{pt}}{K_L}\left(\dfrac{f_{pt}}{f_{py}} - 0.55\right)$ **(6.14)**

Relaxation-based prestress losses, estimated on the basis of AASHTO LRFD 2004, AASHTO LRFD 2012 and 0-6374 Proposed methods, are presented in Figure 6.6. The result of the recommended expression (6.14) is not influenced by the girder length or cross-section type and will remain constant for typical fabrication procedures (where strand stress is assumed to be $f_{pt} = 0.7 f_{pu}$). The variation in relaxation loss determined using AASHTO LRFD 2012 is a result of the variation in f_{pt} for different design lengths. Implementation of the recommendation will not affect the relaxation loss estimated using AASHTO LRFD 2012 by more than about 0.5 ksi.
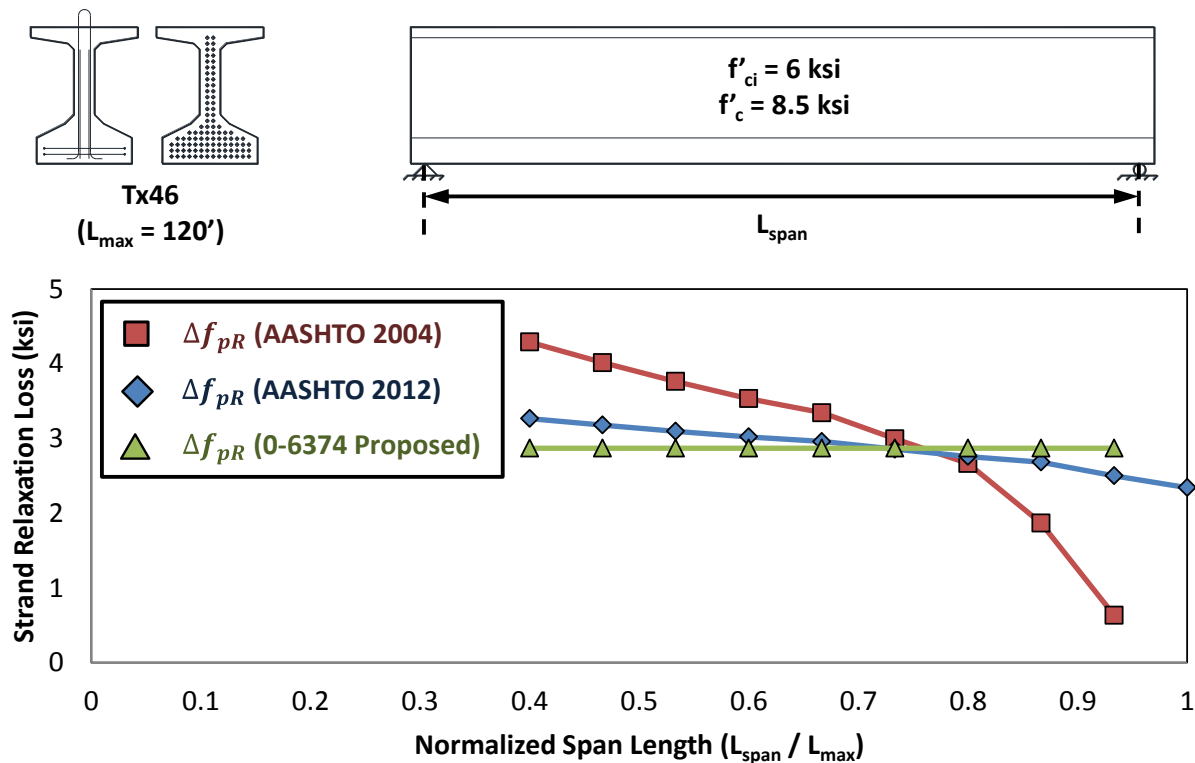
Figure 6.6 – Strand relaxation losses using AASHTO LRFD 2004, AASHTO LRFD 2012, and 0-6374 Proposed methods

6.3.4 Deck Shrinkage

The AASHTO LRFD 2012 prestress loss provisions include an expression (6.15) to account for the "prestress gain" due to the differential shrinkage between the cast-in-place deck and the precast girder. This component of the total prestress loss estimate is both small in magnitude and does not accurately model the true behavior of a bridge system, therefore it should be neglected.

$$\Delta f_{pSS} = \frac{E_p}{E_{ci}} \Delta f_{cdf} K_{df} \left[1 + \psi_b(t_f, t_d)\right]$$

<div align="right">

(6.15)

AASHTO 12 (5.9.5.4.3d-1)

</div>

Where:

Δf_{cdf} = change in concrete stress at centroid of prestressing strands due to shrinkage of deck concrete (ksi)

$$\Delta f_{cdf} = \frac{\varepsilon_{ddf} A_d E_{cd}}{\left[1 + 0.7\psi_d(t_f, t_d)\right]} \left(\frac{1}{A_c} - \frac{e_{pc} e_d}{I_c}\right)$$

<div align="right">

(6.16)

AASHTO 12 (5.9.5.4.3d-2)

</div>

ε_{ddf} = shrinkage strain of deck concrete between placement and final time

A_d = area of deck concrete (in.^{2})

e_d = eccentricity of deck with respect to the gross composite section, positive in typical construction where deck is above girder (in.)

$\psi_d(t_f, t_d)$= creep coefficient of deck concrete at final time due to loading introduced shortly after deck placement (i.e. overlays, barriers, etc.)

The assumptions underlying the deck shrinkage expression of AASHTO LRFD 2012 (Δf_{pSS}) are examined in Figure 6.7 through Figure 6.9. To begin, applicability of the expression is predicated on the use of a full-depth, cast-in-place deck as shown in Figure 6.7 (a). The behavior of the concrete deck, and resulting effects on the prestress loss, assuredly changes when alternate construction methods are utilized. In Texas, typical deck placement includes the use of precast, prestressed concrete panels, as shown in Figure 6.7 (b).
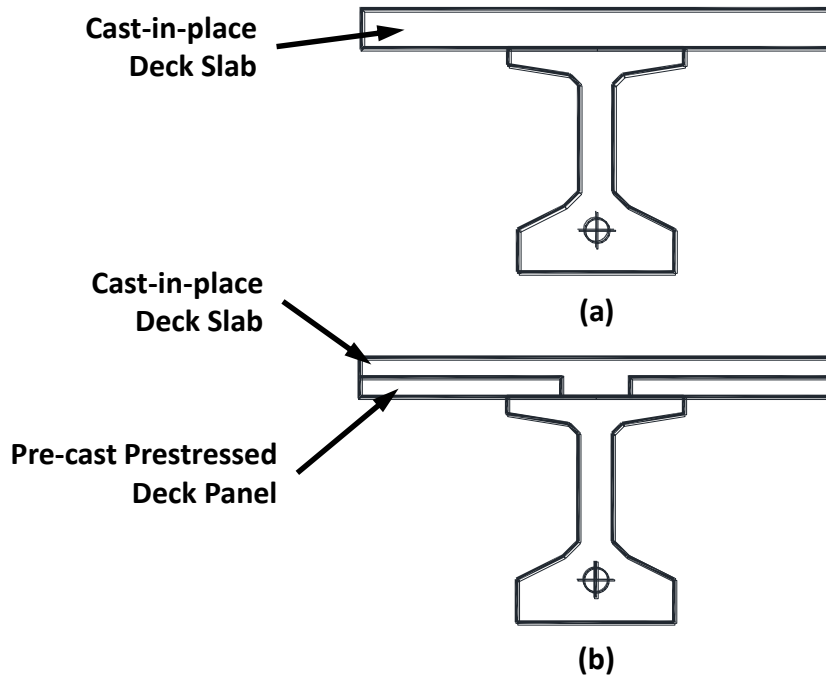
Figure 6.7 – (a) ASHTO LRFD 2012 assumed cross-section and (b) typical cross-section fabricated in Texas

In the case of the full-depth, cast-in-place solution, the deck concrete will begin to shrink shortly after exposure to a drying environment. Shrinkage of the deck will be resisted by the underlying girder through the transfer of stresses at the deck-to-girder interface. As the top fiber of the girder is forced to shrink through compatibility, positive bending stresses will be developed through the cross-section depth (Figure 6.8). The positive bending stresses will impose tension on the prestressing strands as well as the concrete. This "stress gain" in the prestressing strands is inappropriately termed a "prestress gain" within AASHTO LRFD 2012; a true "prestress gain" would imply that the concrete is subject to greater compression, which is not the case here.

Shrinkage of Deck Concrete

(a)

Tension Region

(b)
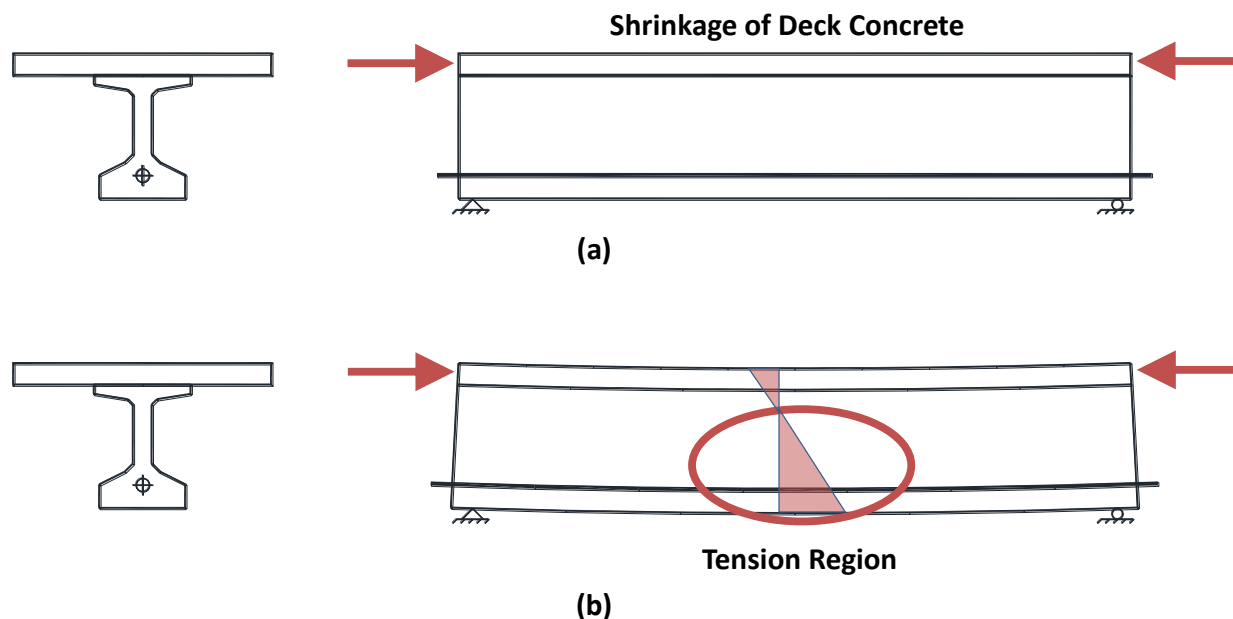
Figure 6.8 – Shrinkage of the deck concrete (a) is assumed to be restrained by the girder in the AASHTO LRFD 2012 procedure

Standard TxDOT bridge designs include the use of precast concrete panels (Figure 6.7 (b)) that are prestressed perpendicular to the longitudinal axes of the girders. These precast panels are generally placed well in advance of the bridge erection and placement of the concrete topping. The majority of the panel creep and shrinkage deformations will have accrued prior to deck placement, and remaining deformations will likely occur perpendicular to the longitudinal axes of the girders. For these reasons, the precast panels are likely the primary source of resistance to shrinkage of the cast-in-place deck topping (Figure 6.9); deck shrinkage demands imposed on the girder in such a system are likely limited in comparison to those imposed by the traditional deck construction details.

Shrinkage of Deck Concrete

Resistance by Precast Panels
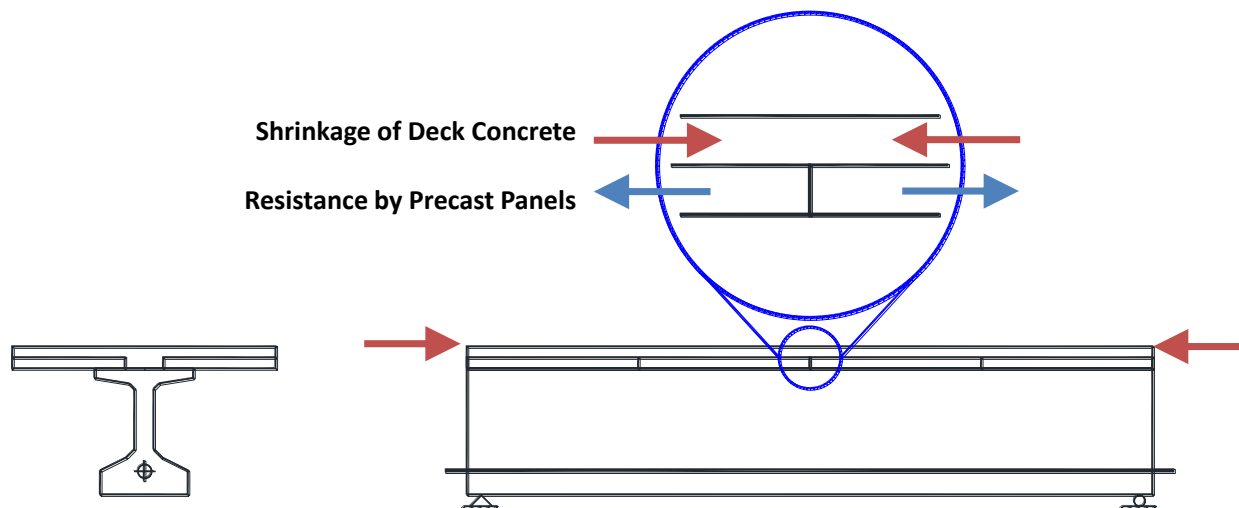
Figure 6.9 – Shrinkage of the deck concrete primarily restrained by precast panels

The AASHTO LRFD 2012 estimates of prestress loss due to deck shrinkage are shown in Figure 6.10 for three different TX-girders. It appears that: (1) deck shrinkage consistently results in increased tensile demands on both the strands and concrete, and (2) the stress demands imposed by deck shrinkage are small in comparison to total prestress losses (about 3 percent). Given the questionable basis and small impact of the provision, the "prestress loss" due to deck shrinkage should be neglected.

Deck Shrinkage Loss
RECOMMENDATION: Neglect Δf_{pSS}
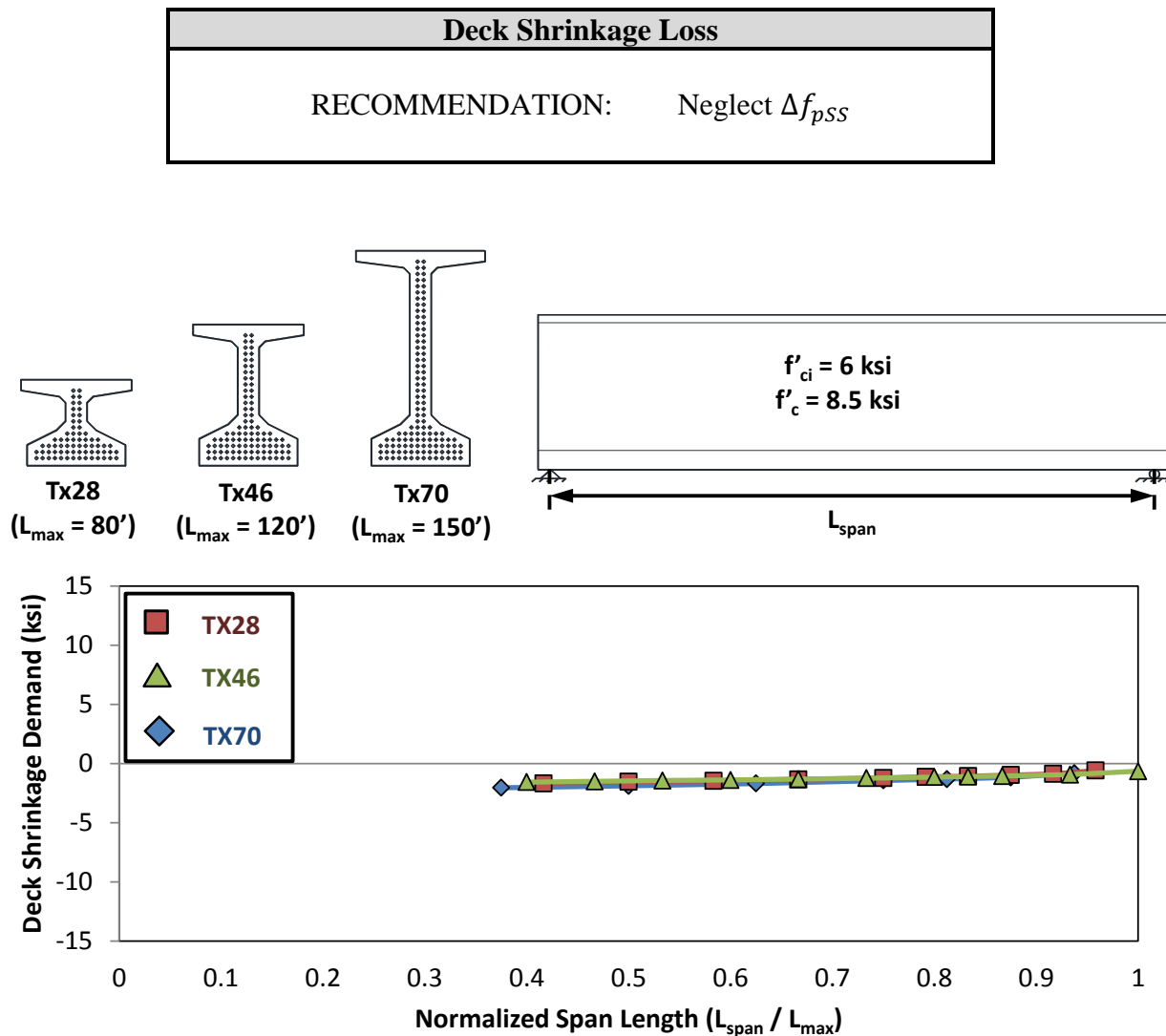
Figure 6.10 – Deck shrinkage demands for Tx28, Tx46 and Tx70

6.4   CONSIDERATION OF TYPICAL CONSTRUCTION DETAILS

Despite dissociation of deck placement and the long-term prestress loss estimates, the resulting provisions still include calculation-intensive variables with limited relevance to the precision and conservatism of the results. The variables examined below were flagged for simplification during the course of the parametric study; variation of the terms within the context

of standard bridge practice was either insignificant and/or design-stage determination of the variable was deemed purposeless. Simplification of all the variables below was completed with due consideration of the typical materials, fabrication practices and climatic conditions within the State of Texas.

6.4.1 Transformed Section Coefficient

As defined in AASHTO LRFD 2012, the transformed section coefficient (Note: $K_{id/df} \rightarrow K_{if}$) of Equation (6.17) accounts for the time-dependent interaction between the concrete and steel in a cross-section. Derivation of the coefficient (fully examined in Chapter 2) is accomplished by enforcing compatibility between the strands and concrete, and assuming that the prestressing strands provide some restraint against concrete shrinkage and creep.

$$K_{if} = \frac{1}{1 + \frac{E_p}{E_{ci}} \frac{A_{ps}}{A_g} \left(1 + \frac{A_g e_{pg}^2}{I_g}\right)\left(1 + 0.7\psi_b(t_f, t_i)\right)} \qquad (6.17)$$

AASHTO 12 (5.9.5.4.2a-2)

Variation of the transformed section coefficient was investigated during the parametric study and a sample of the results is examined here. The transformed section coefficients for three different TX-girders (Tx28, Tx46 and Tx70) of various span lengths are shown in Figure 6.11. Irrespective of the cross-section height, the transformed section coefficient decreased as the span was increased; a trend that was driven by the need for more flexural reinforcement at longer span lengths. Absolute variation of the transformed section coefficient over the range of span lengths and cross-section heights was minor nonetheless; values generally fell between 0.8 and 0.9.
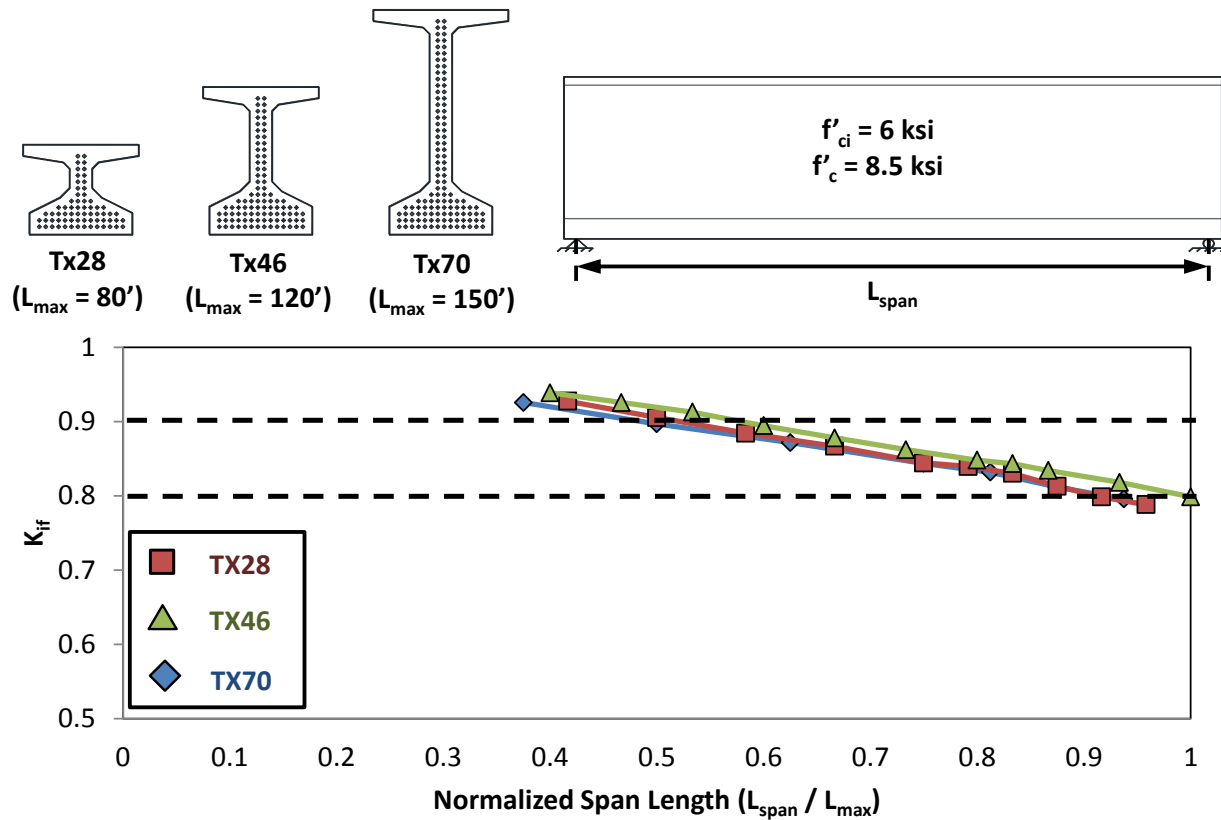
Figure 6.11 – Transformed section coefficient (K_{if}) vs. span length for Tx28, Tx46, and Tx70

The transformed section coefficients were calculated for several different types of bulb-T, I-beam, box beam and U-beam sections at three different span lengths (*0.4L_{max}*, *0.8L_{max}*, and *L_{max}*); results are summarized in Figure 6.12. Although the U-beams generated a slightly higher coefficient, nearly all girders and span lengths resulted in a transformed section coefficient between 0.8 and 0.9.

136
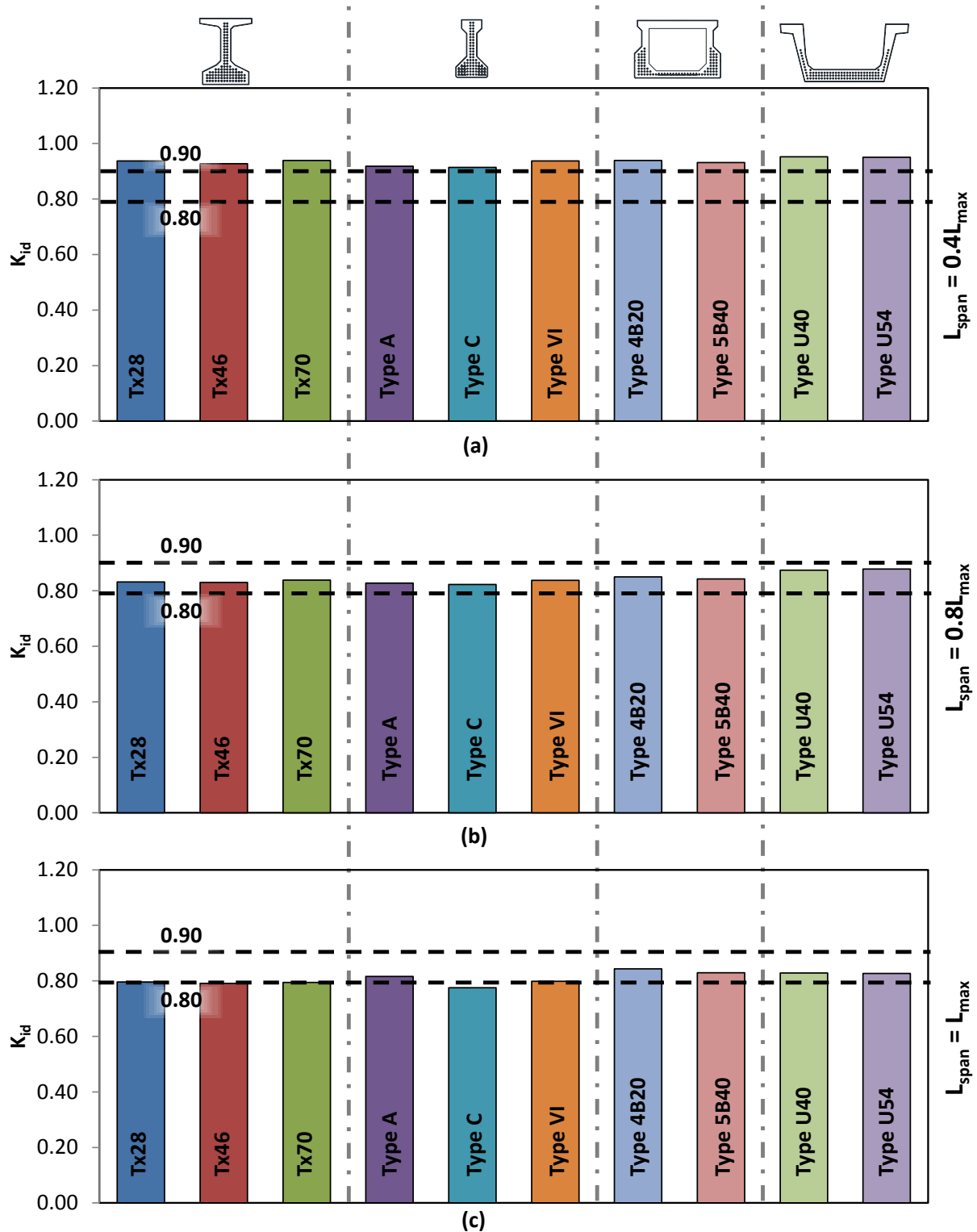
Figure 6.12 – Transformed section coefficient for various span lengths

The transformed section coefficient is a measure of the creep and shrinkage restraint provided by the prestressing strand, where the value of the coefficient is inversely proportional to the restraint provided by the strands. The addition of flexural reinforcement to a cross-section will result in greater restraint, lower prestress losses, and consequently, a lower transformed section coefficient. Based on the data provided above, it would be conservative to utilize an upper bound approximation (i.e. $K_{if} = 0.9$) of the transformed section coefficient. It is therefore recommended that the transformed section coefficient be conservatively set equal to 0.9 for all designs.

Transformed Section Coefficient
RECOMMENDATION: $\quad K_{if} = 0.9$

This recommendation further simplifies the prestress loss provisions by eliminating the calculation of one additional complicated variable. It also adds an additional level of conservatism to the prestress loss calculations for typical design spans.

6.4.2   Volume-to-Surface Area Ratio

The shape factor (k_s), shown in Equation (6.18), is used to account for the effect of the girder volume-to-surface area ratio (*V/S*) on the development of creep and shrinkage. Creep and shrinkage are driven, in part, by the loss of moisture from the girder which is to some extent affected by the volume-to-surface area ratio of the cross-section. Conceptually, a pretensioned girder with a large surface area in relation to its volume (i.e. low *V/S*) will experience greater creep- and shrinkage-related losses than a girder with a small surface area in relation to its volume (i.e. high *V/S*). The factor is explicitly referenced in Equation (6.3) and Equation (6.11) for calculation of the shrinkage strain and creep coefficient, respectively.

(6.18)

$$k_s = 1.45 - 0.13(V/S) \geq 1.0$$

AASHTO 12 (5.4.2.3.2-2)

Where:

    V/S   = volume-to-surface area ratio (in)

The volume-to-surface area ratios for a number of standard girder cross-sections are shown in Figure 6.13 (a); corresponding shape factors are summarized in Figure 6.13 (b). The actual shape factor will vary slightly with the physical length of the beam; only one length beam is shown in Figure 6.13.

Given that the effect of girder length on the shape factor is generally insignificant, calculation of the shape factor on a cross-sectional basis is sufficiently realistic and far more practical. Per Equation (6.18), any girder with a volume-to-surface area ratio greater than approximately 3.5 inches will result in the lower limit shape factor of 1.0 (i.e. $k_s = 1.0$). Only three of the ten girder cross-sections that were investigated resulted in a shape factor greater than 1.0. In the case of a Type A cross-section, a volume-to-surface area ratio of 3.0 results in a shape factor of 1.05; which effectively represents a 5 percent increase in the shrinkage strain and creep coefficient calculated per Equation (6.3) and Equation (6.11), respectively.
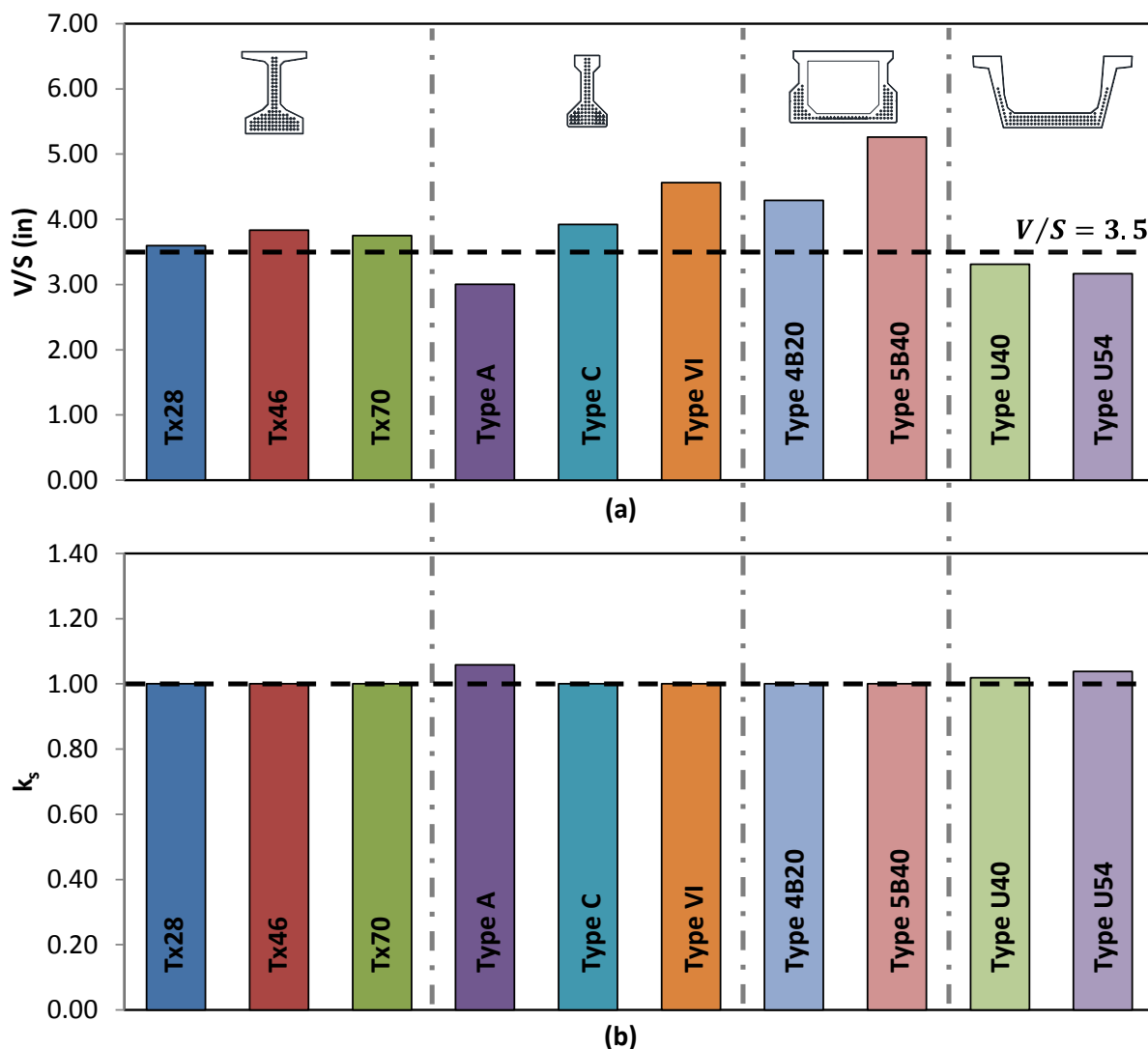
Figure 6.13 – (a) Volume-to-surface area ratios and (b) shape factors (k_s) for various cross-section types and sizes

Due to the minor impact of the shape factor, in terms of both the magnitude of the prestress loss changes and the scope of the girders affected, the shape factor should be set equal to 1.0 to further simplify the prestress loss provisions. This simplification is already suggested in AASHTO LRFD 2012 §5.4.2.3.1 for pretensioned stemmed members with an average web thickness of 6.0 to 8.0 inches.

Shape Factor
RECOMMENDATION: $k_s = 1.0$

6.4.3   Timing of Prestress Transfer and Deck Placement

There are two additional recommendations concerning timing for typical fabrication cycles. The prestress loss provisions are used in the design stages, during which, (1) times of transfer and deck placement and (2) contractors and methods are not precisely known. Control of these variables is purposeless and should be eliminated, for this reason the time of release should be taken as one day and the time of deck placement as 120 days. For typical fabrication cycles, release of the prestressing tendons occurs around 24 hours. The actual time of deck placement can vary, but it is recommended in AASHTO LRFD 2012 to be taken as 120 days. These recommendations will help to simplify the creep expressions for standard pretensioned girders.

Fabrication Timing (Release and Deck Placement)	
RECOMMENDATION:	$t_i = 1.0$ day $t_d = 120$ days

6.5   REINCORPORATION OF SELECT AASHTO LRFD 2004 RECOMMENDATIONS

Introduction of the new prestress loss provisions in 2005 was intended to address the future needs of bridge design community: sophisticated, computer-based analyses would be tailored for application to high-strength concrete bridge members. In truth, the new prestress loss provisions of AASHTO LRFD 2012 are not reflective of the current state of practice. Two additional recommendations are therefore proposed to bridge the gap between current and future design/construction practices. Both of these recommendations reincorporate expressions and assumptions made in AASHTO LRFD 2004.

6.5.1   Concrete Release Strength Coefficient

As noted in Chapter 2, AASHTO LRFD 2012 accounts for the effect of the concrete release strength through the use of the release strength coefficient, k_f. The effect of the concrete release strength on the long-term prestress losses was previously unaccounted for within AASHTO LRFD 2004. In fact, the introduction of the release strength coefficient by Tadros et al. (2003) was driven by a desire to provide more accurate loss estimates for high strength concrete members. A database evaluation of the relationship between the concrete release strength and the precision of the AASHTO LRFD 2012 approach is indicative of the bias toward high concrete release strengths. Disregarding the generally unconservative nature of the AASHTO LRFD 2012 approach, it appears that a greater level of precision (and a correspondingly greater level of unconservatism) is attained for high concrete release strengths (refer to Figure 6.14). In practice, this bias would result in lower strength member requiring a disproportionately greater margin of strands, where the difference in margin between a high and low strength member is effectively proportionate to the disparity in the distribution of E/M (ratio of estimated and measured losses) values shown in Figure 6.14.
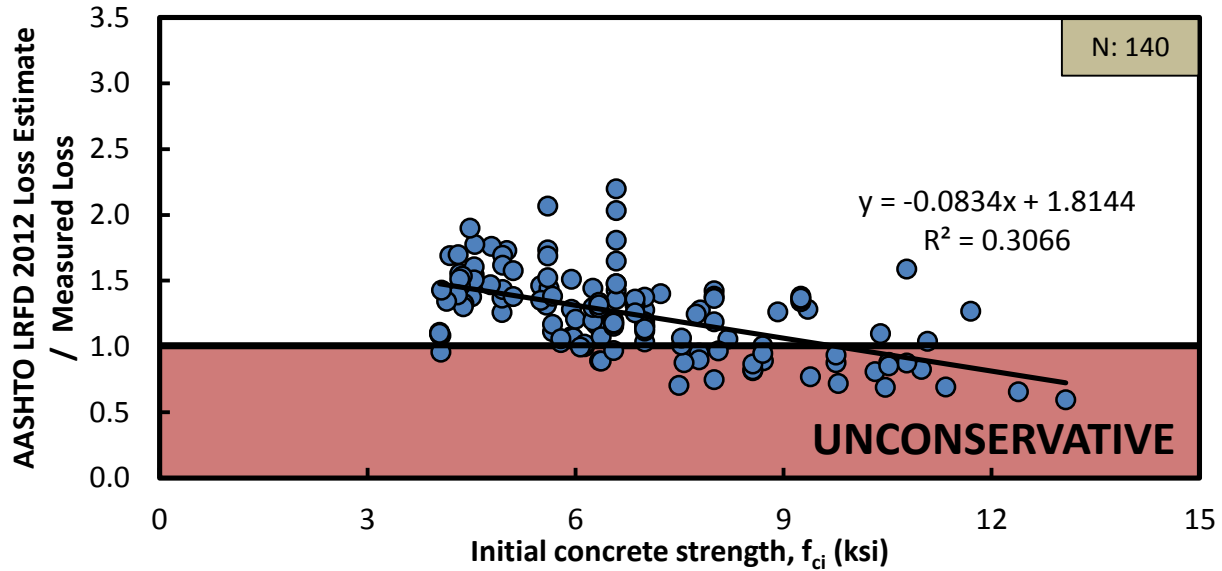
Figure 6.14 – Estimate-to-measured prestress loss ratio for AASHTO LRFD 2012 versus concrete release strength

With this in mind, a concrete release strength coefficient was desired that would have less of an impact on the estimated prestress loss with varying release strengths. Although the material properties section is not used in the AASHTO LRFD 2004 loss provisions, a concrete strength coefficient is provided for calculating the creep coefficient, shown in Equation (6.19). This expression was derived based on work done by Collins and Mitchell (1991) for 28-day concrete compressive strengths. In order to use the concrete release strength in the expression, it is assumed that the release strength is approximately 80 percent of the 28-day strength, proposed by Tadros (2003). Using this assumption, Equation (6.19) can be simplified down to Equation (6.20).

$$k_f = \frac{1}{0.67 + \left(\frac{f'_c}{9}\right)}$$

(6.19)

AASHTO 04 (5.4.2.3.2-2)

Concrete Release Strength Factor (k_f)		
RECOMMENDATION:	$k_f = \dfrac{7.2}{4.8 + f'_c}$	**(6.20)**

The recommended concrete release strength coefficient is compared with the AASHTO LRFD 2012 coefficient in Figure 6.15. Using the recommended release strength coefficient will result in less of a penalty for using lower release strengths and less reward for using high release strengths. The recommended factor better represents the trends observed in the evaluation database.
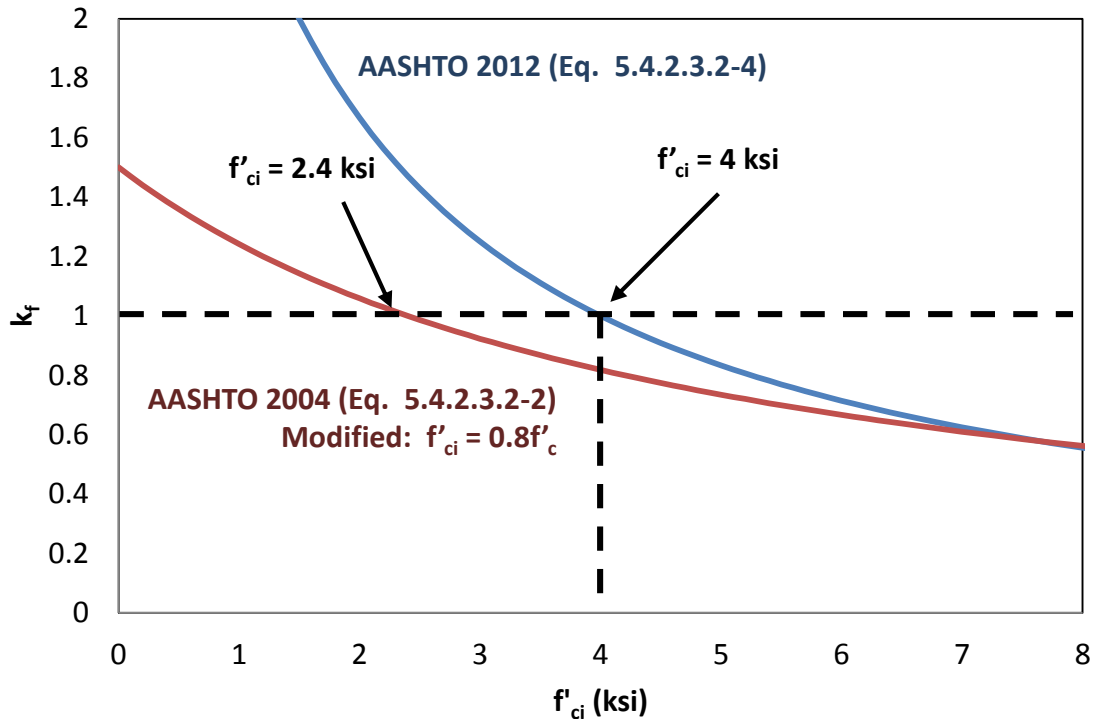
Figure 6.15 – Concrete release strength coefficient (k_f) versus concrete release strength (f'_{ci}) for AASHTO LRFD 2004 and AASHTO LRFD 2012

6.5.2 Strand Stress after Transfer

The AASHTO LRFD 2012 provisions currently include two options for calculation of the concrete stress imposed by the initial prestressing force (f_{cgp}): (1) an iterative method defined on the basis of beam theory, and (2) a direct expression derived through approximation of the iterative method. Both methods are based on the assumption that the effective prestress transferred to the girder will be less than the initial jacking stress placed on the strands (f_{pi}). The iterative and direct methods, respectively included in the specifications and commentary of AASHTO LRFD 2012, are the subject of further examination in Chapter 2.

Prior to the introduction of the AASHTO LRFD 2005 prestress loss provisions, calculation of the concrete stress at the centroid of the prestressing steel was completed on the basis of an effective prestress transfer of 70 percent of the ultimate tensile strength of the prestressing strands (or $0.7f_{pu}$, refer to Equation 2.7 of Chapter 2). Please recall that the initial jacking stress placed on the prestressing strands is generally 75 percent of the ultimate tensile strength (i.e. $f_{pi} = 0.75f_{pu}$). While the AASHTO LRFD 2004 prestress loss provisions did discount the initial prestressing force (similar to AASHTO LRFD 2012), determination of the concrete stress at the centroid of the prestressing steel did not require iterative calculations.

The results from a database evaluation of the AASHTO LRFD 2004 and 2012 elastic shortening loss estimation procedures are presented in Table 6.3. In spite of the sophistication or simplicity of either method, the AASHTO LRFD 2004 and 2012 estimates of the elastic shortening are very similar, in terms of both conservatism and precision.

142

Table 6.3 – Comparison of elastic shortening loss using the estimated-to-actual ratio (E/M) from the evaluation database

	AASHTO LRFD 2004	AASHTO LRFD 2012
N	36	36
Min.	0.71	0.69
Average	0.92	0.87
Max.	1.31	1.15
Co. Var.	0.15	0.14

In light of the simplicity of past approaches, the prestressing force immediately after transfer (f_{pt}) should be taken as 70 percent of the ultimate strand stress, shown in Equation (6.21), to calculate the concrete stress at the centroid of the prestressing strands (f_{cgp}). Although this recommendation is not as theoretically correct as the iterative method currently outlined in AASHTO LRFD 2012, it is a simpler, non-iterative solution that results in better (slightly more conservative) estimates of prestress loss due to elastic shortening.

Strand Stress After Transfer (f_{pt})

RECOMMENDATION: $$f_{pt} = 0.7 f_{pu}$$ **(6.21)**

6.6   FURTHER SIMPLIFICATION OF DESIGN EXPRESSIONS

Thus far, simplifications have been recommended for both the time dependency of the current loss provision and the material and section properties. In order to eliminate the differentiation between before and after deck placement prestress loss estimations, the following recommendations are made:

- *Time development factor*: A time development factor of 1.0 is recommended to combine the before and after deck placement loss contributions of girder creep and shrinkage loss.

$$k_{td} = 1.0$$

- *Change in concrete stress due to before deck losses*: When estimating the long-term creep the stress change caused by long-term prestress loss prior to deck placement is recommended to be neglected.

$$Neglect\ \Delta f_{cd,\Delta P}$$

- *Strand relaxation*: The before and after deck placement contributions of relaxation loss should be combined and the strand stress immediately prior to transfer should be used.

$$\Delta f_{pR} = \frac{2f_{pt}}{K_L}\left(\frac{f_{pt}}{f_{py}} - 0.55\right)$$

- *Deck shrinkage demands*: This component of the total prestress loss estimate is both small in magnitude and does not accurately model the true behavior of a bridge system, so it should be neglected.

$$Neglect\ \Delta f_{pSS}$$

Despite dissociation of deck placement and the long-term prestress loss estimates, the resulting provisions still include calculation-intensive variables with limited relevance to the precision and conservatism of the results. After a thorough investigation of these variables, the following recommendations are made:

- *Transformed section coefficient*: Based on data from the parametric study, it was found that an upper bound approximation of the transformed section coefficient of 0.9 could conservatively be used for all designs.

$$K_{if} = 0.9$$

- *Volume-to-surface area ratio*: Little variation was observed in the volume-to-surface area ratio between all commonly used sections in TxDOT design. For this reason, the shape factor is recommended to be set equal to 1.0.

$$k_s = 1.0$$

- *Timing of transfer and deck placement*: Due to the fact that times of release and deck placement are entirely unknown during the design phase, they should be taken as one day and 120 days, respectively.

$$t_i = 1\ day \qquad\qquad t_d = 120\ days$$

Two additional modifications were determined appropriate through analysis of the evaluation database. These two modifications incorporated recommendations made in AASHTO LRFD 2004:

- *Concrete release strength coefficient*: Based on analysis of the evaluation database, the current release strength coefficient was determined to have too great an impact on loss estimates for varying release strengths. For this reason, the release strength coefficient is recommended to be:

$$k_f = \frac{7.2}{4.8 + f'_c}$$

- *Strand Stress After Transfer*: In order to simplify the elastic shortening loss estimation, the strand stress after transfer is recommended to be 70 percent of the ultimate strand stress:

$$f_{pt} = 0.7 f_{pu}$$

The implications of the above recommendations will be addressed in this section as well as a few additional recommendations for simplifications to AASHTO LRFD 2012. These further simplifications generally did not fit well within the context of the efforts described above.

6.6.1 Shrinkage

The current AASHTO LRFD 2012 expression for estimation of the prestress loss due to girder shrinkage prior to deck placement is presented as Equation (6.22). By setting the time development factor (k_{td}) equal to 1.0, as recommended in Section 6.4.1, the expression may be used to estimate the shrinkage-related prestress losses over the service life of the girder. Additional simplifications to the expression are recommended below.

(6.22)

$$\Delta f_{pSR} = \varepsilon_{bid} K_{if} E_p$$

AASHTO 12 (5.9.5.4.2a-1)
(Modified)

The effect of the recommendations on the expression for prestress loss due to girder shrinkage is outlined in Table 6.4. Implementation of the constants and reduction of the remaining terms results in a simple expression (6.23) that is only dependent on the relative humidity (*H*) and concrete compressive strength at the time of prestress transfer (*f'$_{ci}$*).

Table 6.4 - Effect of simplified constants on girder shrinkage losses

Equation (6.22)	$\Delta f_{pSR} = \varepsilon_{bid} K_{if} E_p$ $$\Delta f_{pSR} = \left(k_s k_{hs} k_f k_{td} 0.48 * 10^{-3}\right) K_{if} E_p$$
Recommendations	$k_{td} = 1$ $\quad$ $k_s = 1.0$ $\qquad$ $k_f = \dfrac{7.2}{4.8 + f'_c}$ $\quad$ $K_{if} = 0.9$
Result	$\Delta f_{pSR} = \left(k_{hs} k_f 0.48 * 10^{-3}\right)(0.9) E_p$ $$\Delta f_{pSR} = \left[\frac{(7.2)(0.48 * 10^{-3})(2.0 - 0.014H)}{4.8 + f'_{ci}}\right](0.9) E_p$$ $$\Delta f_{pSR} = E_p \left(\frac{143 - H}{4.8 + f'_{ci}}\right) 4.35 * 10^{-5}$$

Total Shrinkage Loss		
RECOMMENDATION:	$\Delta f_{pSR} = E_p \left(\dfrac{140 - H}{4.8 + f'_{ci}}\right) 4.4 * 10^{-5}$	**(6.23)**

6.6.2 Creep

The recommended expression for the estimation of prestress loss due to girder creep is presented Equation (6.24). Equation (6.24) includes the before deck placement component of the creep-related losses, as presented in AASHTO LRFD 2012, and the after deck placement component as previously simplified in Section 6.3.2. The expression does not account for the variable simplifications made in Section 6.4; substitution of the resulting constants and further reduction of the expression is completed below.

$$\Delta f_{pCR} = \frac{E_p}{E_{ci}} K_{if} \left(f_{cgp}\psi_b(t_f, t_i) + \Delta f_{cd}\psi_b(t_f, t_d) \right)$$

(6.24)

Where:

Δf_{cd} = change in concrete stress at centroid of prestressing strands due to deck weight and superimposed loads (ksi)

$$\Delta f_{cd} = -\frac{M_g e_{pg}}{I_g}$$

(6.25)

Recommended

ψ_b = creep coefficient

$$\psi_b(t_f, t_i) = 1.9 k_s k_{hc} k_f k_{td} t_i^{-0.118}$$

(6.26)

AASHTO 12 (5.4.2.3.2-1)

$$\psi_b(t_f, t_d) = 1.9 k_s k_{hc} k_f k_{td} t_d^{-0.118}$$

(6.27)

AASHTO 12 (5.4.2.3.2-1)

The impact of the recommendations on the creep coefficients will be examined first. Substitution of the constants into, as well as reduction of, the full service life and after deck creep coefficients (ϕ_{bif} and ϕ_{bdf}) is outlined in Table 6.5. The simplified creep coefficients are further substituted into Equation (6.24), yielding the recommended expression (6.28) for the estimation of prestress loss due to girder creep.

<div align="center">

Table 6.5 – Effect of simplified constants on creep coefficients

</div>

Equation (6.26) and (6.27)	$\psi_b(t_f, t_i) = 1.9 k_s k_{hc} k_f k_{td} t_i^{-0.118}$	$\psi_b(t_f, t_d) = 1.9 k_s k_{hc} k_f k_{td} t_d^{-0.118}$
Recommendations	$k_{td} = 1$ $k_s = 1.0$ $K_{if} = 0.9$	$t_i = 1.0$ $t_d = 120$ $k_f = \dfrac{7.2}{4.8 + f'_c}$
Result	$\psi_b(t_f, t_i) = 1.9 \left[\dfrac{7.2(1.56 - 0.008H)}{4.8 + f_{ci}}\right]$ $\psi_b(t_f, t_i) = 0.109 \left(\dfrac{195 - H}{4.8 + f'_{ci}}\right)$	$\psi_b(t_f, t_i) = 1.9 \left[\dfrac{7.2(1.56 - 0.008H)}{4.8 + f_{ci}}\right] (120)^{-0.118}$ $\psi_b(t_f, t_d) = 0.062 \left(\dfrac{195 - RH}{4.8 + f'_{ci}}\right)$

Total Creep Loss
RECOMMENDATION: $\quad \Delta f_{pCR} = 0.1 \left(\dfrac{195 - H}{4.8 + f'_{ci}} \right) \left(\dfrac{E_p}{E_{ci}} \right) \left(f_{cgp} + 0.6 \Delta f_{cd} \right)$ $\qquad$ **(6.28)**

6.6.3   Elastic Shortening

The prestress loss due to elastic shortening of the girder at the time of prestress transfer may be estimated via Equation (6.29). The magnitude of the prestress loss due to elastic shortening is primarily dependent on the concrete modulus (E_{ci}) and the concrete stress imposed by the initial prestressing force (f_{cgp}).

$$\Delta f_{pES} = \frac{E_p}{E_{ci}} f_{cgp}$$

(6.29)

AASHTO 12 (5.9.5.2.3a-1)

In the calculation of f_{cgp}, shown in Equation (6.30), the strand stress immediately after transfer should be assumed equal to 70 percent of the ultimate strand stress. This assumption allows for f_{cgp} to be calculated for directly, without an iterative procedure as was previously required. The f_{cgp} should be used when calculating both elastic shortening and creep loss.

Concrete Stress At transfer
RECOMMENDATION: $\qquad f_{cgp} = f_{pt} A_{ps} \left(\dfrac{1}{A_g} + \dfrac{e_p^2}{I_g} \right) - \dfrac{M_g e_p}{I_g}$ $\qquad$ **(6.30)** $\qquad\qquad\qquad\qquad$ *OR* $\qquad\qquad\qquad\qquad$ $f_{cgp} = 0.7 f_{pu} A_{ps} \left(\dfrac{1}{A_g} + \dfrac{e_p^2}{I_g} \right) - \dfrac{M_g e_p}{I_g}$

6.7   TxDOT PROJECT 0-6374 PRESTRESS LOSS PROVISIONS

One of the primary objectives of TxDOT Project 0-6374 was to simplify the prestress loss provisions of the current 2012 AASHTO LRFD Bridge Design Specifications. The simplification process was driven by a desire to develop a set of expressions that provided conservative, yet precise estimates of the final prestress loss through consideration of only the most influential parameters. The result of the simplification process detailed above is summarized in Table 6.6.

Table 6.6 – Summary of recommended prestress loss expressions

Component	Recommended Expressions
Total Prestress Loss (Δf_{pT})	$$\Delta f_{pT} = \Delta f_{pES} + \Delta f_{pSR} + \Delta f_{pCR} + \Delta f_{pR}$$
Elastic Shortening (Δf_{pES})	$$\Delta f_{pES} = \frac{E_p}{E_{ci}} f_{cgp}$$ $where:$ $$f_{cgp} = 0.7 f_{pu} A_{ps} \left(\frac{1}{A_g} + \frac{e_p{}^2}{I_g} \right) - \frac{M_g e_p}{I_g}$$
Shrinkage Loss (Δf_{pSR})	$$\Delta f_{pSR} = E_p \left(\frac{140 - H}{4.8 + f'_{ci}} \right) 4.4 * 10^{-5}$$
Creep Loss (Δf_{pCR})	$$\Delta f_{pCR} = 0.1 \left(\frac{195 - H}{4.8 + f'_{ci}} \right) \left(\frac{E_p}{E_{ci}} \right) \left(f_{cgp} + 0.6 \Delta f_{cd} \right)$$ $where:$ $$\Delta f_{cd} = - \frac{M_{sd} e_p}{I_g}$$
Relaxation Loss (Δf_{pR})	$$\Delta f_{pR} = \frac{2 f_{pt}}{K_L} \left(\frac{f_{pt}}{f_{py}} - 0.55 \right)$$

In the following sections, the performance of the recommended prestress loss provisions versus the performance of AASHTO LRFD 2004 and 2012 will be investigated in terms of (1) simplicity, (2) conservatism, and (3) design implications. These investigations will be aided by the use of the Evaluation Database and the results from the parametric study.

6.7.1 Simplicity

The level of simplicity achieved through implementation of the aforementioned recommendations is illustrated in Table 6.7. The simplicity is expressed in two forms: (1) the total number of mathematical operations required by the procedure and (2) the total number of different variables required to complete the procedure. It can be seen that the TxDOT Project 0-6374 prestress loss provisions require approximately one-tenth of the total number of mathematical operations required by AASHTO LRFD 2012. Moreover, the 0-6374 provisions included approximately one-third of the total number of variables included within the AASHTO LRFD 2012 procedure.

Table 6.7 – Simplicity of AASHTO 2012 vs. 0-6374 Proposed

	AASHTO 2012	0-6374 Proposed
Total Operations	≈ 600	≈ 60
Total Variables	70	24

The prestress loss provisions of AASHTO LRFD 2012 were developed for implementation in computer software. The prestress loss estimates are burdensome to compute by hand, leaving the designer to rely solely on software. If implemented within a software package, output of the TxDOT Project 0-6374 prestress loss provisions may be easily checked by hand calculations; enabling better control and understanding of the design process.

6.7.2 Conservatism

The main goal of the simplification of the AASHTO LRFD 2012 prestress loss provisions was to reduce the unnecessary complexity of the method. It is important to recall that database evaluation of the AASHTO LRFD 2012 prestress loss provisions (in Chapter 2) confirmed that introduction of the method represented a profound shift in code philosophy, from conservatism to accuracy. A significantly larger number of the experimentally determined prestress losses included in the Evaluation Database were unconservatively estimated by AASHTO LRFD 2012.

The impact of the simplification process on the conservatism of the TxDOT Project 0-6374 prestress loss provisions will now be examined through extension of the database evaluation of Chapter 2. The performance of each set of prestress loss provisions (TxDOT Project 0-6374, AASHTO LRFD 2004 and AASHTO LRFD 2012) is evaluated through comparison of the estimated prestress loss to the measured prestress loss of each specimen in the Evaluation Database. As noted in Chapter 2, examination of the ratio of the estimated-to-measured prestress losses (*E/M*) is helpful in this regard. Key statistics from the *E/M* ratios calculated for all three sets of prestress loss provisions are presented in Table 6.8.

Table 6.8 – Comparison of AASHTO LRFD 2004 and 2012 performance vs. 0-6374 performance using estimated-to-actual ratio (*E/M*) from the evaluation database

	AASHTO 2004	AASHTO 2012	0-6374 Proposed
Minimum	0.89	0.59	0.84
Average	1.74	1.25	1.32
Maximum	3.69	2.20	2.31
Co. of Variation	0.26	0.24	0.20
St. Deviation	0.45	0.30	0.27
E/M < 1 (Specimens)	1	30	21

The relationship between the estimated prestress losses and the measured prestress losses is further examined in Figure 6.16 (AASHTO LRFD 2004), Figure 6.17 (AASHTO LRFD 2012), and Figure 6.18 (TxDOT Project 0-6374). All results contained within the Evaluation Database are plotted against the prestress loss estimate on the vertical axis and the measured prestress loss on the horizontal axis. Concepts from Chapter 2 for examination of the plots are reiterated here for the benefit of the reader. If a procedure exhibits perfect precision, all of the specimens will fall on a straight line that originates from the origin. A procedure with no excess conservatism and perfect accuracy will place all of the specimens on the line of equality, which is the solid black line extending from the origin in Figure 6.16. It should also be noted that all of the specimens that fall below the line of equality are estimated unconservatively by the particular set of prestress loss provisions. The statistics within Table 6.8 are a direct reflection of the trends observed in the database.
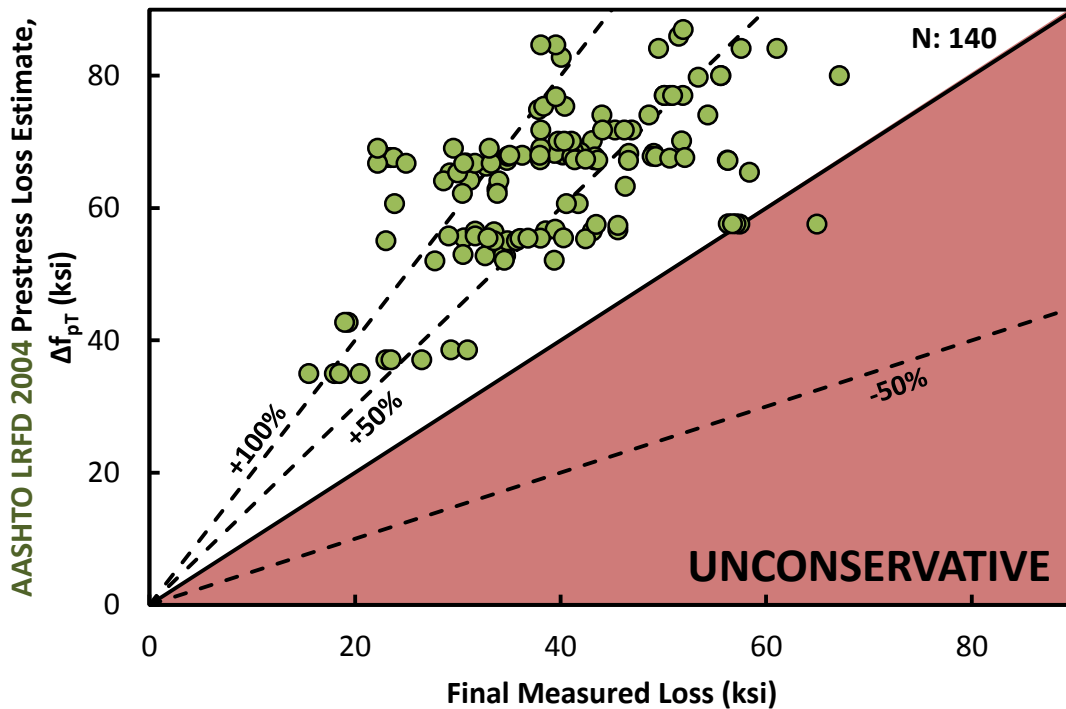
Figure 6.16 – AASHTO LRFD 2004 prestressed loss estimate vs. final measured loss
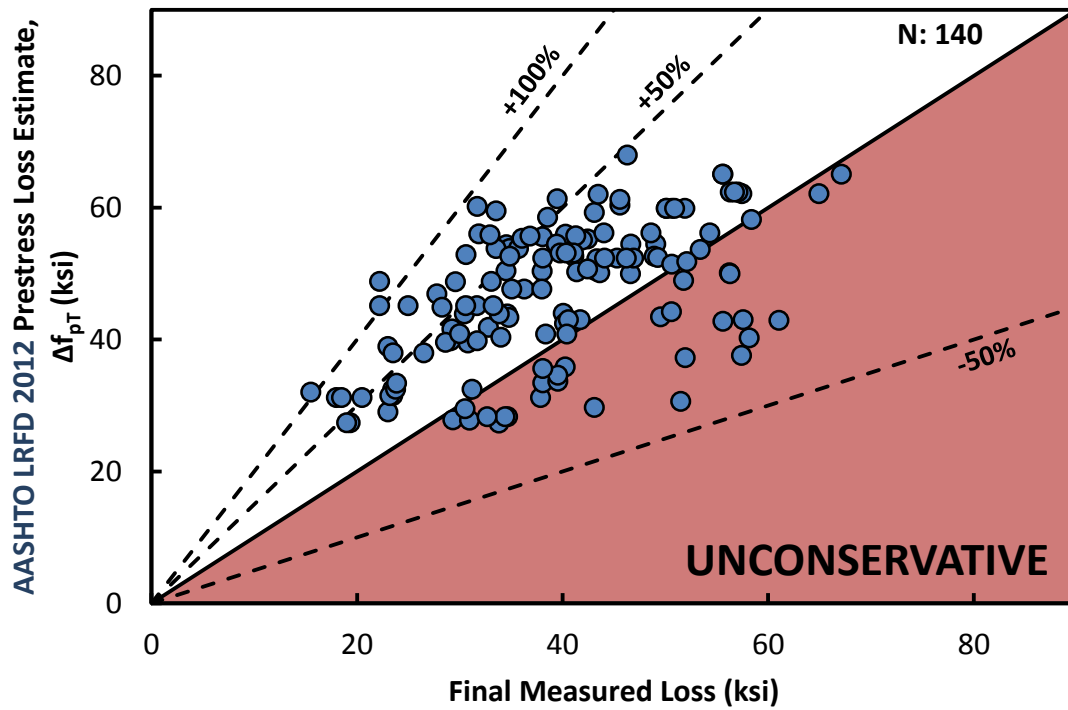
Figure 6.17 – AASHTO LRFD 2012 prestressed loss estimate vs. final measured loss
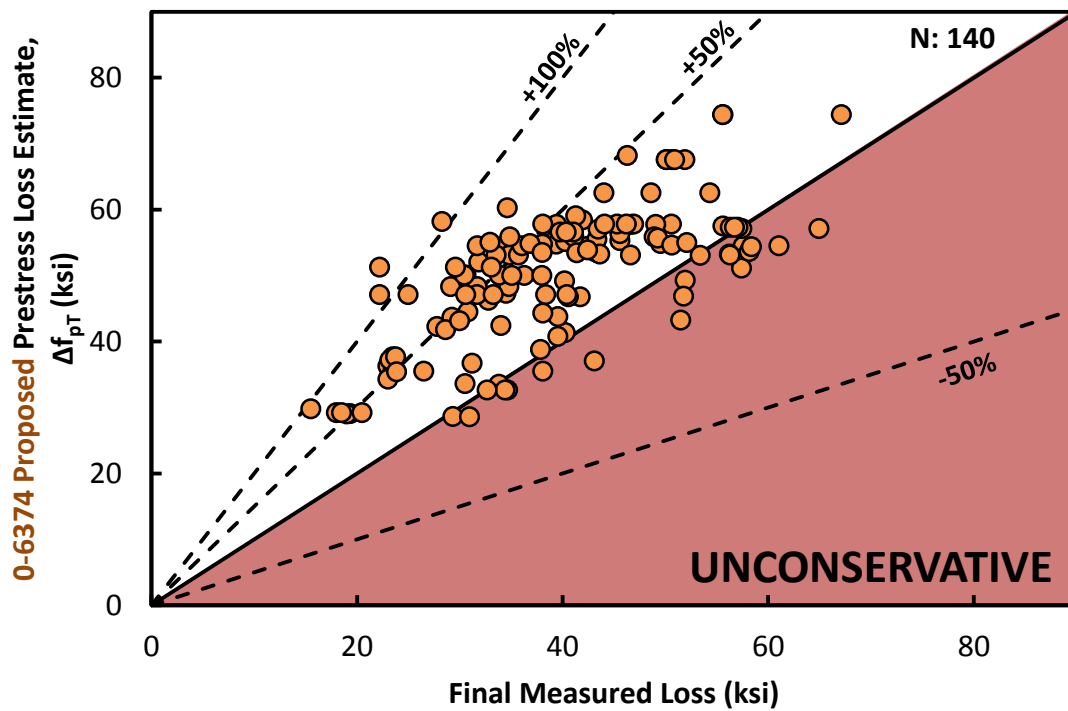
Figure 6.18 – 0-6374 Proposed prestressed loss estimate vs. final measured loss

The performance of AASHTO LRFD 2004 is marked by a significant amount of scatter and a high level of conservatism. Measured losses were under-estimated by as much as 14 percent (E/M = 0.86) and over-estimated by as much as 269 percent (E/M = 3.69). The estimated losses were on average 74 percent greater than the measured losses. The coefficient of variation, which is a quantifiable measure of the data scatter, is comparable to that of the AASHTO LRFD 2012 prestress loss provisions (COV = 0.26 and 0.24, respectively). The large scatter within the results of both provisions would suggest that the expressions are not properly modeling the actual behavior. As noted previously, the performance of AASHTO LRFD 2012 is reflective of the NCHRP Project D18-07 focus on accuracy. Measured losses were under-estimated by as much as 41 percent (E/M = 0.59) and over-estimated by as much as 120 percent (E/M = 2.20). On average, the estimated losses were 25 percent greater than the measured losses. Given the care taken to account for a number of primary and even secondary influential parameters, the lack of precision achieved by AASHTO LRFD 2012 is unanticipated. Simplification of the method was fully justified on this basis alone.

The TxDOT Project 0-6374 prestress loss provisions, when subjected to a similar database evaluation, met the expectations established at the outset. The method required a minimal number of calculations and resulted in a reasonable level of conservatism at a reduced level of scatter (COV = 0.20). The conservatism provided by the recommendations was well balanced with respect to that provided by AASHTO LRFD 2004 and 2012. On average, the losses estimated by TxDOT Project 0-6374 prestress loss provisions were 32 percent greater than the measured losses.

The value of conservative, yet precise prestress loss estimates cannot be overstated. As noted by Tadros et al. (2003), "If one underestimates prestress losses, there is a risk of cracking the girder bottom fibers under full service loads," leading to long-term serviceability and durability concerns for the damaged structure.

6.7.3 Design Implications

The design implications of the TxDOT Project 0-6374 prestress loss expressions were compared with that of AASHTO LRFD 2004 and 2012 through use of results from the parametric analysis of Chapter 5. Only the results from the critical case within each different cross-section type are provided in this section. Results from other section types investigated may be found in Appendix D. Results from the following sections will be briefly discussed: Tx46 (bulb-T), Type C (I-beam), Type 5B40 (box beam), Type U40 (U-beam). It should also be noted that the design implications are only quantified in terms of the number of strands that may be removed from an equivalent girder designed according to the AASHTO LRFD 2004 prestress loss provisions (the current TxDOT standard). The effect of the different loss provisions on the flexural capacity, shear capacity, and camber estimations may be found in Appendix D.

Two different approaches were taken when evaluating the design implications of the recommended loss expressions: (1) the effect on TxDOT girders with the current design philosophy and (2) the effect on TxDOT girders if release strengths of 6 ksi were used. The performance of the recommendations using the current design philosophy was evaluated by allowing the analysis tool to design for concrete release and 28-day strengths (greater than 4 ksi). It was found through this investigation that the recommendations would have little effect on current TxDOT designs; only in a handful of cases would the number of strands change from that previously required. The recent trend in industry is the use of higher release strengths (5 to 6 ksi

and higher), allowing for construction of longer span bridges. The recommendations will have the highest impact on designs within this higher concrete release strength range. For this reason, results from the second investigation (using concrete release strength of 6 ksi) will be presented in this section and within Appendix D.

It should be noted that for each of the design cases shown below, the design is either controlled flexural strength or flexural stress requirements. The designs are typically controlled by flexural strength requirements at shorter span lengths and by flexural stress requirements at longer span lengths. The largest difference in the prestressing strand requirements was typically observed at the longest span lengths, where the magnitude of the flexural stresses was directly impacted by the prestress loss estimation methods. Flexural capacity, on the other hand, is primarily controlled by the ultimate strength of the reinforcement and was unaffected by discrepancies in the prestress loss estimations. Design impacts were therefore limited for shorter span lengths.

The total prestress losses calculated per the provisions of AASHTO LRFD 2004, AASHTO LRFD 2012 and TxDOT Project 0-6374 are summarized in Figure 6.19 (a) for the Tx46 cross-section. As anticipated on the basis of the database evaluation, the prestress losses estimated by the recommendations fall between those estimated by AASHTO LRFD 2004 and 2012. The resulting difference in the number of strands required by either AASHTO LRFD 2012 or the recommendations and that required by AASHTO LRFD 2004 is shown in Figure 6.19 (b). The effect of AASHTO LRFD 2012 and the recommendations on Tx46 design is highlighted at a span of about 90% of the maximum allowable span length. AASHTO LRFD 2004 design of such a Tx46 girder would necessitate the use of 54 strands to satisfy the flexural stress and strength requirements. The same girder designed per AASHTO LRFD 2012 would only feature 48 strands, 6 strands less than the AASHTO LRFD 2004 design. The TxDOT Project 0-6374 prestress loss provisions would allow as many as four strands to be removed from the AASHTO LRFD 2004 design.
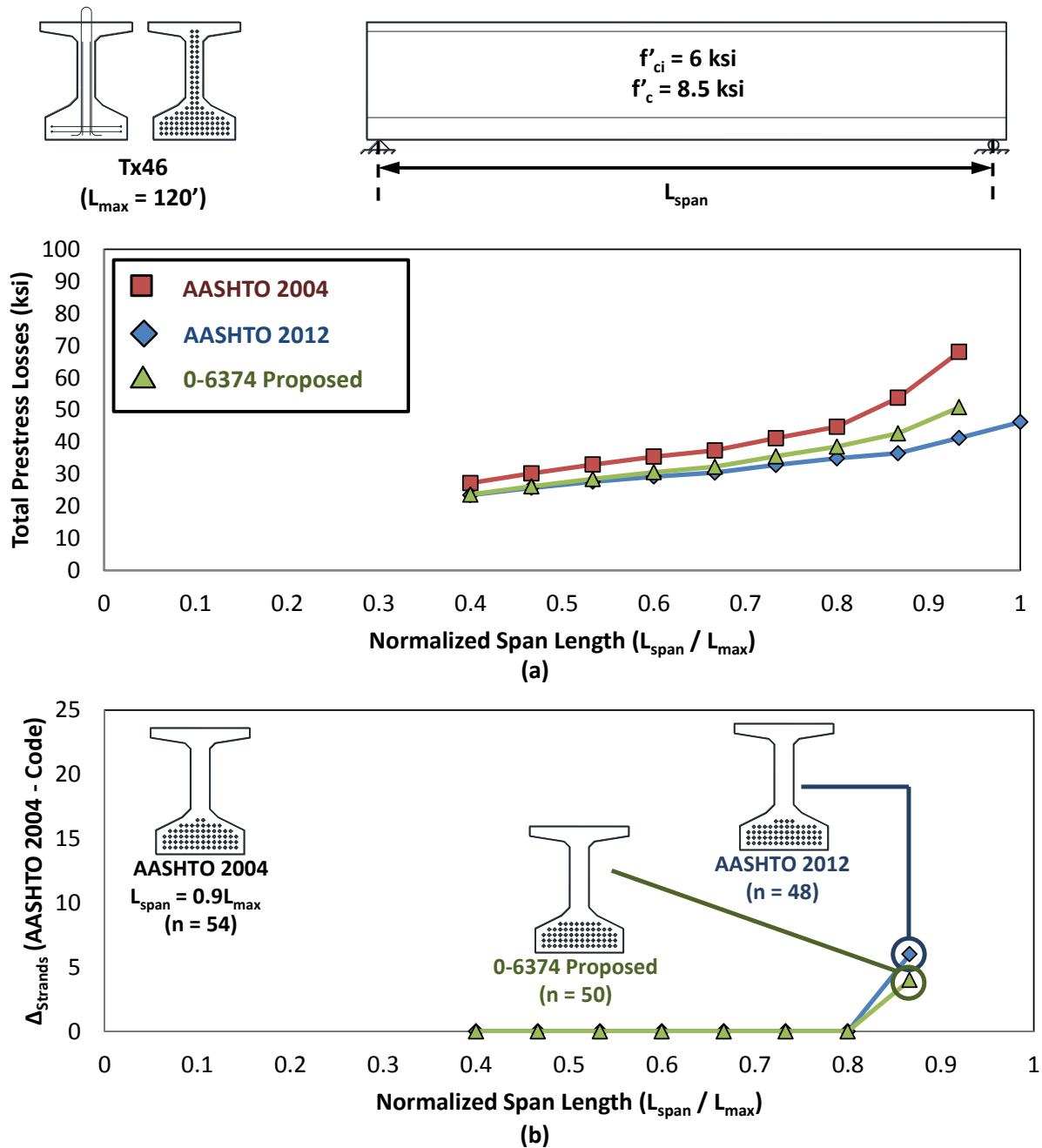
Figure 6.19 – (a) Total prestress loss and (b) change in number of required strands from AASHTO LRFD 2004 for Tx46 section

The prestress loss estimates and prestressing strand requirements for the Type C cross-section are summarized in parts (a) and (b) of Figure 6.20, respectively. The impact of the different specifications on the final cross-section design was most severe in this case. As shown in Figure 6.20 (b), a Type C girder of near-maximum length, designed per AASHTO LRFD 2012, would feature 10 less strands than an equivalent girder designed per AASHTO LRFD 2004. The impact of the TxDOT Project 0-6374 recommendations are more reasonable, with six less strands provided in relation to AASHTO LRFD 2004.
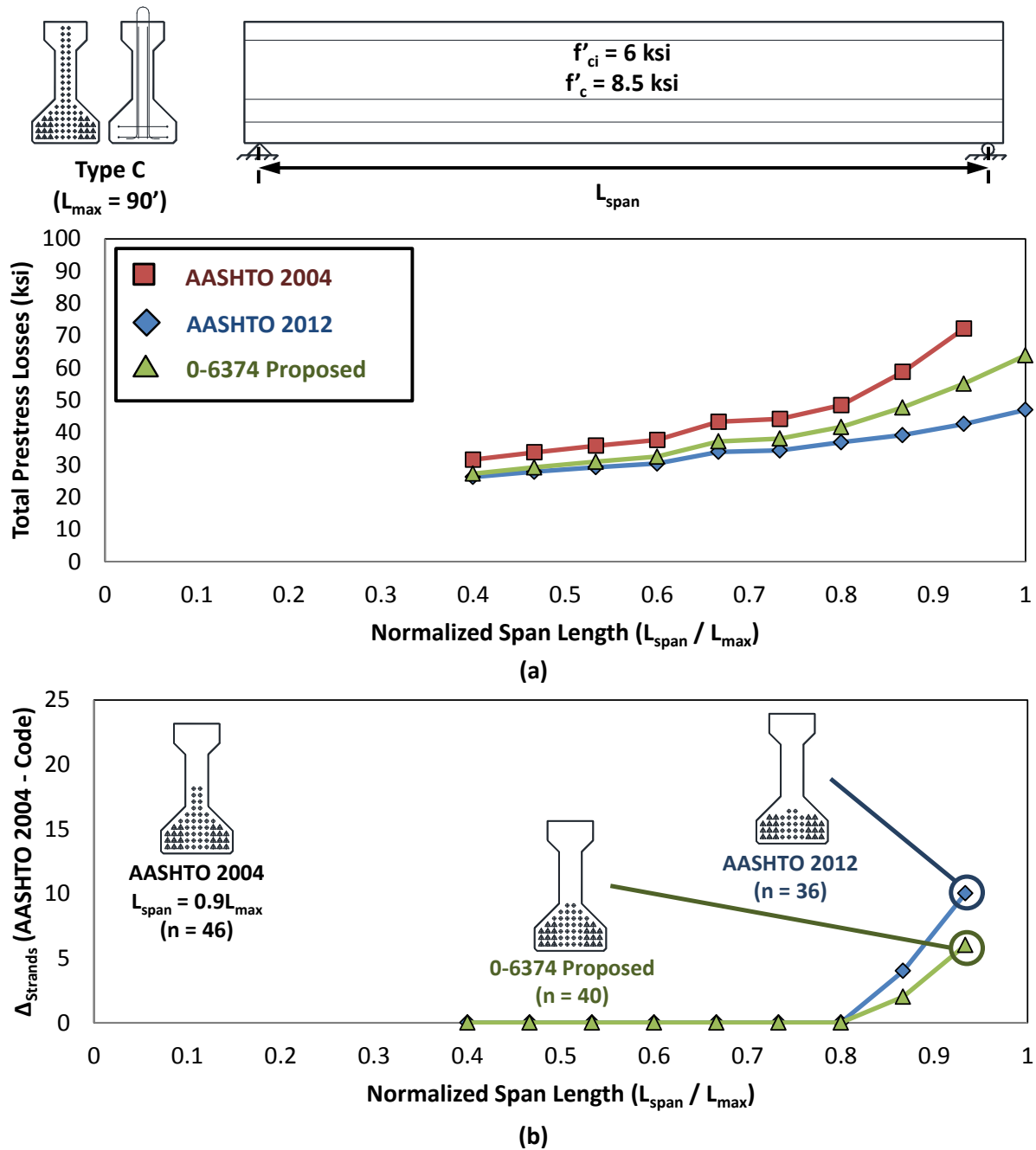
Figure 6.20 - (a) Total prestress loss and (b) change in number of required strands from AASHTO LRFD 2004 for Type C section

The total prestress losses estimated for Type 5XB40 and Type U40 cross-sections are shown in Figure 6.21 and Figure 6.22, respectively. Consistent with the previous observations, the TxDOT Project 0-6374 recommendations in both cases yielded prestress loss estimates that fell between the outcomes of AASHTO LRFD 2004 and 2012. The impact of the different specifications on the final cross-section design was similar to the previous observations. As

shown in Figure 6.21, a Type 5XB40 girder designed per either AASHTO LRFD 2012 or the TxDOT 0-6374 recommended loss provisions would result in four less strands than an equivalent beam designed per AASHTO LRFD 2004. As shown in Figure 6.22, a Type U40 girder designed per AASHTO LRFD 2012 loss provisions would result in eight less strands than an equivalent beam designed per AASHTO LRFD 2004, compared to six less strands in a girder designed per TxDOT Project 0-6374 recommendations.

Type 5XB40
(L$_{max}$ = 120')

f'$_{ci}$ = 6 ksi
f'$_{c}$ = 8.5 ksi

L$_{span}$

(a)

AASHTO 2004
AASHTO 2012
0-6374 Proposed

Total Prestress Losses (ksi)

Normalized Span Length (L$_{span}$ / L$_{max}$)

(b)

AASHTO 2004
L$_{span}$ = 0.9L$_{max}$
(n = 62)

AASHTO 2010
0-6374 Proposed
(n = 58)

Δ$_{Strands}$ (AASHTO 2004 - Code)

Normalized Span Length (L$_{span}$ / L$_{max}$)
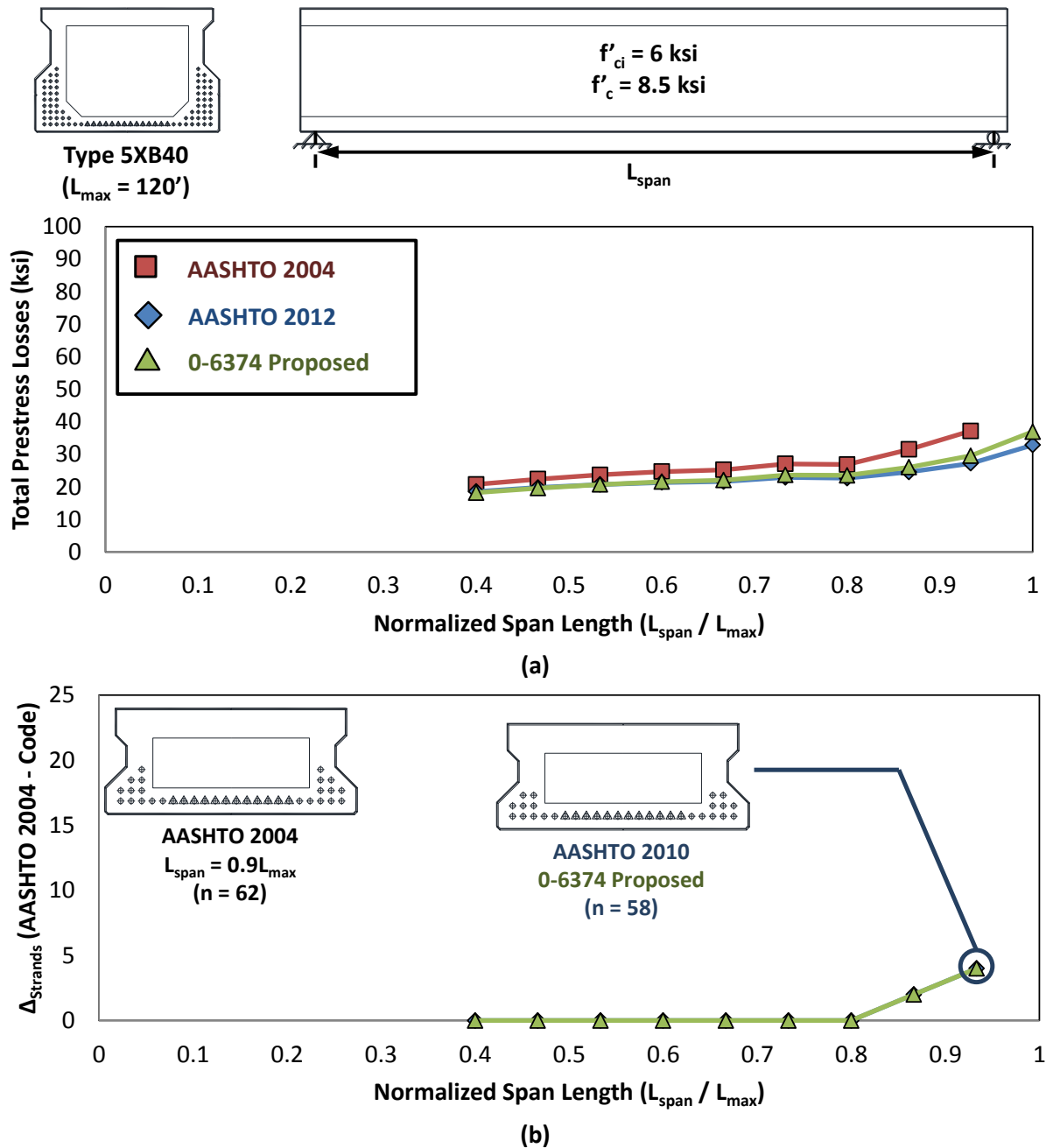
Figure 6.21 - Total prestress loss for Type 5XB40 section

157
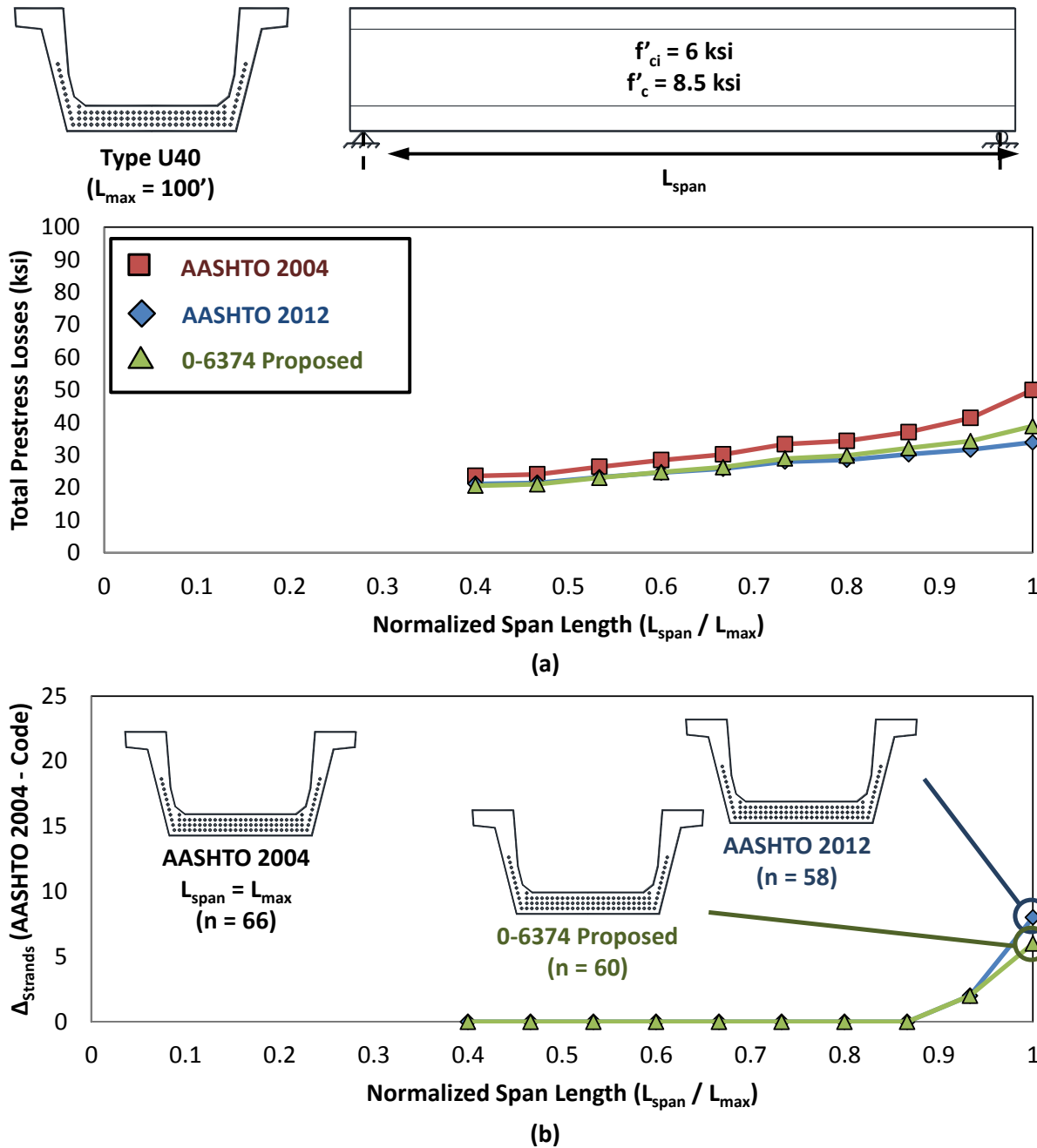
Figure 6.22 - Total prestress loss for Type U40 section

In all of the cases investigated during the extended parametric study, the TxDOT Project 0-6374 prestress loss estimates consistently fell between the AASHTO LRFD 2004 and 2012 prestress loss estimates. In cases where the flexural stress requirements drove proportioning of the flexural reinforcement, the TxDOT Project 0-6374 recommendations generally allowed for the removal of a few strands in relation to TxDOT's current design standard (AASHTO LRFD 2004). In general, the design implications of the project recommendations were much more reasonable than those of the AASHTO LRFD 2012 prestress loss provisions.

6.8   SUMMARY

Findings obtained during the course of TxDOT Project 0-6374 were used to develop new prestress loss provisions that would provide an appropriate amount of conservatism, precision and practicality. The prestress loss provisions currently outlined in AASHTO LRFD 2012 were utilized as a starting point. Simplifications were made where appropriate and can be subdivided into three main categories (1) dissociation of deck placement and long-term estimates, (2) consideration of typical construction details, and (3) reincorporation of AASHTO LRFD 2004 recommendations. The result of this simplification process was the recommended prestress loss provisions outlined in Section 6.7.

The TxDOT Project 0-6374 prestress loss provisions performed well compared to AASHTO LRFD 2012. The final set of provisions was found to be:

- *Simpler*: Looking at the expressions in the provisions, it was observed that the TxDOT Project 0-6374 prestress loss provisions require approximately one-tenth of the total number of mathematical operations required by and one-third the total number of variables included in AASHTO LRFD 2012.

- *More conservative and precise*: The minimum E/M value for AASHTO LRFD 2012 was found to be 0.59, compared to 0.84 for the TxDOT Project 0-6374 prestress loss provisions. The recommendations also provided a reduced scatter, with a COV = 0.20 compared to 0.24 for AASHTO LRFD 2012.

- *Less significant of a design impact*: In some designs using AASHTO LRFD 2012 up to 10 less strands are required than a design using AASHTO LRFD 2004. The same designs using the recommended procedure would require only up to 6 less strands.

Simplification of the AASHTO LRFD 2012 prestress loss provisions served two purposes: (1) to reduce the unnecessary complexity of the method and (2) to introduce additional conservatism through the use of lower bound constants and parameter expressions. Both of these were accomplished through the development of the recommended loss provisions.

This page is intentionally left blank

CHAPTER 7
Summary, Conclusions and Recommendations

7.1   PROJECT SUMMARY

The prestress loss provisions within the 2012 AASHTO LRFD Bridge Design Specifications account for a large number of factors that are thought to influence prestress losses, with the expressed objective of achieving accurate estimations. The resulting complexity of the method far exceeds that of the preceding provisions of the 2004 AASHTO LRFD Bridge Design Specifications. In addition to increased complexity, the prestress loss estimates of AASHTO LRFD 2012 are considerably less than those of AASHTO LRFD 2004, prompting TxDOT and others to question the conservatism of the method.

With these concerns in mind, the primary objectives of TxDOT Project 0-6374 were:

1. To *assess the conservatism and accuracy* of the current prestress loss provisions, introduced in the 2005 Interim Revision of the AASHTO LRFD Bridge Design Specifications, and still included in the 2012 Edition of the Specifications.

2. To *identify the benefits and weaknesses* of using the prestress loss provisions contained within the 2004 and 2012 Editions of the AASHTO LRFD Bridge Design Specifications.

3. To *make recommendations to simplify* the prestress loss provisions of the 2012 AASHTO LRFD Bridge Design Specifications such that the final prestress loss can easily be estimated without the consideration of time.

Development of design recommendations was accomplished through a synthesis of knowledge gathered during the course of the research project. Work completed during each of the major project tasks is outlined below:

1. *Literature Review*: The origin of the prestress loss expressions was investigated in order to understand the logic and reasoning behind each expression. Recent efforts examining the performance of the new loss procedure and recommending simplifications to the procedure were also studied.

2. *Database Assembly*: A comprehensive database of available experimental investigations pertaining to prestress loss was compiled as part of the project. This database contains information on 237 specimens, including 140 specimens for which prestress loss was reported or enough information was provided to calculate prestress loss that occurred at the time of testing. Compared with previously assembled databases, the database assembled in this project is unmatched in size and diversity. The use of this database was invaluable in evaluation of the current prestress loss provisions and the project recommendations.

3. *Fabrication, Conditioning and Experimental Evaluation of Pretensioned Girders*: A total of 30 full-scale prestressed concrete beams were fabricated to provide a relevant empirical basis for assessment of the existing prestress loss provision (and for the development of new provisions). These specimens were representative of a broad

range of the most influential factors that may affect prestress losses in structures fabricated within the State of Texas including:

- type of concrete (CC and SCC),

- coarse aggregate (Limestone and River Gravel),

- sectional geometry (Type C and Tx46), and

- climate (humidity from 51% to 63%).

Prestress loss monitoring was conducted on 18 of the specimens. This was achieved through the use of internal instrumentation. As part of the experimental program, tests for compression, tension and modulus of elasticity were conducted on a large number of cylinders at multiple concrete ages. These concrete properties were used to assess the effect of the different concrete mixes. Flexural testing was conducted at the end of the conditioning period, and the load at the time of first cracking (together with measured concrete tensile strength) was used to back-calculate the total prestress loss. Results from the flexural testing were compared with results from the internal instrumentation and included in the database for evaluation.

4. *Parametric Study of Design Implications*: In order to assess the impact of the new prestress loss provisions of the 2012 AASHTO LRFD Bridge Design Specifications, a comprehensive parametric study was completed. Over 1800 different bridge designs were completed to account for all of the influential design parameters, including cross-section type, girder spacing, bridge span length and concrete release strength. Through completion and comparison of the 2004 and 2012 AASHTO LRFD bridge designs, it was possible to identify the impact of the new loss provisions on the design of standard TxDOT bridges, summarized in terms of flexural reinforcement, flexural capacity, shear capacity and camber.

5. *Development of Design Recommendations*: New prestress loss provisions were developed through simplification of the method outlined in AASHTO LRFD 2012. The simplification process included consideration of the results obtained from experimental and analytical efforts outlined above. The primary objectives of the simplification were:

- To exclude prestress loss components with a minor contribution and/or limited relevance to the final prestress loss estimate.

- To account for typical materials and construction practices in calculation of the prestress loss components for simple span, pretensioned girders.

- To eliminate time-dependency of the provisions and limit estimation of the prestress loss to that corresponding to the full service life of a girder.

- To introduce additional conservatism where warranted by comparison of measured and estimated prestress losses.

It should be noted that this study was limited to pretensioned members used for the construction of simple span bridges. Post-tensioned, multi-stage construction was not examined within the context of this study. The provisions provided in this report are expected to be

conservative for post-tensioned, multi-stage construction due to the fact that loading applied to more mature concrete will have less of a long-term effect on prestress loss.

7.2   CONCLUSIONS: AASHTO LRFD PRESTRESS LOSS PROVISIONS

Conclusions regarding the relative complexity, conservatism and design implications of the prestress loss provisions in the 2004 and 2012 Editions of the AASHTO LRFD Bridge Design Specifications are presented here. The conservatism of each code approach was established during the database evaluations of Chapter 2. The relative complexity and design implications of each code approach were evaluated during the parametric study of Chapter 5.

7.2.1   AASHTO LRFD 2004

The prestress loss provisions within the 2004 AASHTO LRFD Bridge Design Specifications were found to be overly conservative, though relatively straightforward to implement.

- *Implementation is straightforward*: The empirically derived expressions of AASHTO LRFD 2004 were relatively simple to implement in relation to AASHTO LRFD 2012. The Specifications provide clear definitions for both the intention and implementation of the variables and expressions.

- *Elastic shortening estimates are slightly unconservative*: The AASHTO LRFD 2004 estimation of the prestress loss due to elastic shortening was consistently 10 to 15 percent less than the prestress loss measured within the 18 instrumented specimens of the experimental program.

- *Total prestress loss estimates are overly conservative*: The AASHTO LRFD 2004 prestress loss estimates were on average 74 percent greater than the measured losses contained in the Evaluation Database. The conservatism is attributed to an excessive overestimation of the creep-related prestress losses.

7.2.2   AASHTO LRFD 2012

The prestress loss provisions within 2012 AASHTO LRFD Bridge Design Specifications were found to be unnecessarily complex and both less conservative and no more precise than the AASHTO LRFD 2004 provisions.

- *Implementation is difficult*: Estimation of the short-term and long-term prestress losses is complicated by consideration of effects and parameters that bear little relevance to the calculated prestress loss (e.g. stepping through time, composite section effects, cross-section properties, etc.). Approximately 600 mathematical operations are necessary to estimate the total prestress within one pretensioned girder.

- *Elastic shortening estimates are slightly unconservative*: As observed for AASHTO 2004, the AASHTO LRFD 2012 estimation of the prestress loss due to elastic shortening was consistently 10 to 15 percent less than the prestress loss measured within the 18 instrumented specimens of the experimental program.

- *Total prestress loss estimates are unconservative*: A significant number of the prestress loss measurements (30 specimens) included within the Evaluation Database were underestimated by AASHTO LRFD 2012. The unconservative nature of

AASHTO LRFD 2012 is attributed to the 'accurate' approach adopted by the authors of NCHRP Report 496 during derivation of the provisions.

- *Significant design impact*: Designs completed according to AASHTO LRFD 2012 allowed as many as 10 strands to be removed in relation an equivalent design completed according to AASHTO LRFD 2004. Given the performance of AASHTO LRFD 2012 within the context of the Evaluation Database, there is a risk for serviceability problems associated with implementation of the method.

7.3   RECOMMENDATIONS: TxDOT PROJECT 0-6374 PRESTRESS LOSS PROVISIONS

The development of new prestress loss provisions was accomplished through simplification of AASHTO LRFD 2012. The simplification process primarily consisted of: (1) dissociation of deck placement and long-term estimates, (2) consideration of typical construction details, and (3) reincorporation of AASHTO LRFD 2004 recommendations.

In order to eliminate the differentiation between before and after deck placement prestress loss estimations, the following recommendations were made:

- *Time development factor*: A time development factor of 1.0 was recommended to combine the before and after deck placement contributions of girder creep and shrinkage.

$$k_{td} = 1.0$$

- *Change in concrete stress due to before deck losses*: When estimating the long-term creep, the stress change caused by long-term prestress loss prior to deck placement is to be neglected.

$$Neglect \ \Delta f_{cd,\Delta P}$$

- *Strand relaxation*: It was recommended that the before and after deck placement contributions of relaxation loss be combined.

$$\Delta f_{pR} = \frac{2 f_{pt}}{K_L} \left(\frac{f_{pt}}{f_{py}} - 0.55 \right)$$

- *Deck shrinkage demands*: This component of the total prestress loss estimate is both small in magnitude and does not accurately model the true behavior of a bridge system, so it is recommended that it be neglected.

$$Neglect \ \Delta f_{pSS}$$

Despite dissociation of deck placement and the long-term prestress loss estimates, the resulting provisions still included calculation-intensive variables with limited relevance to the precision and conservatism of the results. After a thorough investigation of these variables, the following recommendations were made:

- *Transformed section coefficient*: Based on data from the parametric study, it was found that an upper bound approximation of the transformed section coefficient of 0.9 could conservatively be used for all designs.

$$K_{if} = 0.9$$

- *Volume-to-surface area ratio*: Little variation was observed in the volume-to-surface area ratio between all commonly used sections in TxDOT design. For this reason, the shape factor was conservatively recommended to be set equal to 1.0.

$$k_s = 1.0$$

- *Timing of transfer and deck placement*: Due to the fact that times of release and deck placement are not known exactly during the design phase, it was recommended that they be taken as one day and 120 days, respectively.

$$t_i = 1 \ day \qquad\qquad t_d = 120 \ days$$

Two additional modifications were prompted by analysis of the evaluation database. These modifications reincorporated recommendations made in AASHTO LRFD 2004.

- *Concrete release strength coefficient*: Database evaluation of AASHTO LRFD 2012 revealed that it was biased toward high concrete release strengths. Use of the release strength coefficient found within the creep provisions of AASHTO LRFD 2004 is a more balanced means of accounting for the effect of concrete release strength.

$$k_f = \frac{7.2}{4.8 + f'_c}$$

- *Strand stress after transfer*: In order to eliminate the iterative procedure prescribed by AASHTO LRFD 2012, the strand stress after transfer is recommended to be taken as 70 percent of the ultimate capacity.

$$f_{pt} = 0.7 f_{pu}$$

Implementation of the above recommendations and further simplification of the AASHTO LRFD 2012 expressions resulted in the TxDOT Project 0-6374 prestress loss provisions, summarized in Table 7.1. The proposed prestress loss provisions performed well in comparison to both the AASHTO LRFD 2004 and 2012 methods. The final set of provisions was found to be:

- *Simple to implement*: The TxDOT Project 0-6374 prestress loss provisions require approximately one-tenth of the total number of mathematical operations required by, and one-third the total number of variables included in, AASHTO LRFD 2012.

- *More conservative and precise*: The minimum E/M value for AASHTO LRFD 2012 was found to be 0.59, compared to 0.84 for the TxDOT Project 0-6374 prestress loss provisions. The recommendations also resulted in less scatter, with a characteristic coefficient of variation (COV) equal to 0.20 (as compared to COV = 0.24 for AASHTO LRFD 2012).

- *Less significant of a design impact*: Use of the AASHTO LRFD 2012 provisions would result in up to 10 less strands, relative to AASHTO LRFD 2004, in some design scenarios using a 6 ksi release strength. Use of the TxDOT Project 0-6374 prestress loss provisions would result in up to 6 less strands in the same design scenarios.

Simplification of the AASHTO LRFD 2012 prestress loss provisions served two purposes: (1) to reduce the unnecessary complexity of the method and (2) to introduce additional conservatism through the use of lower bound constants and parameter expressions. Both of these were accomplished through the development of the TxDOT Project 0-6374 prestress loss provisions.

Table 7.1 – Summary of recommended prestress loss provisions

Component	Recommended Expressions
Total Prestress Loss (Δf_{pT})	$$\Delta f_{pT} = \Delta f_{pES} + \Delta f_{pSR} + \Delta f_{pCR} + \Delta f_{pR}$$
Elastic Shortening (Δf_{pES})	$$\Delta f_{pES} = \frac{E_p}{E_{ci}} f_{cgp}$$ *where:* $$f_{cgp} = 0.7 f_{pu} A_{ps} \left(\frac{1}{A_g} + \frac{e_p^2}{I_g} \right) - \frac{M_g e_p}{I_g}$$
Shrinkage Loss (Δf_{pSR})	$$\Delta f_{pSR} = E_p \left(\frac{140 - H}{4.8 + f'_{ci}} \right) 4.4 * 10^{-5}$$
Creep Loss (Δf_{pCR})	$$\Delta f_{pCR} = 0.1 \left(\frac{195 - H}{4.8 + f'_{ci}} \right) \left(\frac{E_p}{E_{ci}} \right) \left(f_{cgp} + 0.6 \Delta f_{cd} \right)$$ *where:* $$\Delta f_{cd} = - \frac{M_{sd} e_p}{I_g}$$
Relaxation Loss (Δf_{pR})	$$\Delta f_{pR} = \frac{2 f_{pt}}{K_L} \left(\frac{f_{pt}}{f_{py}} - 0.55 \right)$$

This page is intentionally left blank

REFERENCES

ACI Committee 209. (1992 (Reapproved 2008)). *Prediction of Creep, Shrinkage, and Temperature Effects in Concrete Structures.* American Concrete Institute.

American Association of State Highway and Transportation Officials (AASHTO). (2004). *AASHTO LRFD Bridge Design Specifications, Customary U.S. Units, 3rd Edition.* Washington, DC.

American Association of State Highway and Transportation Officials (AASHTO). (2005). *2005 Interim Revisions: AASHTO LRFD Bridge Design Specification, Customary U.S. Units.* Washington, DC.

American Association of State Highway and Transportation Officials (AASHTO). (2012). *AASHTO LRFD Bridge Design Specification, Customary U.S. Units, 6th Edition.* Washington, DC.

American Society for Testing and Materials (ASTM). (2002). *ASTM C469 - Standard Test Method for Static Modulus of Elasticity and Poisson's Ratio of Concrete in Compression.* West Conshohocken, PA: ASTM International.

American Society for Testing and Materials (ASTM). (2004). *ASTM C496 - Standard Test Method for Splitting Tensile Strength of Cylindrical Concrete Specimens.* West Conshohocken, PA: ASTM International.

American Society for Testing and Materials (ASTM). (2005). *ASTM C39 - Standard Test Method for Compressive Strength of Cylindrical Concrete Specimens.* West Conshohocken, PA: ASTM International.

Barr, P., Halling, M., Boone, S., Toca, R., & Angomas, F. (2009). *UDOT's Calibration of AASHTO's New Prestress Loss Design Equations.* Logan, UT: Utah State University.

Bazant, Z. (1972). Prediction of Concrete Creep Effects Using Age-Adjusted Effective Modulus Method. *Journal of the American Concrete Institute*, 212-217.

Cousins, T. E. (2005). *Investigation of Long-Term Prestress Losses In Pretensioned High Performance Concrete Girders.* Charlottesville: Virginia Transportation Research Council.

Magura, D. D., Sozen, M. A., & Siess, C. P. (1964). A Study of Stress Relaxation in Prestressing Reinforcment. *PCI Journal*, 13-57.

National Oceanic and Atmospheric Administration (NOAA). (2012). *National Climatic Data Center*. Retrieved 2009 - 2012, from http://www.ncdc.noaa.gov/

Roller, J. J., Russell, H. G., Bruce, R. N., & Alaywan, W. R. (Winter 2011). Evaluation of prestress losses in high-strength concrete bulb-tee girders for the Rigolets Pass Bridge. *PCI Journal*, 110 - 134.

Roller, J. J., Russell, H. G., Bruce, R. N., & Martin, B. T. (1995). Long-Term Performance of Prestressed, Pretensioned High Strength Concrete Bridge Girders. *PCI Journal*, 48-59.

Schnittker, B. A. (2008). *Allowable Compressive Stress at Prestress Transfer.* Austin: The University of Texas at Austin.

Swartz, B. D. (2010). *Time-Dependent Analysis of Pretensioned Concrete Bridge Girders.* State College: The Pennsylvania State University.

Swartz, B. D., Schokker, A. J., & Scanlon, A. (2010). Evaluation of the LRFD Bridge Design Specifications Method for Estimating Prestress Losses. *Concrete Bridge Conference (CBC)*, (pp. 200-222). Phoenix.

Tadros, M. K., Al-Omaishi, N., Seguirant, S. J., & Gallt, J. G. (2003). *Prestress Losses in High-Strength Concrete Bridge Girders.* Washington, D.C.: National Cooperative Highway Research Program.

Texas Department of Transportation (TxDOT). (2005). Bridge Division Standard Drawings: English Prestressed Concrete I-Beam Standards. *www.dot.state.tx.us*. Austin.

Texas Department of Transportation (TxDOT). (2006). Bridge Division Standard Drawings: English Prestressed Concrete Box Beam Standards. *www.dot.state.tx.us*. Austin.

Texas Department of Transportation (TxDOT). (2006). Bridge Division Standard Drawings: English Prestressed Concrete U-Beam Standards. *www.dot.state.tx.us*. Austin.

Texas Department of Transportation (TxDOT). (2009). Bridge Division Standard Drawings: English Prestressed Concrete I-Girder Standards. *www.dot.state.tx.us*. Austin.

Texas Department of Transportation (TxDOT). (2012). *Standard Specifications for Construction and Maintenance of Highways, Streets, and Bridges.* Austin: Texas Department of Transportation.

Yang, Y., & Myers, J. J. (2005). Prestress Loss Measurements in Missouri's First Fully Instrumented High-Performance Concrete Bridge. *Transportation Research Record: Journal of the Transportation Research Board*, 118-125.

APPENDIX A
Proposed Prestress Loss Specification

A.1 OVERVIEW

The prestress loss procedure developed as part of TxDOT Project 0-6374 is presented in this appendix. The underlying rationale for the recommendations presented in this appendix is presented in Chapter 6, where the refined method is discussed, and Appendix D, where the approximate loss estimate is explained. In short, the recommendations were developed to simplify the procedure for estimating prestress loss while adding a reasonable level of conservatism. A recommended Article "5.4.2.4 – Modulus of Elasticity" and "5.9.5 – Loss of Prestress" are presented with recommendations in bold.

A.2 PROPOSED REVISIONS TO THE AASHTO LRFD BRIDGE DESIGN SPECIFICATIONS

The prestress loss procedure presented below is a proposed revision to AASHTO LRFD (2012). The articles are therefore numbered to correspond with their placement within the AASHTO LRFD loss of prestress specifications. The proposed changes to the current provisions are denoted with bold text.

5.4.2.4—Modulus of Elasticity

In the absence of measured data, the modulus of elasticity, E_{ci}, for concrete with unit weights between 0.090 and 0.155 kcf and specified compressive strengths up to 15.0 ksi may be taken as:

$$E_c = 33{,}000K_1w_c^{1.5}\sqrt{f'_c} \qquad (5.4.2.4\text{-}1)$$

where:

K_1 = correction factor for source of aggregate to be taken as 1.0 unless determined by physical test, and as approved by the authority of jurisdiction

w_c = unit weight of concrete (kcf); refer to Table 3.5.1-1 or Article C5.4.2.4

f'_c = specified compressive strength of concrete (ksi)

C5.4.2.4

See commentary for specified strength in Article 5.4.2.1.

For normal weight concrete with $w_c = 0.145$ kcf, E_c may be taken as:

$$E_c = 1{,}820\sqrt{f'_c} \qquad (C5.4.2.4\text{-}1)$$

Test data show that the modulus of elasticity of concrete is influenced by the stiffness of the aggregate. The factor K_1 is included to allow the calculated modulus to be adjusted for different types of aggregate and local materials. Unless a value has been determined by physical tests, K_1 should be taken as 1.0. Use of a measured K_1 factor permits a more accurate prediction of modulus of elasticity and other values that utilize it.

5.9.5—Loss of Prestress

5.9.5.1—Total Loss of Prestress

Values of prestress losses specified herein shall be applicable to normal weight concrete only and for specified concrete strengths up to 15.0 ksi, unless stated otherwise.

In lieu of more detailed analysis, prestress losses in members constructed and prestressed in a single stage, relative to the stress immediately before transfer, may be taken as:

- In pretensioned members:

$$\Delta f_{pT} = \Delta f_{pES} + \Delta f_{pLT} \qquad (5.9.5.1-1)$$

- In post-tensioned members:

$$\Delta f_{pT} = \Delta f_{pF} + \Delta f_{pA} + \Delta f_{pES} + \Delta f_{pLT} \qquad (5.9.5.1-2)$$

where:

Δf_{pT} = total loss (ksi)

Δf_{pF} = loss due to friction (ksi)

Δf_{pA} = loss due to anchorage set (ksi)

Δf_{ES} = sum of all losses or gains due to elastic shortening or extension at the time of application of prestress and/or external loads (ksi)

Δf_{pLT} = losses due to long-term shrinkage and creep of concrete, and relaxation of the steel (ksi)

C5.9.5.1

For segmental construction, lightweight concrete construction, multi-stage prestressing, and bridges where more exact evaluation of prestress losses is desired, calculations for loss of prestress should be made in accordance with a time-step method supported by proven research data. See references cited in Article C5.4.2.3.2.

Data from control tests on the materials to be used, the methods of curing, ambient service conditions, and pertinent structural details for the construction should be considered.

Accurate estimate of total prestress loss requires recognition that the time-dependent losses resulting from creep, shrinkage, and relaxation are also interdependent. However, undue refinement is seldom warranted or even possible at the design stage because many of the component factors are either unknown or beyond the control of the Designer.

Losses due to anchorage set, friction, and elastic shortening are instantaneous, whereas losses due to creep, shrinkage, and relaxation are time-dependent.

This Article has been revised on the basis of new analytical investigations. The presence of a substantial amount of nonprestressed reinforcement, such as in partially prestressed concrete, influences stress redistribution along the section due to creep of concrete with time, and generally leads to smaller loss of prestressing steel pretension and larger loss of concrete precompression.

The loss across stressing hardware and anchorage devices has been measured from two to six percent (Roberts, 1993) of the force indicated by the ram pressure times the calibrated ram area. The loss varies depending on the ram and the anchor. An initial design value of three percent is recommended.

The extension of the provisions to 15.0 ksi was based on Tadros (2003), which only included normal weight concrete. Consequently, the extension to 15.0 ksi is only valid for member made with normal weight concrete.

5.9.5.2—Instantaneous Losses

5.9.5.2.1—Anchorage Set

The magnitude of the anchorage set shall be the greater of that required to control the stress in the prestressing steel at transfer or that recommended by the manufacturer of the anchorage. The magnitude of the set assumed for the design and used to calculate set loss shall be shown in the contract documents and verified during construction.

C5.9.5.2.1

Anchorage set loss is caused by the movement of the tendon prior to seating of the wedges or the anchorage gripping device. The magnitude of the minimum set depends on the prestressing system used. This loss occurs prior to transfer and causes most of the difference between jacking stress and stress at transfer. A common value for anchor set is 0.375 in., although values as low as 0.0625 in. are more appropriate for some anchorage devices, such as those for bar tendons.

For wedge-type strand anchors, the set may vary between 0.125 in. and 0.375 in., depending on the type of equipment used. For short tendons, a small anchorage seating value is desirable, and equipment with power wedge seating should be used. For long tendons, the effect of anchorage set on tendon forces is insignificant, and power seating is not necessary. The 0.25 in. anchorage set value, often assumed in elongation computations, is adequate but only approximate.

Due to friction, the loss due to anchorage set may affect only part of the prestressed member.

Losses due to elastic shortening may also be calculated in accordance with Article 5.9.5.2.3 or other published guidelines (PCI 1975; Zia et. al. 1979). Losses due to elastic shortening for external tendons may be calculated in the same manner as for internal tendons.

5.9.5.2.2—Friction

5.9.5.2.2a Pretensioned Constuction

For draped prestressing tendons, losses that may occur at the hold-down devices should be considered.

5.9.5.2.2b Post-Tensioned Construction

Losses due to friction between the internal prestressing tendons and the duct wall may be taken as:

C.5.9.5.2.2b

Where large discrepancies occur between measured and calculated tendon elongations, in-place friction tests are required.

$$\Delta f_{pF} = f_{pj}\left(1 - e^{-(Kx+\mu\alpha)}\right) \qquad (5.9.5.2.2b\text{-}1)$$

Losses due to friction between the external tendon across a single deviator pipe may be taken as:

$$\Delta f_{pF} = f_{pj}\left(1 - e^{-\mu(\alpha+0.04)}\right) \qquad (5.9.5.2.2b\text{-}2)$$

where:

f_{pj} = stress in the prestressing steel at jacking (ksi)

x = length of a prestressing tendon from the jacking end to any point under consideration (ft)

K = wobble friction coefficient (per ft. of tendon)

μ = coefficient of friction

α = sum of the absolute values of angular change of prestressing steel path from jacking end, or from the nearest jacking end if tensioning is done equally at both ends, to the point under investigation (rad.)

e = base of Napierian logarithms

Values of K and μ should be based on experimental data for the materials specified and shall be shown in the contract documents. In the absence of such data, a value within the ranges of K and μ as specified in Table 5.9.5.2.2b-1 may be used.

For tendons confined to a vertical plane, α shall be taken as the sum of the absolute values of angular changes over length x.

The 0.04 radians in Eq. 5.9.5.2.2b-2 represents an inadvertent angle change. This angle change may vary depending on job-specific tolerances on deviator pipe placement and need not be applied in cases where the deviation angle is strictly controlled or precisely known, as in the case of continuous ducts passing through separate longitudinal bell-shaped holes at deviators. The inadvertent angle change need not be considered for calculation of losses due to wedge seating movement.

For slender members, the value of x may be taken as the projection of the tendon on the longitudinal axis of the member. A friction coefficient of 0.25 is appropriate for 12 strand tendons. A lower coefficient may be used for larger tendon and duct sizes. See also Article C5.14.2.3.7 for further discussion of friction and wobble coefficients.

α_v and α_h may be taken as the sum of absolute values of angular changes over length, x, of the projected tendon profile in the vertical and horizontal planes, respectively.

The scalar sum of α_v and α_h may be used as a first approximation of α.

For tendons curved in three dimensions, the total tridimensional angular change α shall be obtained by vectorially adding the total vertical angular change, α_v, and the total horizontal angular change α_h.

When the developed elevation and plan of the tendons are parabolic or circular, the α can be computed from:

$$\alpha = \sqrt{\alpha_v{}^2 + \alpha_h{}^2} \qquad \text{(C5.9.5.2.2b-1)}$$

When the developed elevation and the plan of the tendon are generalized curves, the tendon may be split into small intervals, and the above formula can be applied to each interval so that:

$$\alpha = \Sigma\Delta\alpha = \Sigma\sqrt{\Delta\alpha_v{}^2 + \Delta\alpha_h{}^2} \qquad \text{(C5.9.5.2.2b-2)}$$

As an approximation, the tendon may be replaced by a series of chords connecting nodal points. The angular changes, $\Delta\alpha_v$ and $\Delta\alpha_h$, of each chord may be obtained from its slope in the developed elevation and in plan.

Field tests conducted on the external tendons of a segmental viaduct in San Antonio, Texas, indicate that the loss of prestress at deviators is higher than the usual friction coefficient ($\mu = 0.25$) would estimate.

This additional loss appears to be due, in part, to the tolerances allowed in the placement of the deviator pipes. Small misalignments of the pipes can result in significantly increased angle changes of the tendons at the deviation points. The addition of an inadvertent angle change of 0.04 radians to the theoretical angle change accounts for this effect based on typical deviator length of 3.0 ft. and placement tolerance of ±3/8 in. The 0.04 value is to be added to the theoretical value at each deviator. The value may vary with tolerances on pipe placement.

The measurements also indicated that the friction across the deviators was higher during the stressing operations than during the seating operations.

See Podolny (1986) for a general development of friction loss theory for bridges with inclined webs and for horizontally curved bridges.

Table 5.9.5.2.2b-1 – Friction Coefficients for Post-Tensioning Tendons

Type of Steel	Type of Duct	K	μ
Wire or strand	Rigid and semirigid galvanized metal sheathing	0.0002	0.15-0.25
	Polyethylene	0.0002	0.23
	Rigid steel pipe deviators for external tendons	0.0002	0.25
High-strength bars	Galvanized metal sheathing	0.0002	0.30

5.9.5.2.3—Elastic Shortening

5.9.5.2.3a—Pretensioned Members

The loss due to elastic shortening in pretensioned members shall be taken as:

$$\Delta f_{pES} = \frac{E_p}{E_{ci}} f_{cgp} \qquad (5.9.5.2.3a\text{-}1)$$

in which:

$$f_{cgp} = f_{pt} A_{ps} \left(\frac{1}{A_g} + \frac{e_m{}^2}{I_g} \right) - \frac{M_g e_m}{I_g} \qquad (5.9.5.2.3a\text{-}2)$$

where:

f_{cgp} = the concrete stress at the center of gravity of prestressing tendons due to the prestressing force immediately after transfer and the self-weight of the member at the section of maximum moment (ksi)

E_p = modulus of elasticity of prestressing steel

E_{ci} = modulus of elasticity of concrete at transfer or time of load application (ksi)

f_{pt} = stress in prestressing strands immediately after transfer, taken as 0.7f_{pu} if a more detailed analysis is not performed (ksi)

A_{ps} = area of prestressing steel (in.²)

A_g = gross area of section (in.²)

e_m = average prestressing steel eccentricity at midspan (in.)

I_g = moment of inertia of the gross concrete section (in.⁴)

M_g = midspan moment due to member self-weight (kip-in.)

C5.9.5.2.3a

Changes in prestressing steel stress due to the elastic deformations of the section occur at all stages of loading. Historically, it has been conservative to account for this effect implicitly in the calculation of elastic shortening and creep losses considering only the prestress force present after transfer. **Even though elastic shortening may be calculated on a purely theoretical basis, it has been shown that using an assumed strand stress immediately after transfer of 0.7f_{pu} more accurately estimates the actual behavior.**

The change in prestressing steel stress due to the elastic deformations of the section may be determined for any load applied. The resulting change may be a loss, at transfer, or a **stress gain**, at time of superimposed load application. Where a more detailed analysis is desired, Eq. 5.9.5.2.3a-1 may be used at each section along the beam, for the various loading conditions.

The loss due to elastic shortening in pretensioned members may be determined by the following alternative equation:

$$\Delta f_{pES} = \frac{A_{ps} f_{pbt} \left(I_g + e_m{}^2 A_g \right) - e_m M_g A_g}{A_{ps} \left(I_g + e_m{}^2 A_g \right) + \frac{A_g I_g E_{ci}}{E_p}} \qquad (C5.9.5.2.3a\text{-}1)$$

where:

A_{ps} = area of prestressing steel (in.²)

A_g = gross area of section (in.²)

E_{ci} = modulus of elasticity of concrete at transfer (ksi)

E_p = modulus of elasticity of prestressing tendons (ksi)

e_m = average prestressing steel eccentricity at midspan (in.)

f_{pbt} = stress in prestressing steel immediately prior to transfer (ksi)

The total elastic loss or gain may be taken as the sum of the effects of prestress and applied loads.

5.9.5.2.3b—Post-Tensioned Members

The loss due to elastic shortening in post-tensioned member, other than slab systems, may be taken as:

$$\Delta f_{pES} = \frac{N-1}{2N} \frac{E_p}{E_{ci}} f_{cgp}$$

(5.9.5.2.3b-1)

where:

N = number of identical prestressing tendons
f_{cgp} = sum of concrete stresses at the centroid of gravity of prestressing tendons due to the prestressing force after jacking and the self-weight of the member at the section of maximum moment (ksi)

f_{cgp} values may be calculated using a steel stress reduced below the initial value by a margin dependent on elastic shortening, relaxation, and friction effects.

For post-tensioned structures with bonded tendons, f_{cgp} value may be taken at the center section of the span or, for continuous construction, at the section of maximum moment.

For post-tensioned structures with unbounded tendons, the f_{cgp} value may be calculated as the stress at the center of gravity of the prestressing steel averaged along the length of the member.

For slab systems, the value of Δf_{pES} may be taken as 25 percent of that obtained from Eq. 5.9.5.2.3b-1.

I_g = moment of inertia of the gross concrete section (in.⁴)

M_g = midspan moment due to member self-weight (kip-in.)

C5.9.5.2.3b

The loss due to elastic shortening in post-tensioned members, other than slab systems, may be determined by the following alternative equation:

$$\Delta f_{pES} = \frac{N-1}{2N} \frac{A_{ps} f_{pbt}\left(I_g + e_m^2 A_g\right) - e_m M_g A_g}{A_{ps}\left(I_g + e_m^2 A_g\right) + \frac{A_g I_g E_{ci}}{E_p}}$$

(C5.9.5.2.3b-1)

where:

A_{ps} = area of prestressing steel (in.²)

A_g = gross area of section (in.²)

E_{ci} = modulus of elasticity of concrete at transfer (ksi), K₁ to be taken as 0.85 unless determined by physical test

E_p = modulus of elasticity of prestressing tendons (ksi)

e_m = average prestressing steel eccentricity at midspan (in.)

f_{pbt} = stress in prestressing steel immediately prior to transfer as specified in Table 5.9.3-1 (ksi)

I_g = moment of inertia of the gross concrete section (in.⁴)

M_g = midspan moment due to member self-weight (kip-in.)

N = number of identical prestressing tendons

f_{pj} = stress in the prestressing steel at jacking (ksi)

178

For post-tensioned structures with bonded tendons, Δf_{pES} may be calculated at the center section of the span or, for continuous construction, at the section of maximum moment.

For post-tensioned structures with unbounded tendons, Δf_{pES} can be calculated using the eccentricity of the prestressing steel averaged along the length of the member.

For slab systems, the value of Δf_{pES} may be taken as 25 percent of that obtained from Eq. C5.9.5.2.3b-1.

For post-tensioned construction, Δf_{pES} losses can be further reduced below those implied by Eq. 5.9.5.2.3b-1 with proper tensioning procedures such as stage stressing and retensioning.

If tendons with two different number of strand per tendon are used, N may be calculated as:

$$N = N_1 + N_2 \frac{A_{sp2}}{A_{sp1}} \qquad \text{(C5.9.5.2.3b-2)}$$

where:

N_1 = number of tendons in the larger group

N_2 = number of tendons in the smaller group

A_{sp1} = cross-sectional area of a tendon in the larger group (in.^{2})

A_{sp2} = cross-sectional area of a tendon in the smaller group (in.^{2})

5.9.5.2.3c   Combined Pretensioning and Post-Tensioning

C.5.9.5.2.3c

In applying the provisions of Articles 5.9.5.2.3a and 5.9.5.2.3b to components with combined pretensioning and post-tensioning, and where post-tensioning is not applied in identical increments, the effects of subsequent post-tensioning on the elastic shortening of previously stressed prestressing tendons shall be considered.

See Castrodale and White (2004) for information on computing the effect of subsequent post-tensioning on the elastic shortening of previously stressed prestressing tendons.

179

5.9.5.3—Approximate Estimate of Time-Dependent Losses

For standard precast members subject to normal loading and environmental conditions, where:

- members are made from normal-weight concrete,
- the concrete is either steam- or moist-cured
- prestressing is by bars or strands with normal and low relaxation properties, and
- average exposure conditions and temperatures characterize the site,

the long-term prestress loss, Δf_{pLT}, due to creep of concrete, shrinkage of concrete, and relaxation of steel shall be estimated using the following formula:

$$\Delta f_{pLT} = 10.0 \frac{f_{pi} A_{ps}}{A_g} \gamma_h \gamma_{st} + 15 \gamma_h \gamma_{st} + \Delta f_{pR}$$

(5.9.5.3-1)

in which:

$$\gamma_h = 1.7 - 0.01H \qquad (5.9.5.3\text{-}2)$$

$$\gamma_{st} = \frac{5}{(1 + f'_{ci})} \qquad (5.9.5.3\text{-}3)$$

where:

f_{pi} = prestressing steel stress immediately prior to transfer (ksi)

H = the average annual ambien relative humidity (%)

γ_h = correction factor for relative humidity of the ambient air

γ_{st} = correction factor for specified concrete strength at time of prestress transfer to the concrete member

The losses or gains due to elastic deformations at the time of transfer or load application should be added to the time-dependent losses to determine total losses. However, these elastic losses (or gains) must be taken equal to zero if transformed section properties are used in stress analysis.

The approximate estimates of time-dependent prestress losses given in Eq. 5.9.5.3-1 are intended for sections with composite decks only. The losses in Eq. 5.9.5.3-1 were derived as approximations of the terms in the refined method for a wide range of standard precast prestressed concrete I-beams, box beams, inverted tee beams, and voided slabs. The members were assumed to be fully utilized, i.e., level of prestressing is such that concrete tensile stress at full service loads is near the maximum limit. It is further assumed in the development of the approximate method that live load moments produce about on-third of the total load moments, which is reasonable for I-beam and inverted tee composite construction and conservative for noncomposite boxes and voided slabs. They were calibrated with full-scale test results and with the results of the refined method, and found to give conservative results (Al-Omaishi, 2001; Tadros, 2003). The approximate method should not be used for members of uncommon shapes, i.e., having V/S ratios much different from 3.5 in., level of prestressing, or construction staging. The first term in Eq. 5.9.5.3-1 corresponds to creep losses, the second term to shrinkage losses, and the third to relaxation losses.

The commentary to Article 5.9.5.4.2 also gives an alternative relaxation loss prediction method.

Δf_{pR} = an estimate of relaxation loss taken as 2.4 ksi for low relaxation strand, 10.0 ksi for stress relieved strand, and in accordance with manufacturers recommendation for other types of strand (ksi)

For girders other than those made with composite slabs, the **final** prestress losses resulting from creep and shrinkage of concrete and relaxation of steel shall be determined using the refined method of Article 5.9.5.4.

For segmental concrete bridges, **Article 5.9.5.3** may be used only for preliminary design purposes.

For members of unusual dimensions, level of prestressing, construction staging, or concrete constituent materials, the refined method of Article 5.9.5.4 or computer time-step methods shall be used.

5.9.5.4——Refined Estimates of Time-Dependent Losses

5.9.5.4.1—General

For nonsegmental prestressed members, more accurate values of creep-, shrinkage-, and relaxation-related losses, than those specified in Article 5.9.5.3 may be determined in accordance with the provisions of this Article. For cast-in-place nonsegmental post-tensioned girders, the provisions of Article 5.9.5.4.5 shall be considered before applying the provisions of this Article.

For segmental construction and post-tensioned spliced precast girders, other than during preliminary design, prestress losses shall be determined by the time-step method and the provisions of Article 5.9.5, including consideration of the time-dependent construction stages and schedule shown in the contract documents. For components with combined pretensioning and post-tensioning, and where post-tensioning is applied in more than one stage, the effects of subsequent prestressing on the creep loss for previous prestressing shall be considered.

C5.9.5.4.1

See Castrodale and White (2004) for information on computing the interaction of creep effects for prestressing applied at different times.

Estimates of losses due to each time-dependent source, such as creep, shrinkage, or relaxation, can lead to a better estimate of total losses compared with the values obtained using Article 5.9.5.3.

The individual losses are based on research published by Garber (2012). The new approach was calibrated on the basis of an experimental database containing 140 specimens with both low- and high-strength concrete, of a common shape, and with normal prestress ratios. Long-term prestress loss will be conservatively estimated for prestressed member with an excessively high prestress ratio or a low volume-to-surface area ratio.

The change in prestressing steel stress due to time-dependent loss, Δf_{pLT}, shall be determined as follows:

$$\Delta f_{pLT} = \Delta f_{pSR} + \Delta f_{pCR} + \Delta f_{pR} \qquad (5.9.5.4.1\text{-}1)$$

where:

Δf_{pSR} = **loss due to shrinkage (ksi)**

Δf_{pCR} = **loss due to creep of concrete (ksi)**

Δf_{pR} = **loss due to relaxation of steel after transfer (ksi)**

For concrete containing lightweight aggregates, **very soft aggregates**, very hard aggregates, or unusual chemical admixtures, the estimated material properties used in this Article and Article 5.4.2.3 may be inaccurate. Actual test results should be used for their estimation.

For segmental construction, for all considerations other than preliminary design, prestress losses shall be determined as specified in Article 5.9.5, including consideration of the time-dependent construction method and schedule shown in the contract documents.

5.9.5.4.2—Shrinkage of Girder Concrete

Loss of prestress, in ksi, due to shrinkage of girder concrete may be taken as:

$$\Delta f_{pSR} = E_p \left(\frac{140 - H}{4.8 + f'_{ci}} \right) 4.4 * 10^{-5}$$

$$(5.9.5.4.2\text{-}1)$$

where:

H = **relative humidity (%). In the absence of better information, H, may be taken from Figure 5.4.2.3.3-1.**

f'_{ci} = **specified concrete compressive strength at transfer (ksi)**

C.5.9.5.4.2

This expression is calibrated for typical concrete mixtures and environmental conditions. Soft aggregate, low-strength concrete, high ambient temperature, and some types of chemical admixtures may cause larger values of shrinkage loss.

5.9.5.4.3—Creep of Girder Concrete

The prestress loss due to creep of girder concrete may be taken as:

$$\Delta f_{pCR} = 0.1 \left(\frac{195 - H}{4.8 + f'_{ci}}\right) \left(\frac{E_p}{E_{ci}}\right) (f_{cgp} + 0.6 \Delta f_{cdp})$$

(5.9.5.4.3-1)

where:

Δf_{cdp} = change in concrete stress at the center of gravity of prestressing steel due to permanent loads, with the exception of the load acting at the time the prestressing force is applied. (ksi)

$$\Delta f_{cdp} = -\frac{M_{sd} e_{pg}}{I_g}$$

(5.9.5.4.3-2)

e_{pg} = eccentricity of prestressing force with respect to the centroid of girder (in.); positive in common construction where it is below girder centroid

M_g = moment due to self-weight of girder (k-in)

M_{sd} = moment due to deck weight and other superimposed dead loads (k-in)

C.5.9.5.4.3

The equation given in Article 5.9.5.4.3 is derived based on common construction practices: time of transfer of 1 day and time of deck placement of 120 days.

For prestress applied later than 1 day after casting, the prestress loss due to creep of girder concrete may be taken as:

$$\Delta f_{pCR} = 0.1 t_i^{-0.118} \left(\frac{195 - H}{4.8 + f'_{ci}}\right) \left(\frac{E_p}{E_{ci}}\right) (f_{cgp} + 0.6 \Delta f_{cdp})$$

(C5.9.5.4.3-1)

where:

t_i = concrete age at transfer (days)

Some of the additional sustained dead loads may be applied after the composite action is effective. If these additional sustained dead loads are substantial compared to the deck weight, then the changes in concrete stress due to these loads should be calculated using composite section properties. Equation 5.9.5.4.3-2 uses gross section properties for simplicity.

5.9.5.4.4——Relaxation of Prestressing Strands

Losses due to relaxation of prestressing steel may be taken as:

$$\Delta f_{pR} = \frac{2 f_{pt}}{K_L} \left(\frac{f_{pt}}{f_{py}} - 0.55\right)$$

(5.9.5.4.3-1)

C5.9.5.4.4

Generally, the initial relaxation loss, prior to transfer, is now determined by the fabricator. If a time dependent equation is needed, e.g. for calculation of relaxation loss prior to transfer, the relaxation loss over a given period of time may be taken as:

183

where:

f_{pt} = stress in prestressing strands immediately after transfer, taken as $0.7f_{pu}$ if a more detailed analysis is not performed (ksi)

f_{py} = specified yield strength of prestressing steel (ksi)

K_L = 30 for low-relaxation strands and 7 for other prestressing steel, unless more accurate manufacturer's data are available

The relaxation loss, Δf_{pR}, may be assumed equal to **2.4** ksi for low-relaxation strands.

$$\Delta f_{pRi} = \frac{f_{pt}}{45}\left[\frac{f_{pt}}{f_{py}} - 0.55\right]\log\left(\frac{24t_2 + 1}{24t_1 + 1}\right)$$

(C5.9.5.4.3-1)

where:

t_1 = time from initial strand stressing to the beginning of desired time period (days)

t_2 = time in which relaxation loss is desired (days)

This equation is only valid for low-relaxation strands. It is based on the work of Magura et al. (1964) and calibrated for strands kept at a constant strain, similar to before transfer. Relaxation loss will be conservatively estimated when the strand strain decreases over time.

Eqs. 5.9.5.4.3-1 and C5.9.5.4.3-1 are given for relaxation losses and are appropriate for normal temperature ranges only. Relaxation losses increase with increasing temperatures.

5.9.5.4.5—Post-Tensioned Nonsegmental Girders

Long-term prestress losses for post-tensioned members after tendons have been grouted may be calculated using the provisions of Articles 5.9.5.4.1 through 5.9.5.4.4.

The creep loss may be calculated using the following equation:

$$\Delta f_{pCR} = 0.1 t_i^{-0.118}\left(\frac{195 - H}{4.8 + f'_{ci}}\right)\left(\frac{E_p}{E_{ci}}\right)\left(f_{cgp} + 0.6\Delta f_{cdp}\right)$$

(5.9.5.4.5-1)

where:

t_i = concrete age at transfer (days)

184

5.9.5.5———Losses For Deflection Calculations

For camber and deflection calculations of prestressed nonsegmental member made of normal weight concrete with a strength in excess of 3.5 ksi at the time of prestress, f_{cgp} and Δf_{cdp} may be computed as the stress at the center of gravity of prestressing steel averaged along the length of the member.

This page is intentionally left blank

APPENDIX B
Design Example

B.1 OVERVIEW

The purpose of this design example is to compare the loss provisions of AASHTO LRFD 2004 and 2012 with those recommended in Chapter 6. In order to show the impact of the loss procedures, a hypothetical bridge (Figure B.1) exhibiting a large difference in estimated prestress losses between provisions was chosen.

The bridge and cross-sectional properties required to calculate the prestress loss are presented in the following section. The bridge consists of four Type-C girders spaced at 6.67 feet on center spanning 80 feet center-to-center of bearings. The number of strands in the girder was chosen based on a girder design using the AASHTO LRFD 2004 Bridge Design Specification. The same number of strands was then used for each of the other loss procedures in order to give a direct comparison of the loss calculations. Keeping the same number of strands allows the loss procedures to be directly compared but does not provide a true design comparison.

Figure B.1 – Model of the hypothetical bridge used for design example

B.2   PROPERTIES

The cross-section properties required for the loss calculations are presented in Table B.1 and illustrated in Figure B.2. The majority of the properties in the table are section properties associated with all Type-C beams (i.e. they do not change with different bridge designs). The only properties that vary between bridge designs are those associated with the location of the centroid of the prestressing strands (e_p, $y_{p,cl}$, etc.).
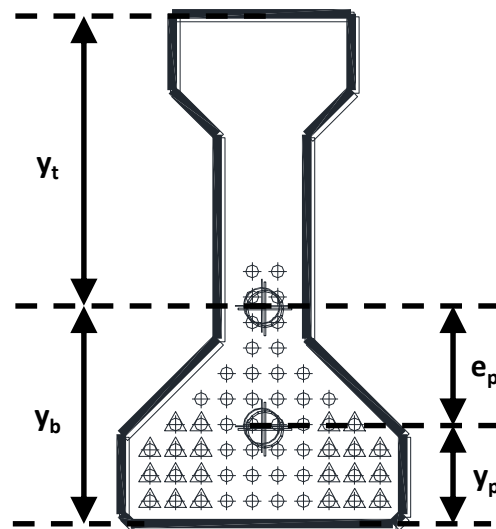
Figure B.2 – As built strand layout for section at mid-span

The bridge properties are presented in Table B.2. The timing of the bridge was chosen based on common fabrication practices (24 hour time of release) and suggested time of deck placement found in AASHTO LRFD 2012 of 120 days. The final time was chosen for a bridge with a 100-year design life; choosing a 50-year or 75-year design life would make no difference in the prestress loss estimates. The age of the both the girder and deck concrete at the end of their respective curing periods is required for calculation of shrinkage strains. In order to illustrate unique aspects of the shrinkage calculations, the girder curing time was chosen so that it would (1) be different than the time of transfer and (2) be less than five days and therefore require an additional 20 percent shrinkage strain.

The length of the bridge chosen (80 feet) is around 90% of the maximum allowable span length for Type-C beams (90 feet). The choice of this length ensured that the design was controlled by stress checks and the design was influenced by the prestress loss estimates. The span length is based on TxDOT prescribed distance of 6.5 inches from the beam end to bearing centroid.

Table B.1 – Section properties required for loss calculations

	Section Properties	
h	40.0 in.	Section height
y_t	22.9 in.	Distance from top fiber to centroid
y_b	17.1 in.	Distance from bottom fiber to centroid
A_g	494.9 in.^{2}	Area of gross section
I_g	82,600 in.^{4}	Moment of inertia of gross section
w_{sw}	0.516 kip/ft	Unit weight of section
p_s	125.1 in.	Perimeter of section
y_{p_cl}	4.84 in.	Distance from bottom fiber to centroid of prestress tendons
e_p	12.25 in.	Eccentricity of prestressing tendons at mid-span
$e_{p,end}$	6.40 in.	Eccentricity of prestressing tendons at end
d_b	0.5 in.	Diameter of prestressing tendons
A_{ps1}	0.153 in.^{2}	Area of one prestressing tendon
A_{ps}	5.81 in.^{2}	Total prestress strand area
A_s	0.62 in.^{2}	Total compression steel area

Table B.2 – Bridge properties required for loss calculations

Bridge Properties		
L_{span}	79.0 ft.	Span length
L_{beam}	80.0 ft	Beam length
$L_{holddown}$	10 ft	Hold-down length
V/S	3.9 in	Volume-to-surface area ratio
M_g	4,954 kip-in.	Dead load moment due to self-weight
H	60 %	Average relative humidity
t_i	1.0 day	Age of girder concrete at time of transfer
t_c	2.0 days	Age of girder concrete at end of moist curing
t_d	120 days	Age of girder concrete at time of deck placement
t_{dc}	125 days	Age of girder concrete at end of moist curing of deck
t_{id}	5 days	Age of deck concrete at time of loading
t_f	365,000 days	Age of girder concrete at final time (100-year design life)

Both the concrete and steel material properties required for the loss calculations are presented in Table B.3. The properties were chosen based on common materials and fabrication practices in Texas. The modulus of elasticity at time of transfer, final time, and for the deck concrete were all calculated values using Equation 5.4.2.4-1 from AASHTO LRFD 2012. A correction factor (K_1) of 1.0 was used for the calculations shown in this design example. In the summary section, the estimated prestress loss using a correction factor of 0.85 and 1.2 are presented; these values were chosen to show the effect of limestone aggregate ($K_1 = 0.85$) and river rock aggregate ($K_1 = 1.2$) on prestress loss estimates.

Table B.3 – Material properties required for loss calculations

	Material Properties	
	Concrete Properties	
f_{ci}	6.0 ksi	Strength of girder concrete at time of transfer
f'_c	8.5 ksi	Ultimate strength of girder concrete
K_1	1.0	Correction factor
w_c	150 lb/ft^3	Unit weight of concrete
E_{ci}	4,700 ksi	Modulus of elasticity of girder concrete at time of transfer, AASHTO LRFD 2012 (5.4.2.4-1)
E_c	5,590 ksi	Modulus of elasticity of girder concrete at final time, AASHTO LRFD 2012 (5.4.2.4-1)
f'_{cdi}	3.2 ksi	Strength of deck concrete at end of deck curing
f'_{cd}	4.0 ksi	Ultimate strength of deck concrete
E_{cd}	3,830 ksi	Modulus of elasticity of deck concrete at final time, AASHTO LRFD 2012 (5.4.2.4-1)
	Steel Properties	
f_{pu}	270 ksi	Ultimate strength of prestressing tendons
f_{py}	243 ksi	Yield stress of prestressing tendons
f_{pi}	202.5 ksi	Initial stress in the tendon at the end of stressing
E_p	28,500 ksi	Modulus of elasticity of prestressing tendons

The composite section properties are required for the calculation of after deck placement prestress loss in the provisions of AASHTO LRFD 2012. The composite section properties for the section shown in Figure B.3 are presented in Table B.4. The mid-span moment due to the superimposed dead load, also presented in this table, includes only the weight of the deck slab.
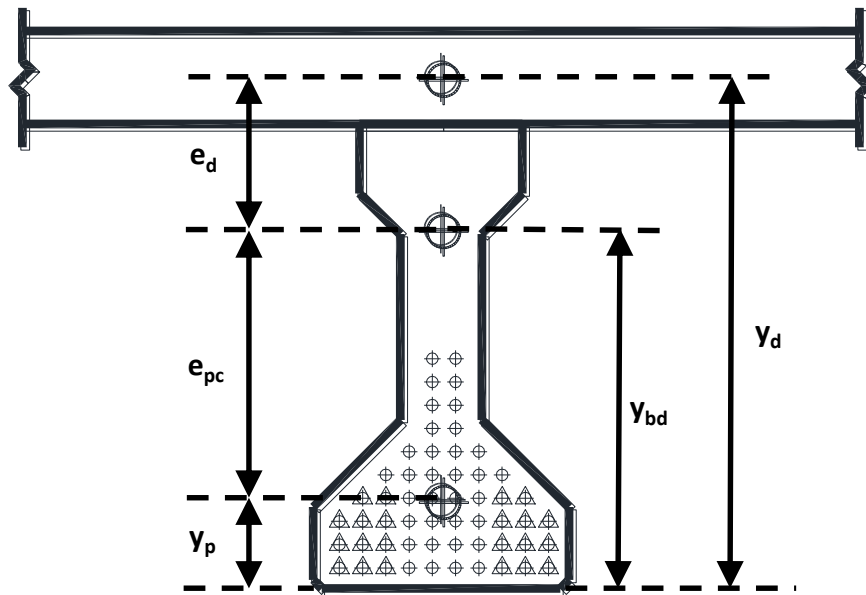
Figure B.3 – As built section with cast-in-place deck

Table B.4 – Deck properties required for loss calculations

Deck Properties and Composite Section Properties		
t_d	8 in.	Deck thickness
b_d	80 in.	Beam spacing
y_d	44.0 in.	Distance from bottom fiber to deck centroid
A_c	934 in.^{2}	Area of composite section
I_c	251,000 in.^{4}	Moment of inertia of composite section
y_{bd}	29.7 in.	Distance from bottom fiber to centroid of composite section
e_d	14.3 in.	Eccentricity of deck
e_{pc}	24.9 in.	Eccentricity of prestressing tendons in composite section at mid-span
M_{sd}	6,400 kip-in.	Dead load moment due to superimposed dead load
$(V/S)_d$	4.4 in.	Volume-to-surface area ratio of deck

B.3 AASHTO LRFD 2004 Loss Procedure

The first loss procedure presented, from the AASHTO LRFD 2004 Bridge Design Specification, has simple, straightforward expressions to estimate prestress loss due to elastic shortening, creep, shrinkage, and strand relaxation. Gross section properties are used for all calculations and there is no dependency of long-term losses on deck placement.

The first calculation made in the procedure is to find the concrete stress at the centroid of the prestressing strands (f_{cgp}). This calculated concrete stress will be used in both the elastic shortening and creep expressions. In AASHTO LRFD 2004, the stress in the prestressing strands immediately after transfer is estimated to be $0.7f_{pu}$.

$$f_{cgp} = 0.7f_{pu}A_{ps}\left(\frac{1}{A_g} + \frac{e_p^2}{I_g}\right) - \frac{M_g e_p}{I_g}$$

$$= 0.7(270\ ksi)(5.81\ in^2)\left(\frac{1}{494.9\ in^2} + \frac{(12.25\ in)^2}{82{,}600\ in^4}\right) - \frac{(4{,}954\ k-in)(12.25\ in)}{(82{,}600\ in^4)}$$

$$= 3.48\ ksi$$

The concrete stress at the centroid of the prestressing strands is then used to calculate the prestress loss due to elastic shortening:

$$\Delta f_{pES} = \frac{E_p}{E_{ci}}f_{cgp}$$

$$= \left(\frac{28{,}500\ ksi}{4{,}700\ ksi}\right)(3.48\ ksi)$$

$$= 21.1\ ksi$$

The long-term prestress loss is broken into loss due to shrinkage, creep, and strand relaxation. The long-term prestress loss is calculated in one step and is independent of time.

Prestress loss due to shrinkage of the girder concrete is dependent only on the average relative humidity at the location of the bridge. In this example, the average relative humidity is 60 percent in the location of the bridge.

$$\Delta f_{pSR} = (17.0 - 0.150H)$$

$$= \left(17.0 - 0.150(60)\right)$$

$$= 8.0\ ksi$$

The prestress loss due to girder creep is dependent on the concrete stress at the centroid of the prestressing strands due to the prestressing force and self-weight (f_{cgp}) and due to any superimposed dead loads (Δf_{cdp}). Both of these stresses are calculated using gross section properties. The "12.0" and "7.0" are empirically derived coefficients that weight the impact of each concrete stress on the total creep loss.

$$\Delta f_{cdp} = -\frac{M_{sd}e_p}{I_g}$$

$$= -\frac{(6{,}400\ k-in)(12.25\ in)}{(82{,}600\ in^4)}$$

$$= 0.95\ ksi$$

$$\Delta f_{pCR} = 12.0 f_{cgp} - 7.0 \Delta f_{cdp}$$

$$= 12.0(3.48\ ksi) - 7.0(0.95\ ksi)$$

$$= 35.1\ ksi$$

Prestress loss due to strand relaxation occurring after transfer is calculated based on the elastic shortening, shrinkage and creep loss calculated above.

$$\Delta f_{pR2} = \frac{3}{10}\left[20.0 - 0.4\Delta f_{pES} - 0.2\left(\Delta f_{pSR} + \Delta f_{pCR}\right)\right]$$

$$= \frac{3}{10}\left[20.0 - 0.4(21.1\ ksi) - 0.2(8.0\ ksi + 35.1\ ksi)\right]$$

$$= 0.88\ ksi$$

B.3.1 Total Loss

The total prestress loss is the summation of the elastic shortening and three long-term loss contributions.

$$\Delta f_{pT} = \Delta f_{pES} + \Delta f_{pSR} + \Delta f_{pCR} + \Delta f_{pR2}$$

$$= 26.6\ ksi + 8.0\ ksi + 46.0\ ksi + 0.9\ ksi$$

$$= 65.1\ ksi$$

B.4 AASHTO LRFD 2012 LOSS PROCEDURE

Use of the provisions of the 2012 AASHTO LRFD Bridge Design Specification is difficult to interpret and little explanation is provided in the commentary. The calculations and values shown in the example are the researcher's best interpretation of the procedure using the language from the specification as well as the assistance of previously published example problems (Tadros 2003, Roller 2011, and Swartz 2010).

B.4.1 Elastic Shortening

An iterative procedure for the estimation of elastic shortening is required by the body of AASHTO LRFD 2012. The procedure is iterated until the concrete stress ($f_{cgp,n}$) and the stress in the strands immediately after transfer ($f_{pt,n}$) converge (i.e. an acceptable accuracy is achieved). The specification suggests that the prestress may be assumed to be 90 percent of the initial prestress before transfer, so this is used as the starting point in the first iteration. Three iterations were required until the reasonable convergence of the concrete and strand stresses. Gross section properties are used for all elastic shortening calculations.

Iteration 1

$$f_{pt,1} = 0.9f_{pi} - \Delta f_{pES,1}$$
$$= 0.9(202.5 \ ksi)$$
$$= 182.2 \ ksi$$

$$f_{cgp,1} = f_{pt,1}A_{ps}\left(\frac{1}{A_g} + \frac{e_p{}^2}{I_g}\right) - \frac{M_g e_p}{I_g}$$

$$= (182.2 \ ksi)(5.81 \ in^2)\left(\frac{1}{494.9 \ in^2} + \frac{(12.25 \ in)^2}{82,600 \ in^4}\right) - \frac{(4,954 \ k-in)(12.25 \ in)}{82,600 \ in^4}$$

$$= 3.33 \ ksi$$

$$\Delta f_{pES,1} = \frac{E_p}{E_{ci}}f_{cgp,1}$$

$$= \frac{(28,500 \ ksi)}{(4,700 \ ksi)}(3.33 \ ksi)$$

$$= 20.2 \ ksi$$

Iteration 2

$$f_{pt,2} = f_{pi} - \Delta f_{pES,1}$$

$$= 202.5 \ ksi - 20.2 \ ksi$$

$$= 182.3 \ ksi$$

Further iterations are not required because the prestress loss due to elastic shortening calculated in the last iteration varied only 0.1 ksi from the value obtained in the previous iteration.

The values for concrete stress at the centroid of the prestressing strands (f_{cgp}), prestress after transfer (f_{pt}) and prestress loss due to elastic shortening (Δf_{pES}) are summarized in Table B.5. These values will be needed in the calculations for creep and strand relaxation below.

Table B.5 – Elastic shortening values calculated using iterative process

$f_{pt} = 182.3 \; ksi$
$f_{cgp} = 3.33 \; ksi$
$\Delta f_{pES} = 20.2 \; ksi$

B.4.2 Required Material Coefficients

Various material coefficients for the girder and deck concrete are required for the calculation of long-term prestress losses. These material coefficients are calculated in this section for both the girder and deck concrete for five different time spans: (1) time of transfer to final time, (2) end of curing to final time, (3) time of transfer to deck placement, (4) end of curing to deck placement, and (5) time of deck placement to final time.

B.4.2.1 Girder Coefficients

The following material coefficients for the girder concrete account for volume-to-surface area ratio (k_s), relative humidity (k_{hs} and k_{hc}), and the strength of the concrete at the time of release (k_f). These coefficients are used in the calculation of shrinkage and creep loss.

$$k_s \quad = 1.45 - 0.13(V/S) \geq 1.0$$

$$= 1.45 - 0.13(3.9) \geq 1.0$$

$$= 1.0$$

$$k_{hs} \quad = 2.0 - 0.014H$$

$$= 2.0 - 0.014(60)$$

$$= 1.16$$

$$k_{hc} \quad = 1.56 - 0.008H$$

$$= 1.56 - 0.008(60)$$

$$= 1.08$$

$$k_f \quad = \frac{5}{1 + f'_{ci}}$$

$$= \frac{5}{1 + 6.0 \; ksi}$$

$$= 0.714$$

The next coefficient accounts for the different time spans being investigated. The time development factor (k_{td}) is required for the five different time spans mentioned above.

$$k_{td}(t_d, t_i) \quad = \frac{(t_d - t_i)}{61 - 4f'_{ci} + (t_d - t_i)}$$

$$= \frac{(120 \; days - 1 \; day)}{61 - 4(6.0 \; ksi) + (120 \; days - 1 \; day)}$$

$$= 0.763$$

$$k_{td}(t_d, t_c) \quad = \frac{(t_d - t_c)}{61 - 4f'_{ci} + (t_d - t_c)}$$

$$= \frac{(120 \; days - 2 \; days)}{61 - 4(6.0 \; ksi) + (120 \; days - 2 \; days)}$$

$$= 0.761$$

$$k_{td}(t_f, t_i) \quad = \frac{(t_f - t_i)}{61 - 4f'_{ci} + (t_f - t_i)}$$

$$= \frac{(36500 \; days - 1 \; day)}{61 - 4(6.0 \; ksi) + (36500 \; days - 1 \; day)}$$

$$= 0.999$$

$$k_{td}(t_f, t_c) = \frac{(t_f - t_c)}{61 - 4f'_{ci} + (t_f - t_c)}$$

$$= \frac{(36500\ days - 2\ day)}{61 - 4(6.0\ ksi) + (36500\ days - 2\ day)}$$

$$= 0.999$$

$$k_{td}(t_f, t_d) = \frac{(t_f - t_d)}{61 - 4f'_{ci} + (t_f - t_d)}$$

$$= \frac{(365,000\ days - 120\ days)}{61 - 4(6.0\ ksi) + (365,000\ days - 120\ days)}$$

$$= 0.999$$

Creep coefficients (ψ_b) are required for the following time intervals: time of transfer to final time, time of transfer to time of deck placement, and time of deck placement to final time. The only difference between the three creep coefficients shown below is a different time development factor.

$$\psi_b(t_d, t_i) = 1.9k_s k_{hc} k_f k_{td}(t_d, t_i)t_i^{-0.118}$$

$$= 1.9(1.0)(1.08)(0.714)(0.763)(1\ day)^{-0.118}$$

$$= 1.12$$

$$\psi_b(t_f, t_i) = 1.9k_s k_{hc} k_f k_{td}(t_f, t_i)t_i^{-0.118}$$

$$= 1.9(1.0)(1.08)(0.714)(0.999)(1\ day)^{-0.118}$$

$$= 1.46$$

$$\psi_b(t_f, t_d) = 1.9k_s k_{hc} k_f k_{td}(t_f, t_d)t_d^{-0.118}$$

$$= 1.9(1.0)(1.08)(0.714)(0.999)(120\ day)^{-0.118}$$

$$= 0.832$$

The shrinkage strain of the girder concrete (ε_{bid}, ε_{bif}, ε_{bdf}) is required for three different time intervals: end of curing to final time, end of curing to deck placement, and time of deck placement to final time. The time interval represented by each shrinkage strain is depicted in the subscript (id = initial to deck placement, etc.). For the purpose of shrinkage calculations, the initial time corresponds to the end of curing. Similar to the creep coefficient, the only difference between the three shrinkage strains below is a different time development factor. The shrinkage

strain is required to be increased by 20 percent because the concrete curing period is less than 5 days.

$$\varepsilon_{bid} = 1.2k_s k_{hs} k_f k_{td}(t_d, t_c)0.48 * 10^{-3}$$

$$= 1.2(1.0)(1.16)(0.714)(0.763)0.48 * 10^{-3}$$

$$= 3.65 * 10^{-4}$$

$$\varepsilon_{bif} = 1.2k_s k_{hs} k_f k_{td}(t_f, t_c)0.48 * 10^{-3}$$

$$= 1.2(1.0)(1.16)(0.714)(0.999)0.48 * 10^{-3}$$

$$= 4.77 * 10^{-4}$$

The shrinkage strain from time of deck placement to final time (ε_{bdf}) is not explicitly defined in the specification. The expression used here is the designer's best interpretation of the variable definition presented in the specification.

$$\varepsilon_{bdf} = \varepsilon_{bif} - \varepsilon_{bid}$$

$$= 4.77 * 10^{-4} - 3.65 * 10^{-4}$$

$$= 1.12 * 10^{-4}$$

Two different transformed section coefficients are required for calculation of the long-term losses: one for the non-composite section from initial release to time of deck placement (K_{id}) and one for the composite section from the time of deck placement to final time (K_{df}). The only difference between the two coefficients is the use of gross section properties in the before deck placement coefficient and composite section properties in the after deck placement coefficient. It can be seen below that these two coefficients are similar in this design example; this was true for all the design examples investigated through the course of the parametric study.

$$K_{id} = \frac{1}{1 + \frac{E_p}{E_{ci}} \frac{A_{ps}}{A_g}\left(1 + \frac{A_g e_p{}^2}{I_g}\right)\left(1 + 0.7\psi_b(t_f, t_i)\right)}$$

$$= \frac{1}{1 + \left(\frac{28,500 \ ksi}{4,700 \ ksi}\right)\left(\frac{5.81 \ in^2}{494.9 \ in^2}\right)\left(1 + \frac{(494.9 \ in^2)(12.25 \ in)^2}{(82,600 \ in^4)}\right)\left(1 + 0.7(1.46)\right)}$$

$$= 0.785$$

$$K_{df} = \cfrac{1}{1 + \cfrac{E_p}{E_{ci}}\cfrac{A_{ps}}{A_c}\left(1 + \cfrac{A_c e_{pc}{}^2}{I_c}\right)\left(1 + 0.7\psi_b(t_f, t_i)\right)}$$

$$= \cfrac{1}{1 + \left(\cfrac{28{,}500\ ksi}{4{,}700\ ksi}\right)\left(\cfrac{5.81\ in^2}{934\ in^2}\right)\left(1 + \cfrac{(934\ in^2)(24.9\ in)^2}{(251{,}000\ in^4)}\right)\left(1 + 0.7(1.46)\right)}$$

$$= 0.798$$

B.4.2.2 Deck Coefficients

Material coefficients are also required for the deck concrete. The shrinkage strain of the deck concrete (ε_{ddf}) is required to calculate one of the contributions of long-term prestress loss. The calculation of this strain requires calculating some of the material coefficients for the deck concrete.

$$k_{sd} = 1.45 - 0.13(V/S) \geq 1.0$$

$$= 1.45 - 0.13(4.4) \geq 1.0$$

$$= 1.0$$

$$k_{fd} = \cfrac{5}{1 + f'_{cdi}}$$

$$= \cfrac{5}{1 + 3.2\ ksi}$$

$$= 1.19$$

$$k_{tdd}(t_f, t_{dc}) = \cfrac{(t_f - t_{dc})}{61 - 4f'_{cdi} + (t_f - t_{dc})}$$

$$= \cfrac{(36500\ days - 125\ days)}{61 - 4(3.8\ ksi) + (36500\ days - 125\ days)}$$

$$= 0.999$$

$$\varepsilon_{ddf} = k_{sd}k_{hs}k_{fd}k_{tdd}(t_f, t_{dc})0.48 * 10^{-3}$$

$$= (1.0)(1.16)(1.19)(0.999)0.48 * 10^{-3}$$

$$= 6.62 * 10^{-4}$$

For this creep coefficient, it is assumed that the shrinkage load begins five days after casting of the deck concrete. The specification states that the loading should be considered "shortly after deck placement" so it is assumed that the loading begins at the end of the moist curing period for the deck.

The variable for the creep coefficient of the deck concrete in Article 5.9.5.4.3d is likely mislabeled; it is shown in the specification as "$\psi_b(t_f, t_d)$" when it likely should be "$\psi_d(t_f, t_d)$". Also, the time at the start, labeled "t_d", may be better labeled "t_{id}," the age of the deck concrete when it experiences loading from the deck shrinkage, overlays, barriers and other dead loads. Both of these assumptions were taken into account in the calculation of the creep coefficient.

$$\psi_d(t_f, t_d) \quad = 1.9 k_{sd} k_{hc} k_{fd} k_{tdd}(t_f, t_{dc}) t_{id}^{-0.118}$$

$$= 1.9(1.0)(1.08)(1.19)(1.0)(5 \; day)^{-0.118}$$

$$= 2.02$$

B.4.3 Long-Term Loss (Prior to Deck Placement)

Now that all the material coefficients have been calculated, the long-term loss expressions will be addressed. The long-term prestress loss estimates in AASHTO LRFD 2012 are broken into shrinkage, creep and strand relaxation occurring before deck placement and after deck placement.

The prestress loss due to girder shrinkage prior to deck placement is calculated using the shrinkage strain from time of transfer to deck placement (ε_{bid}) and the before deck placement transformed section coefficient (K_{id}). Both of these variables were calculated above.

$$\Delta f_{pSR} \quad = \varepsilon_{bid} K_{id} E_p$$

$$= (3.65 * 10^{-4})(0.785)(28,500 \; ksi)$$

$$= 8.16 \; ksi$$

The prestress loss due to girder creep prior to deck placement is calculated using the concrete stress at the centroid of the prestressing strands (f_{cgp}) from the iterative elastic shortening loss procedure. The creep loss is also dependent on the before deck placement transformed section coefficient (K_{id}) and the creep coefficient from time of transfer to deck placement ($\psi_b(t_d, t_i)$).

$$\Delta f_{pCR} = \frac{E_p}{E_{ci}} f_{cgp} K_{id} \psi_b(t_d, t_i)$$

$$= \frac{(28{,}500\ ksi)}{(4{,}700\ ksi)} (3.33\ ksi)(0.785)(1.12)$$

$$= 17.8\ ksi$$

The prestress loss due to strand relaxation prior to deck placement is calculated using the strand stress immediately after transfer (f_{pt}), which was calculated during the iterative elastic shortening procedure. The type of prestressing strand used is accounted for by the factor K_L (30 for low-relaxation and 7 for stress relieved strands). In this example problem low-relaxation strands were chosen as they are much more commonly used in current fabrication practices.

$$\Delta f_{pR1} = \frac{f_{pt}}{K_L}\left(\frac{f_{pt}}{f_{py}} - 0.55\right)$$

$$= \frac{(182.3\ ksi)}{(30)}\left(\frac{(182.3\ ksi)}{(243\ ksi)} - 0.55\right)$$

$$= 1.2\ ksi$$

B.4.4 Long-Term Loss (After Deck Placement)

The after deck placement loss contains components accounting for loss due to girder shrinkage, girder creep, deck shrinkage and strand relaxation. Within these components there are a few ill-defined variables; these will be addressed as they are encountered.

The prestress loss due to the shrinkage of the girder concrete after deck placement is dependent on the shrinkage strain from time of deck placement to final time (ε_{bdf}). This shrinkage strain is not clearly defined in the specification, as previously mentioned, but the value used here is a reasonable interpretation of the specification. The shrinkage strain is also dependent on the after deck placement transformed section coefficient (K_{df}).

$$\Delta f_{pSD} = \varepsilon_{bdf} K_{df} E_p$$

$$= (1.12 * 10^{-4})(0.798)(28{,}500\ ksi)$$

$$= 2.5\ ksi$$

The prestress loss due to the creep of the girder concrete after deck placement is dependent on the concrete stress at the centroid of the prestressing strands (f_{cgp}), which is calculated with the elastic shortening loss. The creep loss also depends on the change in concrete stress at the centroid of the prestressing strands (Δf_{cd}). The change in stress to be considered is due to long-term losses prior to deck placement (P_Δ) and deck weight or other superimposed

dead load (M_{sd}). No expression is explicitly presented for the calculation of the change in stress, but this is a reasonable interpretation of the specification.

$$P_\Delta = -\left(\Delta f_{pSR} + \Delta f_{pCR} + \Delta f_{pR1}\right)A_{ps}$$

$$= -(8.2\ ksi + 17.8\ ksi + 1.2\ ksi)(5.81\ in^2)$$

$$= -158\ kips$$

$$\Delta f_{cd} = \frac{P_\Delta}{A_g} + \frac{P_\Delta e_p{}^2}{I_g} - \frac{M_{sd}e_p}{I_g}$$

$$= \frac{-158\ kips}{494.4\ in^2} + \frac{(-158\ kips)(12.25\ in)^2}{(82{,}600\ in^4)} - \frac{(8170k - in)(12.25\ in)}{(82{,}600\ in^4)}$$

$$= -1.56\ ksi$$

$$\Delta f_{pCD} = \frac{E_p}{E_{ci}} f_{cgp}\left[\psi_b(t_f, t_i) - \psi_b(t_d, t_i)\right]K_{df} + \frac{E_p}{E_c}\Delta f_{cd}\psi_b(t_f, t_d)K_{df}$$

$$= \frac{28{,}500\ ksi}{4{,}700\ ksi}(3.33\ ksi)(1.46 - 1.12)(0.798) + \frac{28{,}500\ ksi}{5{,}590\ ksi}(-1.56\ ksi)(0.832)(0.798)$$

$$= 0.28\ ksi$$

    The prestress gain due to the shrinkage of the deck concrete is dependent on the change in concrete stress at the centroid of the prestressing strands due to the differential shrinkage of the deck concrete compared to the girder concrete (Δf_{cdf}).

    As previously mentioned, there is slight confusion as to which creep coefficient to use in each equation and what times should be used for which material coefficients. Within the expressions the coefficients are clearly defined but the definition of the deck creep coefficient variable is likely mislabeled in the code. The assumptions made and values used for the deck creep coefficient can be found above in the material coefficient section. The assumption in the below calculations is the use of the deck creep coefficient ($\psi_d(t_f, t_d)$) when calculating the change in concrete stress (Δf_{cdf}) and the use of the beam creep coefficient ($\psi_b(t_f, t_d)$) in the loss expression (Δf_{pSS}).

$$\Delta f_{cdf} = \frac{\varepsilon_{ddf} A_d E_{cd}}{[1 + 0.7\psi_d(t_f, t_d)]} \left(\frac{1}{A_c} - \frac{e_{pc} e_d}{I_c}\right)$$

$$= \frac{(6.62 * 10^{-4})(640\ in^2)(3,830\ ksi)}{[1 + 0.7(2.02)]} \left(\frac{1}{934\ in^2} - \frac{(24.9\ in)(14.3\ in)}{(251,000\ in^4)}\right)$$

$$= -0.21\ ksi$$

$$\Delta f_{pss} = \frac{E_p}{E_c} \Delta f_{cdf} K_{df} [1 + 0.7\psi_b(t_f, t_d)]$$

$$= \left(\frac{28,500\ ksi}{5,590 ksi}\right)(-0.21\ ksi)(0.798)[1 + 0.7(0.83)]$$

$$= -1.3\ ksi$$

The prestress loss due to strand relaxation after deck placement is assumed to be equal to the loss prior to deck placement.

$$\Delta f_{pR2} = \Delta f_{pR1}$$

$$= 1.2\ ksi$$

B.4.5   Total Loss

The total prestress loss is the summation of the elastic shortening and long-term loss contributions.

$$\Delta f_{pT} = \Delta f_{pES} + \left(\Delta f_{pSR} + \Delta f_{pCR} + \Delta f_{pR1}\right)_{id} + \left(\Delta f_{pSD} + \Delta f_{pCD} + \Delta f_{pR2} - \Delta f_{pSS}\right)_{df}$$

$$= 20.2\ ksi + (8.2\ ksi + 17.8\ ksi + 1.2\ ksi)$$
$$+ (2.5\ ksi + 0.3\ ksi + 1.2\ ksi - 1.3\ ksi)$$

$$= 50.0\ ksi$$

B.5   RECOMMENDED LOSS PROCEDURE

The recommended loss provisions, proposed in Chapter 6, were broken into elastic shortening and long-term loss contributions, similar to AASHTO LRFD 2004.

B.5.1   Elastic Shortening Loss

The prestress loss due to the elastic shortening of the member is dependent on the concrete stress at the centroid of the prestressing strands (f_{cgp}). In the proposed procedure, this stress is calculated using an assumed stress in the strands immediately after transfer of 70 percent

ultimate. This assumed effective strand stress is typically slightly higher than the stress used in AASHTO LRFD 2012 which leads to higher elastic shortening estimates.

$$f_{cgp} = 0.7 f_{pu} A_{ps} \left(\frac{1}{A_g} + \frac{e_p{}^2}{I_g} \right) - \frac{M_g e_p}{I_g}$$

$$= 0.7(270 \ ksi)(5.81 \ in^2) \left(\frac{1}{494.9 \ in^2} + \frac{(12.25 \ in)^2}{82,600 \ in^4} \right) - \frac{(4,954 \ k - in)(12.25 \ in)}{(82,600 \ in^4)}$$

$$= 3.48 \ ksi$$

$$\Delta f_{pES} = \frac{E_p}{E_{ci}} f_{cgp}$$

$$= \frac{(28,500 \ ksi)}{(4,700 \ ksi)} (3.48 \ ksi)$$

$$= 21.1 \ ksi$$

B.5.2 Long-Term Loss

In the recommended loss provisions, the long-term prestress loss is broken into shrinkage, creep and strand relaxation. The prestress loss due to the girder shrinkage is dependent only on the average relative humidity and the concrete release strength.

$$\Delta f_{pSR} = E_p \left(\frac{140 - H}{4.8 + f'_{ci}} \right) 4.4 * 10^{-5}$$

$$= (28,500 \ ksi) \left(\frac{140 - 60}{4.8 + 6.0 \ ksi} \right) 4.4 * 10^{-5}$$

$$= 9.29 \ ksi$$

The concrete stress at the centroid of the prestressing strand found in the elastic shortening loss calculation is used when calculating girder creep losses. The prestress loss due to creep of the girder concrete is calculated similarly to creep loss in AASHTO LRFD 2004. The loss is dependent on the above calculated concrete stress due to the prestressing force and the self-weight of the girder and on the change in concrete stress caused by deck placement.

$$\Delta f_{cd} = -\frac{M_{sd} e_p}{I_g}$$

$$= -\frac{(6{,}400\ kip - in)(12.25\ in)}{(82{,}600\ in^4)}$$

$$= -0.949\ ksi$$

$$\Delta f_{pCR} = 0.1\left(\frac{195 - H}{4.8 + f'_{ci}}\right)\left(\frac{E_p}{E_{ci}}\right)\left(f_{cgp} + 0.6\Delta f_{cd}\right)$$

$$= 0.1\left(\frac{195 - 60}{4.8 + 6.0\ ksi}\right)\left(\frac{28{,}500\ ksi}{4{,}700\ ksi}\right)\left(3.48\ ksi + 0.6(-0.949\ ksi)\right)$$

$$= 22.1\ ksi$$

The prestress loss cause by strand relaxation is similar to AASHTO LRFD 2012 except the strand stress immediately prior to transfer, rather than after transfer, is used in the proposed expression.

$$\Delta f_{pR} = \frac{2(0.7 f_{pu})}{K_L}\left(\frac{(0.7 f_{pu})}{f_{py}} - 0.55\right)$$

$$= \frac{2(0.7)(270\ ksi)}{30}\left(\frac{(0.7)(270\ ksi)}{243\ ksi} - 0.55\right)$$

$$= 2.87\ ksi$$

B.5.3 Total Loss

$$\Delta f_{pT} = \Delta f_{pES} + \Delta f_{pSR} + \Delta f_{pCR} + \Delta f_{pR}$$

$$= 21.1\ ksi + 9.29\ ksi + 22.1\ ksi + 2.87\ ksi$$

$$= 55.4\ ksi$$

B.6 SUMMARY OF RESULTS

The example problem was completed with a material correction factor (K_1) of 1.0. The prestress loss values calculated during the above example problem are summarized in Table B.6. The first observation to be made is the creep loss has the largest contribution to the total prestress loss, with the elastic shortening making having the second largest. Both of these contributions are dependent on the concrete stress at the centroid of the prestressing strands (f_{cgp}) and the

modulus of elasticity of the concrete (E_{ci}). This would suggest that it is important to properly estimate concrete stress and concrete properties.

The second observation is the elastic shortening, shrinkage, and strand relaxation losses are estimated relatively close between the three provisions. The estimation of creep loss of AASHTO LRFD 2004 is much higher than of the other two provisions. This suggests that the empirical expression of AASHTO LRFD 2004 is excessively conservative compared to the more theoretical methods in the other two procedures.

The final observation is the other loss (deck shrinkage gain) of AASHTO LRFD 2012 is much smaller in magnitude than all of the other loss contributions. This would support the elimination of this contribution in the recommended provisions.

Table B.6 – Summary of calculated prestress loss ($K_1 = 1.0$)

	AASHTO LRFD 2004	AASHTO LRFD 2012	0-6374 Proposed
Elastic Shortening (Δf_{pES})	21.1	20.2	21.1
Shrinkage Loss (Δf_{pSR})	8.0	10.7	9.3
Creep Loss (Δf_{pCR})	35.1	18.1	22.1
Relaxation Loss (Δf_{pR})	0.9	2.4	2.9
Other Loss	0.0	-1.3	0.0
Total Loss (Δf_{pT})	**65.1**	**50.1**	**55.4**

The implications of the material correction factor on this example problem will be investigated using K_1 factors of 0.85 and 1.2, shown in Table B.7 and Table B.8, respectively. These correction factors represent extreme values for the two most commonly used coarse aggregates in Texas (crushed limestone and river gravel), as discussed in Chapter 4.

Table B.7 – Summary of calculated prestress loss ($K_1 = 0.85$)

	AASHTO LRFD 2004	AASHTO LRFD 2012	0-6374 Proposed
Elastic Shortening (Δf_{pES})	21.1	23.3	24.9
Shrinkage Loss (Δf_{pSR})	8.0	10.3	9.3
Creep Loss (Δf_{pCR})	35.1	19.8	26.0
Relaxation Loss (Δf_{pR})	0.9	2.2	2.9
Other Loss	0.0	-1.3	0.0
Total Loss (Δf_{pT})	**65.1**	**54.4**	**63.0**

From comparison of the three summary tables (B.6 through B.8), or comparison of the loss procedure, it can be observed that the K_1 correction factor only impacts the elastic shortening and creep loss components for the provisions of AASHTO LRFD 2012 and the recommendations of this report. Because the correction factor in the proposed loss expressions has a linear relationship with the modulus of elasticity, which has a linear effect on both the elastic shortening and creep loss, a correction factor of 0.85 will increase the elastic shortening and creep loss by 17 percent (1/0.85). This change in elastic shortening and creep loss leads to a 12 percent increase in total prestress loss for the limestone aggregate and a 12 percent decrease in total prestress loss for the river gravel aggregate.

Due to the iterative process in the AASHTO LRFD 2012 procedure, the correction factor does not have a perfectly linear relationship but does have a similar trend. The change in elastic shortening and creep loss leads to a 12 percent increase in the total prestress loss for limestone aggregate and a 9 percent decrease for river gravel aggregate.

Table B.8 – Summary of calculated prestress loss ($K_1 = 1.2$)

	AASHTO LRFD 2004	AASHTO LRFD 2012	0-6374 Proposed
Elastic Shortening (Δf_{pES})	21.1	17.2	17.6
Shrinkage Loss (Δf_{pSR})	8.0	11.1	9.3
Creep Loss (Δf_{pCR})	35.1	16.1	18.4
Relaxation Loss (Δf_{pR})	0.9	2.6	2.9
Other Loss	0.0	-1.4	0.0
Total Loss (Δf_{pT})	**65.1**	**45.7**	**48.2**

The importance of the concrete stiffness is shown by the impact of the K_1 factor on the prestress loss estimates. A stiff aggregate, such as river gravel, can greatly improve the overall behavior of the girder by restricting elastic shortening and creep. It should be noted that the current provisions (AASHTO LRFD 2012) do not require a K_1 factor of less than 1.0 to be used for the estimation of the modulus. Because of this current language, the use of a soft coarse aggregate ($K_1 < 1.0$) would result in even less conservative loss estimates.

APPENDIX C
Additional Database Information

C.1 OVERVIEW

The bibliographies for all of the references contained in the collection database are first presented. Following the list of references is the evaluation database. A select number of important variables were chosen to be reported for all of the specimens contained in the evaluation database.

After this presentation of the content of the database, an in depth analysis of the evaluation database is offered. Within this analysis, the elastic shortening and creep expressions used in AASHTO LRFD 2004 and 2012 and also as recommended are examined using the database. The loss expressions found in AASHTO LRFD 2004 and 2012 and the recommended loss procedure are then investigated using subdivisions of the database (e.g. specimens with decks versus without decks, losses measured using VWG only, etc.). The value of the database and applicability of the recommended loss procedure are shown through these investigations.

At the end of this appendix, the performance of the "Direct Method," suggested by Swartz (2010) and discussed in Chapter 2, will be investigated.

C.2 COLLECTION DATABASE REFERENCES

Barr, P., Eberhard, M., Stanton, J., Khaleghi, B., & Hsieh, J. C. (2000). *High Performance Concrete in Washington State SR18/SR516 Overcrossing: Final Report on Girder Monitoring.* Seattle: Washington Stat Transportation Center.

Birrcher, D. B. (2006). *Effects of Increasing the Allowable Compressive Stress at Release of Prestressed Concrete Girders.* Austin: The University of Texas at Austin.

Brewe, J. E., & Myers, J. J. (2009). Shear Behavior of Reduced Modulus Prestressed High-Strength Self-Consolidating Concrete (HS-SCC) Members Subjected to Elevated Concrete Fiber Stresses. *PCI/NBC*, 1-17.

Brewe, J. E., & Myers, J. J. (2011). High-strength self-consolidating concrete girders subjected to elevated compressive fiber stresses, part 2: Structural behavior. *PCI Journal*, 92-109.

Canfield, S. R. (2005). *Full Scale Testing of Prestressed, High Performance Concrete, Composite Bridge Girders.* Atlanta: Georgia Institute of Technology.

Erkman, B., Shield, C. K., & French, C. E. (2007). Time-Dependent Behavior of Full-Scale Self-Consolidating Conrete Precast Prestressed Girders. *ACI SP-247-12*, 139-153.

Gamble, W. L. (1970). *Field Investigation of a Continuous Composite Prestressed I-Beam Highway Bridge Located in Jefferson County, Illinois.* Urbana: University of Illinois.

Gamble, W. L. (1979). *Long-Term Behavior of a Prestressed I-Girder Highway Bridge in Champaign County, Illinois.* Urbana-Champaign: University of Illinois.

Gross, S. P., & Burns, N. H. (2000). *Field Performance of Prestressed High Performance Concrete Highway Bridges in Texas.* Austin: Texas Department of Transportation.

Gross, S. P., Yost, J. R., & Gaynor, E. (2007). Experimental Study of Prestress Land and Camber in High-Strength SCC Beams. *ACI SP-247-7*, 77-91.

Hale, W. M., & Russell, B. W. (2006). Effect of Allowable Compressive Stress at Release on Prestress Losses and on the Performance of Precast, Prestressed Concrete Bridge Girders. *PCI Journal*, 14-25.

Hodges, H. T. (2006). *Top Strand Effect and Evaluation of Effective Prestress in Prestressed Concrete Beams.* Blacksburg: Virginia Polytechnic Institute and State University.

Houdeshell, D. M., Anderson, T. C., & Gamble, W. L. (1972). *Field Investigation of a Prestressed Concrete Highway Bridge Located in Douglas County, Illinois.* Urbana: University of Illinois.

Idriss, R. L., & Solano, A. (2002). Effects of Steam Curing Temperature on Early Prestress Losses in High-Performance Concrete Beams. *Transportation Research Record*, 218-228.

Labia, Y., Saiidi, M. S., & Douglas, B. (1997). Full-Scale Testing and Analysis of 20-Year-Old Pretensioned Concrete Box Girders. *ACI Structural Journal*, 471-492.

Larson, K. H. (2006). *Evaluating the Time-Dependent Deformations and Bond Characteristics of a Self-Consolidating Concrete Mix and the Implication for Pretensioned Bridge Applications.* Manhattan, Kansas: Kansas State University.

Naito, C., Sause, R., & Thompson, B. (2008). Investigation of Damaged 12-Year Old Prestressed Concrete Box Beams. *Journal of Bridge Engineering*, 139-148.

Nassar, A. J. (2002). *Investigation of Transfer Length, Development Length, Flexural Strength and Prestress Loss Trend in Fully Bonded High Strength Lightweight Prestressed Girders.* Blacksburg: Virginia Polytechnic Institute and State University.

Ozyildirim, C. (2008). *Bulb-T Beams with Self Consolidating Concrete on the Route 33 Bridge Over the Pamunkey River in Virgina.* Charlottesville: Virginia Transportation Research Counsil.

Pessiki, S., Kaczinski, M., & Wescott, H. H. (1996). Evaluation of Effective Prestress Force in 28-Year-Old Prestressed Concrete Bridge Beams. *PCI Journal*, 78-89.

Roller, J. J., Russell, H. G., Bruce, R. N., & Alaywan, W. R. (Winter 2011). Evaluation of prestress losses in high-strength concrete bulb-tee girders for the Rigolets Pass Bridge. *PCI Journal*, 110 - 134.

Roller, J. J., Russell, H. G., Bruce, R. N., & Martin, B. T. (1995). Long-Term Performance of Prestressed, Pretensioned High Strength Concrete Bridge Girders. *PCI Journal*, 48-59.

Ruiz, E. D., Staton, B. W., Do, N. H., & Hale, W. M. (2007). Prestress Losses in Beams Cast with Self-Consolidating Concrete. *ACI SP-247-8*, 93-104.

Schnittker, B. A. (2008). *Allowable Compressive Stress at Prestress Transfer.* Austin: The University of Texas at Austin.

Shenoy, C. V., & Frantz, G. C. (1991). Structural Tests of 27-Year-Old Prestressed Bridge Beams. *PCI Journal*, 80-90.

Smith, M., Shield, C., Eriksson, W., & French, C. (2007). Field and Laboratory Study of the Mn/DOT Precast Slab Span System. *Mid-Continent Transportation Research Symposium*, 1-13.

Tadros, M. K., Al-Omaishi, N., Seguirant, S. J., & Gallt, J. G. (2003). *Prestress Losses in High-Strength Concrete Bridge Girders.* Washington, D.C.: National Cooperative Highway Research Program.

Yang, Y., & Myers, J. J. (2005). Prestress Loss Measurements in Missouri's First Fully Instrumented High-Performance Concrete Bridge. *Transportation Research Record: Journal of the Transportation Research Board*, 118-125.

C.3 EVALUATION DATABASE

The following details are presented in Table C.1 for the specimens in the Evaluation Database:

h = beam height (in.)

A_g = area of gross section (in.^{2})

I_g = moment of inertia of gross section (in.^{4})

f'_{ci} = compressive strength of concrete at release (ksi)

f'_c = compressive strength of concrete at 28 days (ksi)

A_{ps} = total prestressing strand area (in.^{2})

y_p = distance from extreme compression fiber to centroid of prestressing strands (in.)

E_p = modulus of prestressing tendons (ksi)

f_{pi} = stress in prestressing steel immediately prior to transfer (ksi)

RH = average relative humidity (%)

t_f = age of concrete at time of final loss measurement (days)

Δf_{pT} = total measured prestress loss (ksi)

Table C.1 – Evaluation Database (1 of 9)

Beam ID	Section Type	h (in.)	A_g (in.^{2})	I_g (in.^{4})	f'$_{ci}$ (ksi)	f'$_c$ (ksi)	A_{ps} (in.^{2})	y_p (in.)	E_p (ksi)	f_{pi} (ksi)	Deck?	RH (%)	t_f (days)	Δf_{pT} (ksi)
Current Study (2012)														
I-1	Type C	40.0	494.4	82602	7.0	10.8	5.8	6.63	28800	202.9	No	49	979	46
I-2	Type C	40.0	494.4	82602	7.0	10.8	5.8	6.63	28800	202.9	No	65	939	49
I-3	Type C	40.0	494.4	82602	7.0	10.8	5.8	6.63	28800	202.9	No	65	948	46
I-4	Type C	40.0	494.4	82602	7.0	10.8	5.8	6.63	28800	202.9	No	65	962	41
I-5	Type C	40.0	494.4	82602	7.0	10.8	5.8	6.63	28800	202.9	No	49	976	51
I-6	Type C	40.0	494.4	82602	7.0	10.8	5.8	6.63	28800	202.9	No	49	975	56
I-7	Type C	40.0	494.4	82602	7.0	10.8	5.8	6.63	28800	202.9	No	65	946	49
I-8	Type C	40.0	494.4	82602	7.0	10.8	5.8	6.63	28800	202.9	No	65	966	50
II-1	Type C	40.0	494.4	82602	6.6	11.6	5.8	6.63	29400	203.0	No	49	954	32
II-2	Type C	40.0	494.4	82602	6.6	11.6	5.8	6.63	29400	203.0	No	65	922	39
II-3	Type C	40.0	494.4	82602	6.6	11.6	5.8	6.63	29400	203.0	No	65	932	34
II-4	Type C	40.0	494.4	82602	6.6	11.6	5.8	6.63	29400	203.0	No	65	936	32
II-5	Type C	40.0	494.4	82602	6.6	11.6	5.8	6.63	29400	203.0	No	49	953	24
II-6	Type C	40.0	494.4	82602	6.6	11.6	5.8	6.63	29400	203.0	No	49	951	36
II-7	Type C	40.0	494.4	82602	6.6	11.6	5.8	6.63	29400	203.0	No	65	937	24
II-8	Type C	40.0	494.4	82602	6.6	11.6	5.8	6.63	29400	203.0	No	65	923	33
III-1	Tx46	46.0	761.0	198089	6.6	9.6	8.9	6.43	28800	209.0	No	45	693	58
III-2	Tx46	46.0	761.0	198089	6.6	9.6	8.9	6.43	28800	209.0	No	65	988	54

Table C.1 – Evaluation Database (2 of 9)

Beam ID	Section Type	h (in.)	A_g (in.^{2})	I_g (in.^{4})	f'_{ci} (ksi)	f'_c (ksi)	A_{ps} (in.^{2})	y_p (in.)	E_p (ksi)	f_{pi} (ksi)	Deck?	RH (%)	t_f (days)	Δf_{pT} (ksi)
Current Study (2012), continued														
III-3	Tx46	46.0	761.0	198089	6.6	9.6	8.9	6.43	28800	209.0	No	65	676	54
III-4	Tx46	46.0	761.0	198089	6.6	9.6	8.9	6.43	28800	209.0	No	65	674	54
III-5	Tx46	46.0	761.0	198089	6.6	9.6	8.9	6.43	28800	209.0	No	45	699	58
III-6	Tx46	46.0	761.0	198089	6.6	9.6	8.9	6.43	28800	209.0	No	65	686	56
III-7	Tx46	46.0	761.0	198089	6.6	9.6	8.9	6.43	28800	209.0	No	65	680	53
III-8	Tx46	46.0	761.0	198089	6.6	9.6	8.9	6.43	28800	209.0	No	45	699	54
IV-SCC-1	Tx46	46.0	761.0	198089	6.3	11.5	8.6	6.64	28800	202.5	No	65	130	43
IV-SCC-2	Tx46	46.0	761.0	198089	6.3	11.5	8.6	6.64	28800	202.5	No	65	258	42
IV-SCC-3	Tx46	46.0	761.0	198089	6.3	11.5	8.6	6.64	28800	202.5	No	65	220	43
IV-CC-1	Tx46	46.0	761.0	198089	6.9	11.6	8.6	6.64	28800	202.5	No	65	203	39
IV-CC-2	Tx46	46.0	761.0	198089	6.9	11.6	8.6	6.64	28800	202.5	No	65	256	38
IV-CC-3	Tx46	46.0	761.0	198089	6.9	11.6	8.6	6.64	28800	202.5	No	65	250	40
Barr, Eberhard, Stanton, Khalegh and Hsieh (2000)														
1A	Bulb-T	73.5	752.2	546571	7.8	10.0	3.0	3.00	28500	202.5	Yes	80	1095	29
1C	Bulb-T	73.5	752.2	546571	7.8	10.0	3.0	3.00	28500	202.5	Yes	80	1095	31
2A	Bulb-T	73.5	752.2	546571	8.0	11.4	8.7	3.37	28500	202.5	Yes	80	1095	58
2B	Bulb-T	73.5	752.2	546571	7.6	11.4	8.7	3.37	28500	202.5	Yes	80	1095	49
2C	Bulb-T	73.5	752.2	546571	7.6	11.4	8.7	3.37	28500	202.5	Yes	80	1095	61

Table C.1 – Evaluation Database (3 of 9)

Beam ID	Section Type	h (in.)	A_g (in.^{2})	I_g (in.^{4})	f'_{ci} (ksi)	f'_c (ksi)	A_{ps} (in.^{2})	y_p (in.)	E_p (ksi)	f_{pi} (ksi)	Deck?	RH (%)	t_f (days)	Δf_{pT} (ksi)
Birrcher (2006)														
A55-T25	I-Beam	28.0	275.4	22658	5.5	8.3	2.1	4.00	28500	202.5	No	70	28	34
A60-T26	I-Beam	28.0	275.4	22658	5.0	7.8	2.1	4.00	28500	202.5	No	70	29	31
A63-T27	I-Beam	28.0	275.4	22658	4.8	8.5	2.1	4.00	28500	202.5	No	70	28	32
A66-T28	I-Beam	28.0	275.4	22658	4.6	9.6	2.1	4.00	28500	202.5	No	70	28	33
A67-T29	I-Beam	28.0	275.4	22658	4.5	7.1	2.1	4.00	28500	202.5	No	70	28	38
A66-T30	I-Beam	28.0	275.4	22658	4.5	8.1	2.1	4.00	28500	202.5	No	70	28	43
A69-T31	I-Beam	28.0	275.4	22658	4.3	7.7	2.1	4.00	28500	202.5	No	70	28	39
A68-T32	I-Beam	28.0	275.4	22658	4.4	7.8	2.1	4.00	28500	202.5	No	70	28	46
A67-T33	I-Beam	28.0	275.4	22658	4.5	8.4	2.1	4.00	28500	202.5	No	70	29	32
Canfield (2005)														
BT-56	Bulb-T	56.3	717.5	312529	10.4	14.3	9.5	9.05	29682	205.4	Yes	70	182	40
TYPE IV	I-Beam	54.6	795.1	271606	11.7	14.6	11.3	7.37	29682	205.4	Yes	70	161	35
Erkman, Shield, French (2007)														
A-SCC1	Bulb-T	36.0	570.0	93528	8.2	8.7	6.1	6.90	28600	202.5	No	70	325	40
A-CM	Bulb-T	36.0	570.0	93528	11.1	11.6	6.1	6.90	28600	202.5	No	70	325	31
B-SCC1	Bulb-T	36.0	570.0	93528	7.8	10.9	6.1	6.90	29000	202.5	No	70	80	33
B-SCC2	Bulb-T	36.0	570.0	93528	7.7	11.0	6.1	6.90	29000	202.5	No	70	82	35
B-CM	Bulb-T	36.0	570.0	93528	9.4	13.7	6.1	6.90	29000	202.5	No	70	82	31

Table C.1 – Evaluation Database (4 of 9)

Beam ID	Section Type	h (in.)	A_g (in.^{2})	I_g (in.^{4})	f'_{ci} (ksi)	f'_c (ksi)	A_{ps} (in.^{2})	y_p (in.)	E_p (ksi)	f_{pi} (ksi)	Deck?	RH (%)	t_f (days)	Δf_{pT} (ksi)
Gamble (1970)														
BX-1	I-Beam	48.0	524.0	147800	4.2	5.5	4.3	3.74	27000	170.0	Yes	70	1220	28
Gamble (1979)														
BX-5	I-Beam	42.0	464.5	90956	5.6	6.6	2.6	9.0	27750	158.1	Yes	70	367	19
BX-6	I-Beam	42.0	464.5	90956	5.6	6.6	2.6	9.0	27750	158.1	Yes	70	367	19
Gross and Burns (2000)														
N32	U-Beam	54.0	1025	380420	10.5	13.6	13.9	3.82	28500	202.5	Yes	75	761	43
S15	U-Beam	54.0	1025	380420	11.0	14.3	13.9	3.82	28500	202.5	Yes	75	748	38
S16	U-Beam	54.0	1121	404230	8.7	13.3	14.8	4.46	28500	202.5	Yes	75	1262	40
S25	U-Beam	54.0	1121	404230	10.3	13.4	14.8	4.46	28500	202.5	Yes	75	1221	34
E13	I-Beam	54.0	789.0	260400	10.8	13.7	18.2	11.1	28500	202.5	Yes	57	422	51
E14	I-Beam	54.0	789.0	260400	10.8	13.7	18.2	11.1	28500	202.5	Yes	57	422	28
E24	I-Beam	54.0	789.0	260400	13.1	14.2	14.3	7.0	28500	202.5	Yes	57	404	51
E25	I-Beam	54.0	789.0	260400	9.8	14.8	14.3	7.0	28500	202.5	Yes	57	746	52
E34	I-Beam	54.0	789.0	260400	12.4	13.8	18.2	11.1	28500	202.5	Yes	57	316	57
E35	I-Beam	54.0	789.0	260400	11.3	14.5	18.2	11.1	28500	202.5	Yes	57	309	58
E44	I-Beam	54.0	789.0	260400	9.4	14.6	17.4	10.0	28500	202.5	Yes	57	305	56
W14	I-Beam	54.0	789.0	260400	8.6	10.1	8.0	5.62	28500	202.5	Yes	57	771	35
W15	I-Beam	54.0	789.0	260400	8.6	10.1	8.0	5.62	28500	202.5	Yes	57	771	34

Table C.1 – Evaluation Database (5 of 9)

Beam ID	Section Type	h (in.)	A_g (in.^{2})	I_g (in.^{4})	f'_{ci} (ksi)	f'_c (ksi)	A_{ps} (in.^{2})	y_p (in.)	E_p (ksi)	f_{pi} (ksi)	Deck?	RH (%)	t_f (days)	Δf_{pT} (ksi)
Gross and Burns (2000), continued														
W16	I-Beam	54.0	789.0	260400	8.6	10.1	8.0	5.62	28500	202.5	Yes	57	771	33
W17	I-Beam	54.0	789.0	260400	8.1	10.3	8.0	5.62	28500	202.5	Yes	57	766	30
Hale and Russell (2006)														
Girder 1	Bulb-T	24.0	163.3	12400	8.7	11.1	2.2	6.45	28500	204.3	No	60	360	53
Girder 3	Bulb-T	24.0	163.3	12400	6.1	8.4	1.7	7.06	28500	200.8	No	60	360	58
Girder 4	Bulb-T	24.0	163.3	12400	8.7	11.1	1.7	5.81	28500	204.5	No	60	360	52
Houdeshell, Anderson, Gamble (1972)														
BX-3	I-Beam	48.0	569.8	144117	4.9	5.1	4.1	5.95	27700	169.3	Yes	70	784	32
BX-4	I-Beam	48.0	569.8	144117	4.9	5.1	4.1	5.95	27700	169.3	Yes	70	784	29
Idriss and Solano (2008)														
AC	Bulb-T	63.0	713.0	392638	8.0	9.1	6.4	6.00	27000	215.7	Yes	50	374	34
AW	Bulb-T	63.0	713.0	392638	8.0	9.1	6.4	6.00	27000	215.7	Yes	50	374	29
BC	Bulb-T	63.0	713.0	392638	8.0	9.1	6.4	6.00	27000	215.7	Yes	50	374	29
BW	Bulb-T	63.0	713.0	392638	8.0	9.1	6.4	6.00	27000	215.7	Yes	50	374	30
Larson (2006)														
A3	I-Beam	45.0	525.0	127490	5.6	5.9	2.4	7.75	28500	202.5	Yes	65	330	20
B3	I-Beam	45.0	525.0	127490	5.6	5.9	2.4	7.75	28500	202.5	Yes	65	330	18
B1	I-Beam	45.0	525.0	127490	5.6	5.9	2.4	7.75	28500	202.5	Yes	65	330	15

Table C.1 – Evaluation Database (6 of 9)

Beam ID	Section Type	h (in.)	A_g (in.^{2})	I_g (in.^{4})	f'_{ci} (ksi)	f'_c (ksi)	A_{ps} (in.^{2})	y_p (in.)	E_p (ksi)	f_{pi} (ksi)	Deck?	RH (%)	t_f (days)	Δf_{pT} (ksi)
Larson (2006), continued														
C3	I-Beam	45.0	525.0	127490	5.6	5.9	2.4	7.75	28500	202.5	Yes	65	330	18
E3	I-Beam	45.0	525.0	127490	5.0	5.6	2.4	7.75	28500	202.5	Yes	65	330	23
D3	I-Beam	45.0	525.0	127490	5.0	5.6	2.4	7.75	28500	202.5	Yes	65	330	23
E3	I-Beam	45.0	525.0	127490	5.0	5.6	2.4	7.75	28500	202.5	Yes	65	330	26
Nassar (2002)														
LW-4	I-Beam	54.0	789.0	260730	4.8	6.4	6.1	7.20	28500	205.0	No	70	266	46
Pessiki, Kacqinski, Wescott (1996)														
3-J	I-Beam	60.0	848.0	355800	5.1	8.8	5.4	5.60	28500	200.9	No	70	10227	39
4-J	I-Beam	60.0	848.0	355800	5.1	8.2	5.4	5.60	28500	200.9	No	70	10227	34
Roller, Russell, Bruce, Martin (1995)														
Girder 3	Bulb-T	54.0	659.0	268077	8.9	9.9	4.6	3.60	30000	202.5	Yes	75	529	23
Roller, Russell, Bruce, Alaywan (2011)														
43 A	Bulb-T	78.0	1105	935586	9.3	10.9	12.2	7.46	27950	202.5	Yes	75	800	23
43 B	Bulb-T	78.0	1105	935586	9.3	10.9	12.2	7.46	27950	202.5	Yes	75	800	23
43 C	Bulb-T	78.0	1105	935586	9.3	10.9	12.2	7.46	27950	202.5	Yes	75	800	23
43 D	Bulb-T	78.0	1105	935586	9.3	10.9	12.2	7.46	27950	202.5	Yes	75	800	24
Schnittker (2008)														
CA-60-1	I-Beam	40.0	494.9	82602	4.5	10.5	4.0	5.23	29000	202.5	No	70	57	35

Table C.1 – Evaluation Database (7 of 9)

Beam ID	Section Type	h (in.)	A_g (in.^{2})	I_g (in.^{4})	f'$_{ci}$ (ksi)	f'$_c$ (ksi)	A_{ps} (in.^{2})	y_p (in.)	E_p (ksi)	f_{pi} (ksi)	Deck?	RH (%)	t_f (days)	Δf_{pT} (ksi)
Schnittker (2008), continued														
CA-60-2	I-Beam	40.0	494.9	82602	4.5	10.7	4.0	5.23	29000	202.5	No	70	62	33
CA-60-3	I-Beam	40.0	494.9	82602	4.5	11.1	4.0	5.23	29000	202.5	No	70	70	36
CA-65-1	I-Beam	40.0	494.9	82602	4.4	10.2	4.0	5.23	29000	202.5	No	70	70	36
CA-65-2	I-Beam	40.0	494.9	82602	4.4	11.2	4.0	5.23	29000	202.5	No	70	87	42
CA-65-3	I-Beam	40.0	494.9	82602	4.3	11.4	4.0	5.23	29000	202.5	No	70	49	33
CA-65-4	I-Beam	40.0	494.9	82602	4.3	11.5	4.0	5.23	29000	202.5	No	70	93	38
CA-65-5	I-Beam	40.0	494.9	82602	4.3	11.8	4.0	5.23	29000	202.5	No	70	98	37
CA-65-6	I-Beam	40.0	494.9	82602	4.3	11.9	4.0	5.23	29000	202.5	No	70	100	40
CD-70-1	I-Beam	40.0	494.9	82602	5.6	11.0	5.5	6.00	29000	202.5	No	70	29	42
CD-70-2	I-Beam	40.0	494.9	82602	5.5	11.6	5.5	6.00	29000	202.5	No	70	34	41
CD-65-1	I-Beam	40.0	494.9	82602	5.7	9.6	5.5	6.00	29000	202.5	No	70	38	39
CD-65-2	I-Beam	40.0	494.9	82602	5.7	9.6	5.5	6.00	29000	202.5	No	70	42	49
CD-65-3	I-Beam	40.0	494.9	82602	5.7	9.6	5.5	6.00	29000	202.5	No	70	45	47
CD-65-4	I-Beam	40.0	494.9	82602	5.9	10.7	5.5	6.00	29000	202.5	No	70	41	49
CD-65-5	I-Beam	40.0	494.9	82602	5.9	11.2	5.5	6.00	29000	202.5	No	70	46	35
CD-65-6	I-Beam	40.0	494.9	82602	5.9	11.4	5.5	6.00	29000	202.5	No	70	48	41
CD-60-1	I-Beam	40.0	494.9	82602	6.3	11.7	5.5	6.00	29000	202.5	No	70	54	41
CD-60-2	I-Beam	40.0	494.9	82602	6.3	12.0	5.5	6.00	29000	202.5	No	70	61	38

Table C.1 – Evaluation Database (8 of 9)

Beam ID	Section Type	h (in.)	A_g (in.^{2})	I_g (in.^{4})	f'_{ci} (ksi)	f'_c (ksi)	A_{ps} (in.^{2})	y_p (in.)	E_p (ksi)	f_{pi} (ksi)	Deck?	RH (%)	t_f (days)	Δf_{pT} (ksi)
Schnittker (2008), continued														
CD-60-3	I-Beam	40.0	494.9	82602	6.3	12.4	5.5	6.00	29000	202.5	No	70	69	43
CC-65-1	I-Beam	40.0	494.9	82602	6.0	11.1	5.5	6.00	29000	202.5	No	70	64	49
CC-65-2	I-Beam	40.0	494.9	82602	6.0	11.2	5.5	6.00	29000	202.5	No	70	68	43
CC-65-3	I-Beam	40.0	494.9	82602	6.1	11.2	5.5	6.00	29000	202.5	No	70	69	51
CC-65-4	I-Beam	40.0	494.9	82602	6.1	11.5	5.5	6.00	29000	202.5	No	70	76	52
CC-65-5	I-Beam	40.0	494.9	82602	6.4	11.5	5.5	6.00	29000	202.5	No	70	77	44
CC-65-6	I-Beam	40.0	494.9	82602	6.3	11.5	5.5	6.00	29000	202.5	No	70	78	42
CC-60-1	I-Beam	40.0	494.9	82602	6.4	10.8	5.5	6.00	29000	202.5	No	70	72	56
CC-60-2	I-Beam	40.0	494.9	82602	6.4	10.8	5.5	6.00	29000	202.5	No	70	77	56
CC-60-3	I-Beam	40.0	494.9	82602	6.4	10.8	5.5	6.00	29000	202.5	No	70	78	47
BB-01	Box-Beam	28.0	678.8	68745	4.1	11.3	4.6	3.17	29000	202.5	No	70	28	46
BB-02	Box-Beam	28.0	678.8	68745	4.1	11.3	4.6	3.17	29000	202.5	No	70	28	43
BB-06	Box-Beam	28.0	678.8	68745	4.1	9.5	4.6	3.17	29000	202.5	No	70	38	57
BB-07	Box-Beam	28.0	678.8	68745	4.1	9.6	4.6	3.17	29000	202.5	No	70	43	65
BB-08	Box-Beam	28.0	678.8	68745	4.0	8.7	4.6	3.17	29000	202.5	No	70	29	57
BB-09	Box-Beam	28.0	678.8	68745	4.0	8.9	4.6	3.17	29000	202.5	No	70	30	56
BB-10	Box-Beam	28.0	678.8	68745	4.0	9.7	4.6	3.17	29000	202.5	No	70	35	57

Table C.1 – Evaluation Database (9 of 9)

Beam ID	Section Type	h (in.)	A_g (in.^{2})	I_g (in.^{4})	f'_{ci} (ksi)	f'_c (ksi)	A_{ps} (in.^{2})	y_p (in.)	E_p (ksi)	f_{pi} (ksi)	Deck?	RH (%)	t_f (days)	Δf_{pT} (ksi)
Tadros, Al-Omaishi, Seguirant, Gallt (2003)														
IW2-1	Bulb-T	78.7	903.8	790592	6.3	9.0	8.6	4.50	28800	202.5	Yes	65	470	30
IW2-2	Bulb-T	78.7	903.8	790592	6.3	9.0	8.6	4.50	28800	202.5	Yes	65	469	34
G3	Bulb-T	55.1	857.2	351968	5.8	10.1	8.7	5.56	28800	202.8	Yes	70	490	42
G4	Bulb-T	55.1	857.2	351968	5.8	10.1	8.7	5.56	28800	202.8	Yes	70	490	41
G7	U-Beam	54.0	1121	404230	7.2	10.7	13.9	3.47	28800	202.3	Yes	70	400	24
G18	Bulb-T	82.6	972.0	956329	7.5	10.3	13.0	5.00	28800	202.5	Yes	80	380	40
G18	Bulb-T	82.6	972.0	956329	7.5	10.3	13.0	5.00	28800	202.5	Yes	80	380	38
Yang and Myers (2005)														
B13	I-Beam	32.0	311.0	33255	10.5	11.7	3.9	4.22	28000	202.5	Yes	70	275	38
B14	I-Beam	32.0	311.0	33255	10.5	11.7	3.9	4.22	28000	202.5	Yes	70	275	39
B14	I-Beam	32.0	311.0	33255	9.8	12.8	4.3	4.00	28000	202.5	Yes	70	275	39
B14	I-Beam	32.0	311.0	33255	9.8	12.8	4.3	4.00	28000	202.5	Yes	70	275	38

C.4 EXTENDED ANALYSIS

An in depth analysis of the evaluation database will be presented in this section. The information provided is intended to supplement the basic database analysis found in the body of this report. Elastic shortening will be investigated first, followed by refined database analysis and finally a section looking briefly at the creep expressions found in AASHTO LRFD 2004 and 2012. At the end of this appendix, the performance of the "Direct Method," suggested by Swartz (2010) and discussed in Chapter 2, will be investigated.

C.4.1 Elastic Shortening

C.4.1.1 Overview of Procedures

The elastic shortening component of prestressed loss is the most important of the components: it is typically the largest of the loss components; it is the component that is best understood theoretically; and it greatly influences the creep loss component. Because of its high level of importance, a more thorough investigation of elastic shortening estimations was desired.

First, a brief overview of the elastic shortening procedures provided in the 2004 and 2012 AASHTO LRFD Bridge Design Specifications and proposed in this report is provided. A full discussion of these procedures can be found in Chapter 2 and Chapter 6. Following the overview, the performance of each elastic shortening estimation procedure with respect to the evaluation database is provided.

C.4.1.1.1 AASHTO 2004

$$\Delta f_{pES} = \frac{E_p}{E_{ci}} f_{cgp} \qquad\qquad \text{(C.1)}$$

AASHTO 04 (5.9.5.2.3a-1)

Where:
- E_p = modulus of prestressing tendons (ksi)
- E_{ci} = modulus of concrete at time of release (ksi)

$$E_{ci} = 33 w_c^{1.5} \sqrt{f'_{ci}} \qquad\qquad \text{(C.2)}$$

- w_c = unit weight of the concrete (pcf)
- f'_{ci} = compressive strength at release (psi)
- f_{cgp} = concrete stress at center of gravity of prestressing steel at transfer (ksi)

$$f_{cgp} = 0.7 f_{pu} A_{ps} \left(\frac{1}{A_g} + \frac{e_p{}^2}{I_g} \right) - \frac{M_g e_p}{I_g} \qquad \text{(C.3)}$$

f_{pu} = ultimate strength of p/s strand (ksi)
A_{ps} = total p/s strand area (in.^{2})
A_g = area of gross section (in.^{2})
I_g = moment of inertia of gross section (in.^{4})
e_p = eccentricity of prestressing tendons (in)
M_g = dead load moment (in-kips)

C.4.1.1.2 AASHTO 2012

Iteration 1: $f_{cgp,1} = f_{pi} A_{ps} \left(\frac{1}{A_g} + \frac{e_p{}^2}{I_g} \right) - \frac{M_{SW} e_p}{I_g}$

$$f_{p,1} = f_{pi} - f_{cgp,1} \frac{E_p}{E_{ci}}$$

Iteration 2: $f_{cgp,2} = f_{p,1} A_{ps} \left(\frac{1}{A_g} + \frac{e_p{}^2}{I_g} \right) - \frac{M_{SW} e_p}{I_g}$

$$f_{p,2} = f_{pi} - f_{cgp,2} \frac{E_p}{E_{ci}}$$

Iteration n: $f_{cgp,n} = f_{p,n-1} A_{ps} \left(\frac{1}{A_g} + \frac{e_p{}^2}{I_g} \right) - \frac{M_{SW} e_p}{I_g}$

$$f_{p,n} = f_{pi} - f_{cgp,n} \frac{E_p}{E_{ci}}$$
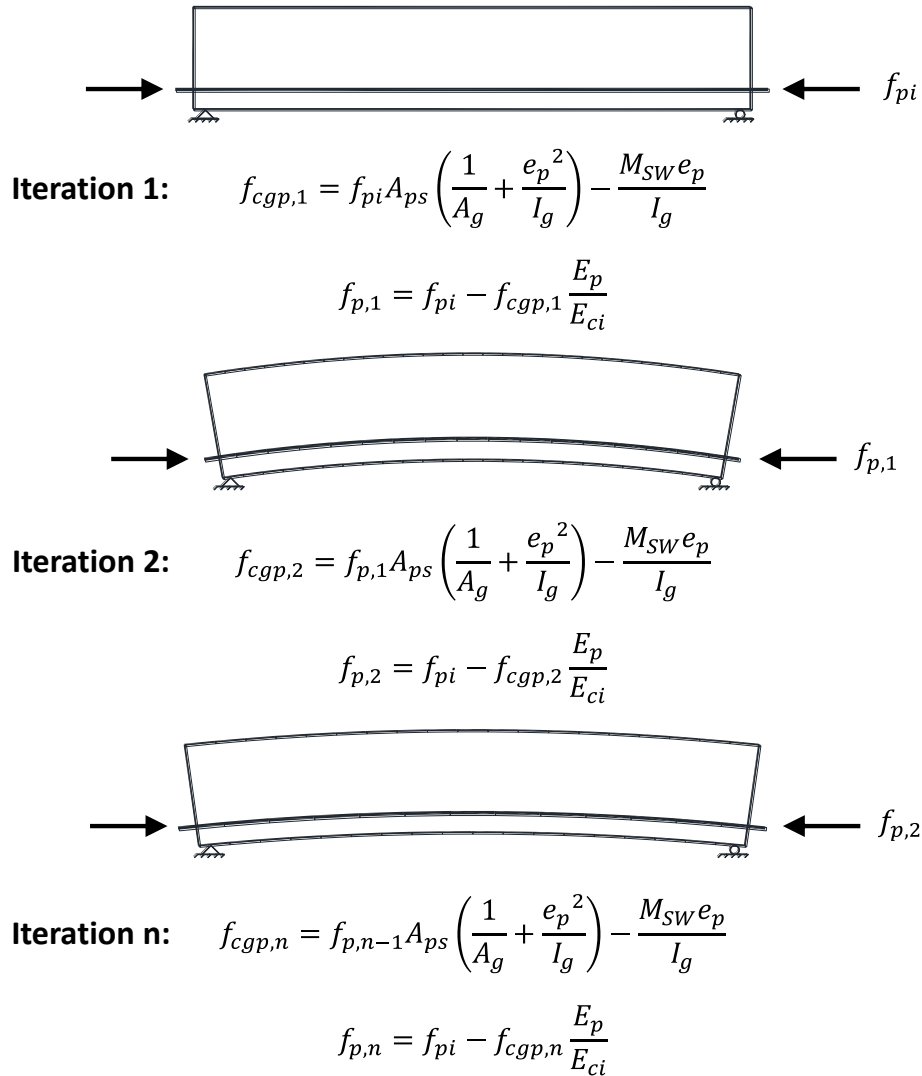
Figure C.1 – AASHTO LRFD 2012 Elastic Shortening Iterative Procedure

C.4.1.2 Results

The performance of the two investigated elastic shortening loss estimates is presented in this section. Despite the fact that the AASHTO LRFD 2004 allows assumption of the prestressing steel stress to calculate f_{cgp}, and AASHTO LRFD 2012 does not (see section C.4.1.1.), there is minimal difference between AASHTO LRFD 2004 and AASHTO LRFD 2012 estimates of elastic shortening. The results are summarized in Table C.2 and presented individually in Figure C.2 and Figure C.3. It can be seen that the estimation found in AASHTO LRFD 2004 and 2012 both perform rather well, but both have an average estimated-to-measured ratio less than 1.0, which is unconservative. The loss estimation found in AASHTO LRFD 2004 is slightly more conservative and much simpler than that found in AASHTO LRFD 2012. It is recommended that the AASHTO LRFD 2004 procedure for elastic shortening loss estimation be re-implemented.

Table C.2 – Comparison of AASHTO LRFD 2004 and 2012 performance vs. 0-6374 performance using estimated-to-actual ratio (E/M) from the evaluation database for Elastic Shortening Loss

	AASHTO 2004	AASHTO 2012	0-6374 Proposed
Minimum	0.71	0.69	0.71
Average	0.94	0.89	0.94
Maximum	1.31	1.17	1.31
Co. of Variation	0.15	0.14	0.15
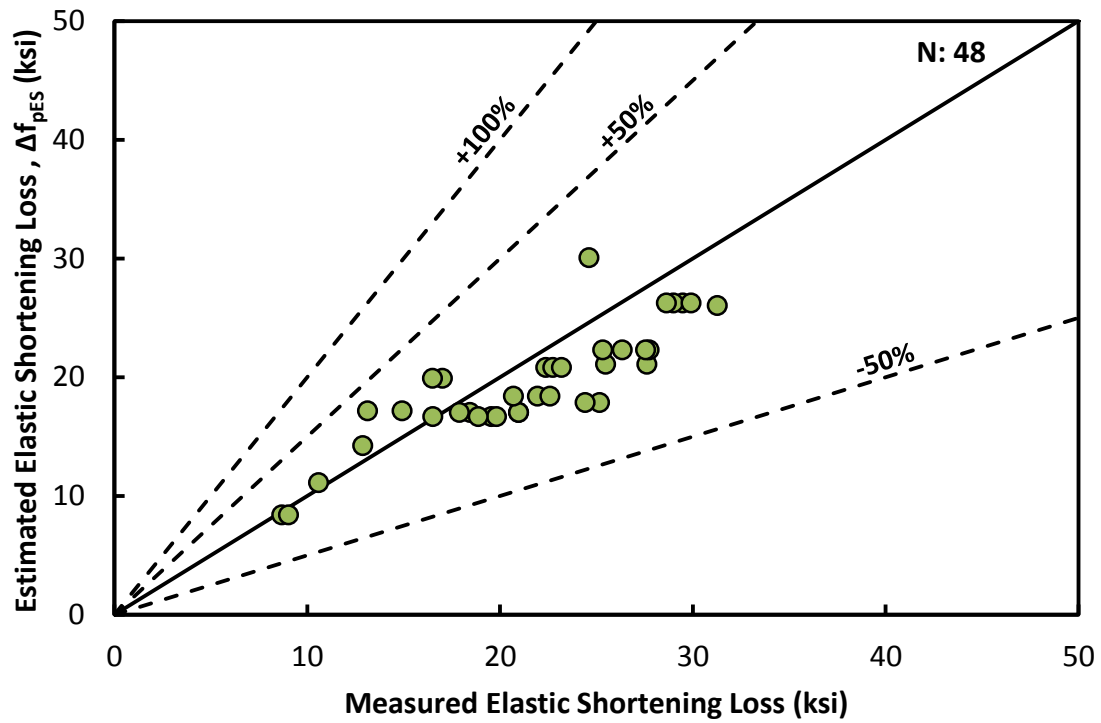
Figure C.2 – AASHTO LRFD 2004 elastic shortening loss estimate vs. measured elastic shortening loss
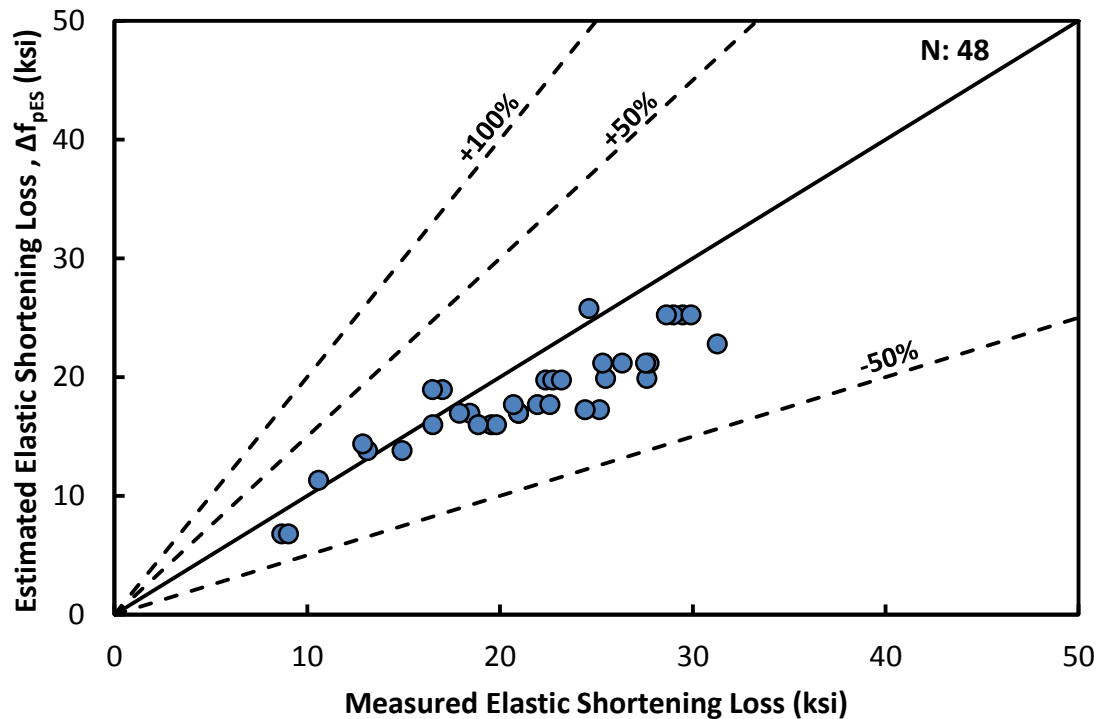
Figure C.3 – AASHTO LRFD 2012 elastic shortening loss estimate vs. measured elastic shortening loss

C.4.2 Refined Results

Within this section results from the evaluation database are broken down into more refined databases to further analyze the different loss procedures. Many specimens were cast using concrete with excessively high release strengths (greater than 7.5 ksi). A refined database containing only specimens with release strengths between 4 and 7.5 ksi was used to evaluate the different loss provisions, which will be presented first.

A few different methods were used for the determination of prestress loss in the database specimens. Some studies used only service load testing to determine the total prestress loss; these will be presented next. The second commonly used method for determining prestress loss was using vibrating wire gages (VWG); these are presented following the service load test losses.

Following the refined database investigations based on loss measurement technique, the evaluation database is separated into specimens with and without a cast in place concrete deck slab. This distinction is important since the majority of the specimens (86 of 140 specimens) did not have a deck, while a deck is always placed in the field. This investigation ensured that the procedures were being calibrated to accurately reflect typical fabrication practices.

C.4.2.1 Concrete Release Strength

First to be presented is the performance of the three prestress loss procedures using the refined evaluation database containing only specimens with concrete release strengths between 4 and 7.5 ksi. The specimens contained in this refined database are most representative of typical past and present design practices. The results from this investigation are summarized in Table C.3 and Figure C.3 through Figure C.5.

Table C.3 – Comparison of performance of AASHTO LRFD 2004 and 2012 procedure and 0-6374 recommendations for specimens with release strength between 4 and 7.5 ksi using estimated-to-actual ratio (E/M) from the evaluation database

	AASHTO 2004	AASHTO 2012	0-6374 Proposed
Minimum	0.89	0.70	0.88
Average	1.64	1.34	1.37
Maximum	3.11	2.20	2.31
Co. of Variation	0.23	0.20	0.18
St. Deviation	0.38	0.27	0.24
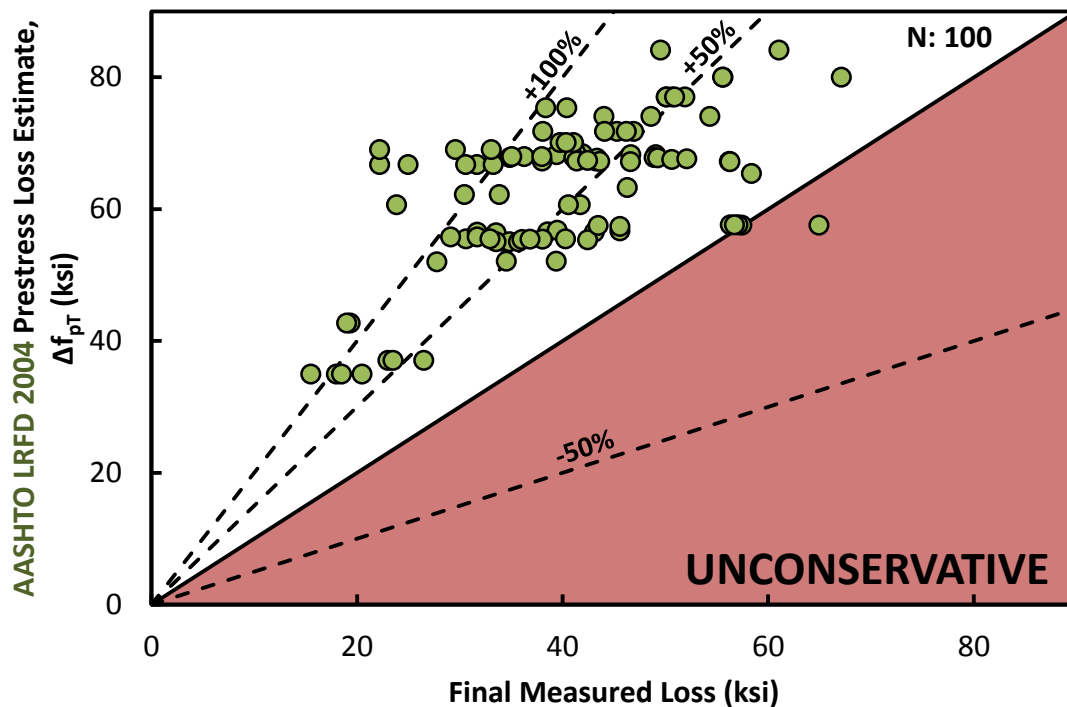
Figure C.4 – AASHTO LRFD 2004 prestress loss estimate vs. final measured loss for specimens with release strengths between 4 and 7.5 ksi
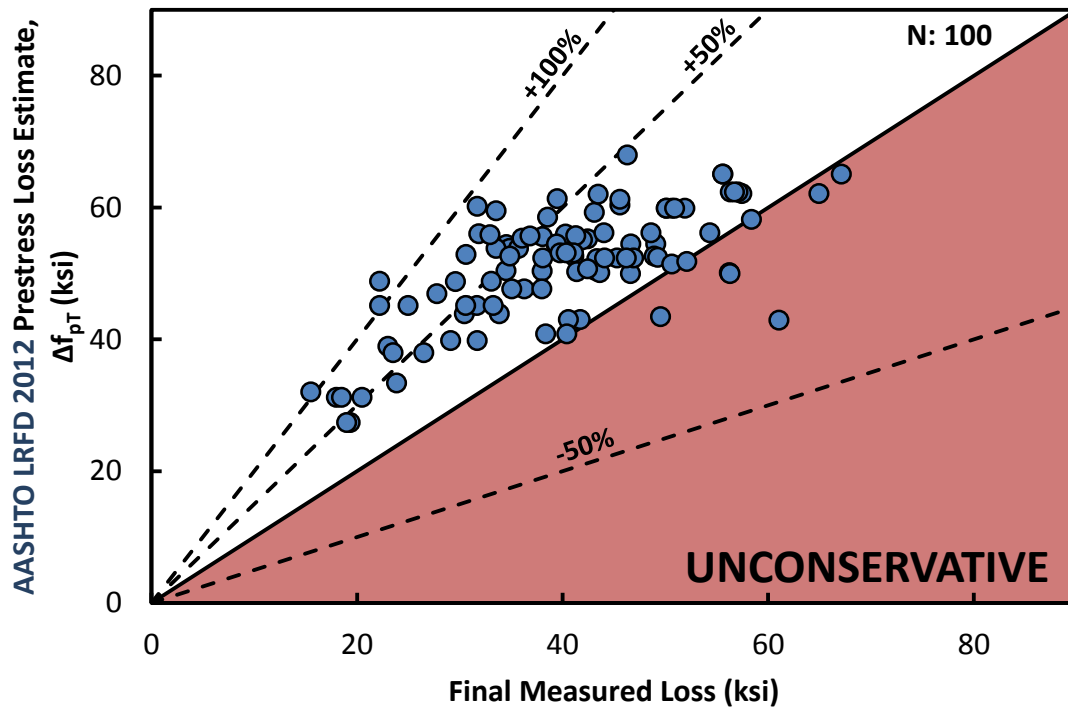
Figure C.5 – AASHTO LRFD 2012 prestress loss estimate vs. final measured loss for specimens with release strengths between 4 and 7.5 ksi
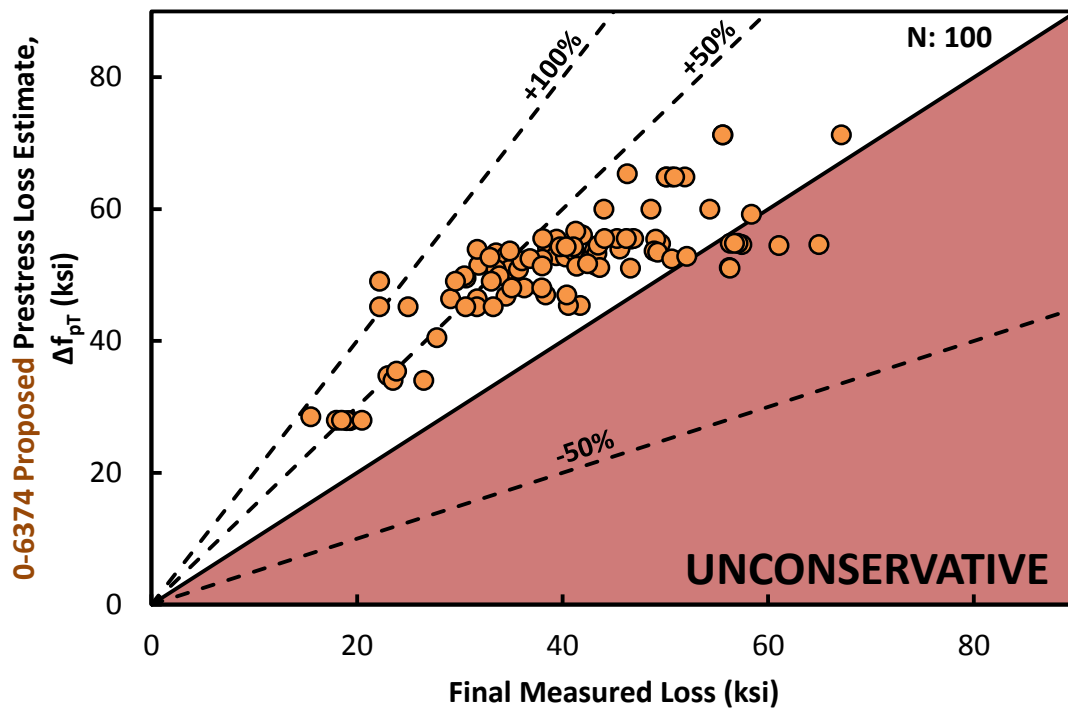
Figure C.6 – 0-6374 Proposed prestress loss estimate vs. final measured loss for specimens with release strengths between 4 and 7.5 ksi

C.4.2.2 Load Tests

First to be presented is the performance of the three prestress loss procedures using the refined evaluation database containing only specimens in which losses were determined using service load testing. It should be noted that the loss measured using service load testing was more variable than loss measured by VWG readings compared to estimated losses.

Table C.4 – Comparison of performance of AASHTO LRFD 2004 and 2012 procedure and 0-6374 recommendations for specimens, where loss was measured by service load testing, using estimated-to-actual ratio (E/M) from the evaluation database

	AASHTO 2004	AASHTO 2012	0-6374 Proposed
Minimum	0.89	0.89	0.88
Average	1.55	1.34	1.35
Maximum	3.11	2.20	2.31
Co. of Variation	0.26	0.21	0.20
St. Deviation	0.40	0.28	0.27
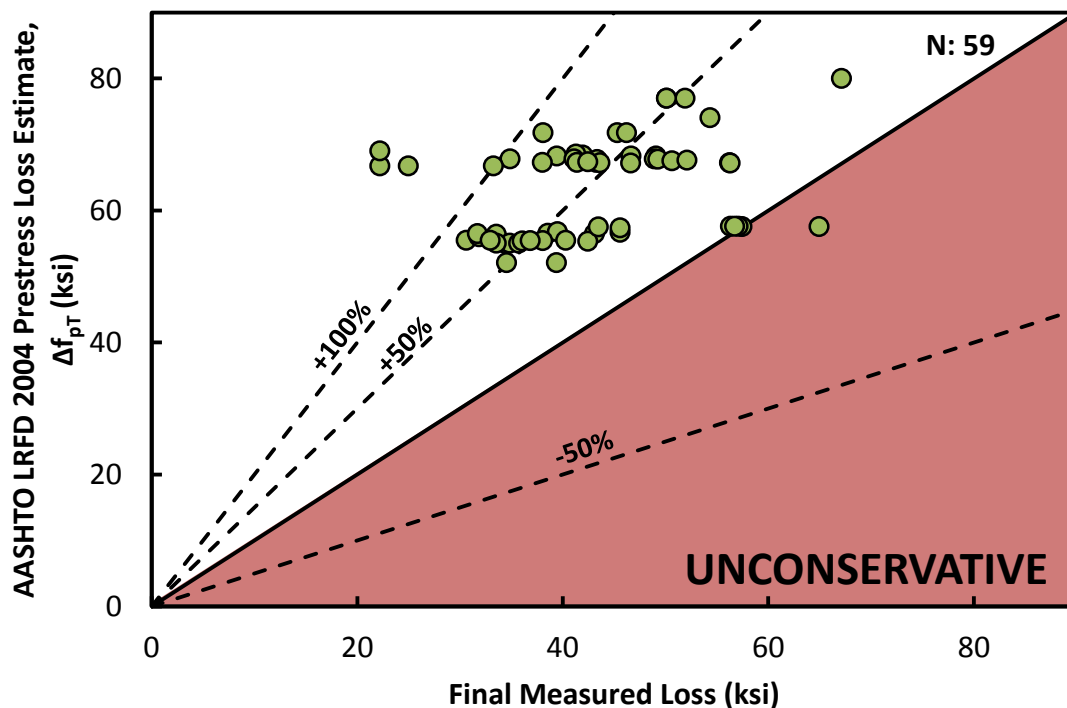
Figure C.7 - AASHTO LRFD 2004 prestress loss estimate vs. final measured loss for specimens where loss was measured by service load testing
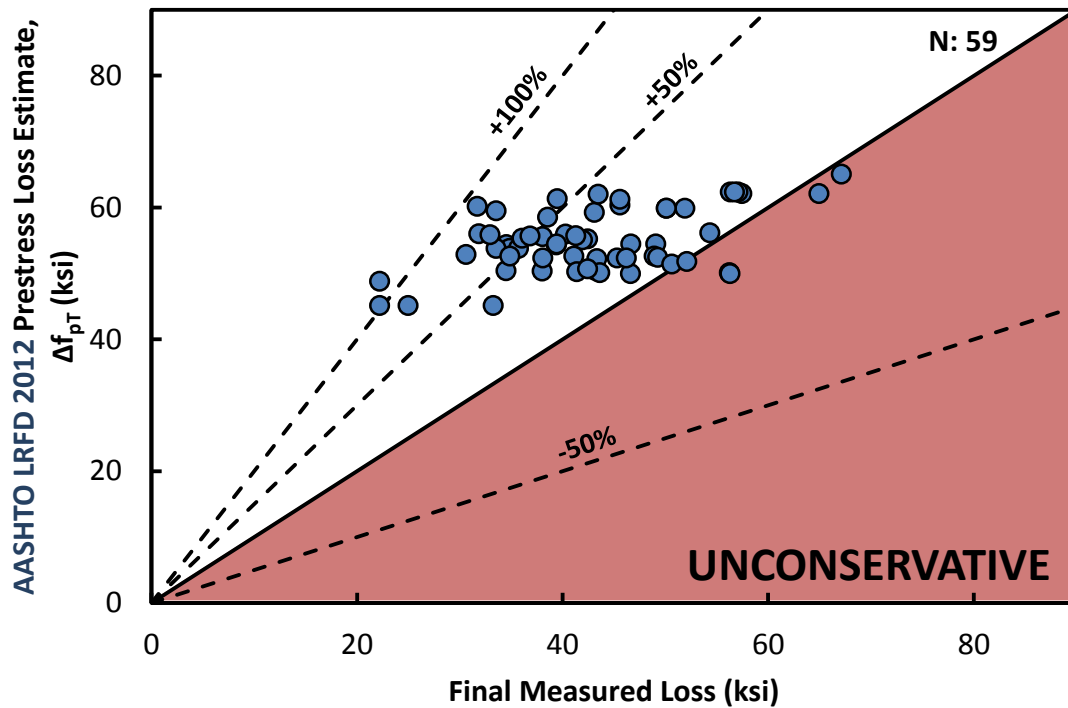
Figure C.8 - AASHTO LRFD 2012 prestress loss estimate vs. final measured loss for specimens where loss was measured by service load testing
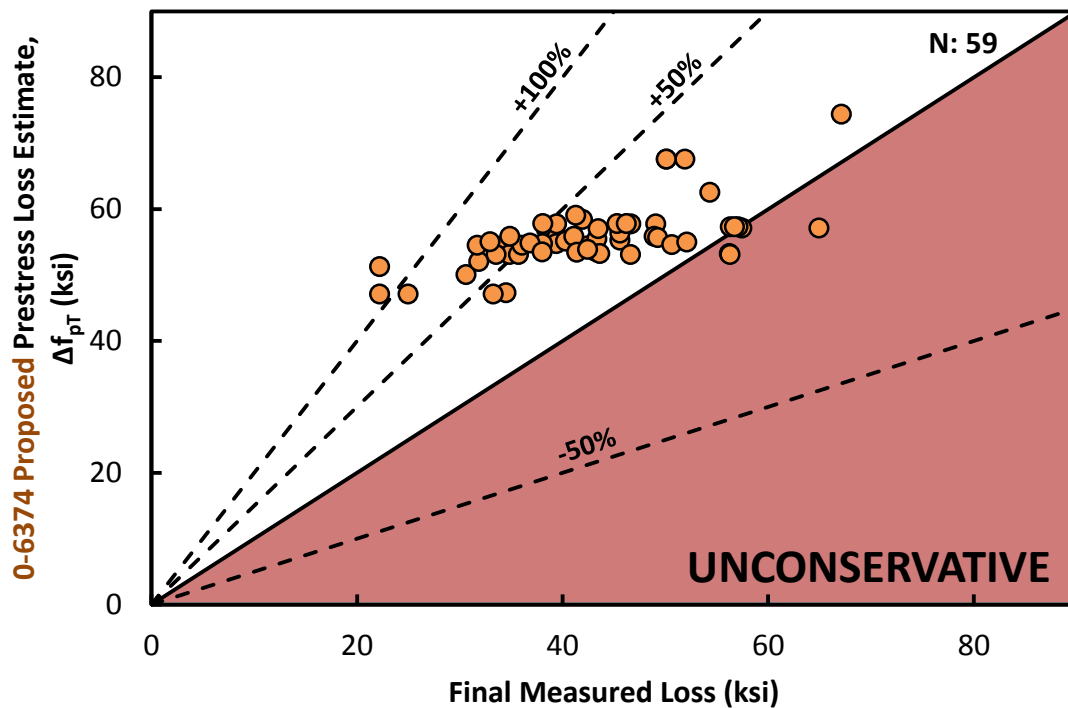
Figure C.9 – 0-6374 Proposed prestress loss estimate vs. final measured loss for specimens where loss was measured by service load testing

C.4.2.3 VWG Readings

Next to be presented is the performance of the three prestress loss procedures using the refined evaluation database containing only specimens in which losses were determined using VWG readings. It can be observed from Figure C.12, compared to Figure C.10 and Figure C.11, that the proposed loss procedure does an excellent job precisely and conservatively estimating prestress loss. The VWG readings are considered to be the more consistent than service load testing.

Table C.5 – Comparison of performance of AASHTO LRFD 2004 and 2012 procedure and 0-6374 recommendations for specimens, where loss was measured by VWG readings, using estimated-to-actual ratio (E/M) from the evaluation database

	AASHTO 2004	AASHTO 2012	0-6374 Proposed
Minimum	1.37	1.01	1.12
Average	1.96	1.30	1.44
Maximum	2.91	1.69	1.74
Co. of Variation	0.23	0.12	0.11
St. Deviation	0.45	0.16	0.16
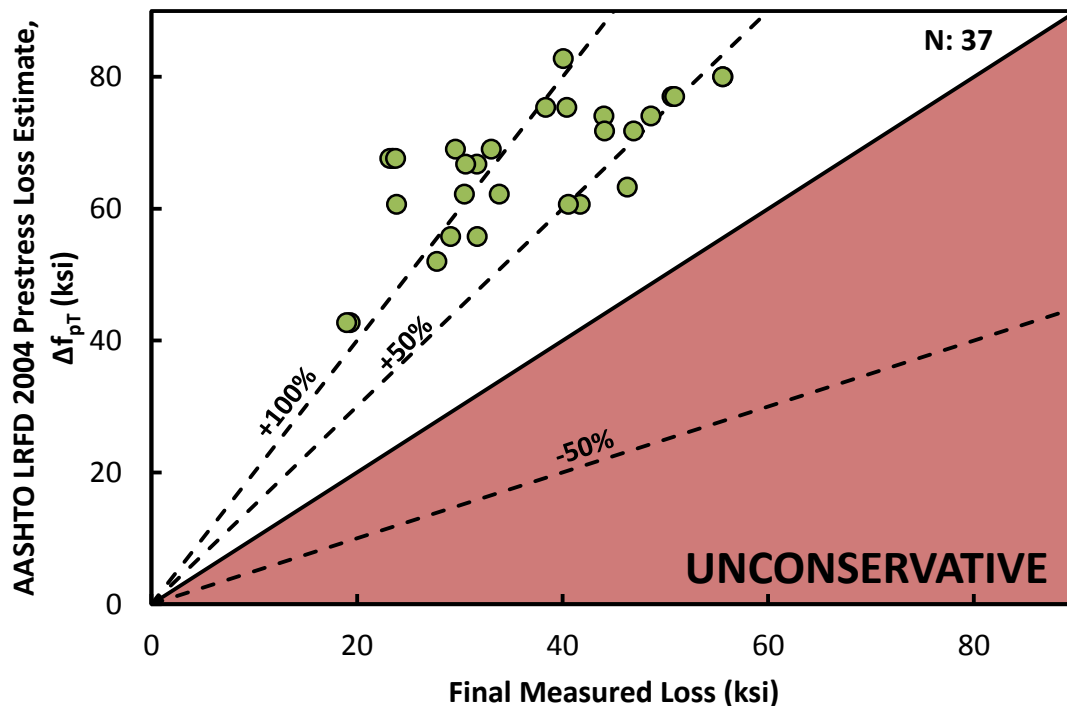
Figure C.10 - AASHTO LRFD 2004 prestress loss estimate vs. final measured loss for specimens where loss was measured by VWG reading

231
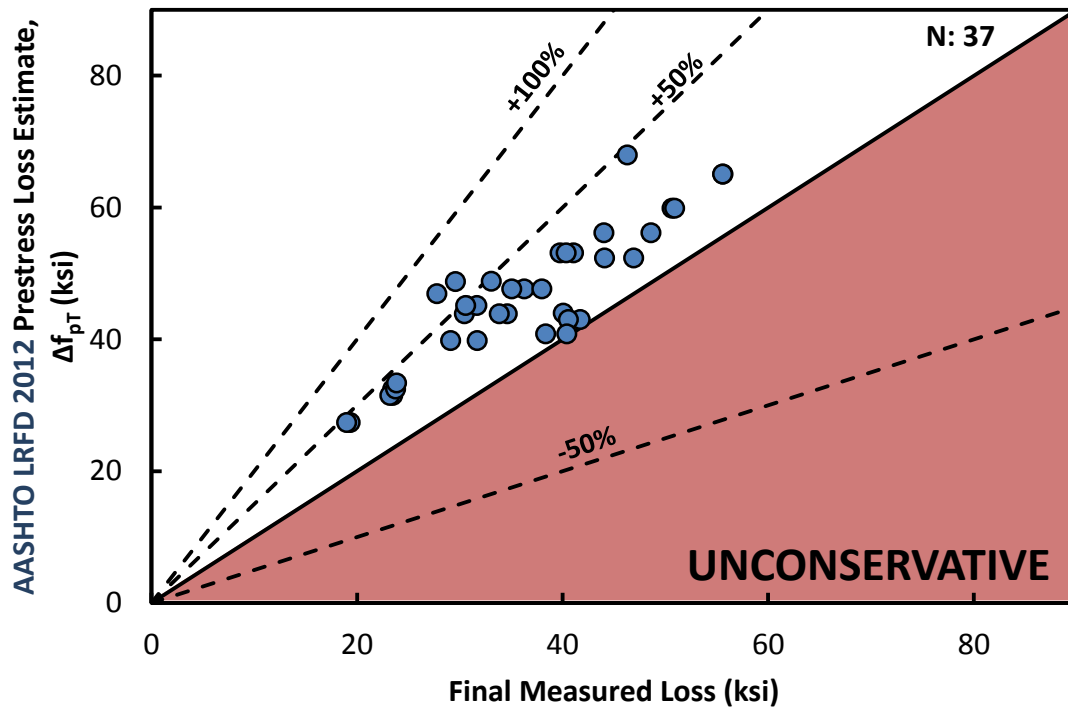
Figure C.11 - AASHTO LRFD 2012 prestress loss estimate vs. final measured loss for specimens where loss was measured by VWG reading
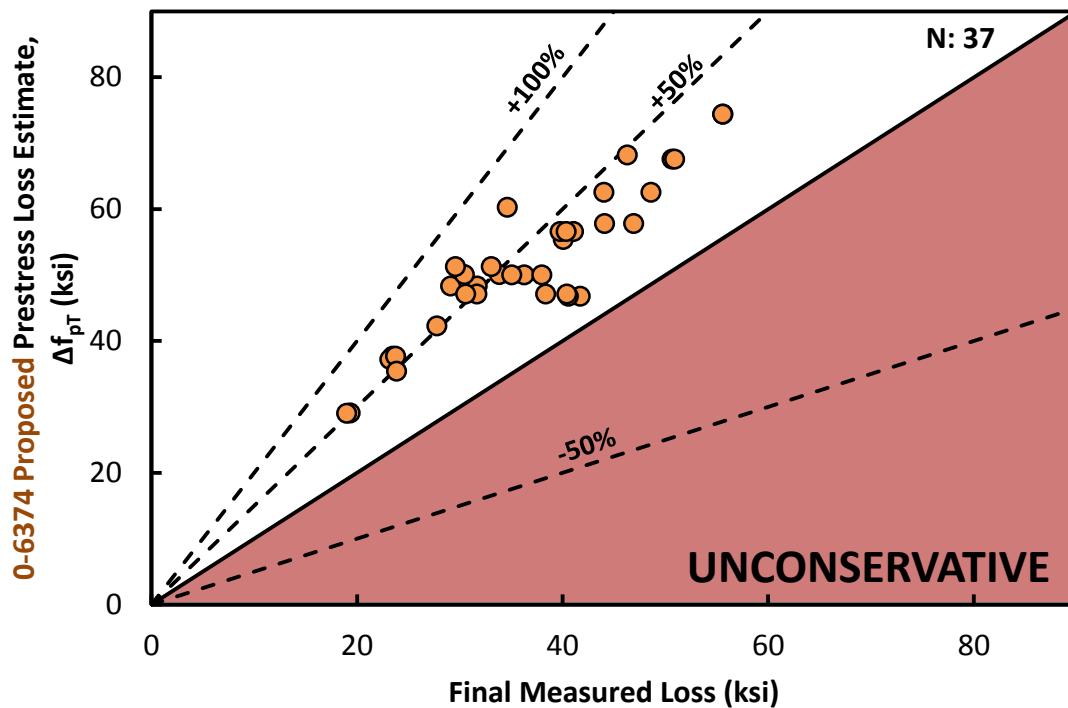
Figure C.12 – 0-6374 Proposed prestress loss estimate vs. final measured loss for specimens where loss was measured by VWG reading

C.4.2.4 Specimens with Decks vs. without Decks

The evaluation database contained specimens both with and without cast-in-place concrete deck slabs. The results from specimens without decks and with decks are presented in Table C.6 and Table C.7, respectively. These results are also shown graphically in Figure C.13 through Figure C.18.

Table C.6 – Comparison of performance of AASHTO LRFD 2004 and 2012 procedure and 0-6374 recommendations for specimens without decks using estimated-to-actual ratio (E/M) from the evaluation database

	AASHTO 2004	AASHTO 2012	0-6374 Proposed
Minimum	0.89	0.89	0.88
Average	1.61	1.31	1.35
Maximum	3.11	2.20	2.31
Co. of Variation	0.24	0.19	0.18
St. Deviation	0.38	0.25	0.24
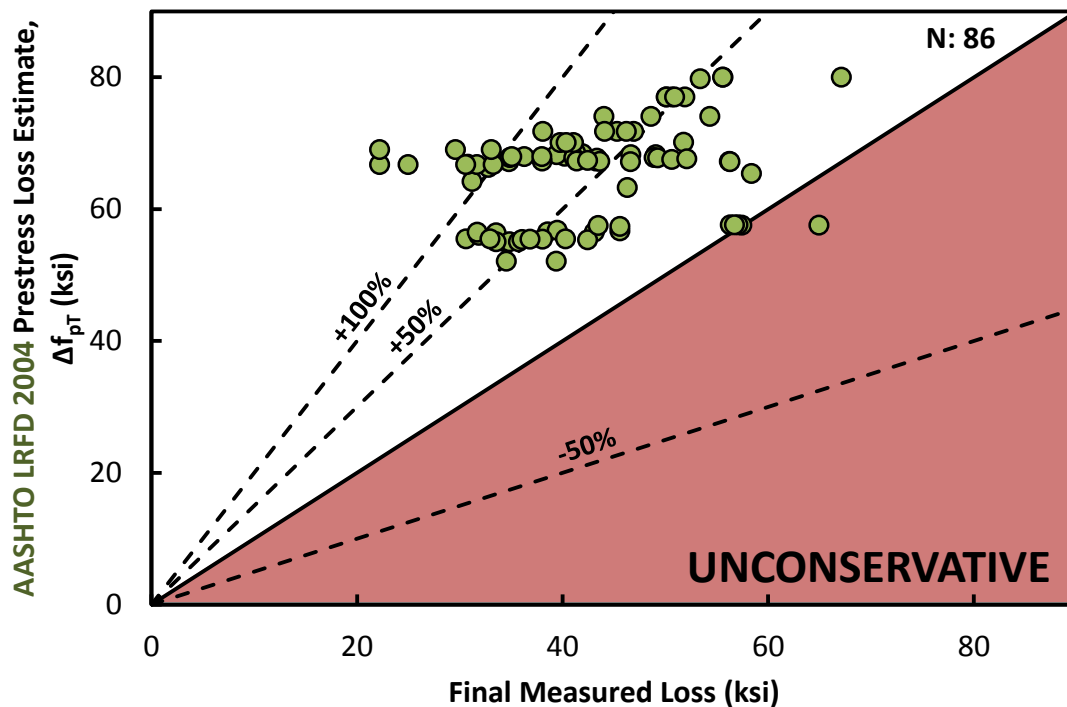
Figure C.13 – AASHTO LRFD 2004 prestress loss estimate vs. final measured loss for specimens without decks
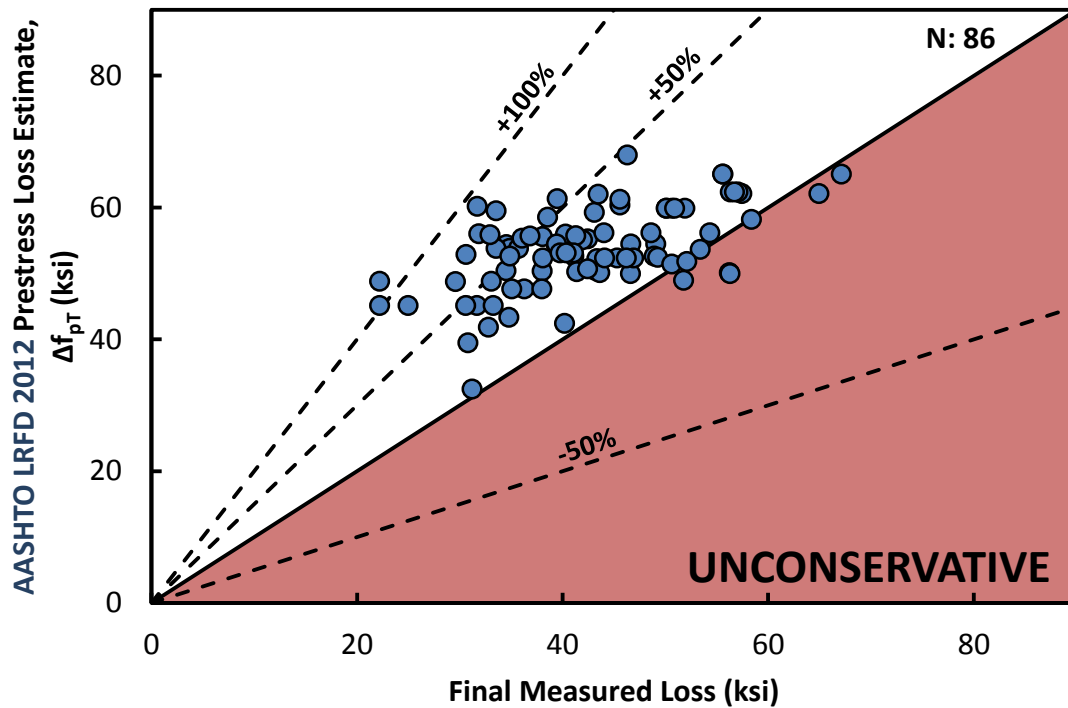
Figure C.14 - AASHTO LRFD 2012 prestress loss estimate vs. final measured loss for specimens without decks
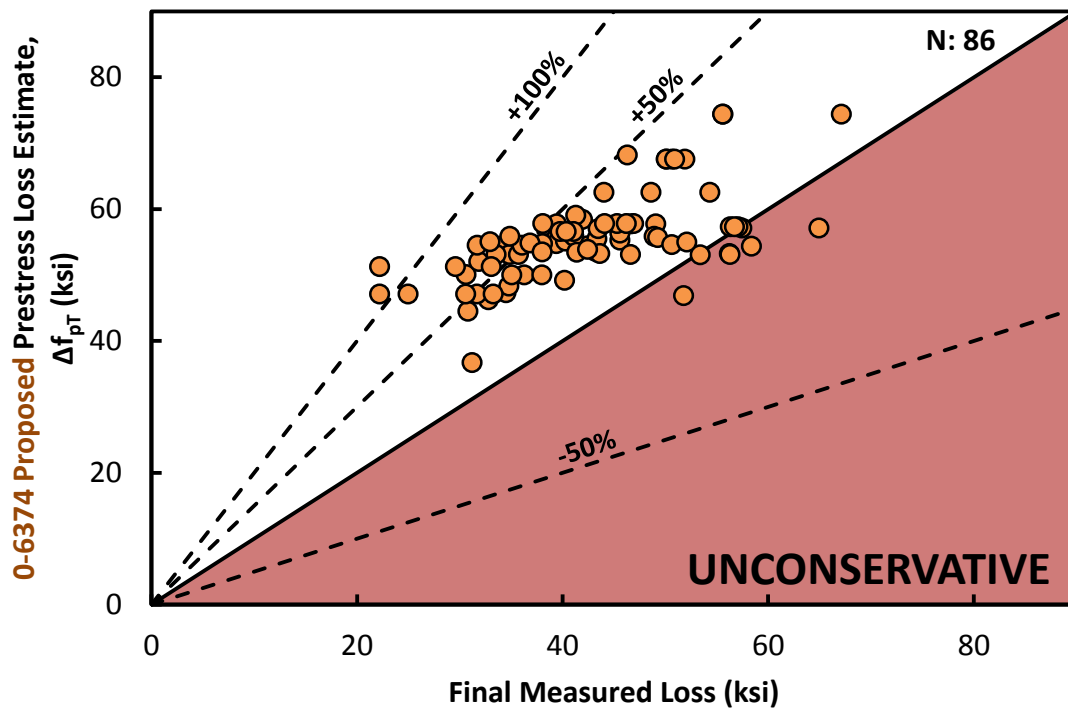
Figure C.15 – 0-6374 Proposed prestress loss estimate vs. final measured loss for specimens without decks

Table C.7 – Comparison of performance of AASHTO LRFD 2004 and 2012 procedure and 0-6374 recommendations for specimens with decks using estimated-to-actual ratio (E/M) from the evaluation database

	AASHTO 2004	AASHTO 2012	0-6374 Proposed
Minimum	1.25	0.59	0.84
Average	1.96	1.15	1.29
Maximum	3.69	2.07	2.06
Co. of Variation	0.24	0.30	0.24
St. Deviation	0.47	0.35	0.30
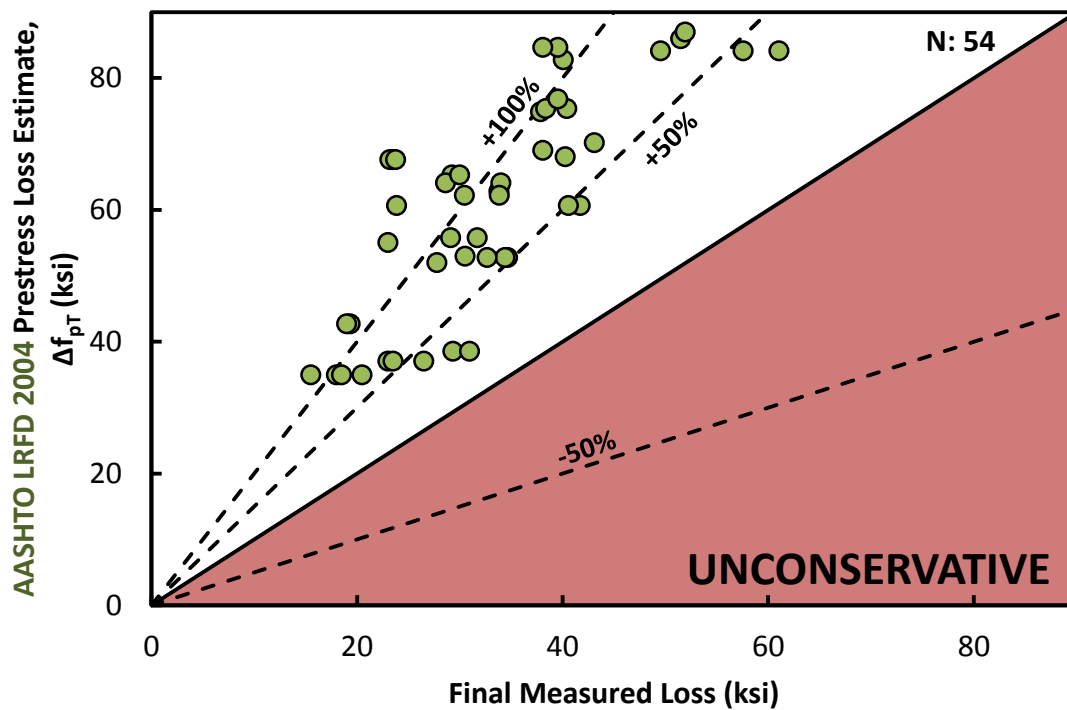
Figure C.16 - AASHTO LRFD 2004 prestress loss estimate vs. final measured loss for specimens with decks
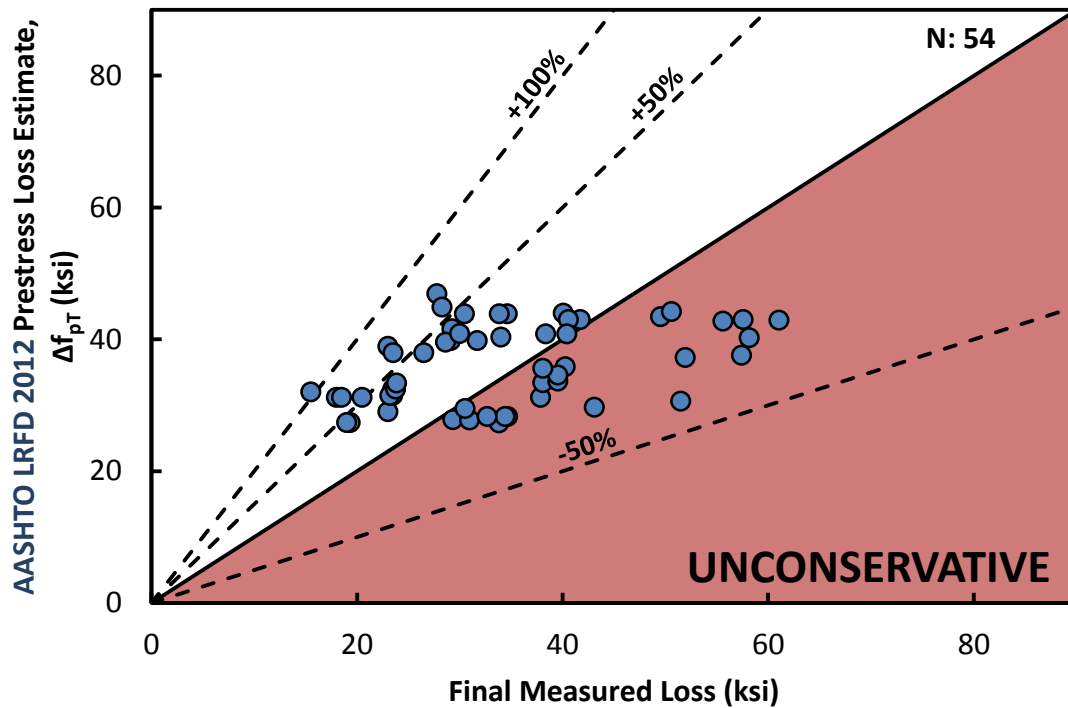
Figure C.17 - AASHTO LRFD 2012 prestress loss estimate vs. final measured loss for specimens with decks
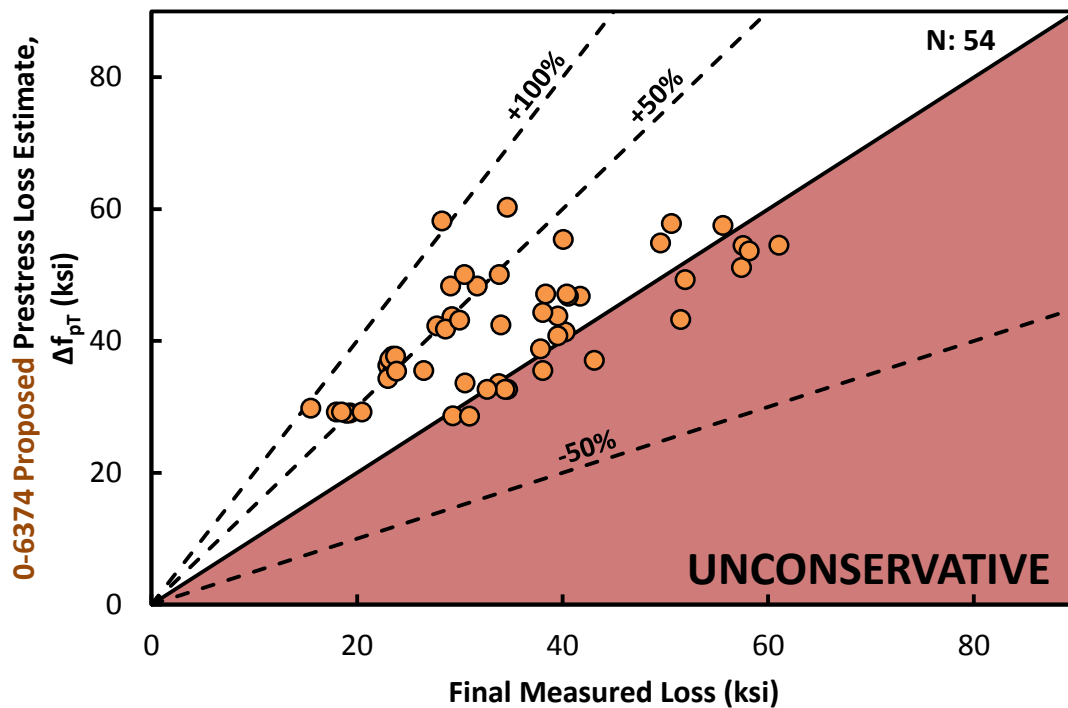
Figure C.18 – 0-6374 Proposed prestress loss estimate vs. final measured loss for specimens with decks

C.4.3 AASHTO LRFD 2004 Creep Loss Expression

The creep expression found in the AASHTO LRFD 2004 procedure is shown in Equation (C.4). Two empirically derived constants are used in this expression, shown as C_1 and C_2 in Equation (C.5). The empirically derived constants used in the AASHTO LRFD 2004 procedure are compared to what these constants would be using the AASHTO LRFD 2012 procedure in the evaluation database.

$$\Delta f_{pCR} = 12.0 f_{cgp} - 7.0 \Delta f_{cdp} \geq 0 \qquad \text{(C.4)}$$

AASHTO 04 (5.9.5.4.3-1)

$$\Delta f_{pCR} = C_1 f_{cgp} - C_2 \Delta f_{cdp} \qquad \text{(C.5)}$$

If the creep expressions found in AASHTO LRFD 2012 are simplified, shown in Equations (C.6) and (C.7), the creep used in AASHTO LRFD 2012 can be compared to that used in AASHTO LRFD 2004.

$$C_1 = \frac{E_p}{E_{ci}} K_{id} \psi_b(t_f, t_i) \qquad \text{(C.6)}$$

$$C_2 = \frac{E_p}{E_{ci}} K_{df} \psi_b(t_f, t_d) \qquad \text{(C.7)}$$

The coefficients used in the creep expressions for both AASHTO LRFD 2004 and 2012 are presented in Table C.8. As stated above, the coefficients used in AASHTO LRFD 2004 are constant for all cases; this is reflected in the table. In the AASHTO LRFD 2012 procedure, these creep coefficients vary, as shown in the above equations and reflected in the values in the below table.

The first observation is that the calculated coefficients in the AASHTO LRFD 2012 procedure are significantly less than the constant values used in 2004. The lower coefficients would lead to lower creep loss estimation. The reason the constants found in AASHTO LRFD 2004 are significantly higher than calculated values in 2012 is that the AASHTO LRFD 2004 loss procedure was calibrated using low-strength specimens. The AASHTO LRFD 2012 procedure was calibrated using specimens with high strength concrete, which would result in smaller creep loss.

Table C.8 – Comparison of AASHTO LRFD 2004 and 2012 creep expressions

	C_1		C_2	
	AASHTO 2004	*AASHTO 2012*	*AASHTO 2004*	*AASHTO 2012*
Minimum	--	2.48	--	1.57
Average	12.0	5.42	7.0	3.05
Maximum	--	12.3	--	6.23
Co. of Variation	--	0.35	--	0.43
St. Deviation	--	1.88	--	1.32

The second observation is the proportion of the coefficients (C_1:C_2) in each of the procedures is the same, around 1.7:1. This shows that in each of the specifications the stress change due to the initial prestress force and that due to deck placement are treated the same with respect to each other.

C.4.4 Swartz et. al. (2010) Procedure Performance

The "Direct Method" recommended by Swartz et. at. (2010) was analyzed using the evaluation database. This method for estimating prestress loss, discussed previously in Chapter 2, is a simplification of the procedure found in the 2012 AASHTO LRFD Bridge Design Specification. It can be seen that this method improves the precision found in AASHTO LRFD 2012 but does not increase conservatism.

Table C.9 – Comparison of performance of AASHTO LRFD 2004 and 2012 procedure, 0-6374 recommendations and Swartz Direct Method using estimated-to-actual ratio (E/M) from the evaluation database

	AASHTO 2004	**AASHTO 2012**	**0-6374 Proposed**	**Swartz (2010)**
Minimum	0.86	0.59	0.84	0.60
Average	1.74	1.25	1.32	1.04
Maximum	3.69	2.20	2.31	1.88
Co. of Variation	0.26	0.24	0.20	0.23
St. Deviation	0.45	0.30	0.27	0.24
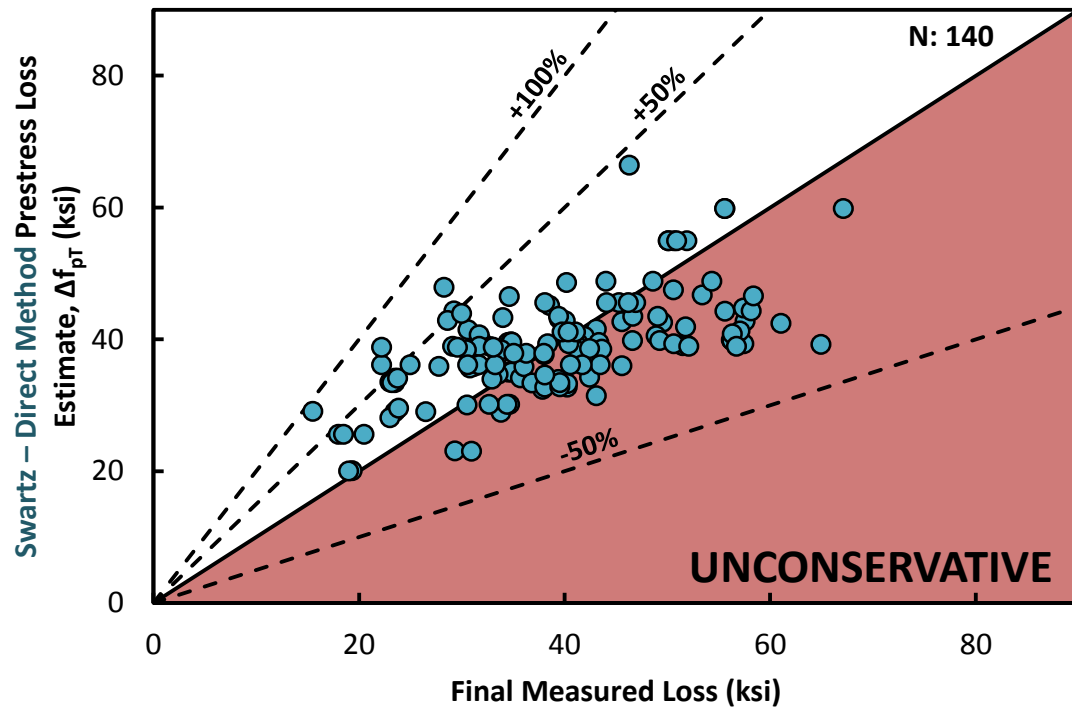
Figure C.19 – Direct Method prestress loss estimate vs. final measured loss

This page is intentionally left blank

APPENDIX D
Parametric Study Results

D.1 OVERVIEW

The results from the parametric study for all of the beam sections are presented in this appendix. The effect of the different loss procedures on (1) prestress loss, (2) number of strands required, (3) flexural capacity, (4) transverse steel required, and (5) initial camber are shown for the following cross-section types:

- Bulb-T: Tx28, Tx46, and Tx70
- I-Beams: Type A, Type C, and Type IV
- Box-Beams: Type 4B20 and Type 5B40
- U-Beams: Type U40 and Type U54

Two different approaches were taken in the parametric study investigation: (1) the effect on TxDOT girders with the current design philosophy and (2) the effect on TxDOT girders if release strengths of 6 ksi were used. The performance of the recommendations using the current design philosophy was evaluated by allowing the analysis tool to design for concrete release and 28-day strengths (greater than 4 ksi). It was found through this investigation that the recommendations would have little effect on current TxDOT designs; only in a handful of cases would the number of strands change from that previously required. The recent trend in industry is the use of higher release strengths (5 to 6 ksi and higher), allowing for construction of longer span bridges. The recommendations will have the highest impact on designs within this higher concrete release strength range. For this reason, results from the second investigation (using concrete release strength of 6 ksi) will be presented in this appendix.

Following this presentation on different cross-sections, the effect of the concrete release strength (f'_{ci}) on design will be investigated. These results are shown for the same cross-sections investigated above.
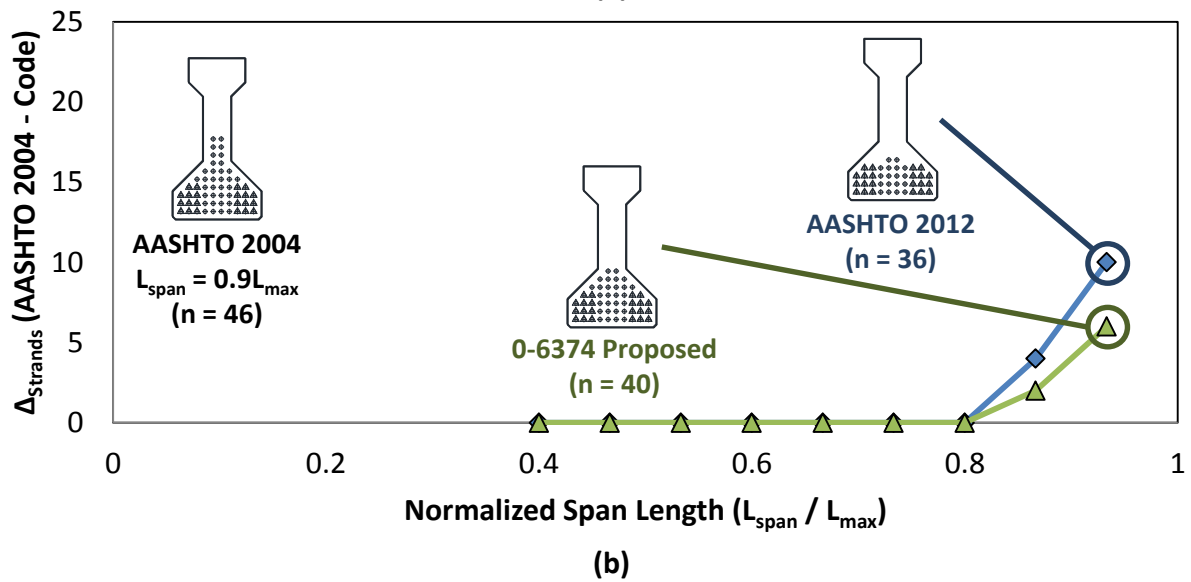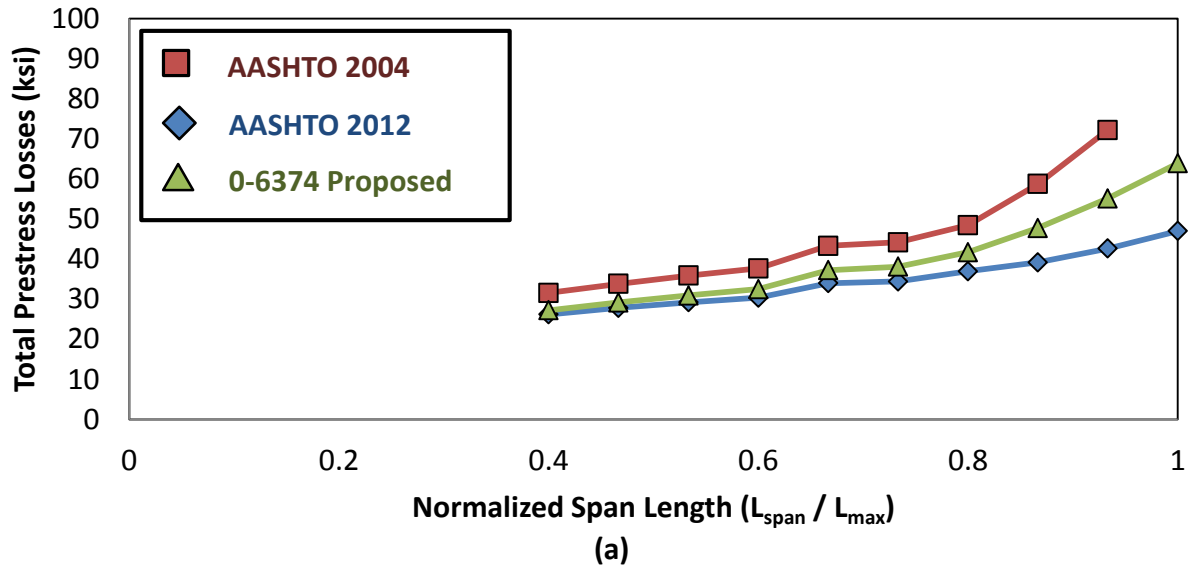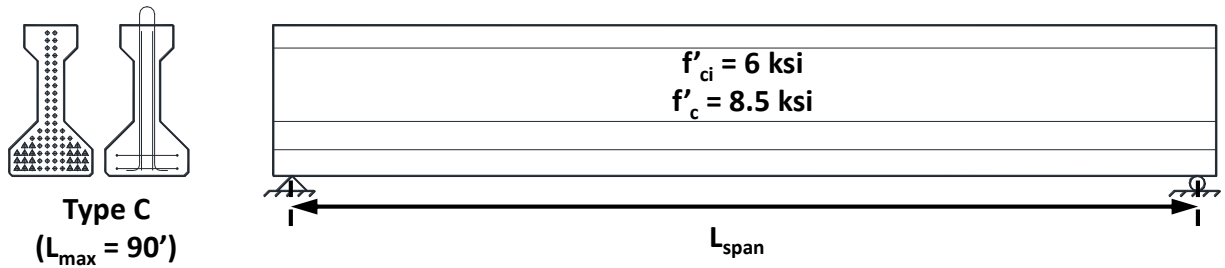
D.2 RESULTS – BY CROSS-SECTION TYPE
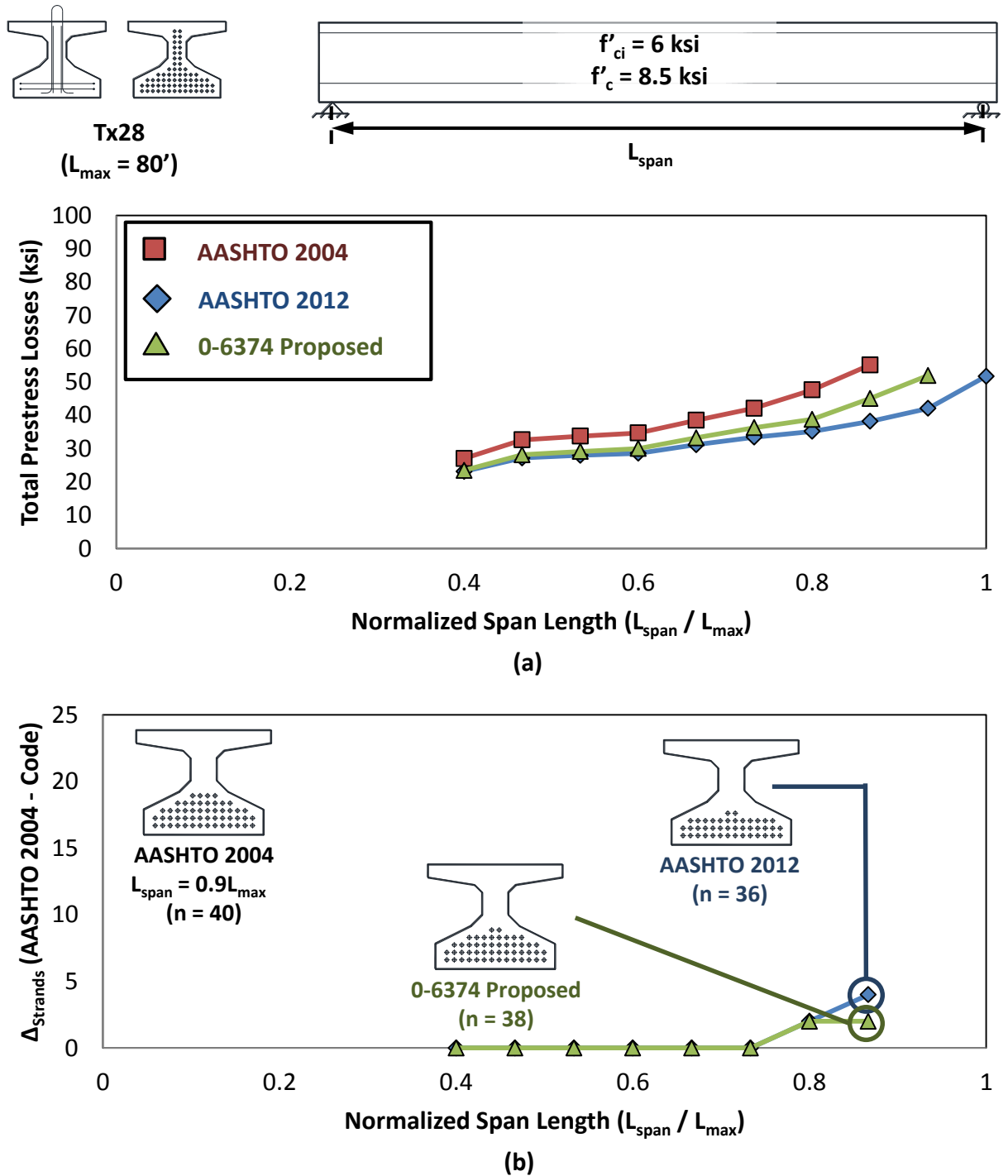
Figure D.1 – Tx28: (a) total prestress loss, (b) Difference in total strands required by AASHTO LRFD 2012 and 0-6374 Proposed versus AASHTO LRFD 2004
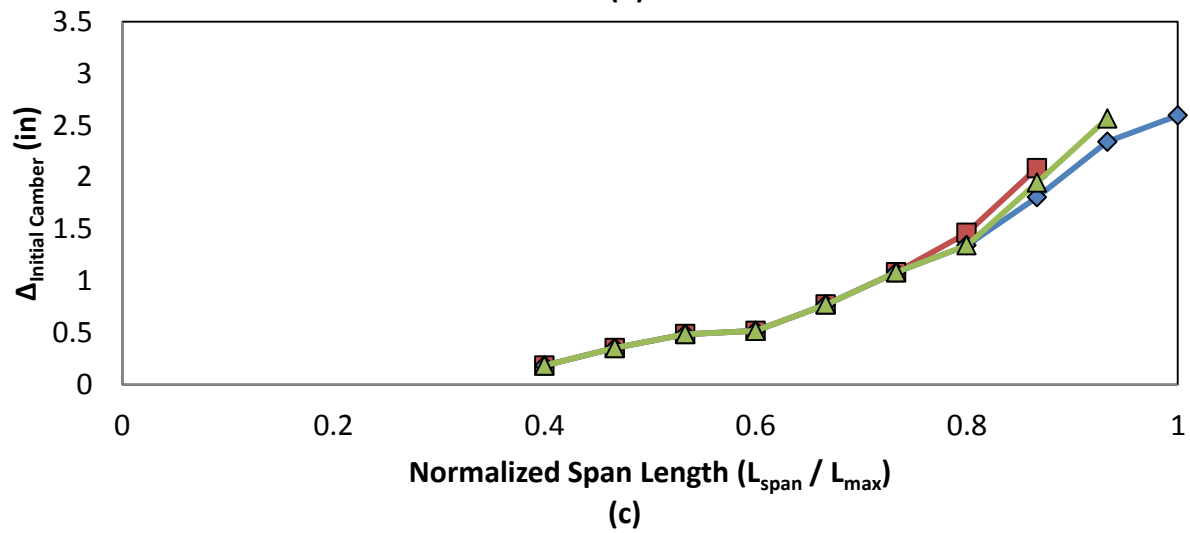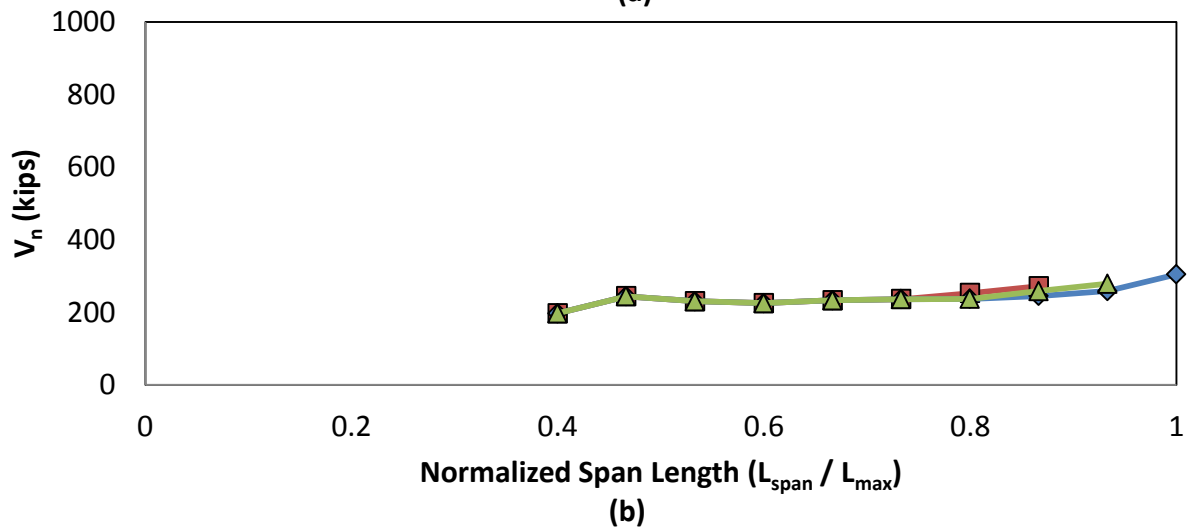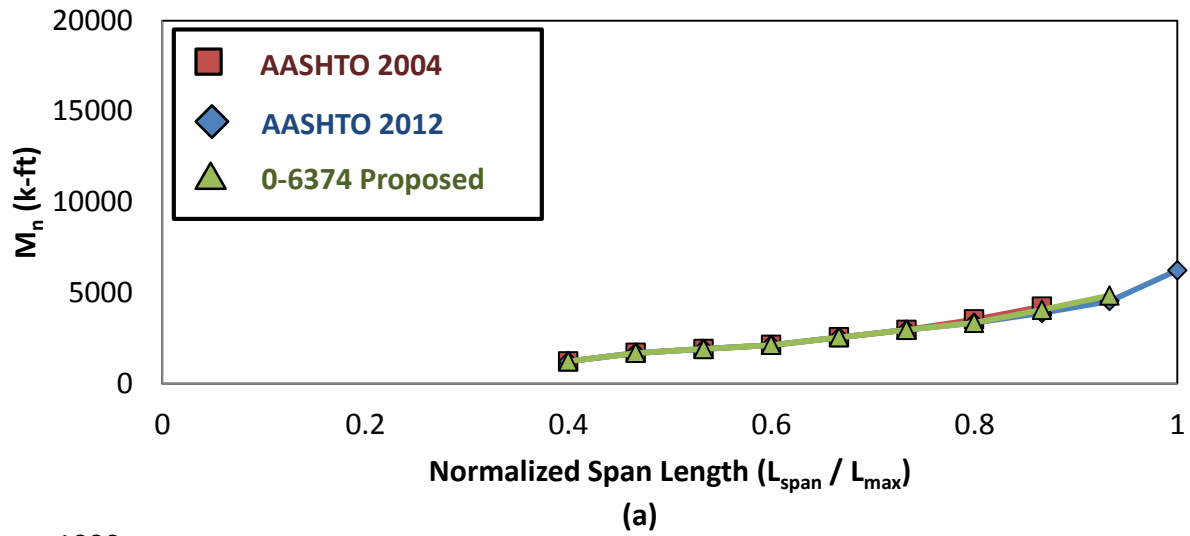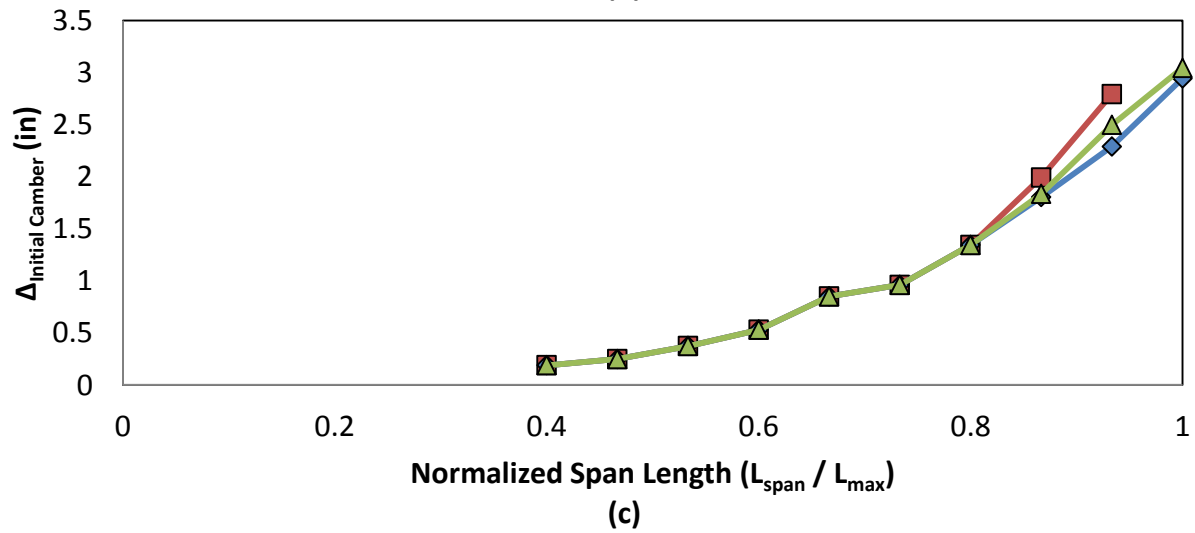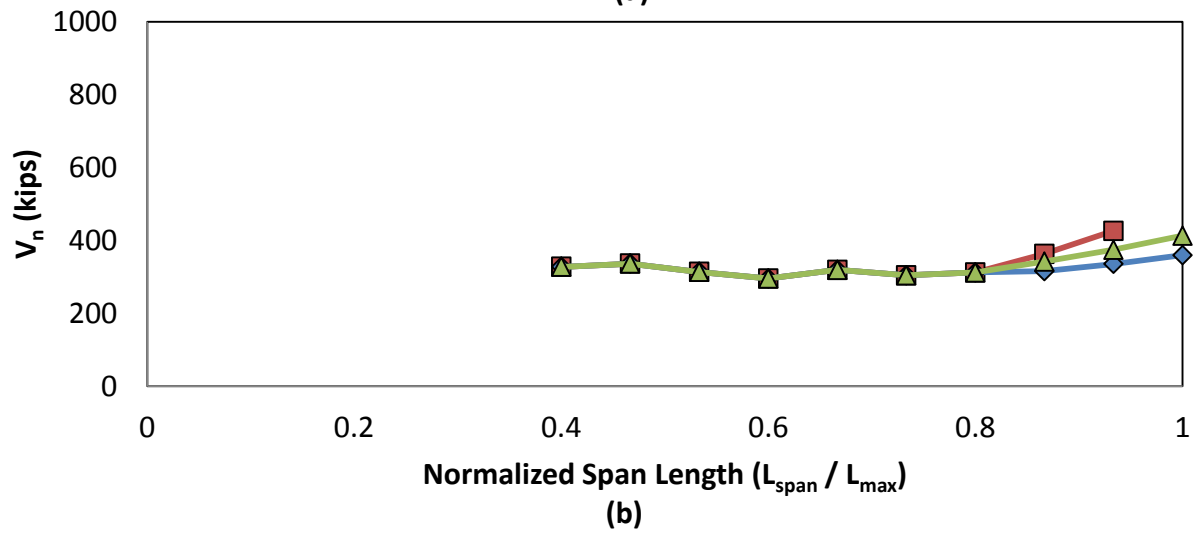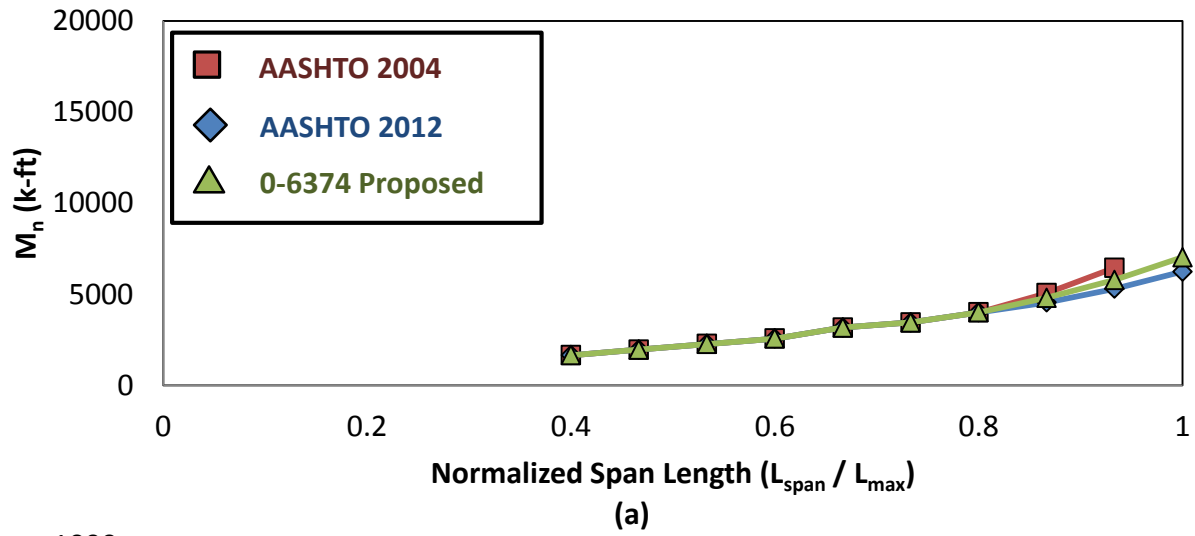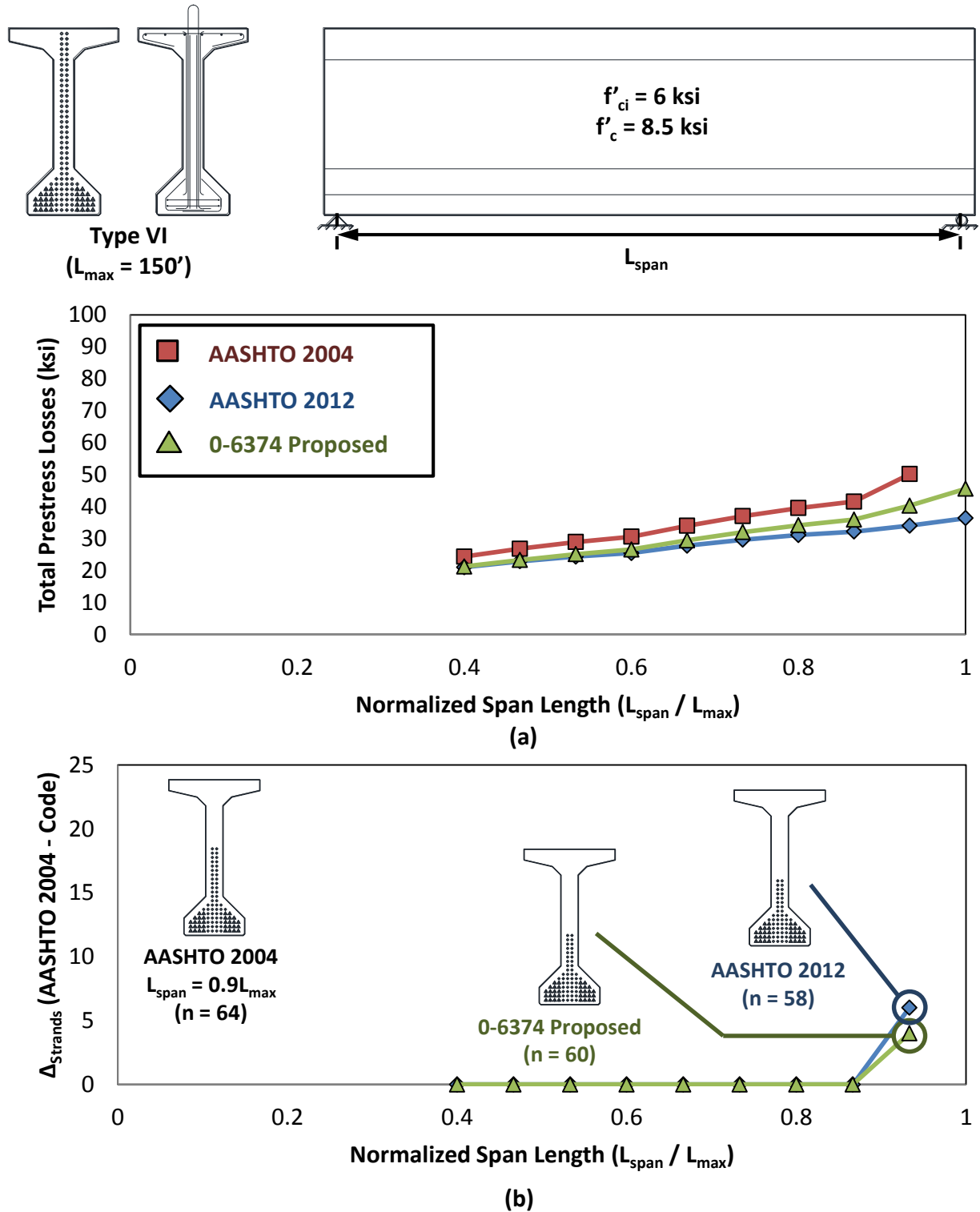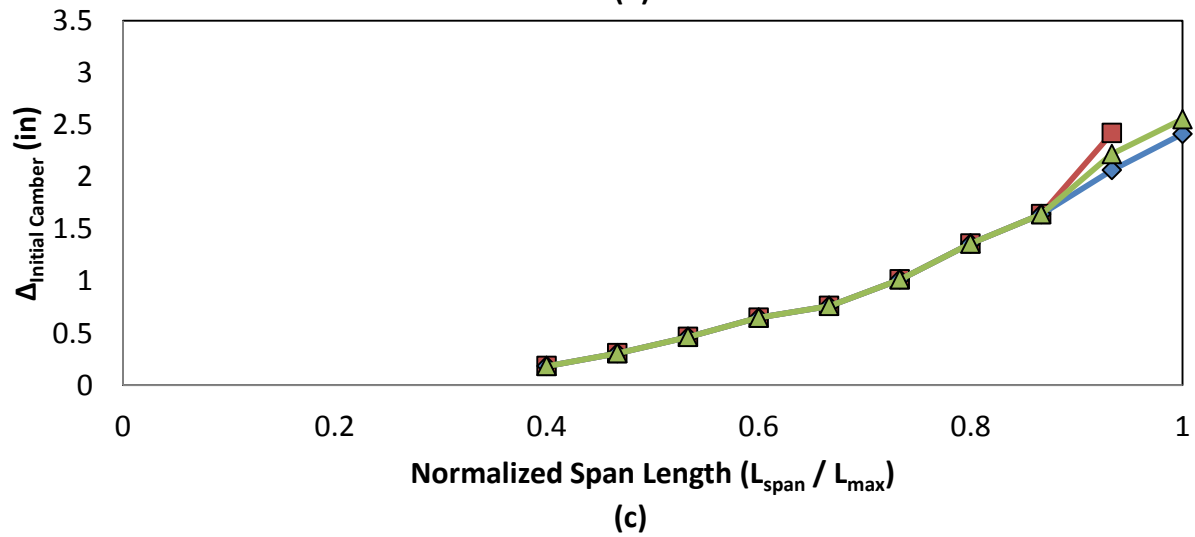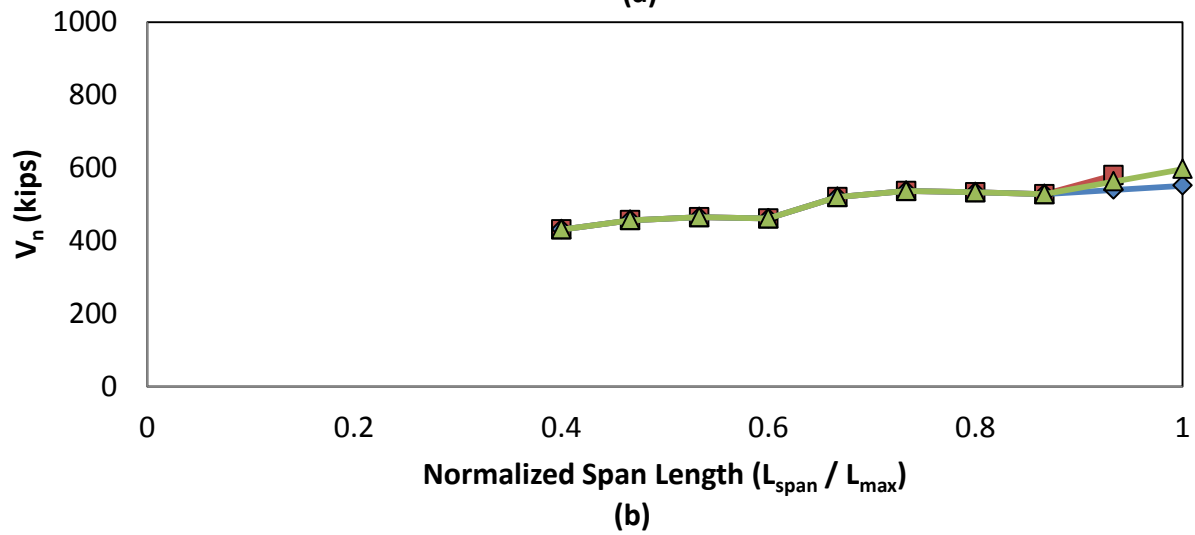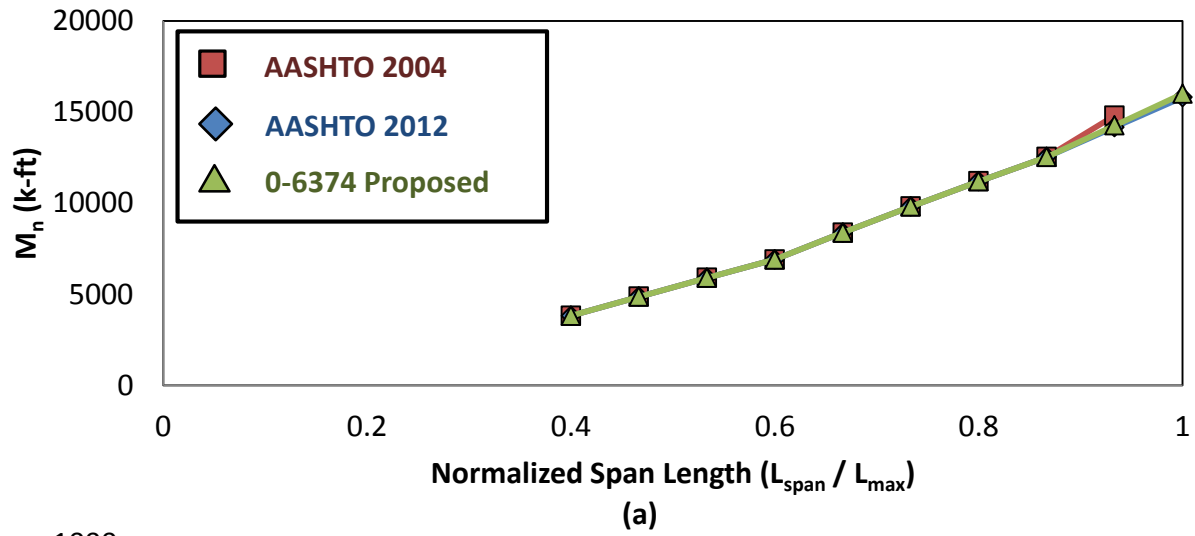
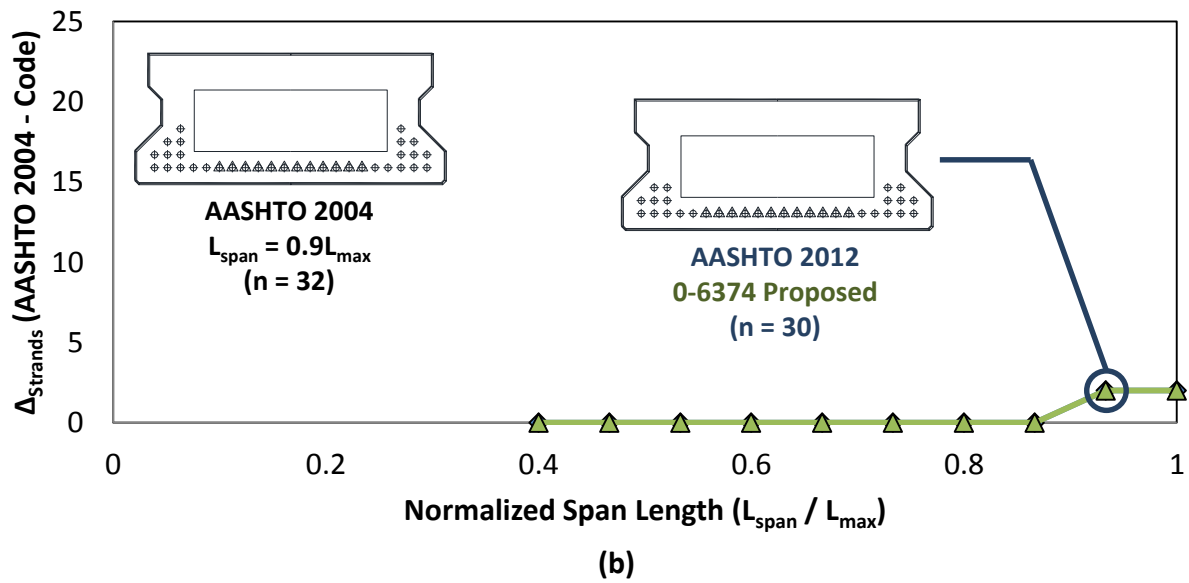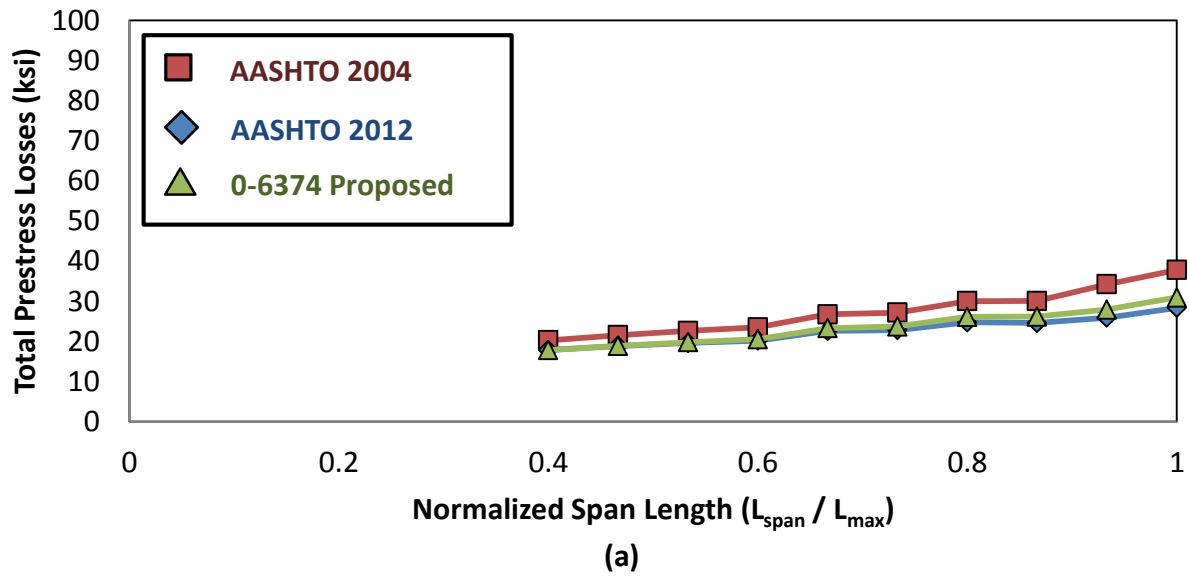*Figure D.2 - Tx28: (a) flexural capacity, (b) required transverse reinforcement, (c) calculated initial camber*
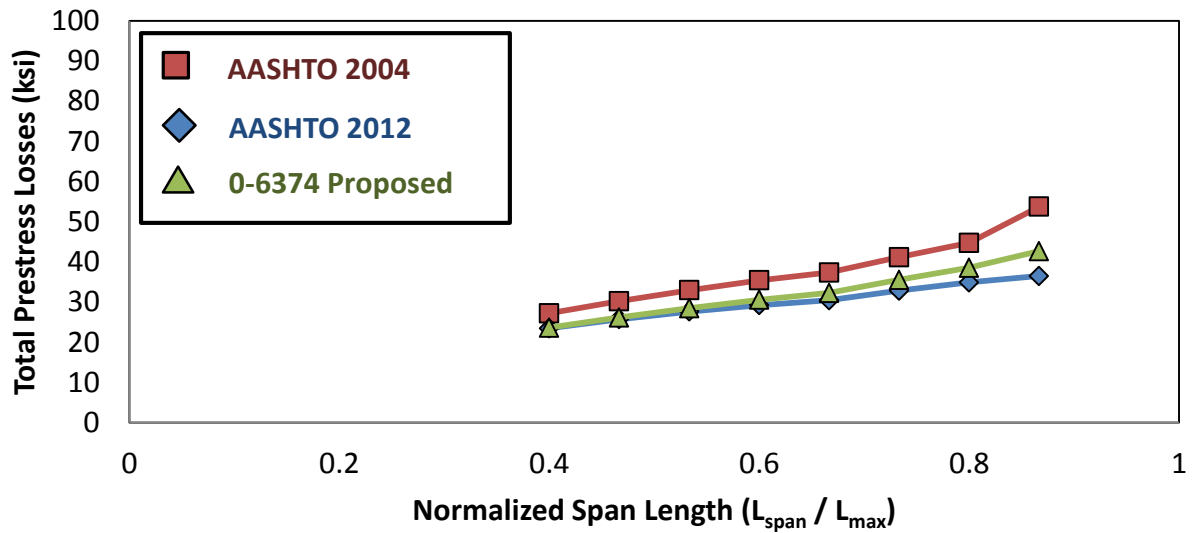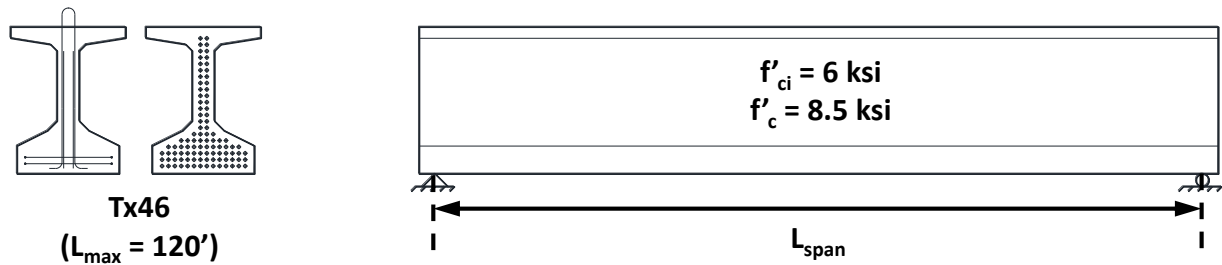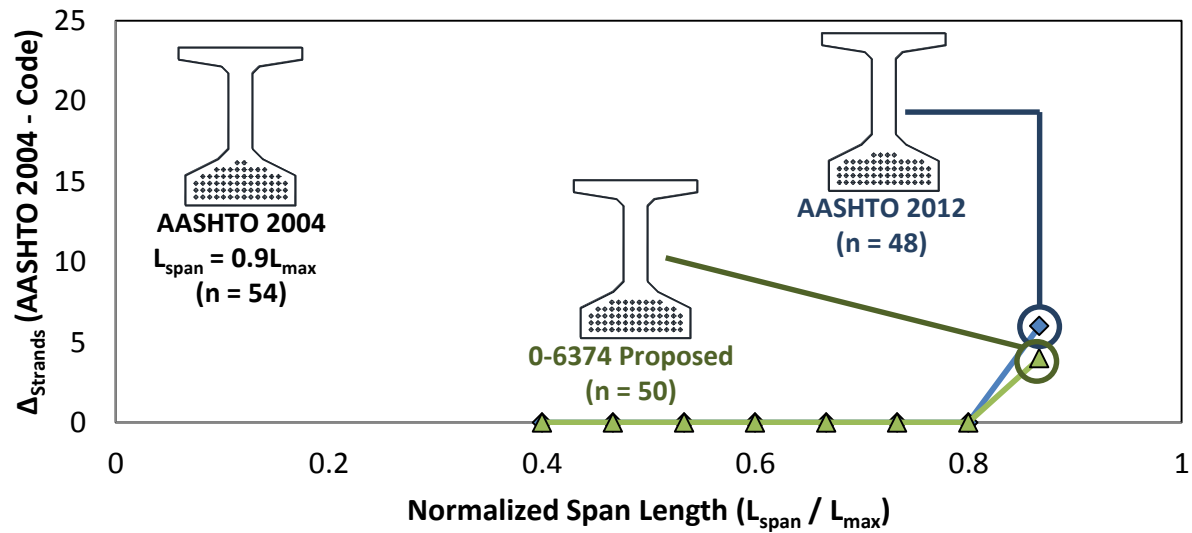
Figure D.3 – Tx46: (a) total prestress loss, (b) Difference in total strands required by AASHTO LRFD 2012 and 0-6374 Proposed versus AASHTO LRFD 2004

244
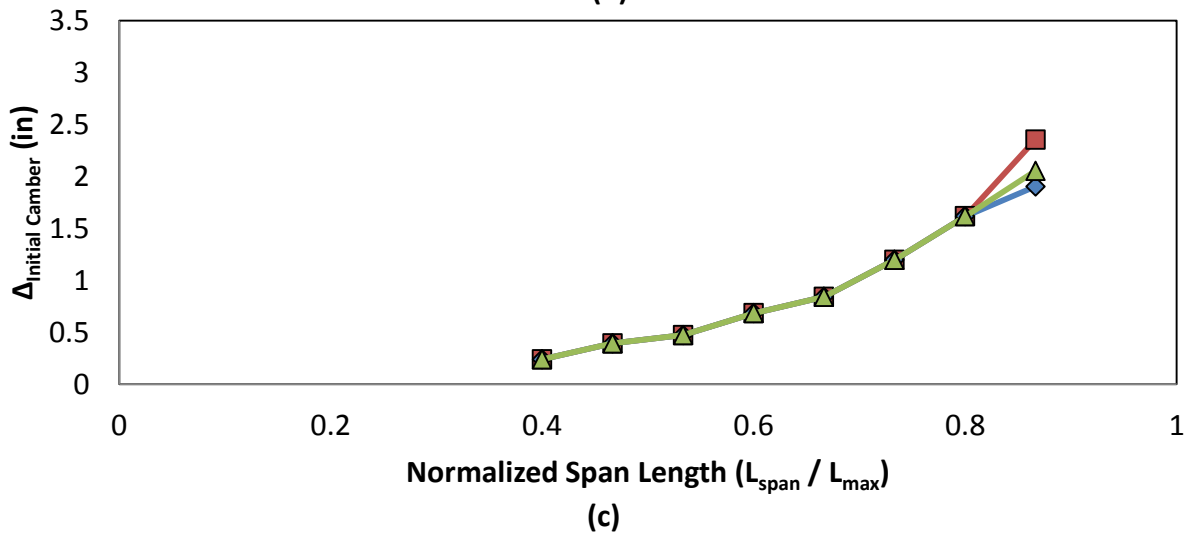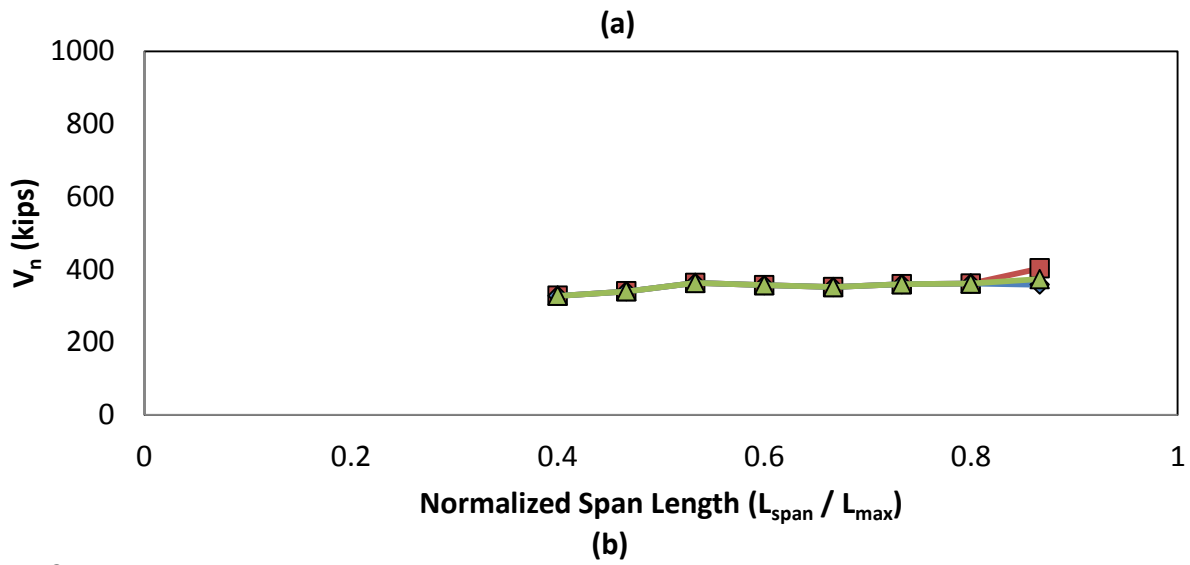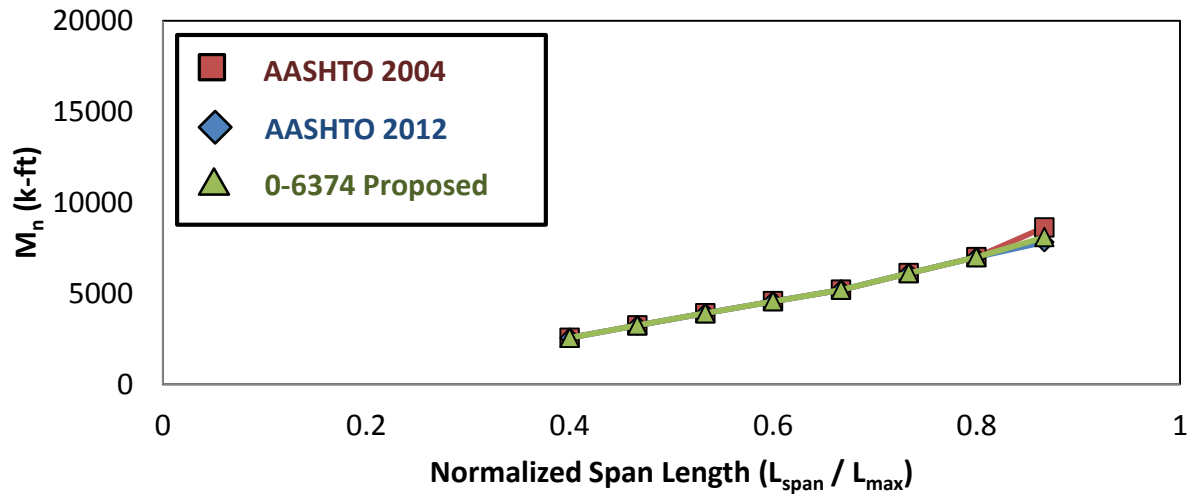
Figure D.4 – Tx46: (a) flexural capacity, (b) required transverse reinforcement, (c) calculated initial camber
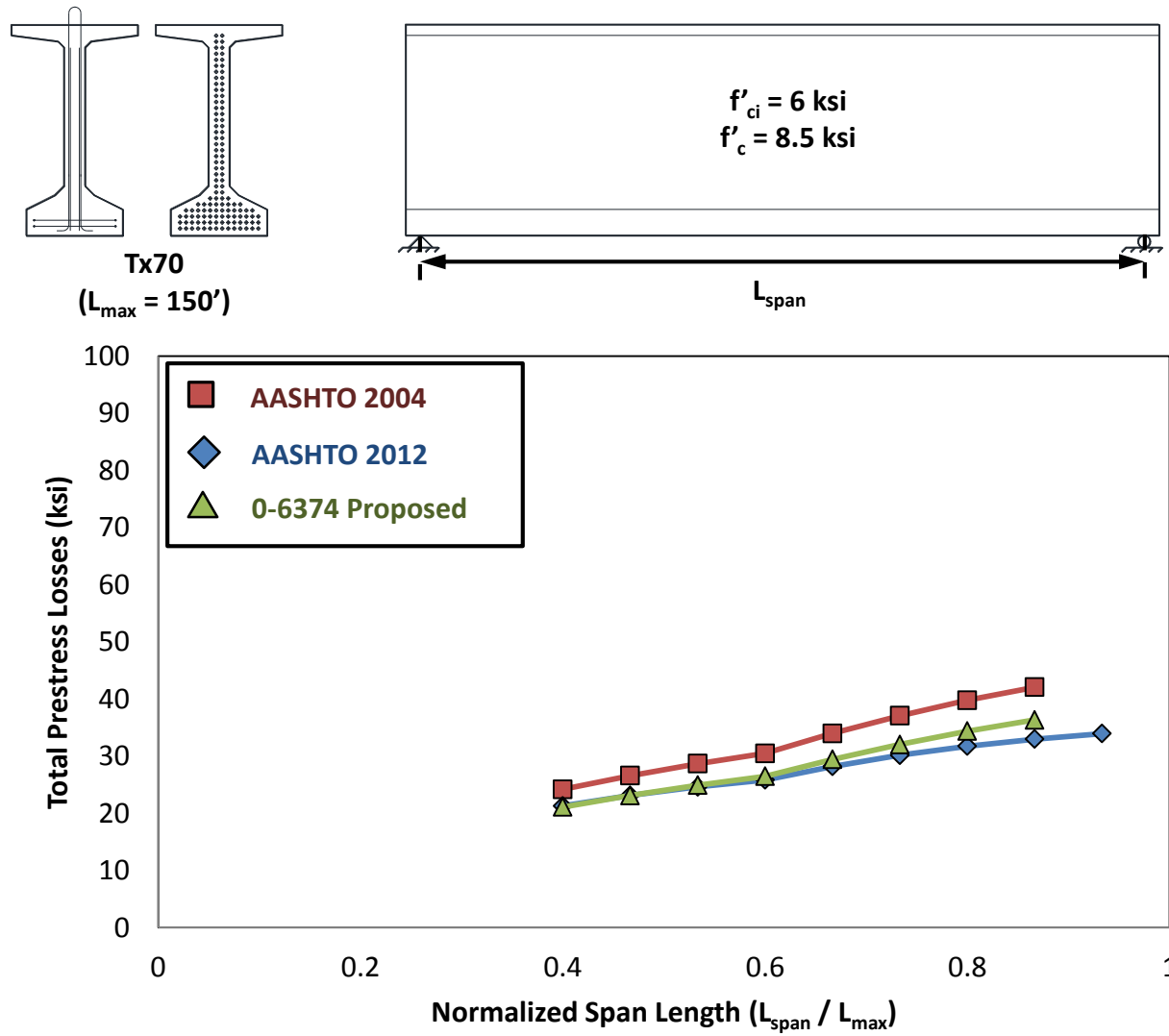
Figure D.5 – Tx70: total prestress loss; no change in strands between designs was observed
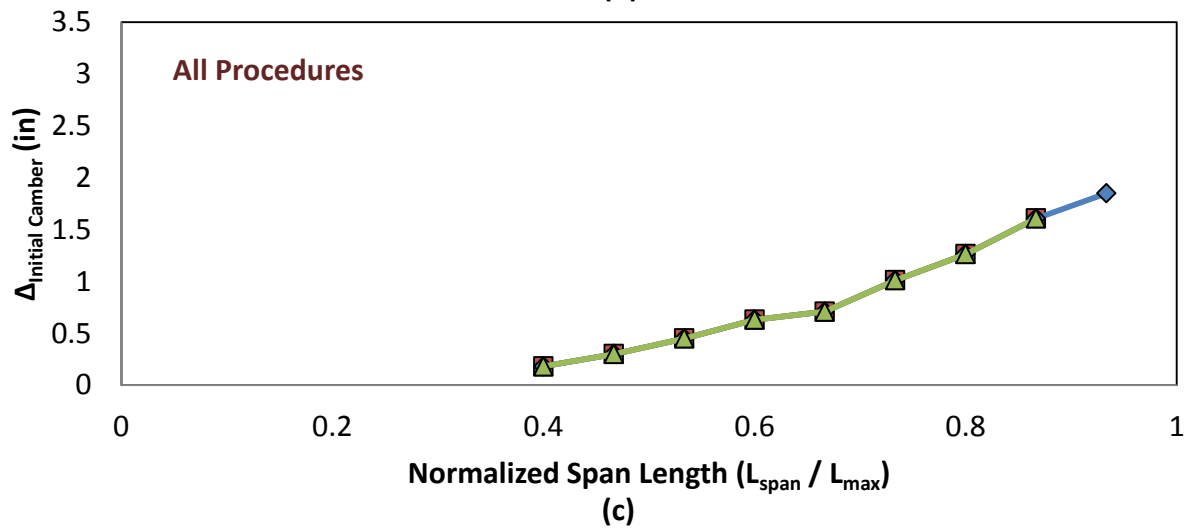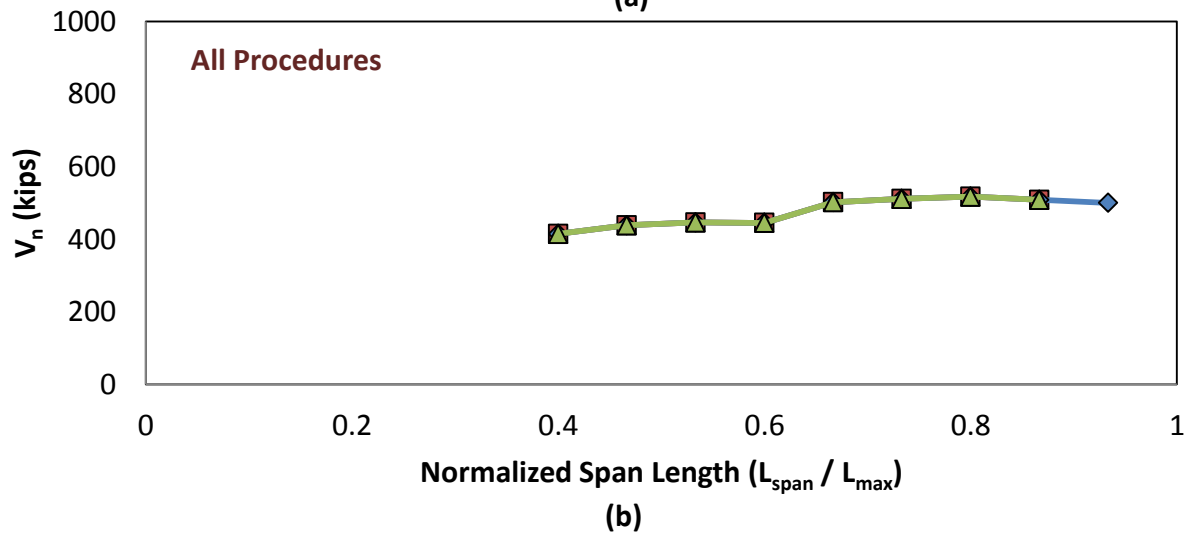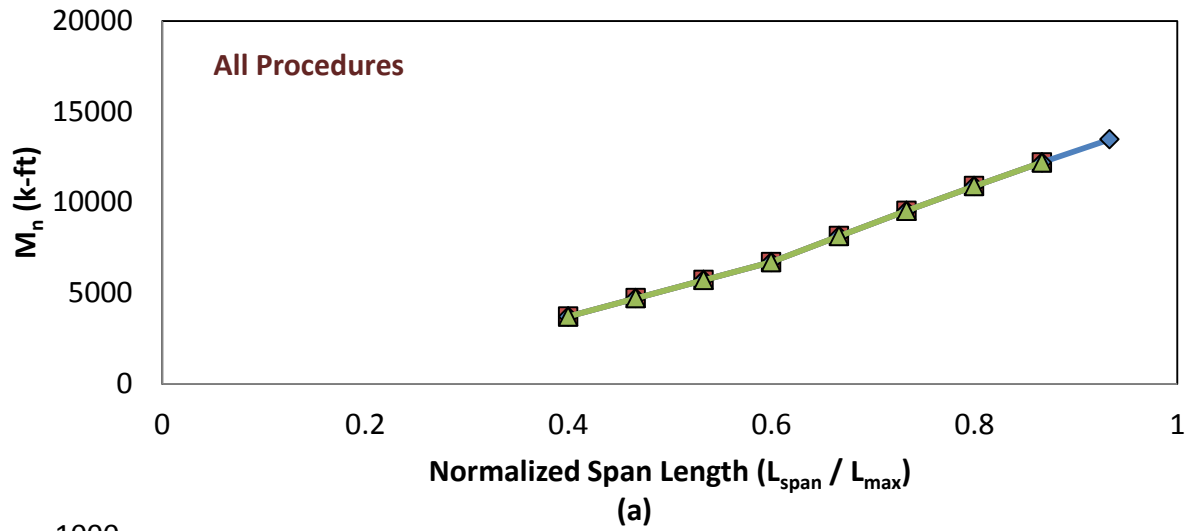
Figure D.6 – Tx70: (a) flexural capacity, (b) required transverse reinforcement, (c) calculated initial camber
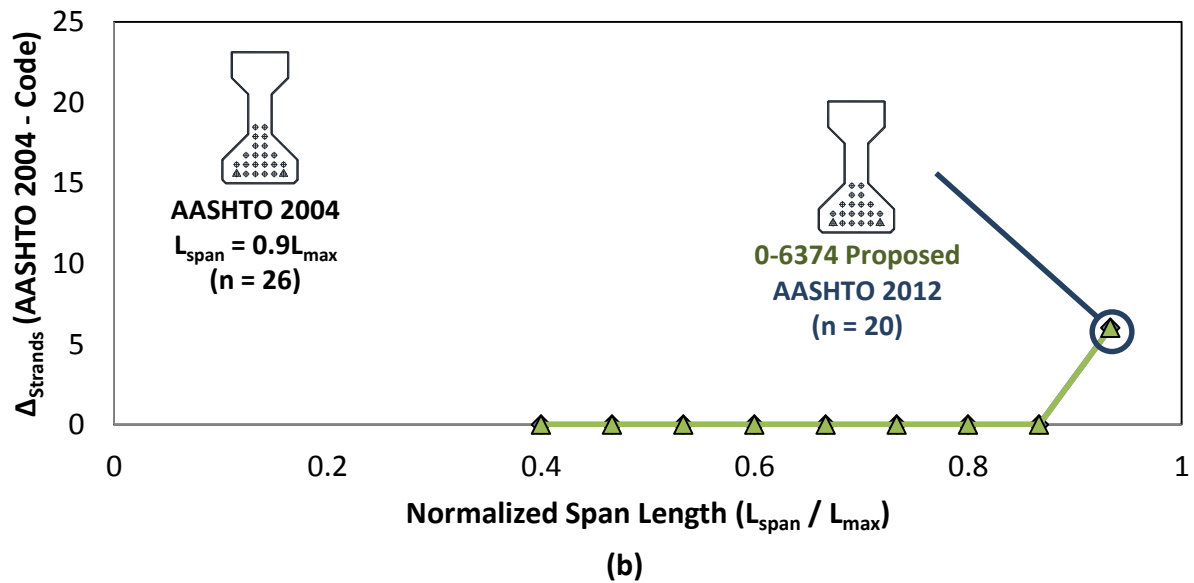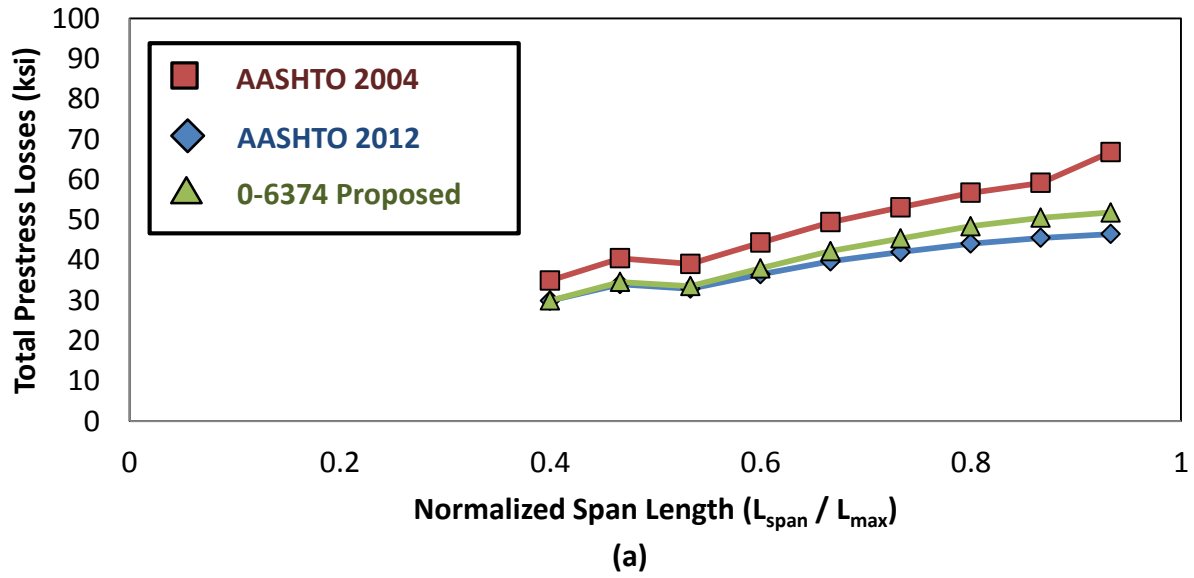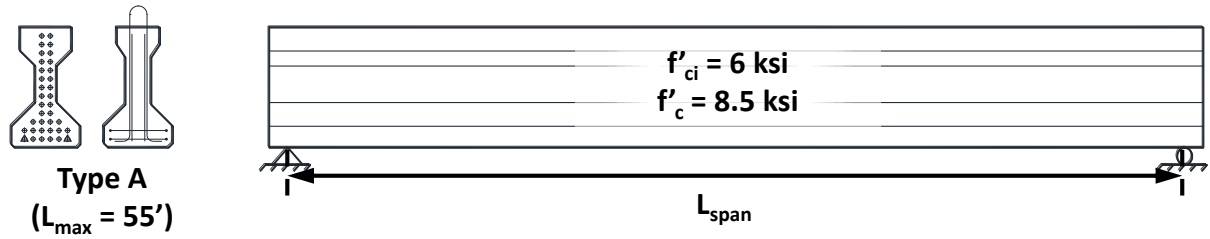
Figure D.7 – Type A: (a) total prestress loss, (b) Difference in total strands required by AASHTO LRFD 2012 and 0-6374 Proposed versus AASHTO LRFD 2004
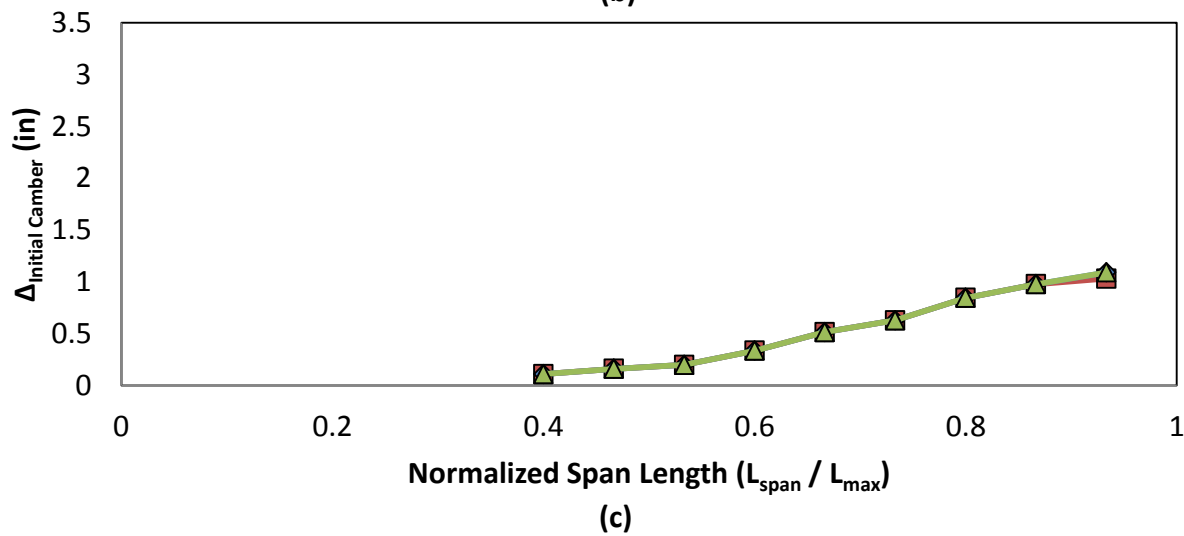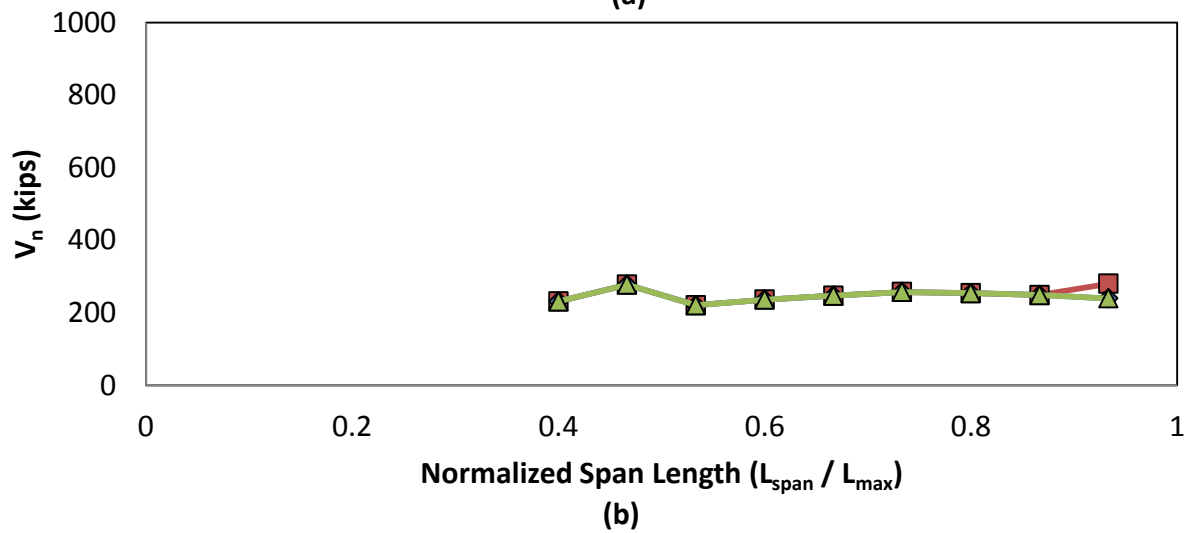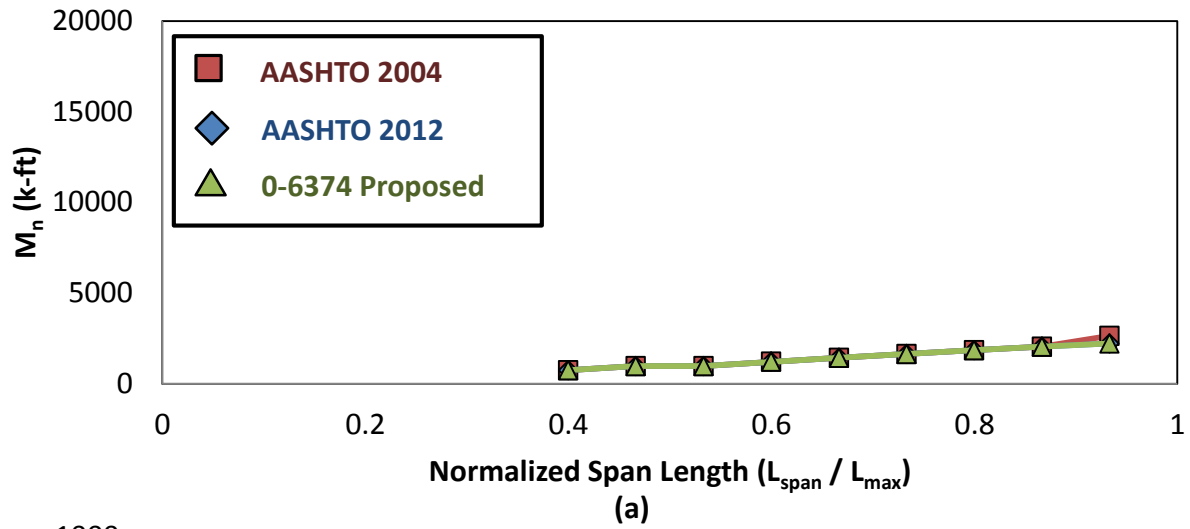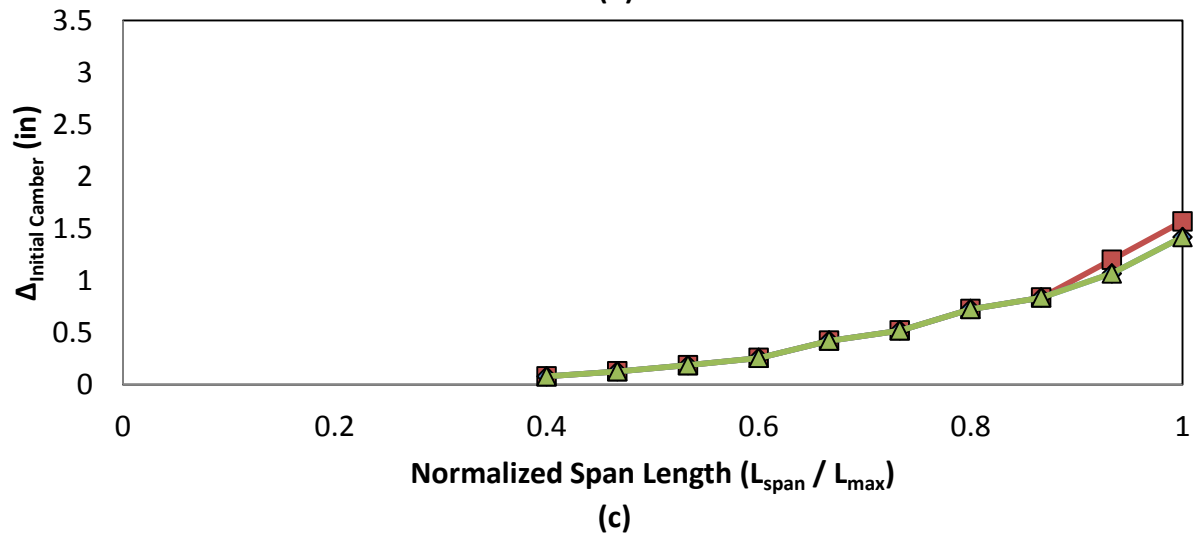
Figure D.8 – Type A: (a) flexural capacity, (b) required transverse reinforcement, (c) calculated initial camber

Figure D.9 - Type C: (a) total prestress loss, (b) Difference in total strands required by AASHTO LRFD 2012 and 0-6374 Proposed versus AASHTO LRFD 2004
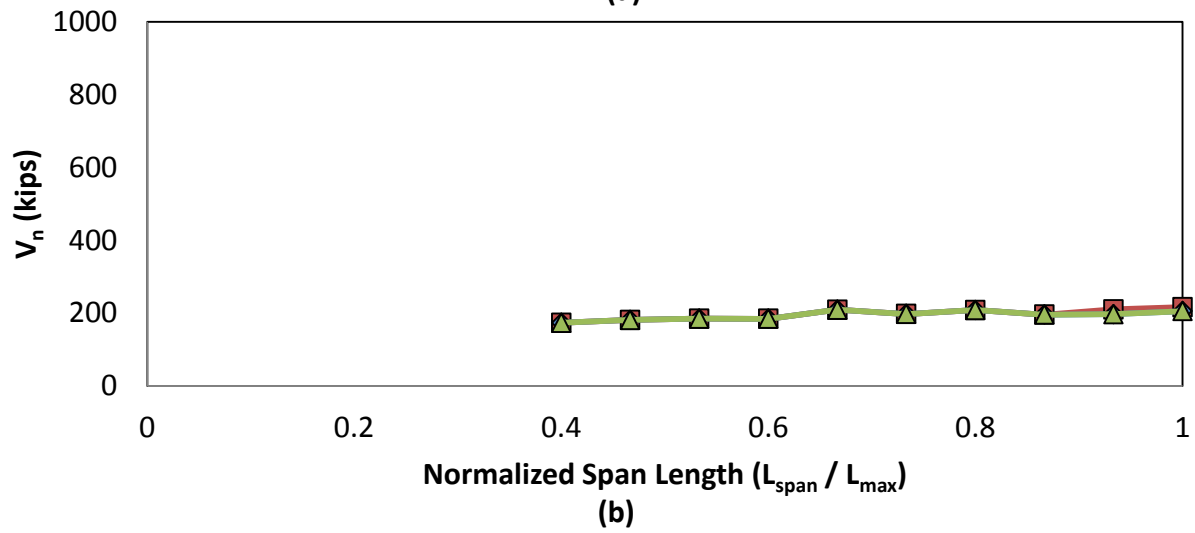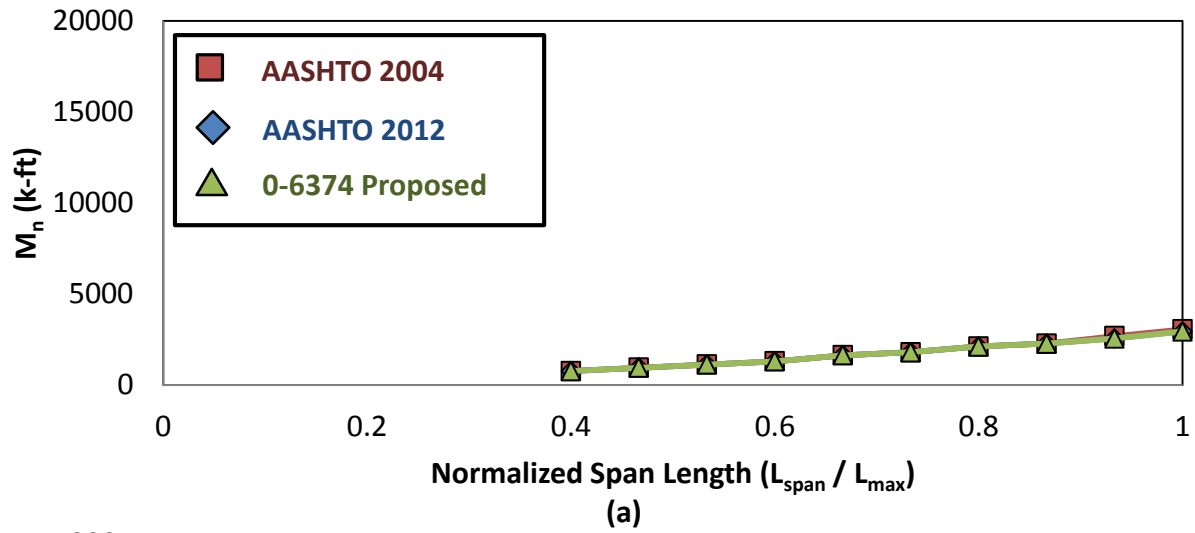
250

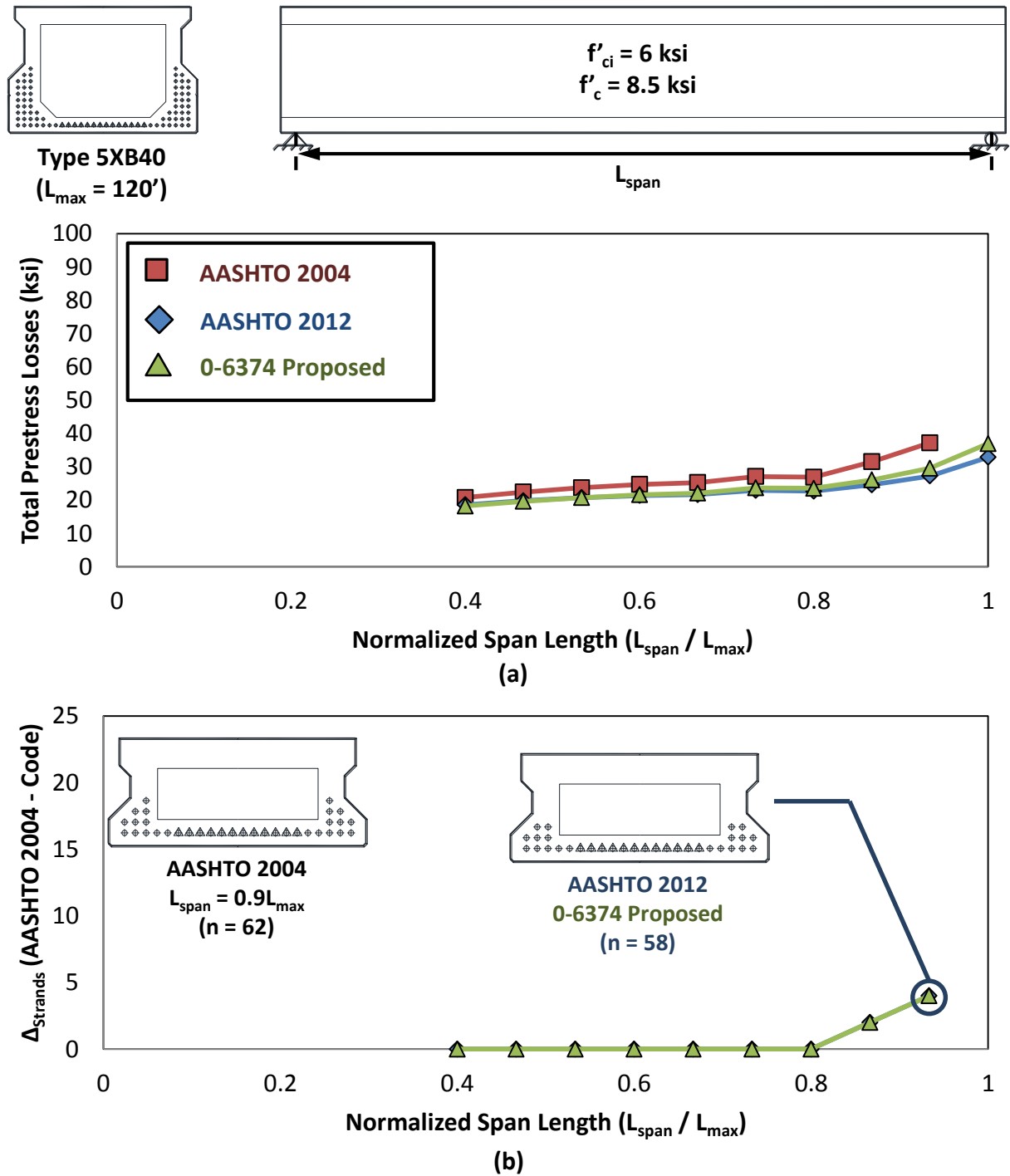*Figure D.10 - Type C: (a) flexural capacity, (b) required transverse reinforcement, (c) calculated initial camber*

Figure D.11 - Type VI: (a) total prestress loss, (b) Difference in total strands required by AASHTO LRFD 2012 and 0-6374 Proposed versus AASHTO LRFD 2004

252

Figure D.12 - Type VI: (a) flexural capacity, (b) required transverse reinforcement, (c) calculated initial camber

Figure D.13 - Type 5XB20: (a) total prestress loss, (b) Difference in total strands required by AASHTO LRFD 2012 and 0-6374 Proposed versus AASHTO LRFD 2004
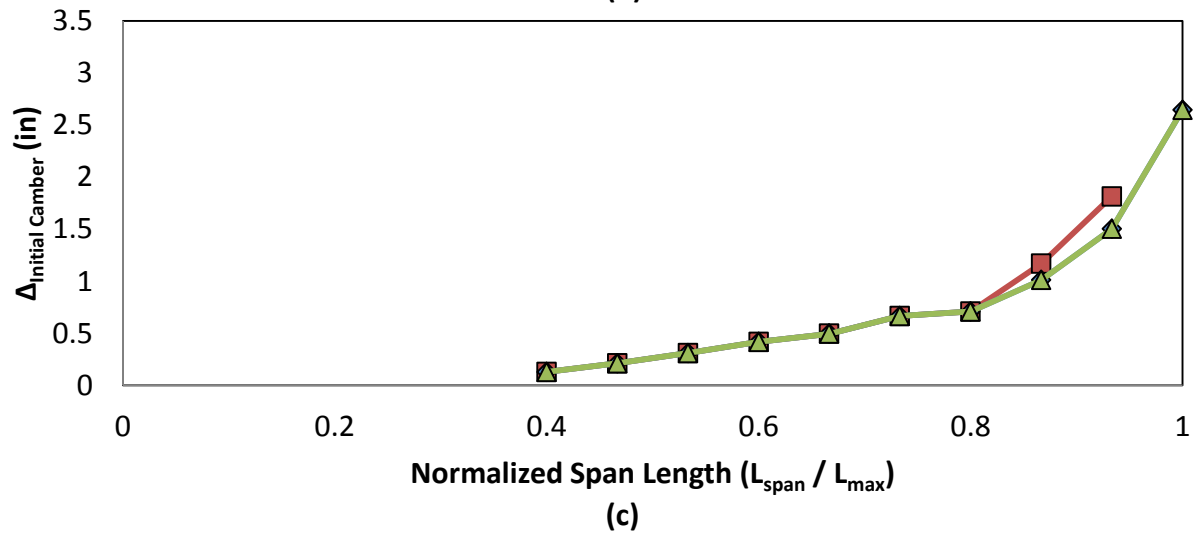
Figure D.14 - Type 5XB20: (a) flexural capacity, (b) required transverse reinforcement, (c) calculated initial camber

Figure D.15 – Type 5XB40: (a) total prestress loss, (b) Difference in total strands required by AASHTO LRFD 2012 and 0-6374 Proposed versus AASHTO LRFD 2004
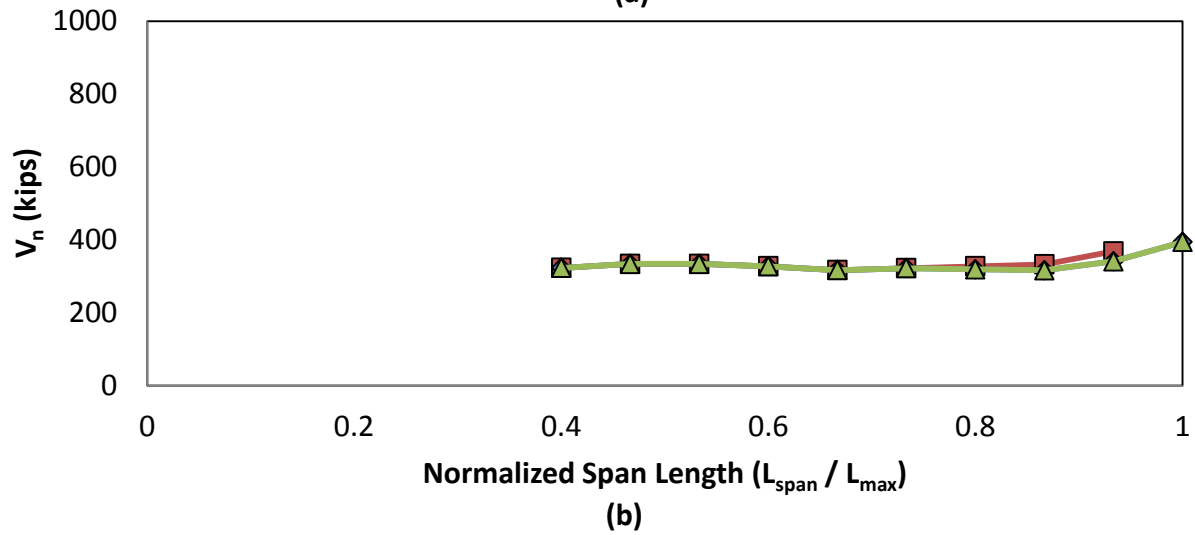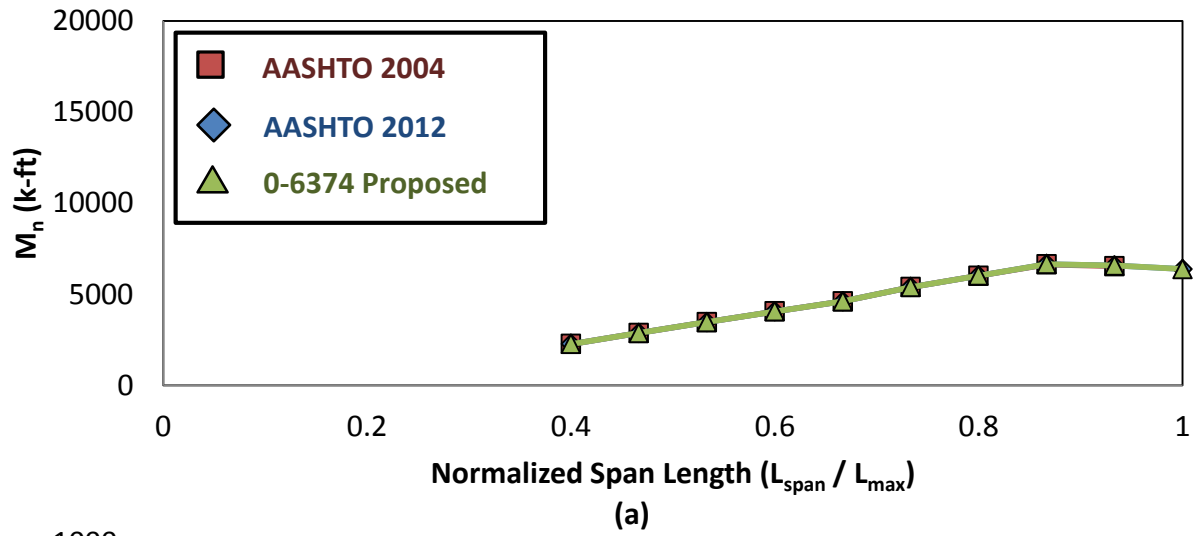
256

Figure D.16 - Type 5XB40: (a) flexural capacity, (b) required transverse reinforcement, (c) calculated initial camber
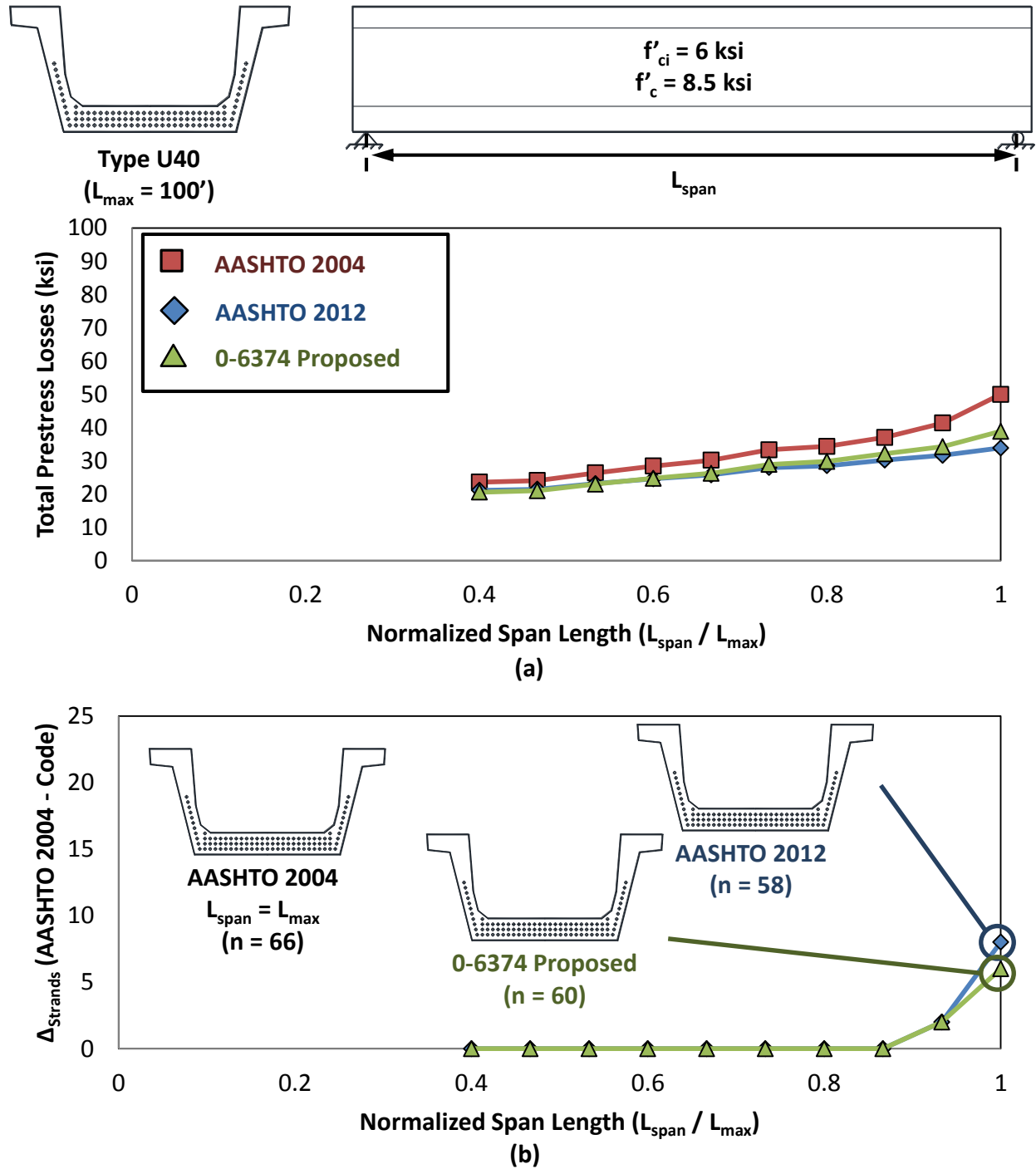
Figure D.17 - Type U40: (a) total prestress loss, (b) Difference in total strands required by
AASHTO LRFD 2012 and 0-6374 Proposed versus AASHTO LRFD 2004

258

Figure D.18 - Type U40: (a) flexural capacity, (b) required transverse reinforcement, (c) calculated initial camber
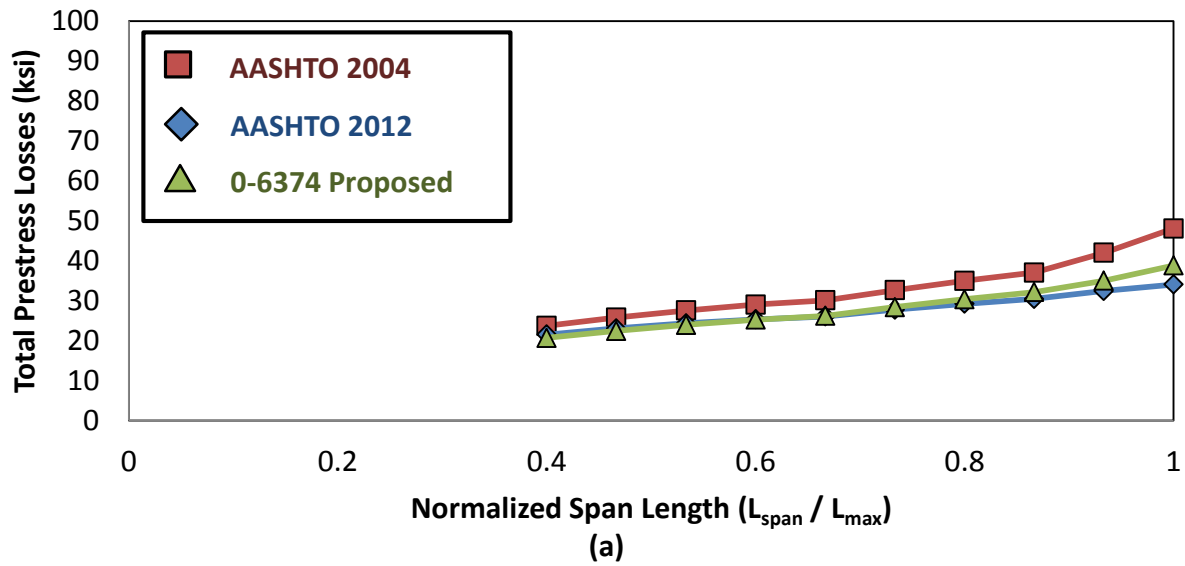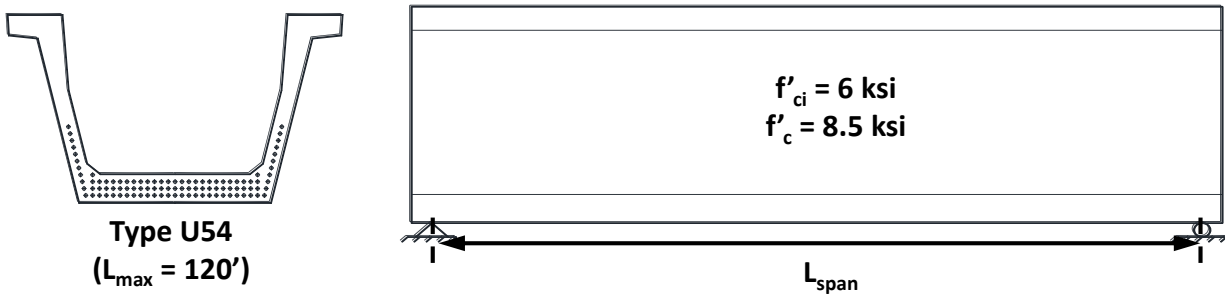
Figure D.19 - Type U54: (a) total prestress loss, (b) Difference in total strands required by AASHTO LRFD 2012 and 0-6374 Proposed versus AASHTO LRFD 2004
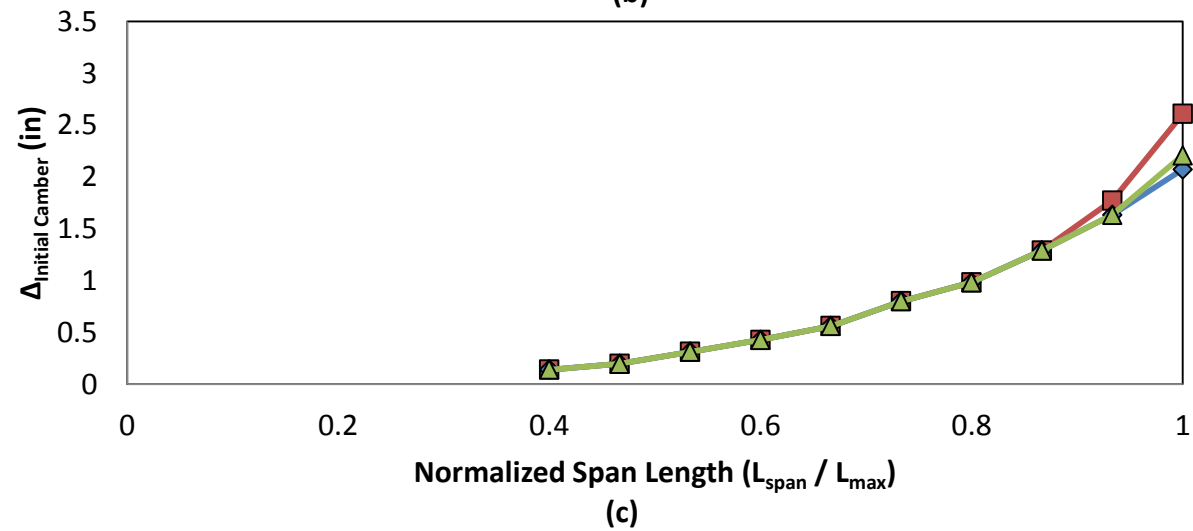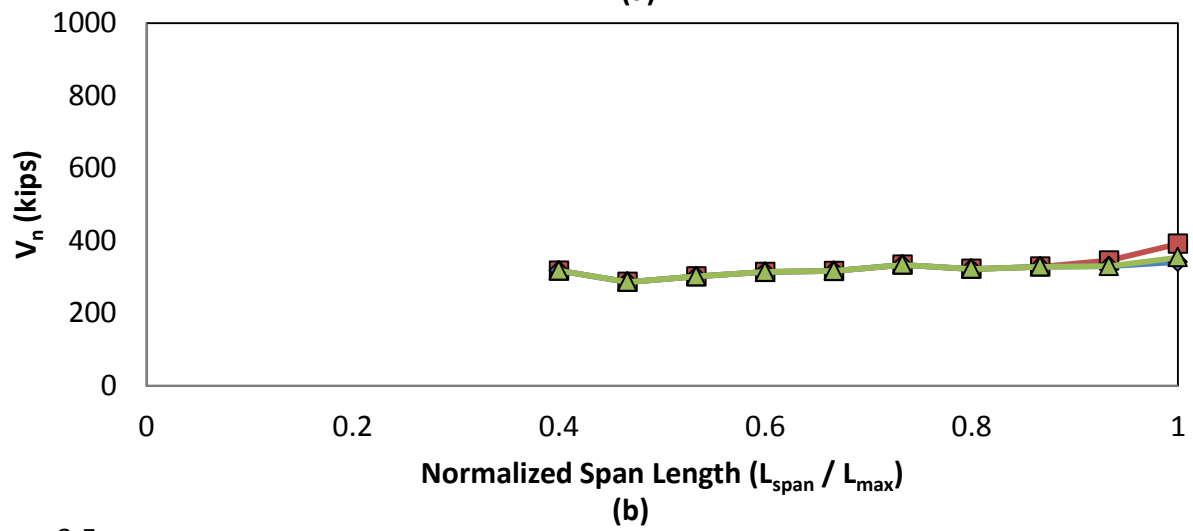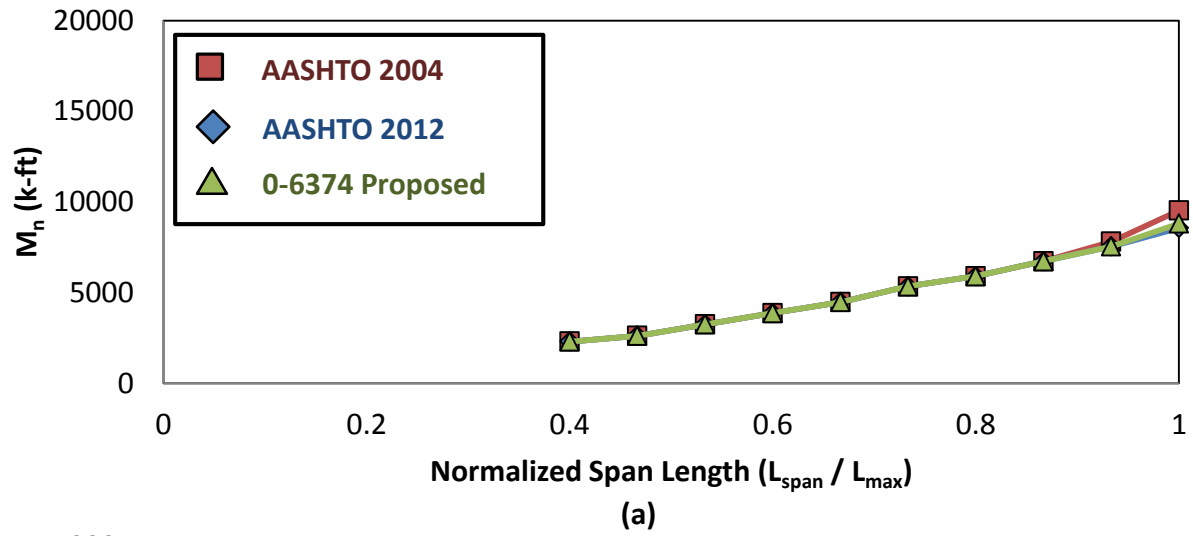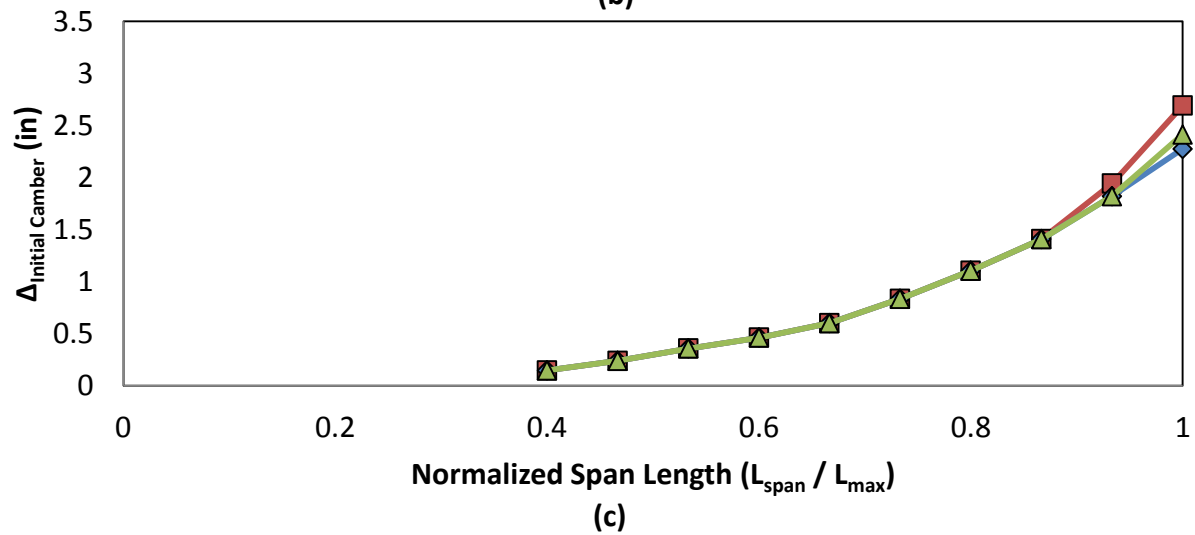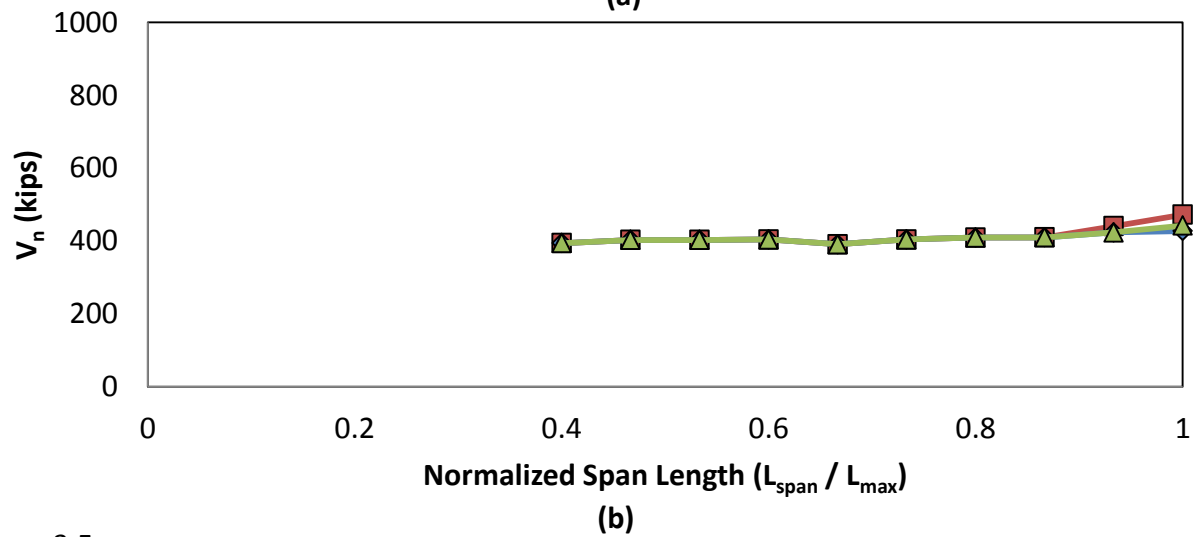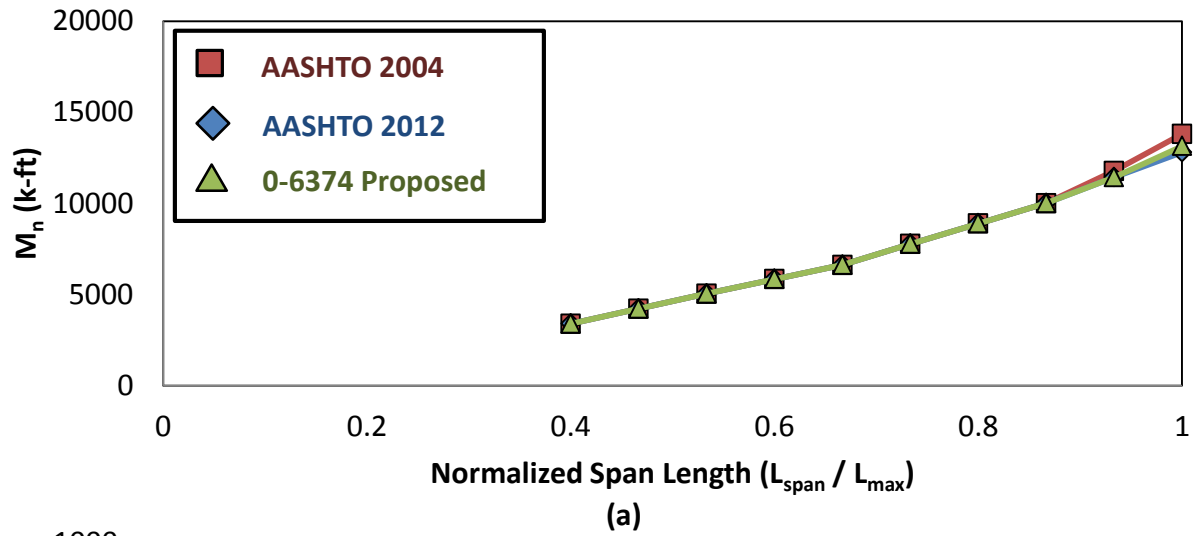
Figure D.20 - Type U54: (a) flexural capacity, (b) required transverse reinforcement, (c) calculated initial camber

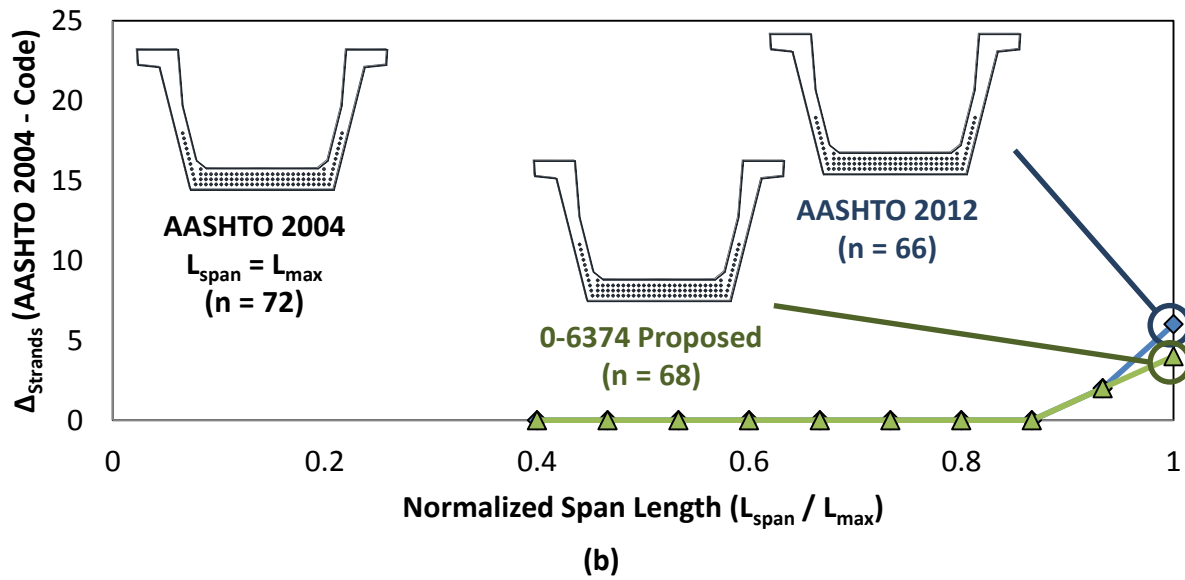## D.3 RESULTS – VARYING RELEASE STRENGTH OF CONCRETE (F_{CI})
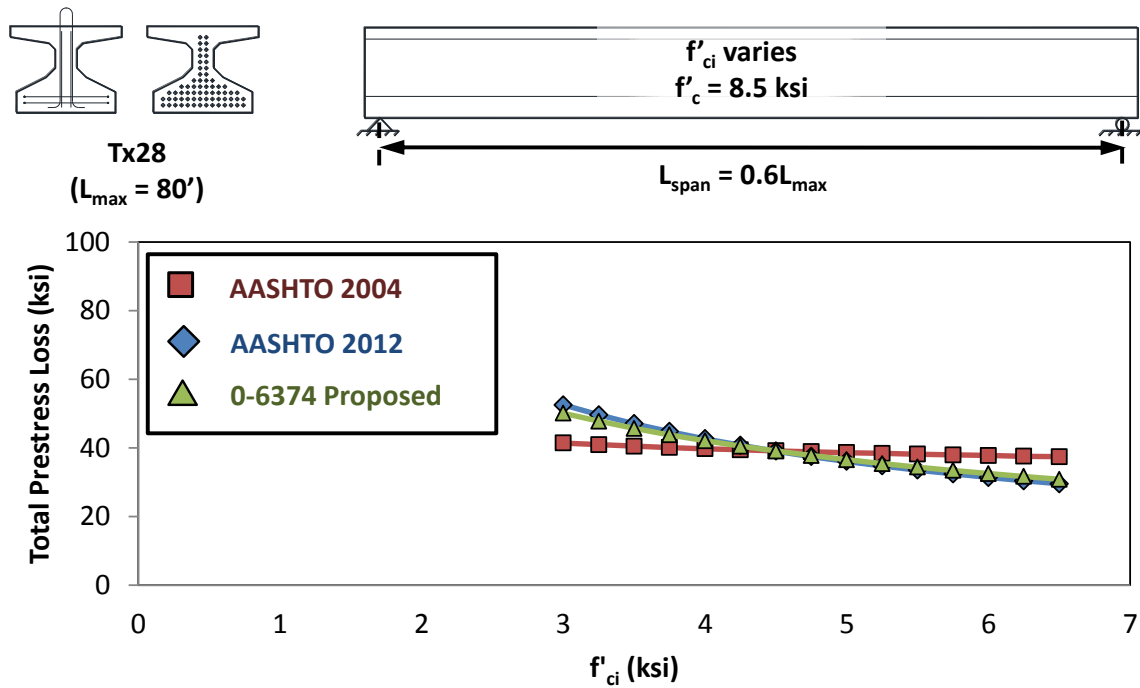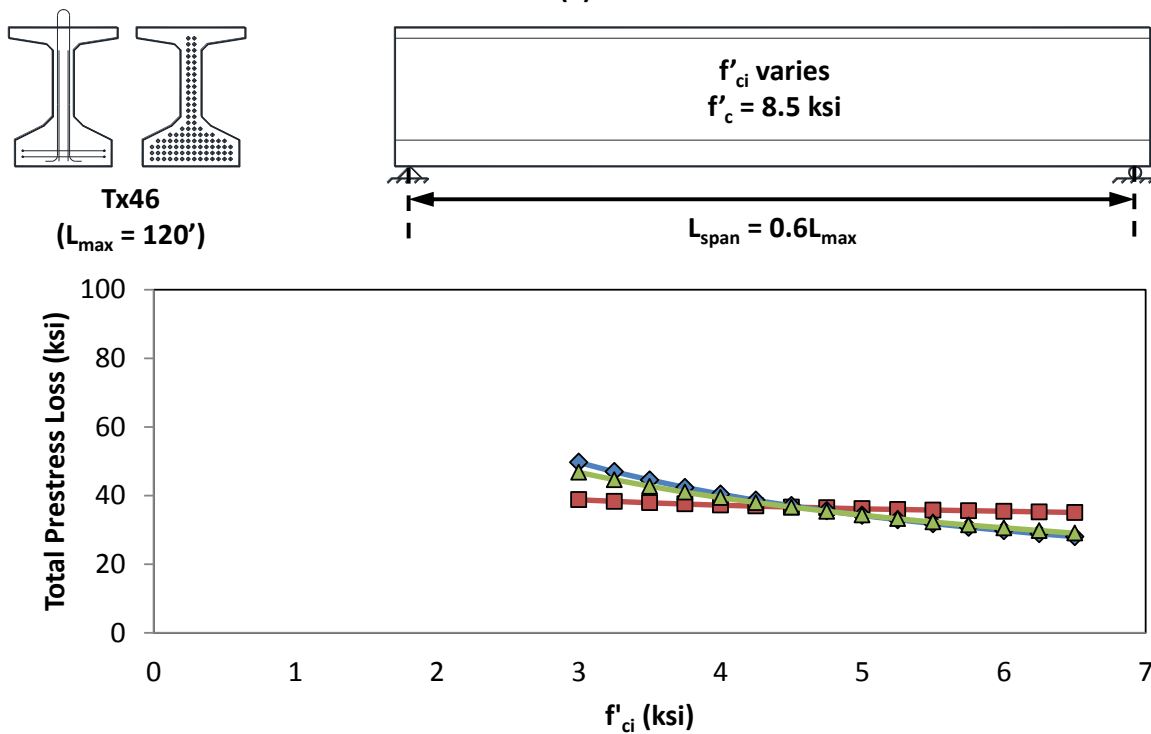
Figure D.21 – Prestress loss with varying release strength for (a) Tx28 and (b) Tx46
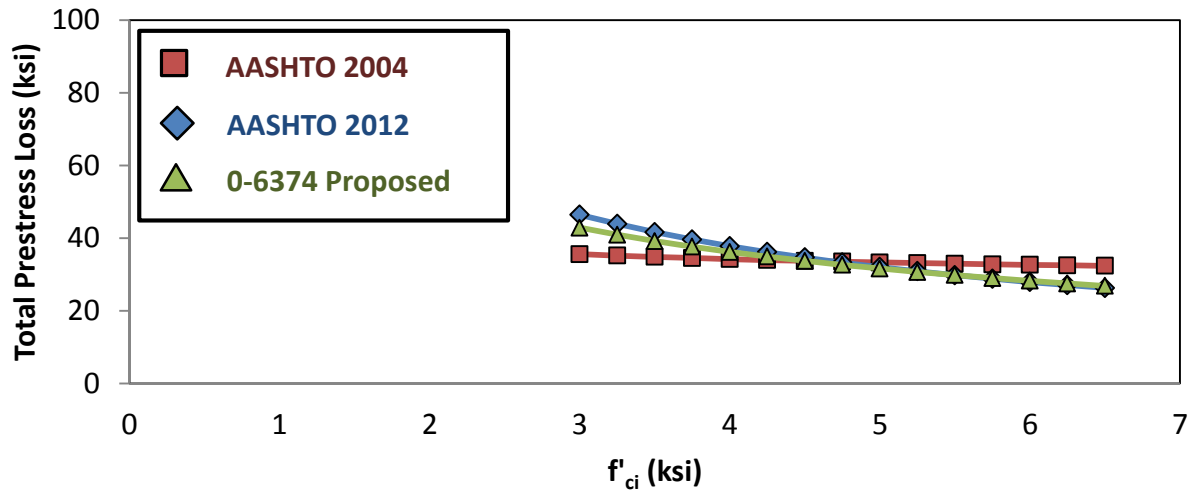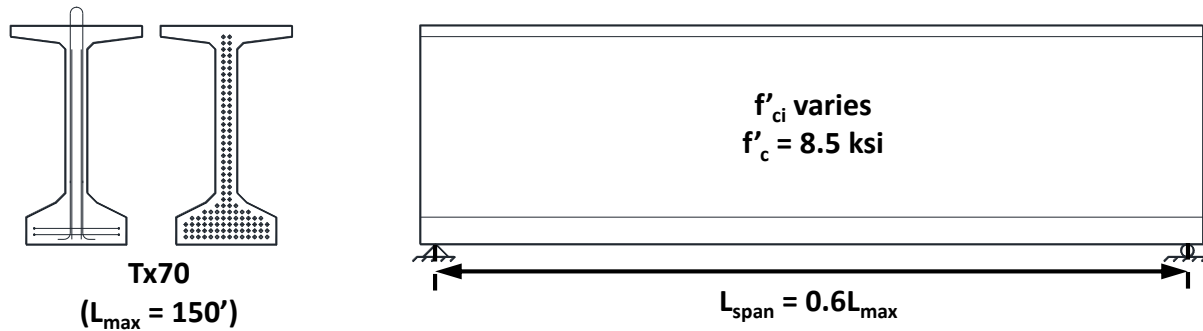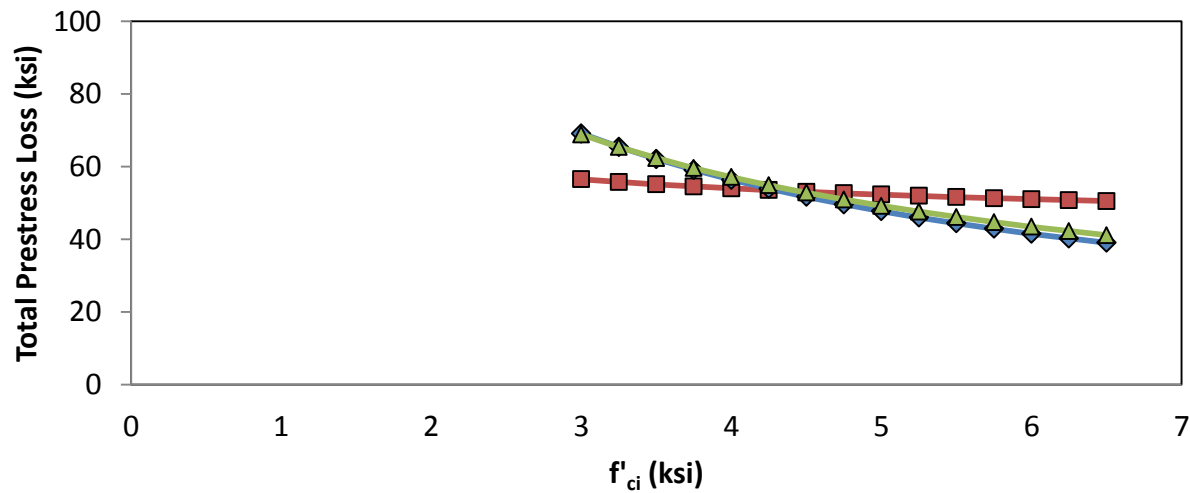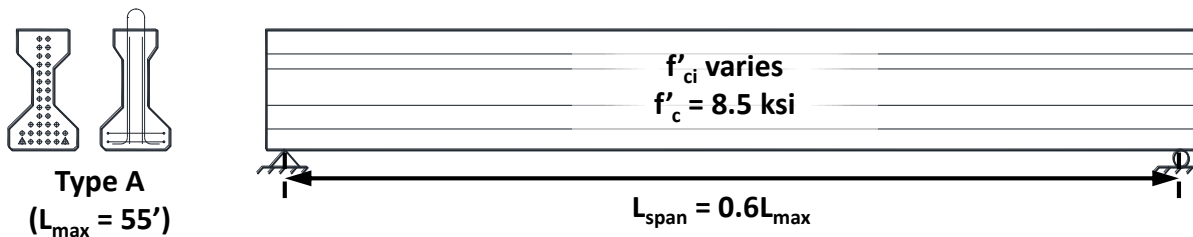
Figure D.22 - Prestress loss with varying release strength for (a) Tx70 and (b) Type A
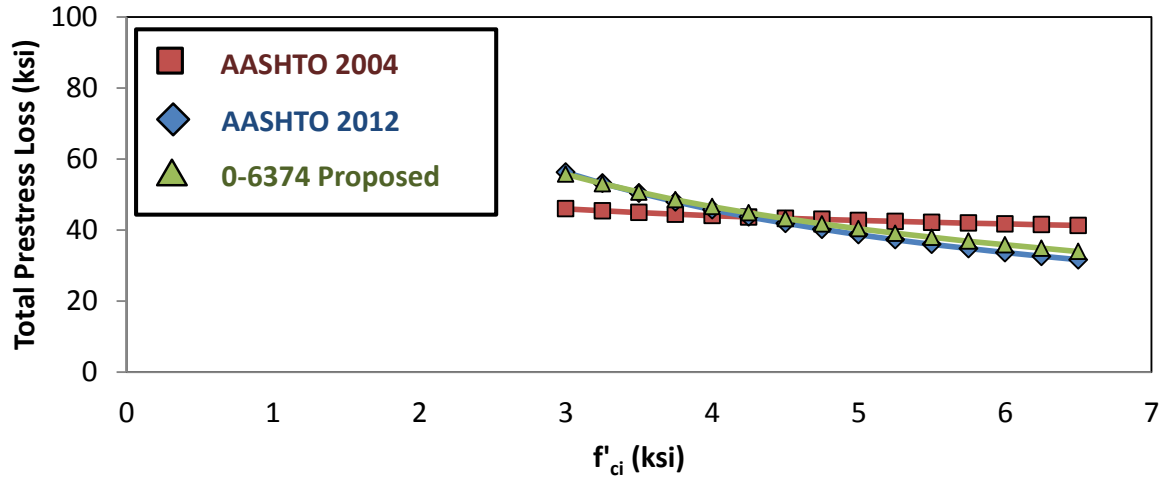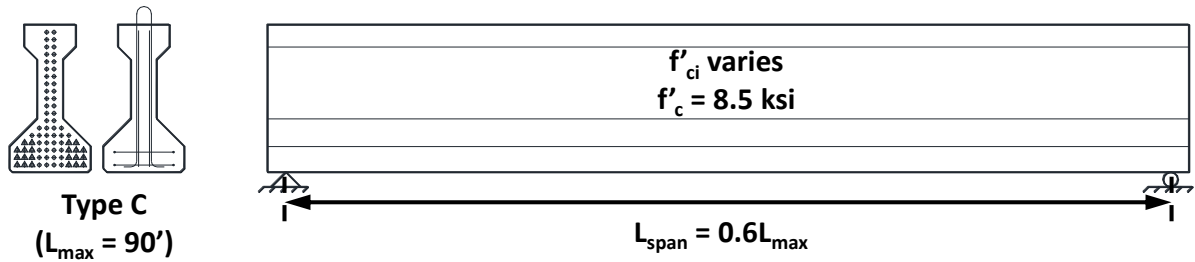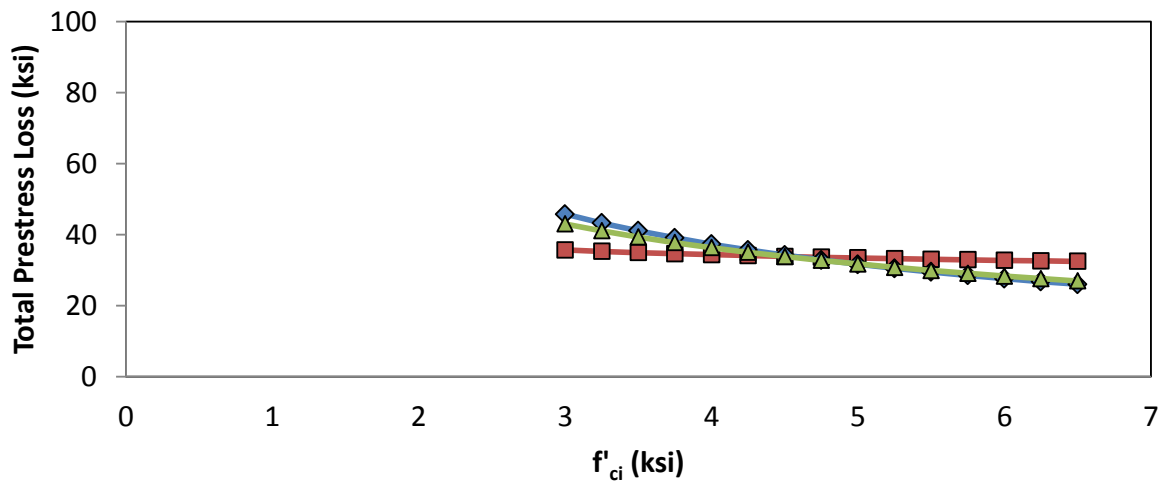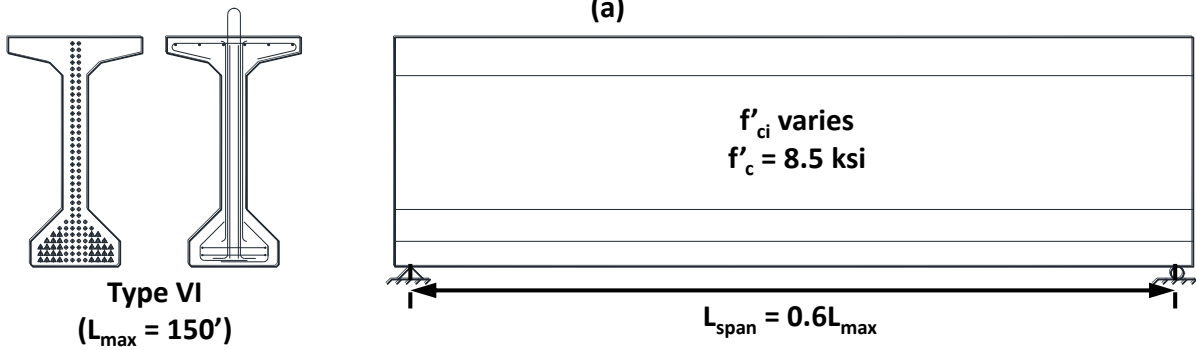
Figure D.23 - Prestress loss with varying release strength for (a) Type C and (b) Type VI
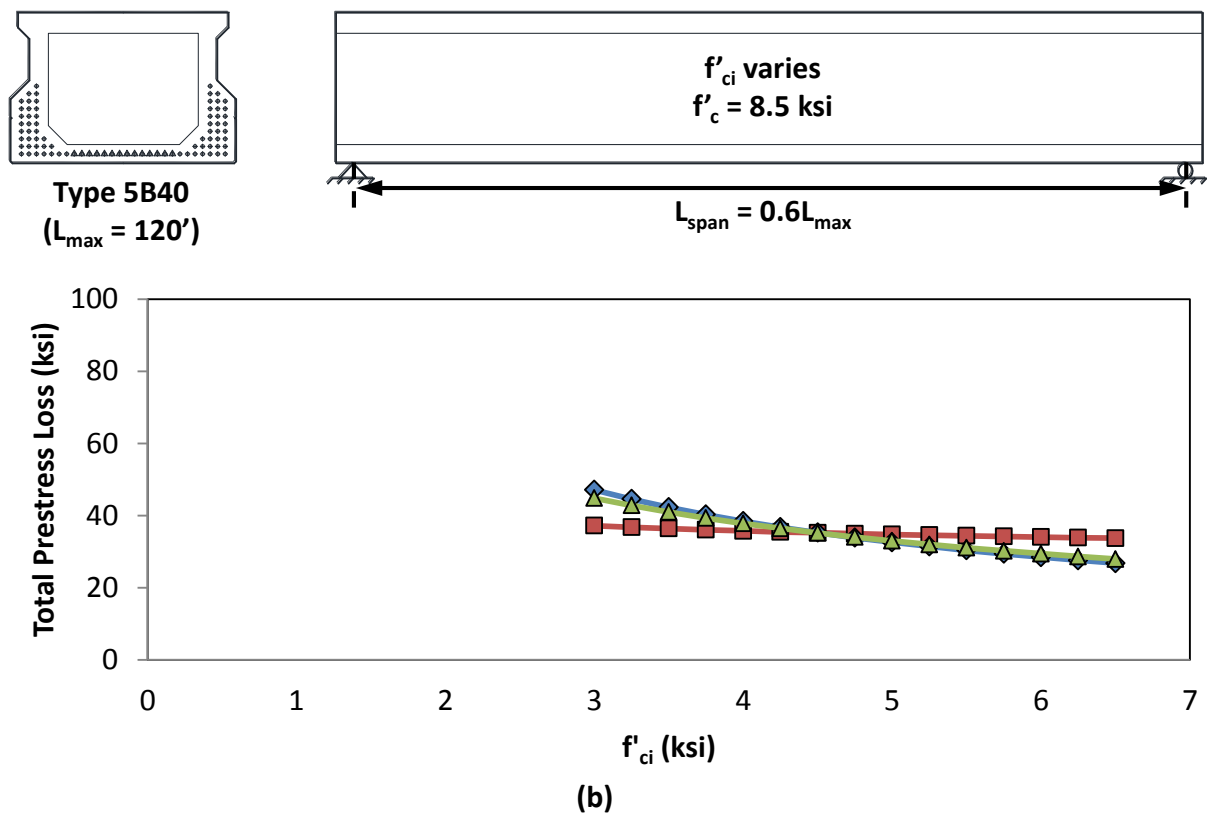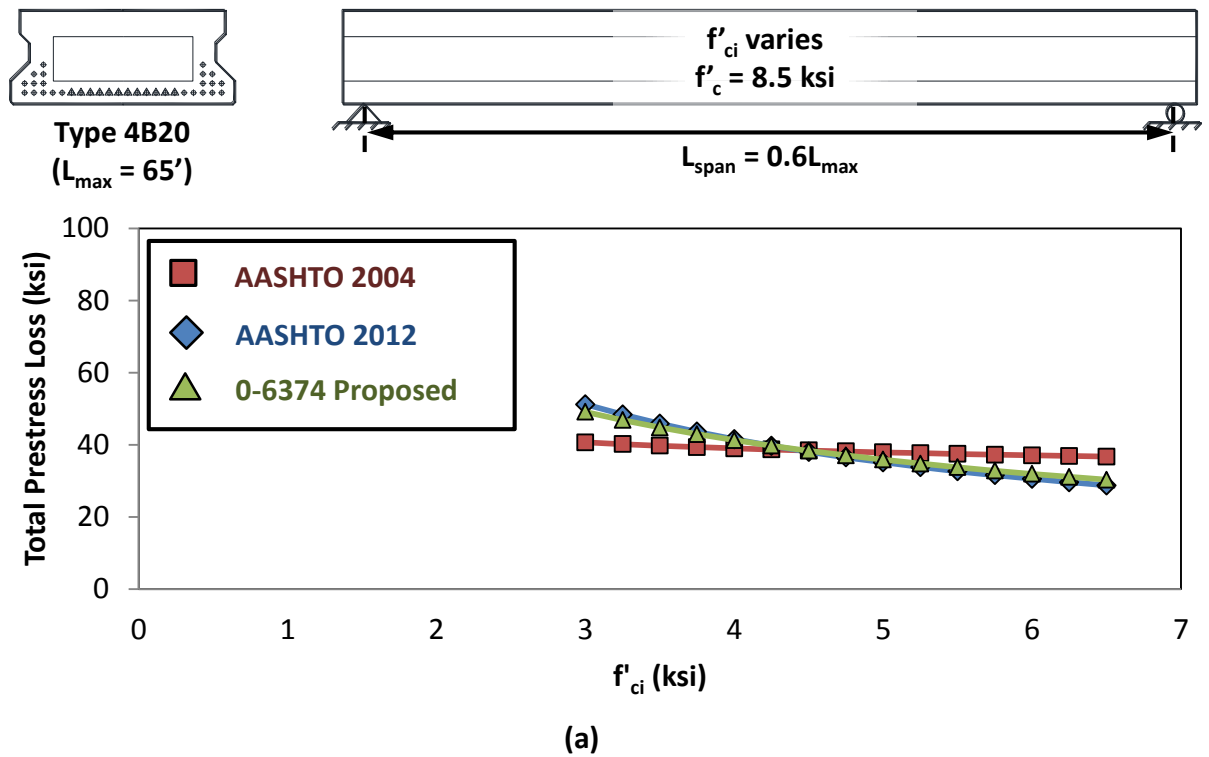
Figure D.24- Prestress loss with varying release strength for (a) Type 4B20 and (b) Type 5B40

Type U40
(L$_{max}$ = 100')

f'$_{ci}$ varies
f'$_c$ = 8.5 ksi

L$_{span}$ = 0.6L$_{max}$

Total Prestress Loss (ksi) vs f'$_{ci}$ (ksi)

- AASHTO 2004
- AASHTO 2012
- 0-6374 Proposed

(a)

Type U54
(L$_{max}$ = 120')

f'$_{ci}$ varies
f'$_c$ = 8.5 ksi

L$_{span}$ = 0.6L$_{max}$

(b)
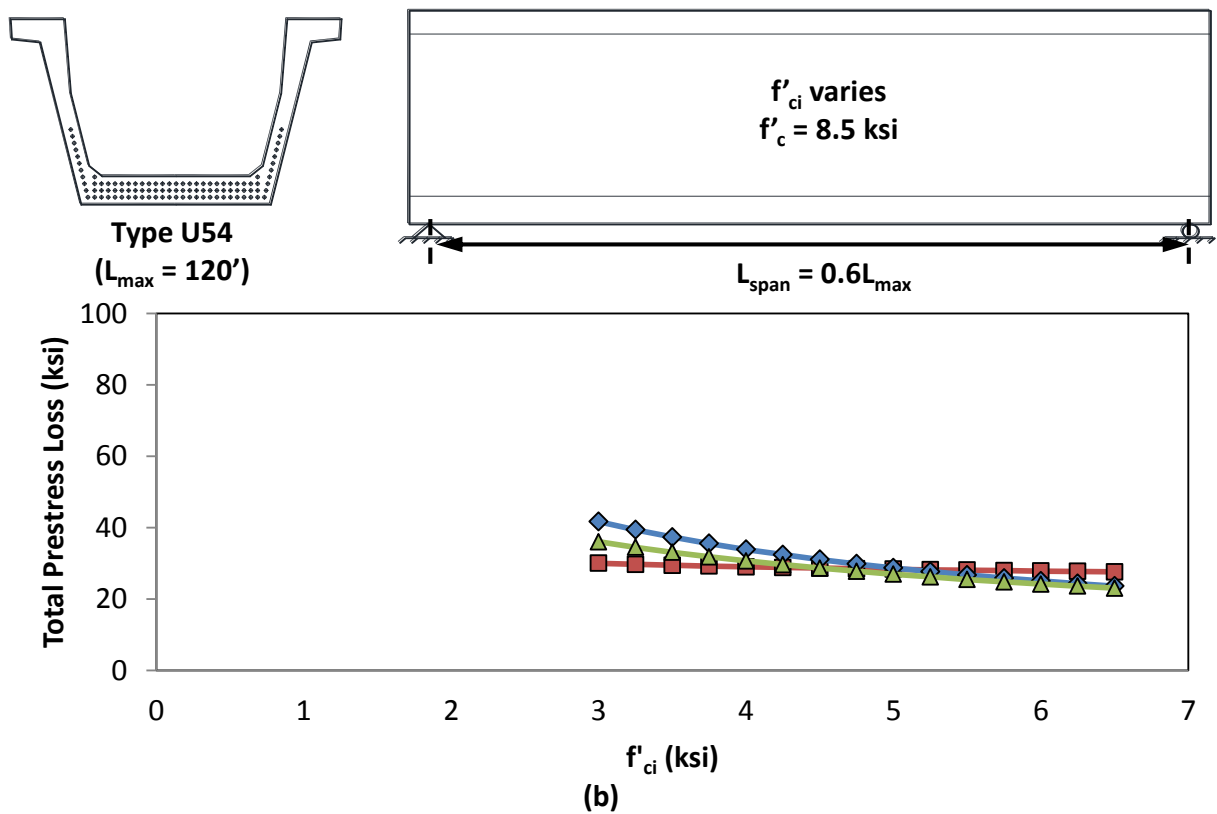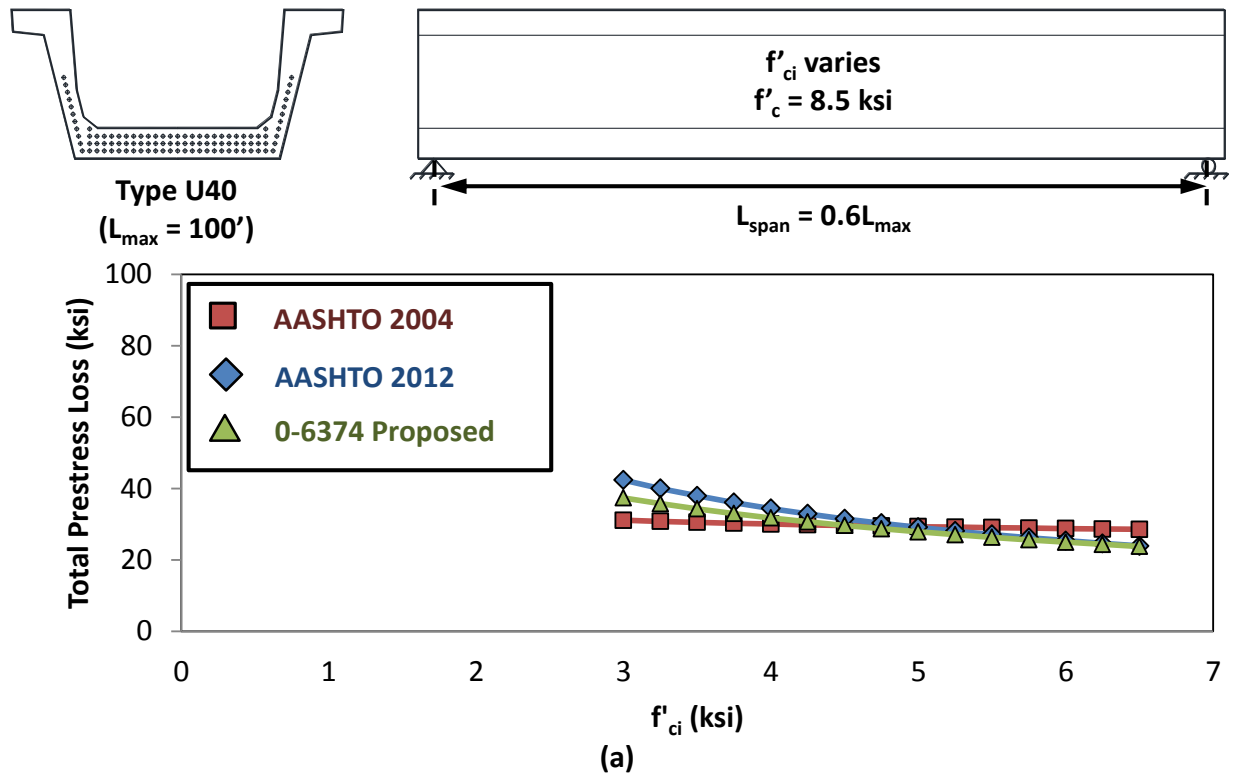
Figure D.25 - Prestress loss with varying release strength for (a) Type U40 and (b) Type U54

APPENDIX E
Approximate / Alternative Methods

E.1 OVERVIEW

Each recent iteration of the AASHTO LRFD Bridge Design Specifications has included a simple, approximate method for estimating prestress losses. In the 2004 AASHTO LRFD Bridge Design Specification there is an approximate lump sum loss value to be used for a variety of bridge types and layouts. In the 2012 AASHTO LRFD Bridge Design Specification, an expression to estimate the approximate long-term loss is provided; this expression being much simpler than the refined loss procedure. Within this appendix, the approximate methods for time dependent loss estimation found in both AASHTO LRFD 2004 and 2012 are introduced, discussed and subjected to a database evaluation.

E.2 CURRENT APPROXIMATIONS AND ALTERNATIVES FOR PRESTRESS LOSSES

The 2004 and 2012 AASHTO LRFD Bridge Design Specifications include approximate/alternative methods for estimation of by the short-term (i.e. elastic shortening) and long-term prestress losses. These methods are included to allow the designer the option to use more simple and straight-forward loss expressions for the purposes of preliminary design.

E.2.1 AASHTO LRFD 2004 and 2012 - Direct Calculation of Elastic Shortening

The loss procedure in both AASHTO LRFD 2004 and 2012 allows for elastic shortening to be calculated directly using Equation (E.1). This equation is an alternative expression; the derivation for this expression is presented in Table E.1.

$$\Delta f_{pES} = \frac{A_{ps}f_{pbt}\left(I_g + e_m{}^2 A_g\right) - e_m M_g A_g}{A_{ps}\left(I_g + e_m{}^2 A_g\right) + \dfrac{A_g I_g E_{ci}}{E_p}}$$

(E.1)

AASHTO (C5.9.5.2.3a-1)

Where:

A_{ps} = area of prestressing steel (in.^{2})
A_g = gross area of section (in.^{2})
E_{ci} = modulus of elasticity of concrete at transfer (ksi)
E_p = modulus of elasticity of prestressing tendons (ksi)
e_m = average eccentricity at midspan (in.)
f_{pbt} = stress in prestressing steel immediately prior to transfer (ksi)
 = 0.75f$_{pu}$ (for low-relaxation strands)
I_g = moment of inertia of the gross concrete section (in.^{4})
M_g = dead load moment (kip-in.)

Table E.1 – Derivation of AASHTO LRFD Alternate Elastic Shortening Equation

Definition of f_{cgp}	$$f_{cgp} = A_{ps}(f_{pbt} - \Delta f_{pES})\left(\frac{1}{A_g} + \frac{e_m^2}{I_g}\right) - \frac{M_g e_m}{I_g} \qquad \text{(E.2)}$$
Definition of Δf_{pES}	$$\Delta f_{pES} = \frac{E_p}{E_{ci}} f_{cgp} \qquad \text{(E.3)}$$
- Plug (E.4) into (E.5)	$$\Delta f_{pES} = \frac{E_p}{E_{ci}}\left[A_{ps}(f_{pbt} - \Delta f_{pES})\left(\frac{1}{A_g} + \frac{e_m^2}{I_g}\right) - \frac{M_g e_m}{I_g}\right]$$
- Separate to isolate terms containing Δf_{pES}	$$\Delta f_{pES} = \frac{E_p}{E_{ci}} A_{ps} f_{pbt}\left(\frac{1}{A_g} + \frac{e_m^2}{I_g}\right)$$ $$- \frac{E_p}{E_{ci}} A_{ps}\Delta f_{pES}\left(\frac{1}{A_g} + \frac{e_m^2}{I_g}\right) - \frac{E_p}{E_{ci}}\frac{M_g e_m}{I_g}$$
- Bring Δf_{pES} to left and factor out	$$\Delta f_{pES}\left[\frac{E_p}{E_{ci}} A_{ps}\left(\frac{1}{A_g} + \frac{e_m^2}{I_g}\right) + 1\right]$$ $$= \frac{E_p}{E_{ci}} A_{ps} f_{pbt}\left(\frac{1}{A_g} + \frac{e_m^2}{I_g}\right) - \frac{E_p}{E_{ci}}\frac{M_g e_m}{I_g}$$
- Solve for Δf_{pES}	$$\Delta f_{pES} = \frac{\frac{E_p}{E_{ci}} A_{ps} f_{pbt}\left(\frac{1}{A_g} + \frac{e_m^2}{I_g}\right) - \frac{E_p}{E_{ci}}\frac{M_g e_m}{I_g}}{\frac{E_p}{E_{ci}} A_{ps}\left(\frac{1}{A_g} + \frac{e_m^2}{I_g}\right) + 1}$$
- Multiply by $$\frac{A_g I_g}{A_g I_g}\cdot\frac{E_{ci}/E_p}{E_{ci}/E_p}$$	$$\Delta f_{pES} = \frac{\frac{E_p}{E_{ci}} A_{ps} f_{pbt}\left(\frac{1}{A_g} + \frac{e_m^2}{I_g}\right) - \frac{E_p}{E_{ci}}\frac{M_g e_m}{I_g}}{\frac{E_p}{E_{ci}} A_{ps}\left(\frac{1}{A_g} + \frac{e_m^2}{I_g}\right) + 1}\frac{A_g I_g \cdot E_{ci}/E_p}{A_g I_g \cdot E_{ci}/E_p}$$
- Simplify	$$\Delta f_{pES} = \frac{A_{ps} f_{pbt}\left(I_g + e_m^2 A_g\right) - e_m M_g A_g}{A_{ps}\left(I_g + e_m^2 A_g\right) + A_g I_g \frac{E_{ci}}{E_p}}$$

E.2.2 AASHTO LRFD 2004 - Approximation of Long-Term Losses

Table E.2 of AASHTO LRFD 2004 contains the approximate lump sum estimates of the long-term prestress loss for four categories of cross-section type and two different reinforcement strengths. Expressions estimating the upper bound and average lump sum loss are provided to allow the designer to choose the level of conservatism.

This approximate method is limited to:

- Post-tensioned non-segmental members with spans up to 160 ft. and stressed at concrete age of 10 to 30 days, and
- Pretensioned members stressed after attaining a compressive strength $f'_{ci} = 3.5$ ksi

where:

- Members are made from normal weight concrete,
- The concrete is either steam- or moist-cured,
- Prestressing is by bars or strands with normal and low relaxation properties, and
- Average exposure conditions and temperatures characterize the site.

Within the approximate lump sum estimate, an estimated prestress loss is provided for each category. The only variable that is accounted for in the estimate is the concrete strength (f'_c) in two categories and the ratio of prestressed to non-prestressed reinforcement (*PPR* of Equation (E.4)).

Table E.2 - AASHTO LRFD 2004 Approximate Lump Sum Estimate of Time-Dependent Losses (Table 5.9.5.3-1)

Type of Beam Section	Level	For Wires and Strands with f_{pu} = 235, 250 or 270 ksi	For Bars with f_{pu} = 145 or 160 ksi
Rectangular Beams, Solid Slab	Upper Bound	$29.0 + 4.0 PPR$	$19.0 + 6.0 PPR$
	Average	$26.0 + 4.0 PPR$	
Box Girder	Upper Bound	$21.0 + 4.0 PPR$	19.0
	Average	$19.0 + 4.0 PPR$	
I-Girder	Average	$33.0 \left[1.0 - 0.15 \dfrac{f'_c - 6.0}{6.0} \right] + 6.0 PPR$	$19.0 + 6.0 PPR$
Single T, Double T, Hollow Core and Voided Slab	Upper Bound	$39.0 \left[1.0 - 0.15 \dfrac{f'_c - 6.0}{6.0} \right] + 6.0 PPR$	$31.0 \left[1.0 - 0.15 \dfrac{f'_c - 6.0}{6.0} \right] + 6.0 PPR$
	Average	$33.0 \left[1.0 - 0.15 \dfrac{f'_c - 6.0}{6.0} \right] + 6.0 PPR$	

Where:

f'_c = compressive strength at release (ksi)

PPR = partial prestress ratio

$$PPR = \frac{A_{ps}f_{py}}{A_{ps}f_{py} + A_s f_y}$$ **(E.4)**

AASHTO 04 (5.5.4.2.1-2)

A_s = area of nonprestressed tension reinforcement (in.^{2})

A_{ps} = area of prestressing steel (in.^{2})

f_y = specified yield strength of reinforcing bars (ksi)

f_{py} = yield strength of prestressing steel (ksi)

E.2.3 AASHTO LRFD 2012 - Approximation of Long-Term Losses

In AASHTO LRFD 2012, a more detailed approximate procedure for estimating prestress loss is provided. The expressions provided in the specification are shown in Equations (E.5) through (E.7). The approximate procedure is intended to be used for standard precast, pretensioned member subject to normal loading and environmental conditions, where:

- members are made from normal-weight concrete,
- the concrete is either steam- or moist-cured,
- prestressing is by bars or strands with normal and low relaxation properties, and
- average exposure conditions and temperatures characterize the site.

The long-term prestress loss, Δf_{pLT}, due to creep of concrete, shrinkage of concrete, and relaxation of steel shall be estimated using the following formula:

(E.5)

$$\Delta f_{pLT} = 10.0 \frac{f_{pi}A_{ps}}{A_g}\gamma_h\gamma_{st} + 12.0\gamma_h\gamma_{st} + \Delta f_{pR}$$ *AASHTO 12 (5.9.5.3-1)*

Where:

γ_h = correction factor for relative humidity of the ambient air

(E.6)

$$\gamma_h = 1.7 - 0.01H$$

AASHTO 12 (5.9.5.3-2)

γ_{st} = correction factor for specified concrete strength at time of prestress transfer to the concrete member

$$\gamma_{st} = \frac{5}{(1 + f'_{ci})}$$

AASHTO 12 (5.9.5.3-3)

f_{pi} = prestressing steel stress immediately prior to transfer (ksi)
H = the average annual ambient relative humidity (%)
Δf_{pR} = an estimate of relaxation loss taken as 2.4 ksi for low relaxation strand, 10.0 for stress relieved strand, and in accordance with manufacturers recommendation for other types of strand (ksi)
A_{ps} = area of prestressing steel (in.^{2})
A_g = gross cross-sectional area (in.^{2})

In Equation (E.5) the first term is an estimate for the creep loss, the second term for the shrinkage loss and the third term for strand relaxation. This approximate estimate is intended for sections with composite decks, but not to be used for sections with uncommon shapes (i.e. V/S much different than 3.5), high level of prestressing, or atypical construction staging.

E.3   PERFORMANCE OF AASHTO LRFD APPROXIMATE METHODS

The performance of the approximate methods for long-term loss estimation found in both AASHTO LRFD 2004 and 2012 was compared with that of the refined methods in both specifications using the assembled evaluation database. As in all the previous chapters and appendices, the performance of each procedure is evaluated by comparing the estimated prestress loss to the actual final measured loss, by using the estimated-to-actual loss ratio (*E/M*).

E.3.1   AASHTO LRFD 2004

The key statistics from the *E/M* ratios for both the refined and approximate procedures in the AASHTO LRFD 2004 bridge specifications are presented in Table E.3. It can be seen that the approximate method is both less conservative and less precise than the refined method. The approximate prestress loss estimates are plotted versus the measured prestress loss in Figure E.1. It appears that use of the approximate method result in about the same estimated prestress loss, regardless of the actual loss that occurred. This would suggest that this approximate method is a poor model of the actual loss.

Table E.3 – Comparison of performance of AASHTO LRFD 2004 refined and approximate procedures using estimated-to-actual ratio (*E/M*) from the evaluation database

	Refined	Approximate
Minimum	0.89	0.67
Average	1.74	1.47
Maximum	3.69	3.06
Co. of Variation	0.26	0.29
St. Deviation	0.45	0.42
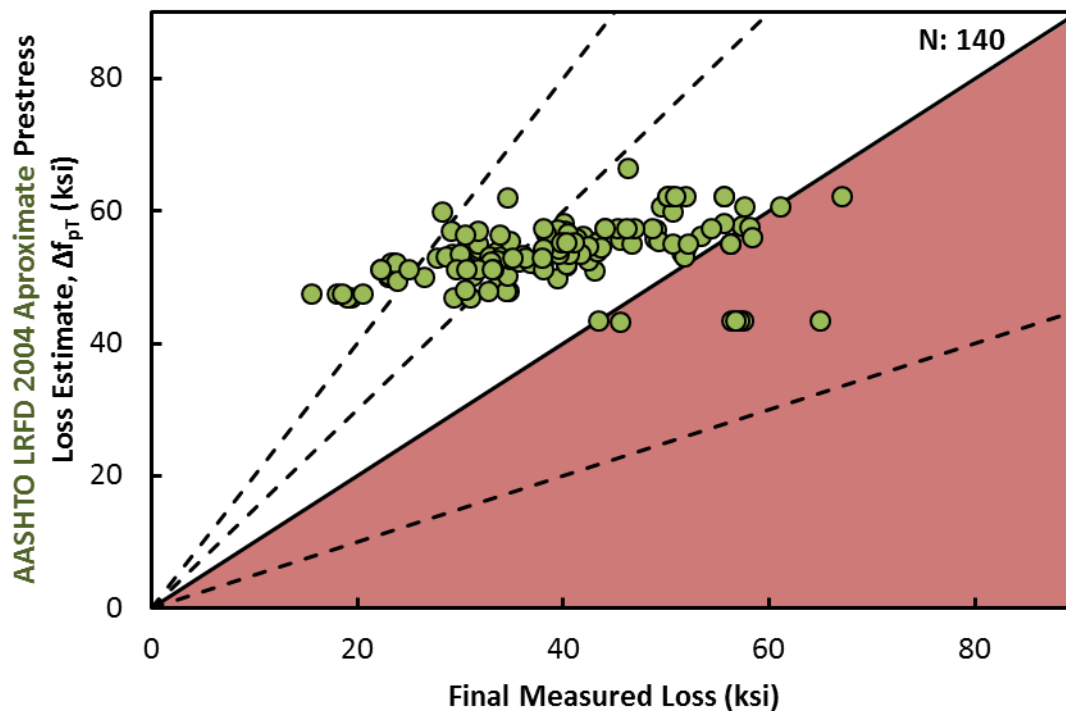
Figure E.1 - AASHTO LRFD 2004 approximate method prestress loss estimate vs. final measured loss

E.3.2 AASHTO LRFD 2012

The key statistics from the *E/M* ratios for both the refined and approximate procedures in AASHTO LRFD 2012 are presented in Table E.4. It can be seen that the approximate method is both more conservative and more precise than the refined method. The approximate prestress loss estimates are plotted versus the measured prestress loss in Figure E.2. It can be seen from this figure that using the approximate method results in reasonable prestress loss estimates, although there are still an excessive number of specimens with unconservatively estimated prestress loss.

Table E.4 – Comparison of performance of AASHTO LRFD 2012 refined and approximate procedures using estimated-to-actual ratio (E/M) from the evaluation database

	Refined	Approximate
Minimum	0.59	0.73
Average	1.25	1.15
Maximum	2.20	2.12
Co. of Variation	0.24	0.22
St. Deviation	0.30	0.25
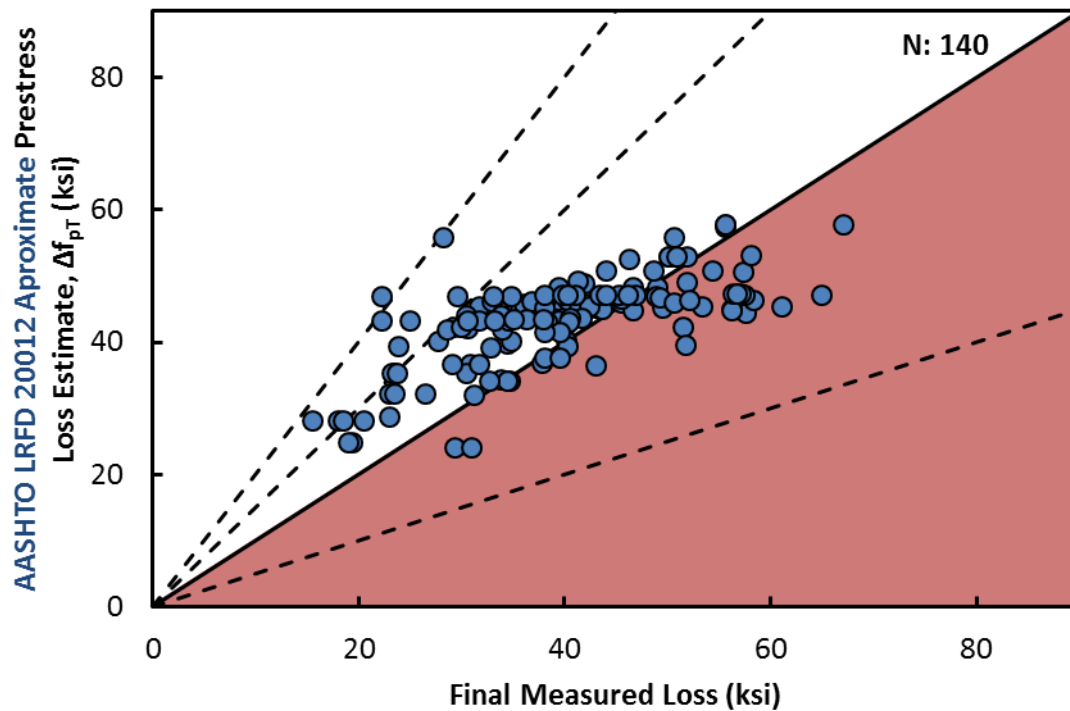
Figure E.2 - AASHTO LRFD 2012 approximate method prestress loss estimate vs. final measured loss

This page is intentionally left blank

APPENDIX F
Design Tables

F.1 OVERVIEW

The purpose of the design tables provided in this appendix is to compare designs completed using the current TxDOT prescribed prestress loss procedure with those completed using the recommended loss procedure.

F.2 DESIGN TABLES FOR I-GIRDERS

For the purpose of brevity, only a sampling from the TxDOT design tables is provided below, Table F.1 through Table F.6. The bridge layout (cross-section type, span length, girder spacing, concrete release strength, etc.) was taken from the TxDOT design tables. The tables below were created based on the I-girder tables for a 24 foot roadway configuration with an 8 inch slab.

Within Table F.1 through Table F.6 the total number of strands required and the total estimated prestress loss for designs using AASHTO LRFD 2004 (the current TxDOT loss provision) and 0-6374 recommended loss provisions are provided. The purpose of the tables is to show the impact of the recommended provisions on typical TxDOT bridge designs.

Table F.1 – Typical design (required strands and total prestress loss) for Tx28 girders of various lengths

Section Properties			Current TxDOT Provisions		0-6374 Recommendation	
Cross-Section Type	Span Length (ft.)	Concrete Release Strength (ksi)	Strands Required (No.)	Total Loss (ksi)	Strands Required (No.)	Total Loss (ksi)
Tx28	40	4.00	12	30.0	12	32.3
	45	4.00	14	32.1	14	34.5
	50	4.00	18	36.7	18	39.5
	55	4.00	22	37.8	22	44.4
	60	4.00	26	45.4	26	49.0
	65	4.25	32	51.3	32	53.8
	70	5.00	40	58.2	38	53.6
	75	5.75	52	66.7	46	54.5

Table F.2 – Typical design (required strands and total prestress loss) for Tx34 girders of various lengths

Section Properties			Current TxDOT Provisions		0-6374 Recommendation	
Cross-Section Type	Span Length (ft.)	Concrete Release Strength (ksi)	Strands Required (No.)	Total Loss (ksi)	Strands Required (No.)	Total Loss (ksi)
Tx34	40	4.00	12	29.9	12	32.1
	45	4.00	14	32.1	14	34.5
	50	4.00	16	33.6	16	36.2
	55	4.00	18	35.0	18	37.7
	60	4.00	20	36.3	20	39.1
	65	4.00	24	40.6	24	43.8
	70	4.00	28	44.8	28	48.3
	75	4.00	36	50.8	36	58.0
	80	5.00	40	54.8	38	50.4
	85	5.50	48	60.8	46	53.7

Table F.3 – Typical design (required strands and total prestress loss) for Tx40 girders of various lengths

Section Properties			Current TxDOT Provisions		0-6374 Recommendation	
Cross-Section Type	Span Length (ft.)	Concrete Release Strength (ksi)	Strands Required (No.)	Total Loss (ksi)	Strands Required (No.)	Total Loss (ksi)
Tx40	40	4.00	10	26.1	10	28.0
	45	4.00	12	28.3	12	30.4
	50	4.00	14	30.4	14	32.7
	55	4.00	16	32.0	16	34.4
	60	4.00	18	33.4	18	36.0
	65	4.00	20	34.7	20	37.4
	70	4.00	24	39.0	24	42.1
	75	4.00	26	40.1	26	43.2
	80	4.00	32	43.8	32	50.3
	85	4.00	38	49.9	38	57.0
	90	4.75	42	54.1	42	53.6
	95	5.25	50	60.1	48	54.6
	100	5.75	62	66.1	54	54.5

Table F.4 – Typical design (required strands and total prestress loss) for Tx46 girders of various lengths

Section Properties			Current TxDOT Provisions		0-6374 Recommendation	
Cross-Section Type	Span Length (ft.)	Concrete Release Strength (ksi)	Strands Required (No.)	Total Loss (ksi)	Strands Required (No.)	Total Loss (ksi)
Tx46	40	4.00	10	24.6	10	26.4
	45	4.00	12	26.6	12	28.5
	50	4.00	12	25.4	12	27.2
	55	4.00	14	27.1	14	29.1
	60	4.00	16	28.4	16	30.5
	65	4.00	18	32.4	20	34.9
	70	4.00	20	33.5	22	36.1
	75	4.00	22	34.6	24	37.2
	80	4.00	26	35.4	26	38.2
	85	4.00	30	38.8	30	41.8
	90	4.00	34	41.7	36	47.8
	95	4.00	40	47.1	40	50.9
	100	4.50	44	48.8	46	52.0
	105	5.00	52	54.5	50	50.6
	110	5.50	60	59.5	56	51.1
	115	6.00	72	66.1	62	51.1

Table F.5 – Typical design (required strands and total prestress loss) for Tx54 girders of various lengths

Section Properties			Current TxDOT Provisions		0-6374 Recommendation	
Cross-Section Type	Span Length (ft.)	Concrete Release Strength (ksi)	Strands Required (No.)	Total Loss (ksi)	Strands Required (No.)	Total Loss (ksi)
Tx54	40	4.00	8	21.5	8	23.0
	45	4.00	10	23.5	10	25.1
	50	4.00	12	25.3	12	27.1
	55	4.00	14	27.0	14	29.0
	60	4.00	16	28.5	16	30.6
	65	4.00	18	29.8	18	32.0
	70	4.00	20	31.0	20	33.4
	75	4.00	22	32.2	22	34.6
	80	4.00	24	33.2	24	35.8
	85	4.00	26	34.2	26	36.8
	90	4.00	28	35.1	28	37.7
	95	4.00	32	38.1	32	41.1
	100	4.00	36	41.1	36	44.3
	105	4.00	42	43.9	42	50.0
	110	4.25	46	46.1	46	50.7
	115	4.75	50	49.8	50	49.4
	120	5.25	58	55.1	54	48.2
	125	5.75	64	57.9	60	48.6

Table F.6 – Typical design (required strands and total prestress loss) for Tx62 girders of various lengths

Section Properties			Current TxDOT Provisions		0-6374 Recommendation	
Cross-Section Type	Span Length (ft.)	Concrete Release Strength (ksi)	Strands Required (No.)	Total Loss (ksi)	Strands Required (No.)	Total Loss (ksi)
Tx62	60	4.00	14	25.7	14	27.5
	65	4.00	16	27.0	16	29.0
	70	4.00	18	28.3	18	30.4
	75	4.00	20	29.5	20	31.7
	80	4.00	22	30.7	22	33.0
	85	4.00	24	31.7	24	34.1
	90	4.00	26	32.7	26	35.1
	95	4.00	28	33.5	28	36.1
	100	4.00	32	36.5	32	39.4
	105	4.00	34	37.1	34	40.0
	110	4.00	38	37.6	38	43.1
	115	4.00	42	40.4	42	46.1
	120	4.00	48	45.1	48	51.1
	125	4.50	52	46.6	52	49.7
	130	5.00	56	50.0	56	48.3
	135	5.50	62	53.0	60	47.0